NUCLEAR SAFETY

VOL 36-1

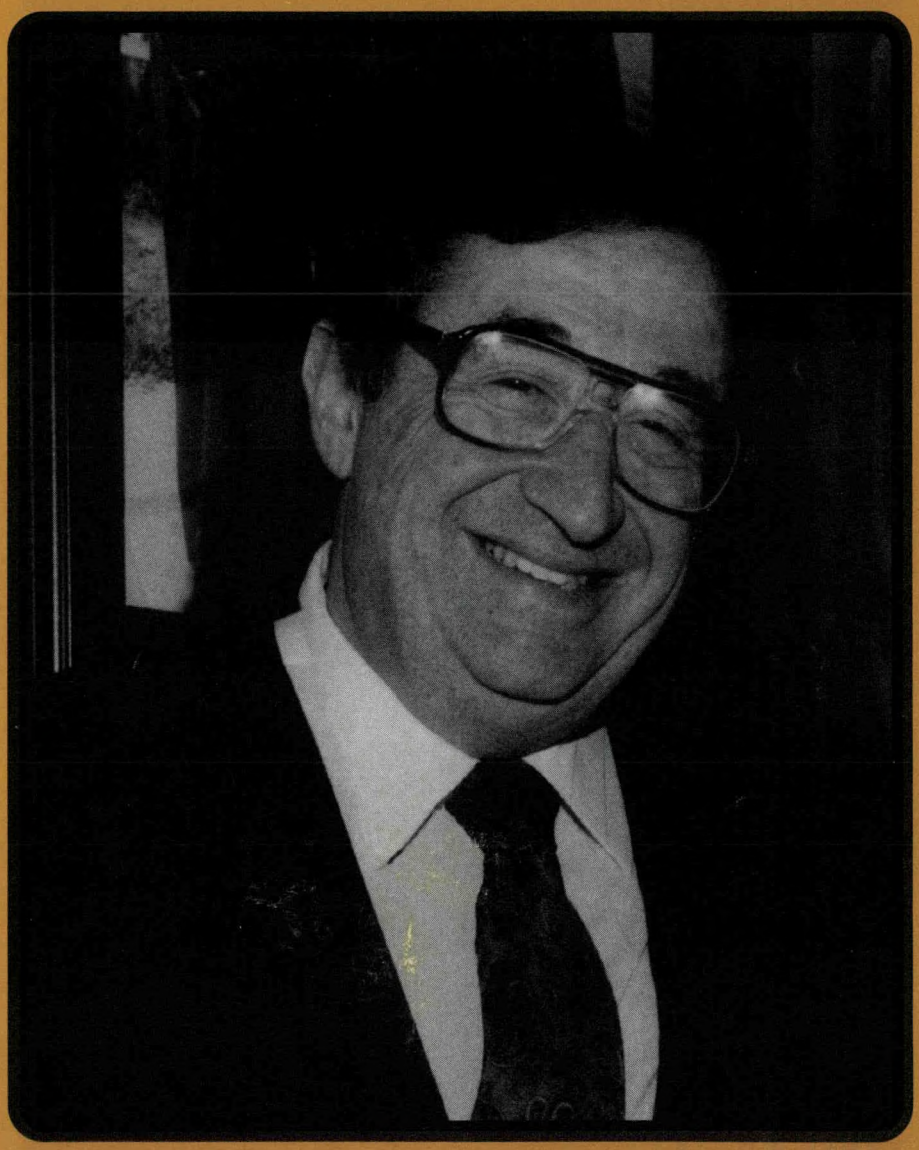

TECHNICAL PROGRESS JOURNAL JANUARY • JUNE 1995

The Operational Performance Technology Section

The Operational Performance Technology (OPT) Section at Oak Ridge National Laboratory (ORNL) conducts analyses, assessments, and evaluations of facility operations for commercial nuclear power plants in support of the Nuclear Regulatory Commission (NRC) operations. OPT activities involve many aspects of facility performance and safety.

OPT was formed in 1991 by combining ORNL's Nuclear Operations Analysis Center with its Performance Assurance Project Office. This organization combined ORNL's operational performance technology activities for the NRC, DOE, and other sponsors aligning resources and expertise in such areas as:

- event assessments
- performance indicators
- data systems development
- trends and patterns analyses
- technical standards
- safety notices

OPT has developed and designed a number of major data bases which it operates and maintains for NRC and DOE. The Sequence Coding and Search System (SCSS) data base collects diverse and complex information on events reported through NRC's Licensee Event Report (LER) System.

OPT has been integrally involved in the development and analysis of performance indicators (PIs) for both the NRC and DOE. OPT is responsible for compiling and analyzing PI data for DOE facilities for submission to the Secretary of Energy.

OPT pioneered the use of probabilistic risk assessment (PRA) techniques to quantify the significance of nuclear reactor events considered to be precursors to potential severe core damage accidents. These precursor events form a unique data base of significant events, instances of multiple losses of redundancy, and infrequent core damage initiators. Identification of these events is important in recognizing significant weaknesses in design and operations, for trends analysis concerning industry performance and the impact of regulatory actions, and for PRA-related information.

OPT has the lead responsibility in support of DOE for the implementation and conduct of DOE's Technical Standards Program to facilitate the consistent application and development of standards across the DOE complex.

OPT is responsible for the preparation and publication of this award-winning journal, *Nuclear Safety,* now in its 36th year of publication sponsored by NRC. Direct all inquiries to Operational Performance Technology Section, Oak Ridge National Laboratory, P.O. Box 2009, Oak Ridge, TN 37831-8065. Telephone (615) 574-0394 Fax: (615) 574-0382.

A semiannual Technical Progress Journal prepared for the U.S. Nuclear Regulatory Commission by the Operational Performance Technology Section at Oak Ridge National Laboratory

Published by the
Office of Scientific and Technical Information
U.S. Department of Energy

NUCLEAR SAFETY

Vol. 36, No. 1 **January–June 1995**

TPJ-NS-36-No. 1
DE95007615

NUSAAZ 36(1), 1995
ISSN: 0029-5604

Nuclear Safety is a journal that covers significant issues in the field of nuclear safety.

Its primary scope is safety in the design, construction, operation, and decommissioning of nuclear power reactors worldwide and the research and analysis activities that promote this goal, but it also encompasses the safety aspects of the entire nuclear fuel cycle, including fuel fabrication, spent-fuel processing and handling, and nuclear waste disposal, the handling of fissionable materials and radioisotopes, and the environmental effects of all these activities.

Qualified authors are invited to submit articles; manuscripts undergo peer review for accuracy, pertinence, and completeness. Revisions or additions may be proposed on the basis of the results of the review process. Articles should aim at 20 to 30 double-spaced typed pages (including figures, tables, and references). Send inquiries or 3 copies of manuscripts (with the draftsman's original line drawings plus 2 copies and with black-and-white glossy prints of photographs plus 2 copies) to M. D. Muhlheim, Oak Ridge National Laboratory, P. O. Box 2009, Oak Ridge, TN 37831-8065.

The material carried in *Nuclear Safety* is prepared at the Oak Ridge National Laboratory's Operational Performance Technology Section, which is responsible for the contents. *Nuclear Safety* is funded by the U.S. Nuclear Regulatory Commission's Office of Nuclear Regulatory Research. Editing, composition, makeup, and printing functions are performed by the DOE Office of Scientific and Technical Information (OSTI). Sale and distribution are by the U.S. Government Printing Office; see the back cover for information on subscriptions.

EDITORIAL

Ernest Silver, Editor-in-Chief 1984–1995

After ten years of service to the nuclear community, Ernest Silver has retired as Editor-in-Chief of *Nuclear Safety*, one of the most respected journals in the nuclear energy field. Silver was only its second Editor, and he has brought it through the last ten years with great style, an unswerving devotion to technical excellence and clear presentation that are the hallmarks of the journal. Even as nuclear energy is passing through a period of travail and distrust, *Nuclear Safety* is increasingly the publication that supplies honest technical answers to the questions that are being asked. Are reactor systems safe? What about diversion of plutonium? What do we do about high level waste? What about relicensing? and so on.

Silver has guided the journal into the present era. He broadened the scope of the journal so that it is not only a review journal but also a general scientific and technical journal that provides descriptions of new work in the nuclear safety area. Through his efforts he has assured for it a respected place in the continuing debate about the use of nuclear energy.

Originally a nuclear physicist who did outstanding neutron research at the Oak Ridge Electron Linac, Silver turned a lively curiosity and appreciation of technical content to the issues discussed in this journal. Silver's deep interest in language and his ability to communicate ideas and to identify areas of interest to the readership all have led to a journal that is outstanding both in content and in form. He took great pleasure in obtaining authors who could do the job, and in this way he kept in touch with a worldwide community of nuclear experts. He felt very much at home in their company.

Editing a journal is, in the final analysis, a cultural activity. This plays to Silver's strength. He is vitally interested in all facets of our culture, from science to art, from history to politics, from economics to the Tennessee Lady Vols. This uncommon breadth of interests is his trademark. It stood him well in his job as Editor, and the result is plain to all: *Nuclear Safety* is a journal of great value, with articles written by the best people in the field on subjects that deal with one of mankind's urgent issues. He has done his job well; with his departure go our thanks and our wishes for a retirement full of the many things he loves and in which he takes pleasure.

Alvin Trivelpiece
Director, Oak Ridge National Laboratory

In Appreciation of Ernest Silver

Ernest Silver, that brilliant and witty polymath, has retired as editor of *Nuclear Safety* after $9^1/_2$ years. I write this editorial to express not only my own appreciation but also that of the entire nuclear engineering community for Ernest's unselfish and dedicated contribution to nuclear energy.

Ernest came to Oak Ridge in 1954 as a student at the Oak Ridge School of Reactor Technology. I quickly recognized his unusual talents: a physicist who had done graduate work at Harvard and who had an excellent instinct for hands-on nuclear and reactor physics as well as an extraordinary, perceptive writing and speaking style. This is all the more unusual because in 1941, at the age of 11, Ernest, a refugee from Hitler's Germany, came to America on the last boat to leave Lisbon. English was his *second* language, and he mastered

(Continues on inside back cover.)

The Chornobyl Accident

Edited by M. D. Muhlheim

The Chornobyl Accident Revisited, Part II: The State of the Nuclear Fuel Located Within the Chornobyl Sarcophagus

By A. A. Borovoi[a] and A. R. Sich[b]

Abstract: *Approximately 135 tonnes of the 190.3-tonne initial core fuel load (≈71%) at Chornobyl Unit 4 melted and flowed into the lower regions of the reactor building to form various kinds of the now-solidified lava-like fuel-containing materials (LFCMs) or corium. The results of radiochemical analyses reveal that only 5% of the LFCM inventory of Ru-106 remains, whereas, surprisingly, 35% of the LFCM inventory of Cs-137 remains. Moreover, the results of these analyses support the fact that little if any of the 5020 tonnes of various materials (dropped from helicopters during the active phase of the accident in an attempt to smother the burning graphite) ever made it into the core shaft, where the bulk of the core was located. The results appear to support earlier Western source-term estimates that significantly more volatile radionuclides may have been released as a result of the accident.*

The 1000-MW(e) RBMK (light-water-cooled, graphite-moderated multichannel reactor) Unit 4 nuclear power reactor at the Chornobyl Nuclear Power Station was "physically started" on November 11, 1983, and achieved criticality 32 days later on December 13, 1983.[c] By April 25, 1986, it had reached the end of its first operating cycle (with a core-average burnup of 10.9 MWd/kg U for its 190.3-tonne UO_2 charge),[d] and a maintenance outage was scheduled for the following day. At approximately 01:23:40 on April 26, 1986, after 865 calendar days and 715 effective full-power days in operation,[1] the most severe accident in the history of commercial nuclear power occurred at this unit—characterized as a Level 7 Major Accident (most severe), according to the International Nuclear Event Scale: "The accident can be

[a]Ukrainian Academy of Sciences, Kyyiv, Ukraine, and Kurchatov Russian Research Institute, Moscow.

[b]Massachusetts Institute of Technology.

[c]This is considered fast for the initial startup of a nuclear power reactor. Normally a period of approximately 4 to 6 months is prescribed for flushing various systems, repairs, tests, etc., between the "physical startup" and first criticality of a power reactor of this size—followed by an additional 4 to 6 months between first criticality and full-power operation. In a March 13, 1984, article in *Pravda Ukrainy*, it was announced that Unit 4 had reached full-power operation 2 months ahead of schedule. Not only was it rare to complete a project ahead of schedule in the Soviet nuclear energy industry but also the startup date as given was incorrect. Unit 4 actually achieved full-power operation on May 25, 1984—more than 2 months later.

[d]Out of the total 1661 technological channels in a 2nd-generation RBMK-1000, for Chornobyl Unit 4 at the time of the accident 1659 channels were fueled (more than 57% of which contained first-load fuel assemblies), one was unfueled, and one contained a "supplemental" absorber. [See Yu. V. Svyntseva and V. A. Kachalova (Eds.), *Chornobyl: Five Difficult Years*, Izdat, Moscow, 1992, p. 102.]

technically classified as a voiding-induced super-prompt critical power excursion that triggered a fuel–coolant interaction steam explosion that simultaneously breached both the primary system and the containment."[2,3]

EXTENT OF DAMAGE TO THE REACTOR BUILDING

As a result of the accident, the reactor core was completely destroyed. Approximately 135 ± 30 tonnes (≈71%) of the fuel melted and flowed into the reactor building's lower regions; about 3.5% of the fuel (6.7 tonnes) was blown upward out of the reactor core "shaft" and released into the atmosphere, where aerosol-sized particles were eventually carried over the northern hemisphere. An estimated 25 to 30 tonnes of fuel, in the form of "dust" or large broken pressure tubes imbedded in graphite, are scattered throughout the upper levels of the damaged reactor building, mostly under debris or concrete poured in after the accident; the balance of the fuel (≈11 tonnes)—most of which is thought to be inside the reactor building and sarcophagus—has yet to be positively located.

The reactor building itself, especially above the floor of the central (reactor) hall, suffered extensive damage and resulted in the complete destruction of the roof and upper building structures, which reduced the height of the building from an initial 71.5 m to an average 46 m (Ref. 4) (see Fig. 1). Other major components of this unit, including the emergency core cooling system (ECCS), deaerator system, steam drums, main coolant pumps, and primary piping, were heavily damaged or destroyed. The explosion's pressure wave significantly displaced those reactor building support columns not completely destroyed—compromising the building's structural integrity and making construction of the sarcophagus extremely difficult. Hot core materials (fuel and graphite) expelled during the explosions started fires in and around the destroyed unit. Particularly heavy damage was caused by these fires and flying debris to the roof that covers Unit 4's two 500-MW(e) turbogenerators. In many places the roof collapsed and thus caused further, widespread damage to equipment below.

BRIEF DESCRIPTION OF THE SARCOPHAGUS

The Chornobyl Unit 4 postaccident containment structure—dubbed Ukryttja, or "Shelter," in Ukrainian, but commonly referred to as the sarcophagus (Figs. 2 and 3)—was completed in November 1986. The sheer size of this containment (constructed upon the ruins of the destroyed reactor building) and the extremely hazardous working conditions (necessitating the use of unique and remote construction methods in very high radiation fields) plus the short time span of 6 months make it a unique accident clean-up and isolation achievement. After considering 18 different project variants, scientists and engineers chose a design that would take advantage of the reactor building's foundation and remaining superstructure.[5] The benefits of their decision were significantly lower costs and high speed of construction. There were, however, also disadvantages: (1) information on the structural integrity of the reactor building was lacking, (2) remote methods for pouring fresh concrete did not always permit observation and review of work, and (3) in a number of cases high radiation fields made welding key structural components impossible. As a result of these construction difficulties, two essential deficiencies exist and continue to threaten the integrity of the sarcophagus: (l) it is unknown how strong are the supports that buttress the upper sections of the structure, and (2) openings and breaks in the walls and the roof of the sarcophagus are estimated to total about 1200 m^2 (Refs. 6 and 7).

During the construction of the sarcophagus, a great deal of "fresh" concrete flowed into the lower sections of the damaged reactor building and made it difficult or impossible to enter many areas for a structural appraisal or for investigations of the remains of the reactor. Conversely, parts of the remains of the reactor core that melted and flowed into the lower regions of the reactor building [the corium, or so-called lava-like fuel-containing materials (LFCMs)] were covered with layers of concrete, which made entrance easier into areas that otherwise would have been impossible because of high radiation fields.

From 1987 to 1991, scientists, engineers, construction specialists, and other members of the Chornobyl Complex Expedition of the Kurchatov Institute of Atomic Energy conducted much scientific and investigative research into the location and state of the nuclear fuel remaining within the sarcophagus. Soon after the collapse of the Soviet Union, all scientific, construction, and technological work at the sarcophagus site fell under the direction of the Ukrainian Academy of Science's Inter-Branch Scientific and Technical Center "Shelter." Day-to-day maintenance and surveillance of Shelter is carried out by the enterprise "Object Shelter," which is

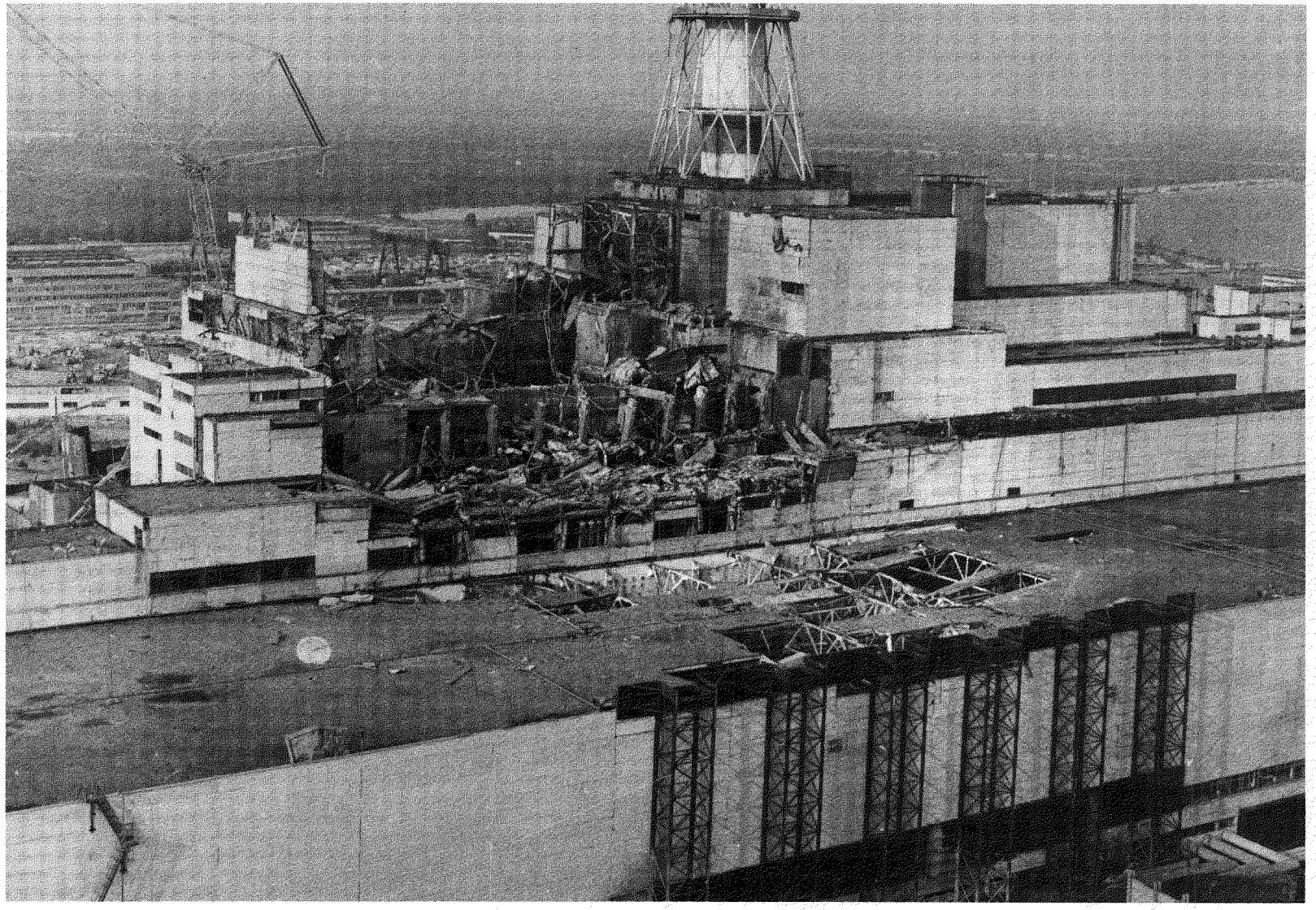

Fig. 1 Photograph of the destroyed Chornobyl Unit 4 reactor building in late July or early August 1986 viewed from the southwest. Note the 1-m-thick reinforced concrete structural support members (at the deaerator level) inclined away from vertical.

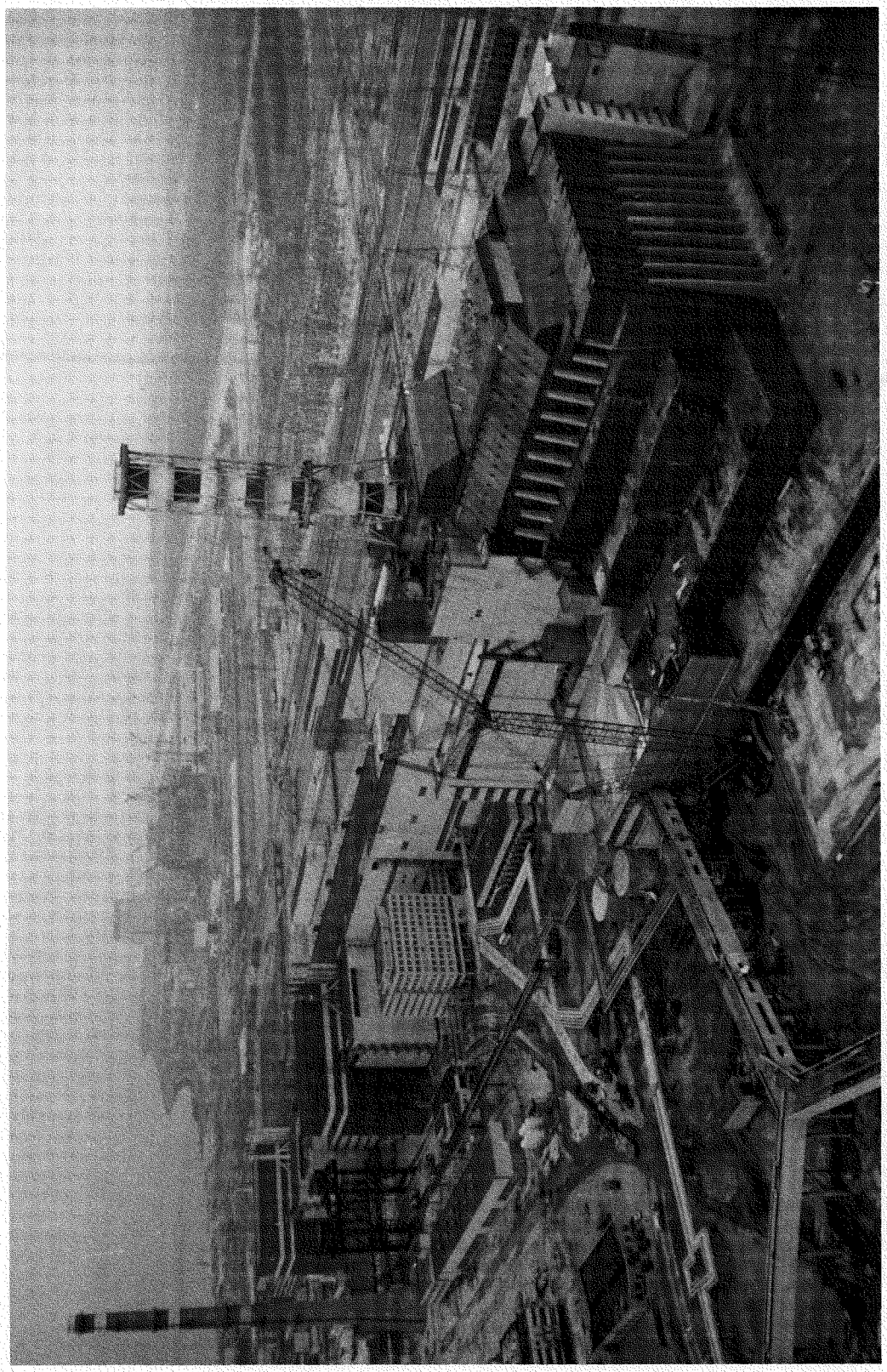

Fig. 2 Photograph of the nearly completed Chornobyl Unit 4 sarcophagus "Shelter" in November 1986 viewed from the northwest. (Photograph courtesy of Valentin Ivanovich Obodzinski of the Kurchatov Institute, Moscow.)

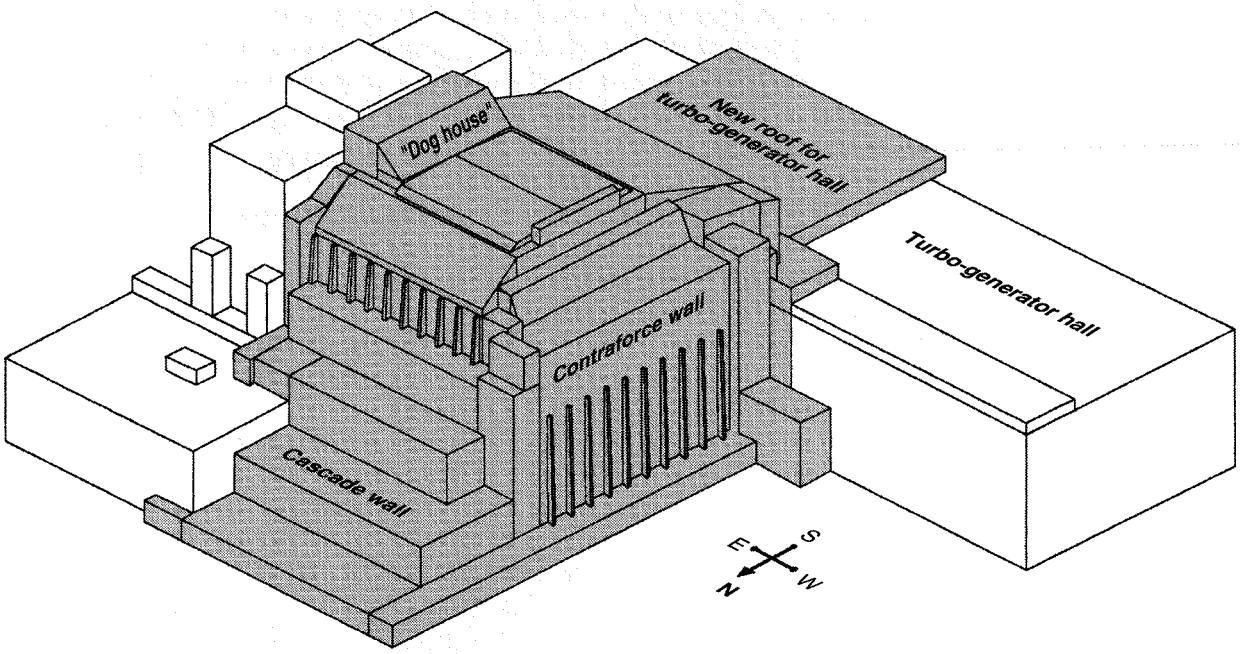

Fig. 3 General view of the Chornobyl Unit 4 sarcophagus "Shelter." (Photograph courtesy of Valentin Ivanovich Obodzinski of the Kurchatov Institute, Moscow.)

formally administered by the staff of the nuclear power plant.

The sarcophagus can be described briefly as follows (refer to Fig. 4a and b): The east side consists of a dividing wall, which separates Unit 3 from the auxiliary systems building "v," and is constructed as a combination of existing building walls and newly erected walls or concrete filler. The north side of the building is defined by the "cascade wall," which is filled with concrete, radioactive materials thrown in from the roof and surroundings, building debris, and structural metals and is in the form of very large cascading steps. These steps conform more or less to the building debris and eventually rise to meet the upper levels of the former high bay area of the reactor's central hall. The western wall is relatively intact and is lined on the inside by a buttressed concrete shielding wall 1 m thick and 45 m high (but only partially filled in) and on the outside by large steel contraforce panels 6 by 45 m and weighing approximately 92 tonnes each (Ref. 5, p. 301). The upper parts of Shelter rest upon three metallic support beams: B1, B2, and the so-called 160-tonne Mammoth Block. The western supports for beams B1 and B2 are served by a reinforced concrete wall about 1 m thick. This wall has a number of serious cracks and is tilted slightly toward the west. During the construction of Shelter, direct inspection of this wall was impossible. The only sources of information concerning its integrity were photos taken from helicopters flying approximately 250 to 300 m from it. Before beams B1 and B2 were placed onto the wall, an effort was made to strengthen it with "fresh" concrete; at the time, however, it was unclear whether this procedure served its intended purpose. On the eastern part of the damaged building the beams rest upon ventilation shafts that appear not to have suffered major damage. On beams B1 and B2 rests a series of steel pipes upon which, in turn, a steel-paneled roof was built. Support for these steel panels on the southern side is served by the 70-m-long (54 m of which is "free hanging" and unsupported) and 5.5-m-wide Mammoth Block, which, in turn, rests upon two concrete columns.[a] These columns stand among the debris of the damaged building and were strengthened by remotely poured concrete.[8]

Work in 1987 and 1988 on strengthening internal structures that suffered heavy damage as a result of the accident has prevented, at least for the time being, an

[a]There is a small inconsistency in the dimensions and mass of the Mammoth Block between those given by Kurnosov et al. (Ref. 5, p. 302) (70 m long × 6 m tall × 2.4 m thick, 147 tonnes) and my review of the sarcophagus construction plans (70 m long × 5.5 m tall × 2.4 m thick, 160 tonnes).

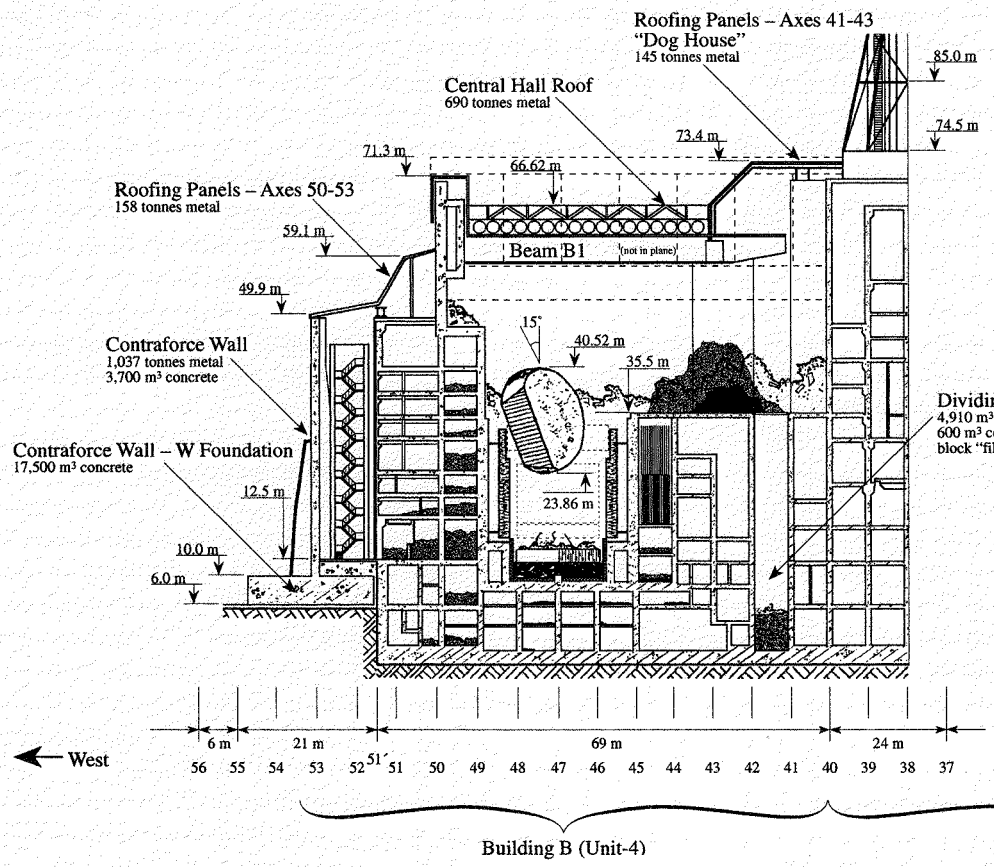

Sarcophagus Component	Metal Mass (t)	Concrete Volume (m³)
Central Hall Roof	690	–
Roofing Panels – Axes P-S	160	–
Roofing Panels – Axes B-Zh	597	–
Roofing Panels – Axes 41-43	145	–
Roofing Panels – Axes 50-53	158	–
Turbo-Generator Hall Roofing Panels	635	–
Turbo-Generator Hall Lateral Wall	85	–
Support Beams B1 & B2	300	–
"Mammoth" Support Beam	140	–
Contraforce Wall – N	253	1,500
Contraforce Wall – W	1,037	3,700
Contraforce Wall – W Foundation	–	17,500
Cascade Wall	800	115,800
Deareator Diving Wall	–	17,000
Dividing Wall – Axis 41	–	5,510
	5,000	**161,010**

Fig. 4a Schematic of the Chornobyl Unit 4 sarcophagus "Shelter." East-west cross section along axis L.

Sarcophagus Component	Metal Mass (t)	Concrete Volume (m³)
Central Hall Roof	690	–
Roofing Panels – Axes P-S	160	–
Roofing Panels – Axes B-Zh	597	–
Roofing Panels – Axes 41-43	145	–
Roofing Panels – Axes 50-53	158	–
Turbo-Generator Hall Roofing Panels	635	–
Turbo-Generator Hall Lateral Wall	85	–
Support Beams B1 & B2	300	–
"Mammoth" Support Beam	140	–
Contraforce Wall – N	253	1,500
Contraforce Wall – W	1,037	3,700
Contraforce Wall – W Foundation	–	17,500
Cascade Wall	800	115,800
Deareator Diving Wall	–	17,000
Dividing Wall – Axis 41	–	5,510
	5,000	**161,010**

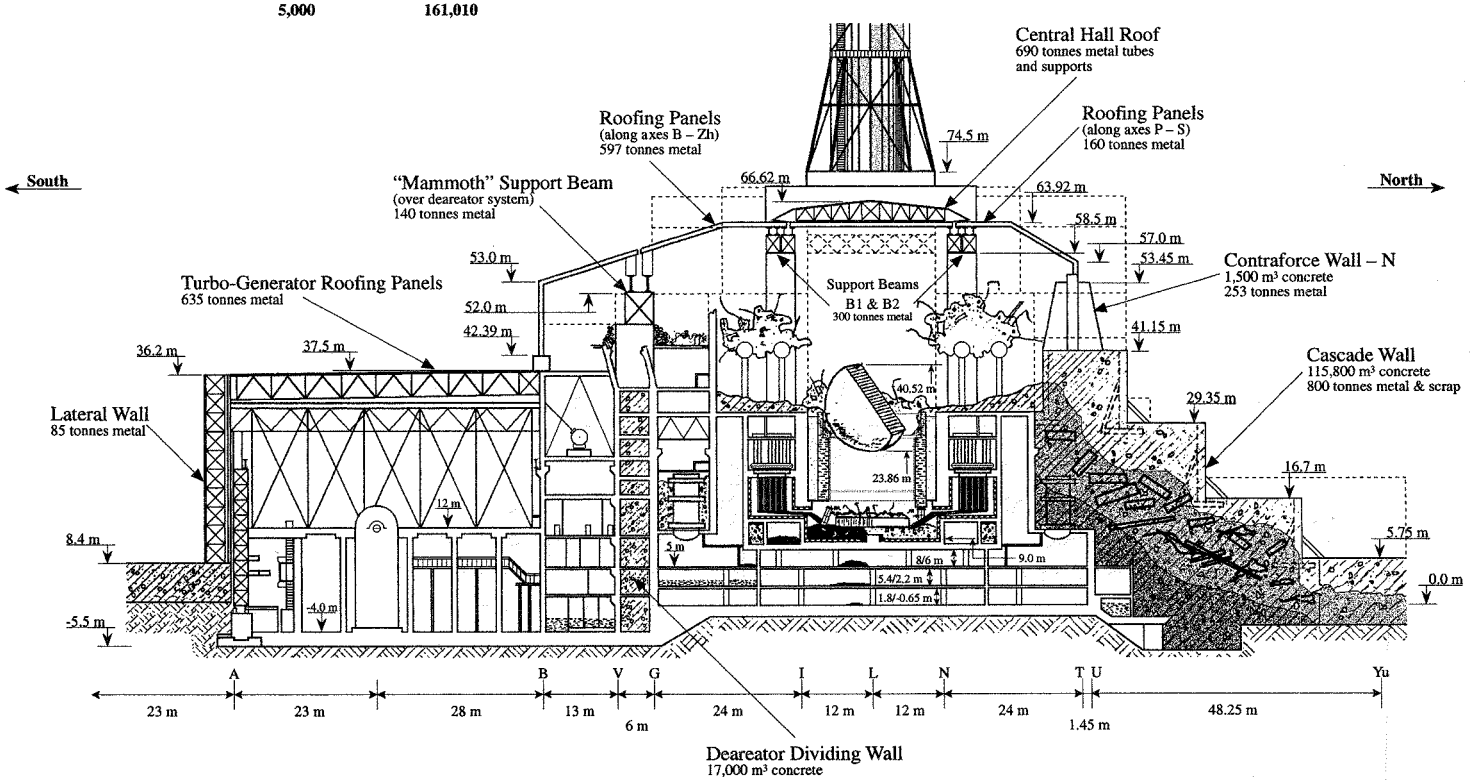

Fig. 4b Schematic of the Chornobyl Unit 4 sarcophagus "Shelter." North-south cross section along axis 47.

internal collapse that could lead to further weakening of Shelter. No noticeable long-term movements of internal structures have been observed—even though an earthquake registering 4.0 on the Richter scale occurred in May 1990, which resulted in only a slight enlargement of currently existing cracks in supporting walls.[9] Visual inspection of the most difficult to reach eastern column support of the Mammoth Block, conducted by an inspection team in 1991, showed that no serious flaws in this support exist, although water was noticed through openings in the structure, which could eventually weaken and wear away the base of this support.

THE STATE OF THE NUCLEAR FUEL REMAINING WITHIN THE SARCOPHAGUS

Remains of the Core and Adjacent Areas

Investigations conducted during 1986 to 1989 showed that previous notions concerning the extent of damage within Unit 4 as a result of the accident in most cases did not correspond to the actual state of the destroyed reactor. After a significant number of bore samples (about 70) were taken of the core region, core-support area and subreactor region, steam-distribution corridor, and a number of other areas, radiation field measurements were taken to determine which areas were safe enough to approach for closer inspection.[10,11] Visual inspections of these areas were then conducted either by remote-control visual aids (video cameras, periscopes, or small robots) or, if approachable, directly by researchers armed with cameras and video equipment. The following account details what was found within the reactor building of Unit 4[12] (refer to Figs. 5 to 9).

The core of the reactor and the steel, hermetic pressure casing that contained the core, "Scheme" or "Component KZh," were destroyed.[a] The upper biological shield (UBS) and lower biological shield (LBS) (Components E and OR, respectively) were displaced from their standard design positions. Cylindrical water tanks surrounding the core, known as the lateral biological shields, Components D and L, remain more or less in their nominal positions. As far as can be ascertained, the 21.6- by 21.6-m reactor shaft remains intact, and little if any of the sand and gravel filler material (between Component L and the shaft) is missing.

Part of the reactor fuel and assemblies (in the form of Zircaloy pressure tubes containing fuel rods, individual pieces of fuel rods, broken or partially intact graphite blocks, granules of these, and dust), as a rule, are found in the upper regions of the reactor building (especially in the control hall). A significant number of graphite blocks and some pieces of Component KZh were hurled onto the roofs of Unit 3 and the turbogenerator hall. A small portion of the reactor graphite block pile along with the associated fuel assemblies are scattered among debris and under concrete[b] on top of Component OR. The rest of the fuel is in the form of LFCMs located in the lower regions of the reactor building starting from below the current location of Component OR. The LFCMs are a combination of various structural materials (stainless steel, serpentine,[c] graphite, etc.) that melted during the active phase of the accident, mixed with molten fuel, and flowed downward into the lower regions of the reactor building to form varied types of frozen corium.

Component OR itself was significantly damaged: besides descending approximately 4 m (compressing the metallic reactor support, Component S, accordion-style beneath it), a pie-shaped section (≈105°) of the southeast quadrant is conspicuously missing. Component OR is also tilted downward through an angle of approximately 10° in the direction of the missing section. It is now believed that Component OR descended not as a result of the initial explosions, but rather because decay heat from the approximately 75 tonnes of melted fuel surrounding Component S served to weaken this support. Component S thus soon reached its yield point, and under a load of approximately 800 tonnes (the remains of Component OR itself and other debris) smoothly descended 4 m (Ref. 13).

---

[a]In architectural-engineering jargon, the Soviets typically use the term *scheme* to indicate a major component of a system. In this case, the steel hermetic pressure casing that contains the core is often referred to by the shorter expression Scheme KZh from the Russian word *KoZha*, or "skin."

[b]This is the so-called "fresh" concrete poured into the reactor building during the construction of Shelter.

[c]Serpentine, a hydrous magnesium silicate $Mg_6[Si_4O_{10}]\cdot[OH]_8$ obtained from the naturally occurring rock Serpentinite, fills the spaces between coolant tubes penetrating both the UBS and LBS in the form of coarse sand, pebbles, and small rocks. Serpentine's most significant and unique feature is that most of the water of crystallization is retained at temperatures as high as 450 to 500 °C. As a consequence, serpentine can be used in shielding applications where high temperatures may be involved. Nominally, approximately 617 tonnes of serpentine is found in the LBS and its peripheral thermal compensator section.

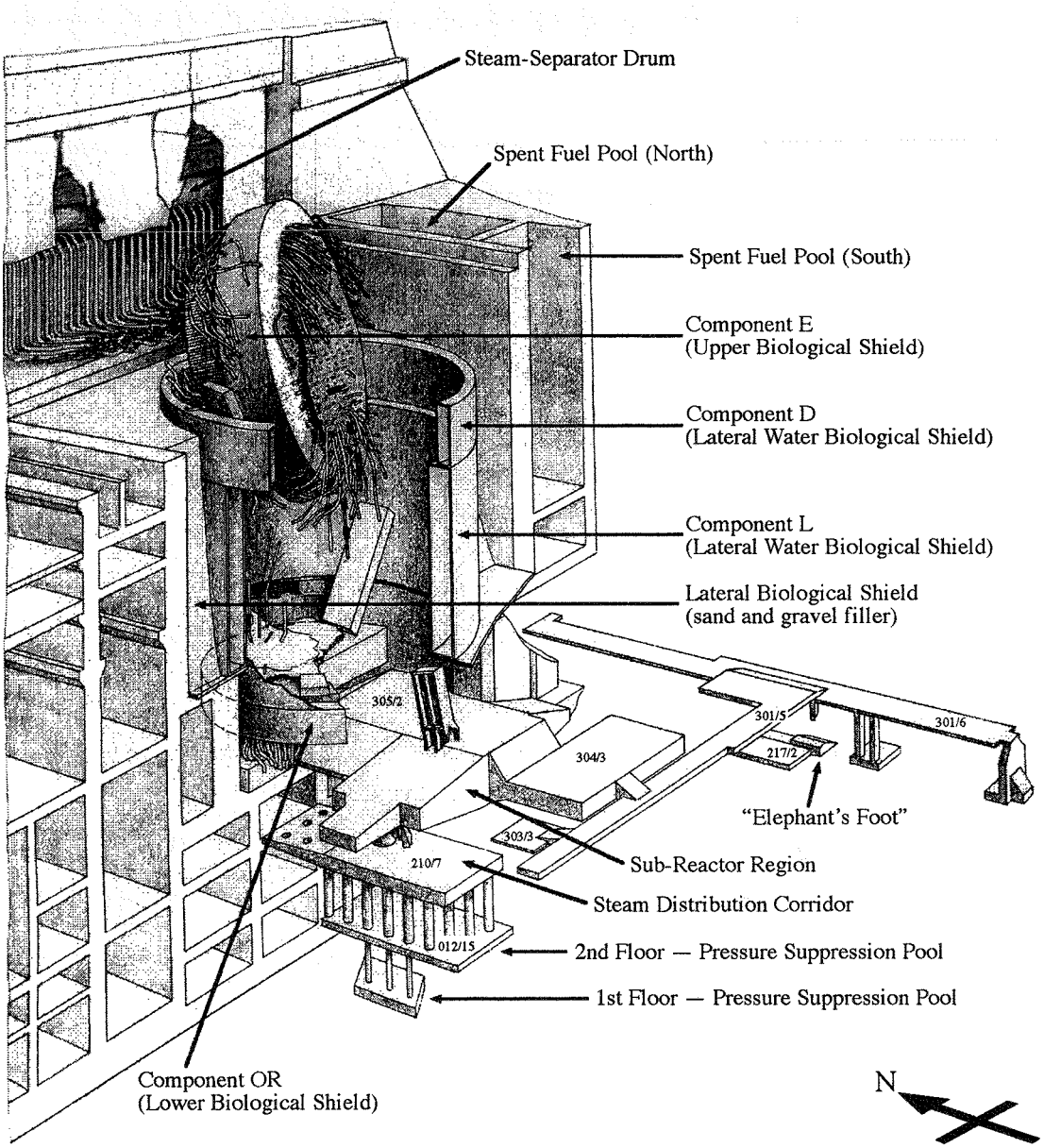

Fig. 5 Sectional view of Chornobyl Unit 4 in its current state. Approximately 71% of the initial 190.3-tonne UO_2 fuel load is now located in areas below the lower biological shield (LBS). Note that virtually no fuel or graphite is found in the reactor shaft region. Also, an approximately one-quarter pie-shaped section of the LBS is missing—presumably taken up by the corium before it flowed into the lower regions of the reactor building and which later cooled into ceramic glass-like and pumice formations.

Component E [together with the remains of approximately 40 upper coolant channels (UCCs), moderator coolant or fuel and instrumentation channels—so-called technological channels (TCs), and fragments of reinforced concrete support structures] is suspended on its side by the walls of the reactor shaft approximately 15° from vertical. On the northeast side of the shaft, Component E rests upon the upper portion of Component D, whereas on the southwest side it rests upon a large fragment (approximately 2 m by 3 m by 1.5 m) of

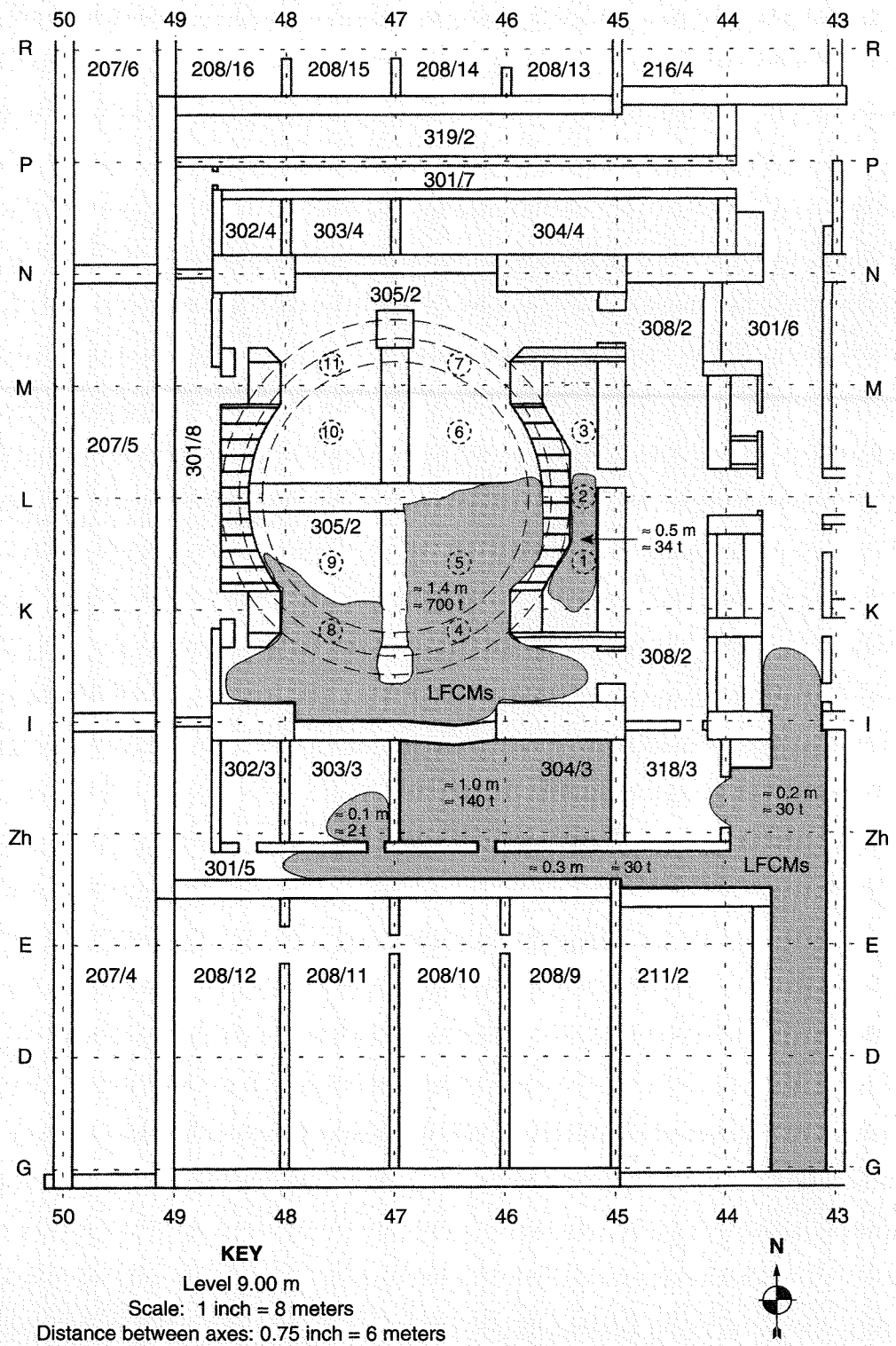

Fig. 6 Level 9 m: subreactor region. Locations of fuel-containing masses in the subreactor region and adjoining areas. LFCMs are lava-like fuel-containing materials. (Note that the LFCMs as depicted here are mostly located under a layer of concrete.)

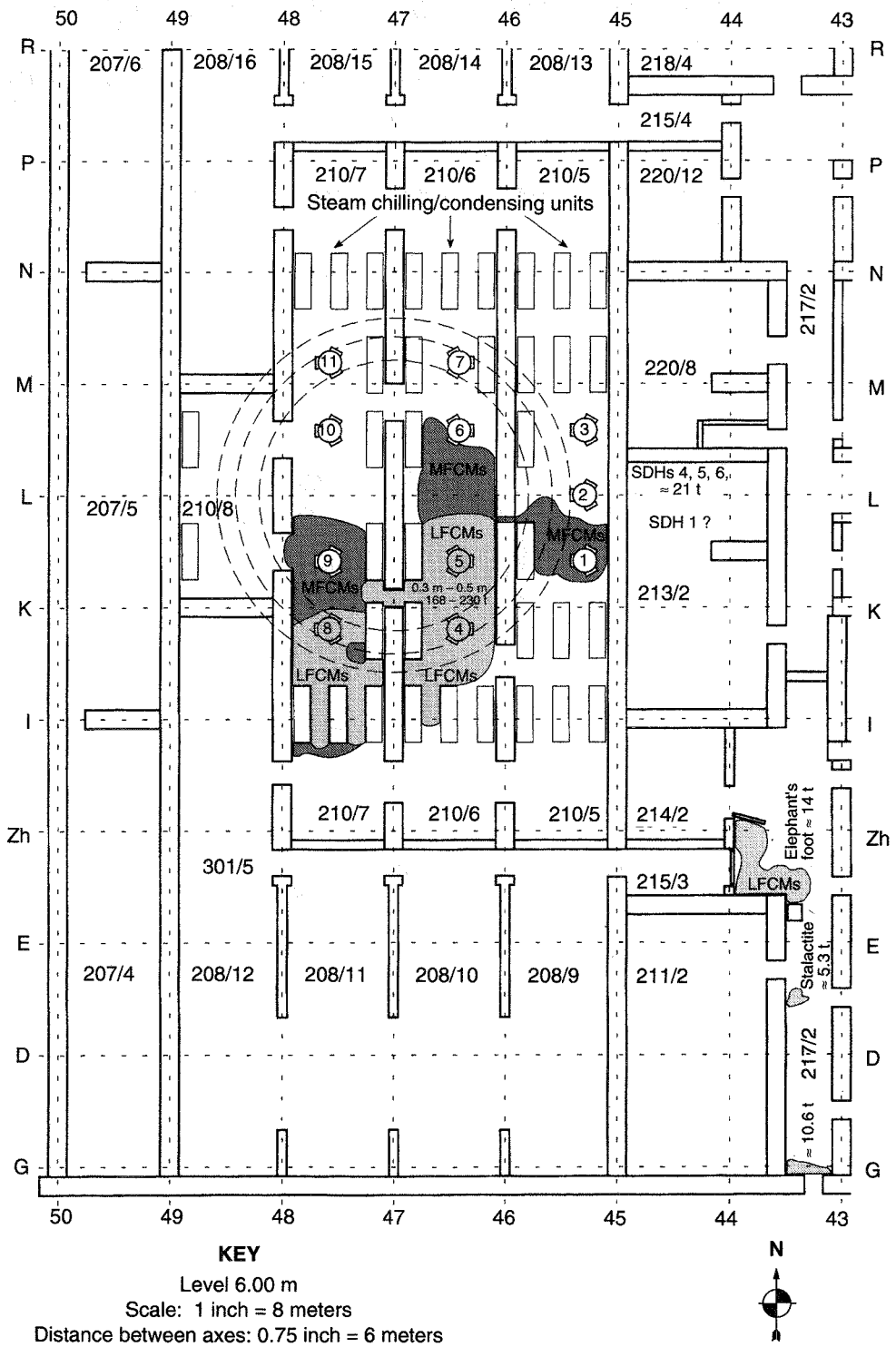

Fig. 7 Level 6 m: steam distribution corridor. Locations of fuel-containing masses in the steam distribution corridor and adjoining areas. LFCMs are lava-like fuel-containing materials, MFCMs are metallic-like fuel-containing materials, and SDH is steam distribution header. (Note that the LFCMs as depicted here are mostly located under a layer of concrete.)

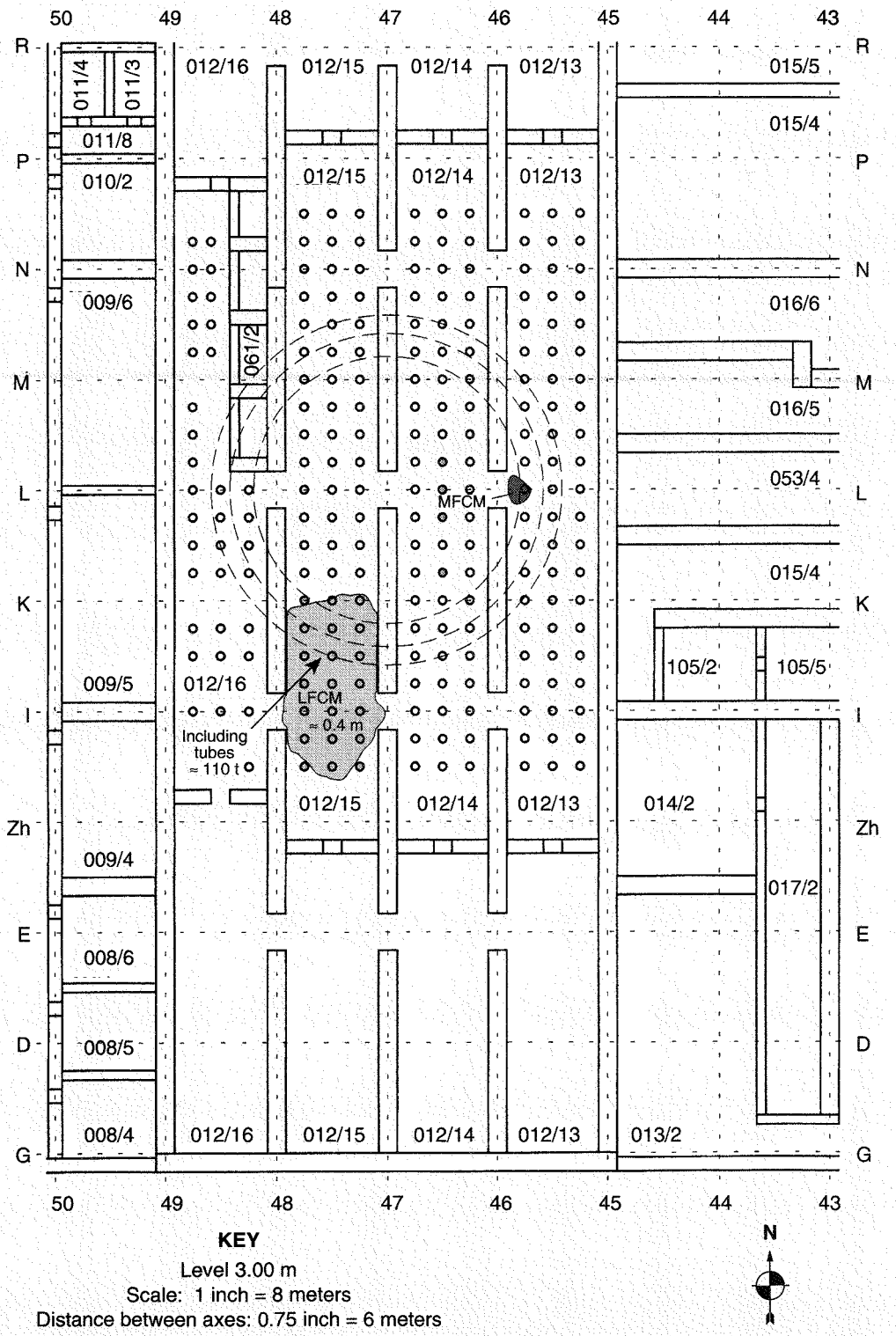

Fig. 8 Level 3 m: pressure suppression pool-2. Locations of fuel-containing masses on the second floor of the pressure suppression pool and adjoining areas. LFCMs are lava-like fuel-containing materials. (Note that the LFCMs as depicted here are mostly located under a layer of concrete.)

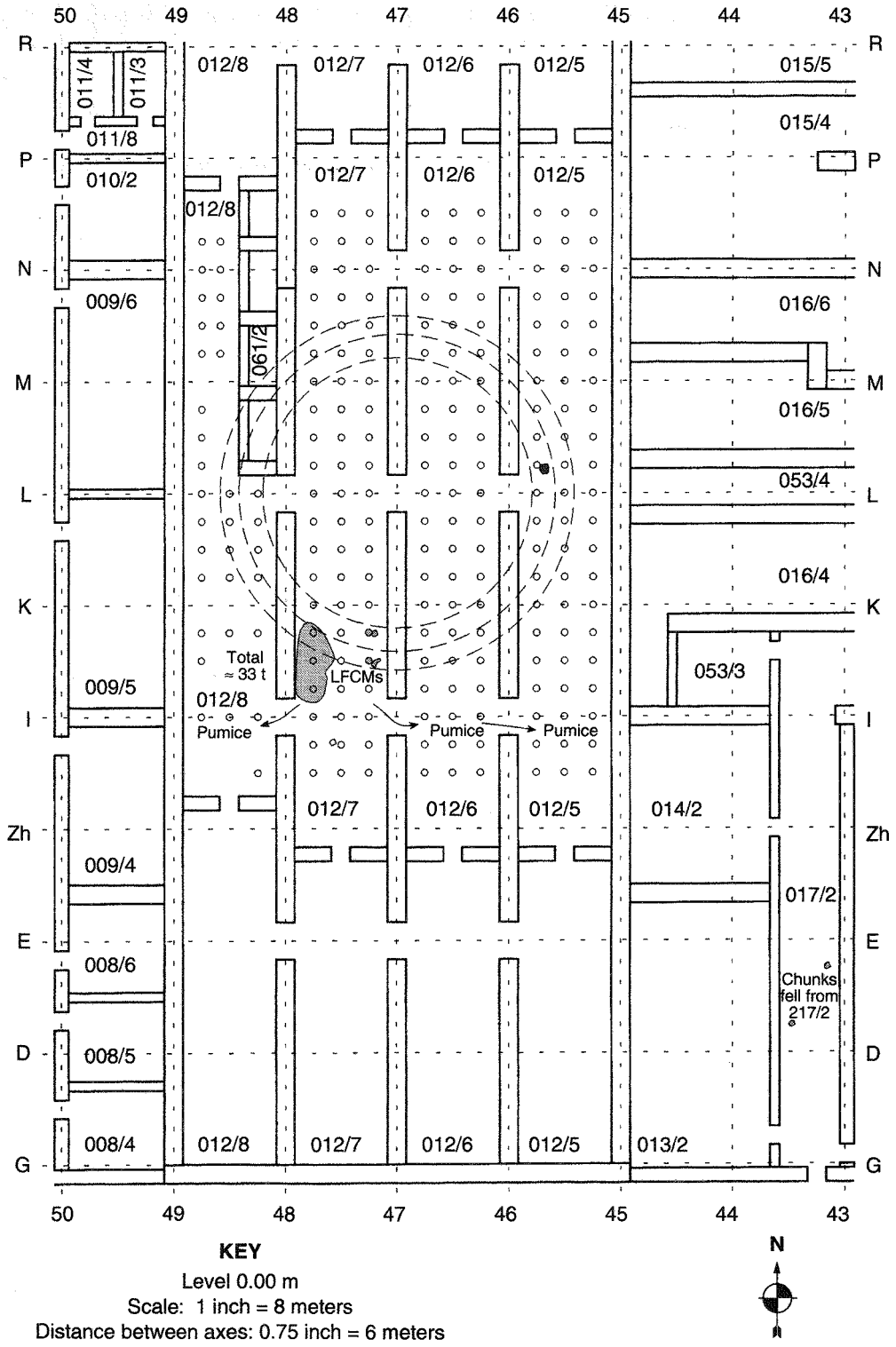

Fig. 9 Level 0 m: pressure suppression pool-1. Locations of fuel-containing masses on the second floor of the pressure suppression pool and adjoining areas. LFCMs are lava-like fuel-containing materials. (Note that the LFCMs as depicted here are mostly located under a layer of concrete.)

reinforced concrete and steel panel pinned against Component D. This panel was later determined to be part of the lower bay wall on the south side of the central hall from approximately Level 45 m, which supported the fueling machine and provided shielding for the steam-drum separators located adjacent to the reactor hall in rooms 804/3 and 4.[a] Virtually the entire space between Component E (normally its upper face) and Component D on the northwest side is filled in with heavily damaged stainless steel coolant pipes (which connect the UCCs to the Zircaloy core pressure tubes) and tangled UCCs. Driven in between these coolant pipes are reinforced concrete blocks about 2 m^3 in volume. Apparently, these blocks were at one time part of the same wall from which the panel pinned on one side beneath Component E (see above) originated. The central section of the (formerly) lower face of Component E (which corresponded to Level 28.5 m) is stripped of its TCs—approximately 50% of the core's total channels are cut off flush with the surface. A small number of severely damaged TCs surrounding the stripped central section on the periphery of Component E's bottom face remain dangling from it. The number of these that are fuel or control channels—as opposed to moderator coolant channels (MCCs)—is not known at this time. From within the core region at Level 24.6 m one can see approximately 40 badly damaged channels dangling from what is now the lower part of Component E. The bottom edge of Component E (which is inside the core region) is at Level 25.0 m, and the top edge (which is clearly seen from the central hall extending out of the core region) is at Level 43.0 m—which places the geometric center of Component E 5 m above its normal position before the accident.

The core region, rather unexpectedly, turned out to be practically empty. Lying in a pile on top of the northeastern upper face of Component OR and on both sides of Component KZh (in the space between the remains of Component KZh and Component L, and between the remains of Component KZh and the center of Component OR) are graphite blocks, eight MCCs oriented vertically and still connected to Component OR, and a reinforced concrete panel approximately 5 m wide (apparently also once forming part of the walls of Room 804/4) that is blocking from sight the northern "emergency alignment" support (Component NAS) resting at a sharp angle (≈70° from horizontal) while pressing MCCs into Component L. Lying horizontally in the southwest quadrant of Component OR are two reinforced concrete panels, one on top of the other, with dimensions approximately 1.2 by 35 by 1.0 m. On the northwest section of the upper face of Component OR is also a pile of graphite blocks, but these are covered somewhat with "fresh" concrete (that seeped in through the damaged wall of Room 804/4 during the construction of Shelter's Cascade Wall in the fall of 1986) approximately up to Level 16 m. A space of about 1 m between the bottom of Component L, the upper remains of Component KZh, and the layer of concrete on Component OR remains.

The southeast section of Component OR (roughly along the reactor central axes 47 and L) no longer exists.[14] It is clear that this section melted [together with its associated lower communications (coolant) channels (LCCs), stainless steel coolant pipes, and support structures]. Evidence to support this is located near the area where the section should be: visible metal structures are either partially melted or warped from heating, the part of Component OR to which its "melted" section should be attached shows signs of some burning and a melting process having taken place, and the top of the southern "emergency alignment" support for Component L (Component SAS) is tilted 15° toward Component OR and burned halfway through approximately in the middle.

Component OR descended approximately 4 m straight down from its normal position and thus crushed Component S beneath. On both sides it also crushed and pulled smoothly downward with itself the LCCs that now rest upon the corner of the upper cover for rooms 302/3 and 4, 303/3 and 4, and 304/3 and 4. Normally, the LCCs enter the space under the reactor (the upper space designated as the subreactor region, the lower space as room 305/2) horizontally from the reinforced "strong boxes" (rooms 404/3 and 4) that protect the group dispensing headers (GDHs). The LCCs that descend vertically from the GDHs before horizontally entering the subreactor region are relatively undamaged, and one may walk through rooms 404/3 and 4 (on top of concrete that seeped in during the construction of Shelter) as during a routine inspection. Component NAS (the northern alignment and support beam) remains in its normal position; in front of it (looking toward the center of Component OR), the lower section of the cylindrical

[a]The question of how pieces of these high-bay wall panels managed to fall to the bottom of the reactor shaft remains unanswered. One credible explanation is that hydrogen generated early during the accident may have accumulated and detonated in the steam-drum separator chambers—blowing parts of the wall in toward the central hall. Another hypothesis is that pressure waves from the steam explosion may have reflected into the steam-drum separator chambers along the water–steam coolant channel paths, also blowing out parts of the wall.

wall, Component KZh, descended together with Component OR and is more or less intact for 1.5 m vertically up to its first thermal expansion compensator.

Overview and Material Balance

Summary Descriptions of the FCMs.[12,15] By current estimates, between 1 270 and 1 350 tonnes of fuel-containing materials (FCMs) (material containing ≈10.5% of partially "burned" nuclear fuel), 64 000 m^3 of other radioactive material (concrete, building metal, etc.), approximately 10 000 tonnes of construction metal, and 800 to 1 000 tonnes of contaminated water are located within the sarcophagus.[16,17] Research conducted during 1987 to 1992 permits classification of the FCMs within the sarcophagus as follows:

1. *Fragments or chunks of destroyed core.* These include parts of destroyed TCs, fuel rods, control rods, graphite, etc., damaged and thrown out of the core shaft as a result of the explosions. The greater portions of these are currently located in the upper floors of the reactor building—in particular, in the central hall into which approximately 15 tonnes were thrown from the roof of the adjacent Auxiliary Building "V," where they were scattered by the explosions. Some pieces of the core (fuel and graphite) were found as far as 150 m from the reactor building and are now either covered with a thick layer of concrete or were collected and deposited into the reactor building's debris. On the scale of millimeters to centimeters, they remain more or less intact.

2. *Finely dispersed fuel particles (dust) or "hot" particles.* To a greater or lesser extent, these particles were distributed over the entire Unit 4 area and beyond the bounds of the station as a result of the explosions and fires that carried them into the atmosphere. They are observed in virtually every area or room of the reactor building—found on open surfaces, imbedded in concrete and other materials, or occurring as dust particles in the air. Dimensions of these particles vary in the range of 0.1 to 100 μ, and their total mass is estimated to be 10 tonnes.

3. *Solidified LFCMs or metallic fuel-containing materials (MFCMs).* These materials formed during the active phase of the accident (April 26 to May 6) as a result of a portion of the core melting and flowing downward along pipes and ducts into the lower regions of the reactor building and the interaction of this "lava" with surrounding metal and concrete structures. The LFCMs are characterized as glass-like or pumice-like siliceous substances containing varying amounts of fuel and other materials of the reactor, including metallic alloys. The MFCMs are in the form of a one-to-several-centimeter layer of solidified and highly radioactive metal (composed of fission-product metals and structural steel) underneath the LFCMs located mainly in the steam distribution corridor.

4. *Contaminated water.* In 1990, it was observed that water located in a number of rooms on several floors under the former reactor [in particular, in the pressure suppression pool (PSP)] contained various quantities of dissolved uranium. Water apparently enters Shelter through the above-mentioned openings and flows into the lower regions where most of the fuel is located. There, both as a result of a slow weakening and breakup of surface layers of LFCMs from high radiation exposure and the subsequent washing away of this newly formed dust by water, the water becomes enriched in uranium. The concentration of uranium is low, varying in the range of several milligrams per liter, yielding an estimated quantity of fuel in water of less than 2 kg.

Quantities and Locations of LFCMs. During the period from the middle of 1987 through the beginning of 1990, the method used most often to determine the location and quantity of LFCMs within the sarcophagus was remote thermographic analysis (thermography). This technique permitted a thermal survey of areas with extremely high levels of radiation greater than 2000 R/h that were also heavily damaged or covered with concrete, which makes access dangerous and nearly impossible for researchers, such as room 305/2, which is directly under Component OR and the subreactor region; and it led to the discovery in these areas of substantial quantities of LFCMs. Furthermore, after determining the location of LFCM accumulations, researchers could estimate the quantity of material by assuming that the source's heat flux (coming through debris and concrete) was directly related to the mass of material found underneath or behind the rubble. This was confirmed by measuring the speed of convective currents of air induced by heat fluxes in areas where the geometry of the surroundings could be well established. Therefore, on the basis of peripheral measurements of heat flux in relatively low areas of radiation and relatively accessible areas of the reactor building, researchers succeeded in estimating quantities of highly radioactive materials buried within the sarcophagus.

In 1989, with the help of heat flux gages mounted on long wands, a survey was conducted from the ceiling of the second floor of the PSP to determine the heat flux from sources above. More than 100 measurements were

taken that permitted the examination not only of this area but also of a number of areas with moderately high but accessible radiation fields between the steam distribution corridor and the subreactor region. Calculations showed that in January 1990 the total LFCM heat generated in the steam distribution corridor was approximately 17 kW(t). Knowing fairly well the amount of decay heat generated per tonne of UO_2 corrected to that time, researchers estimated that this area contained 23 ± 8 tonnes of UO_2. Similarly, in July 1989 the heat generated in room 305/2, the subreactor region, was approximately 60 kW(t) (by far the strongest source found), yielding 75 ± 25 tonnes of UO_2. In this area, even though it is virtually inaccessible, a convection geometry could be quite well established because heated air currents were constrained to exit through the reactor shaft upward into the central hall—thus aiding in the estimation of fuel mass. The balance of the fuel on the fourth floor is located in two corridors (301/5 and 301/6) and one room (304/3), and the total amount of fuel on this level is 95.7 ± 26 tonnes.

Because the PSP was more accessible than other areas, dimensional estimates from photographs, dose-rate measurements, and analysis of samples of LFCMs found there in open "piles" (to determine their radiochemical compositions and densities—see Fig. 10) aided researchers in estimating volumes, fuel content, and thus heat generation more precisely than in other areas. LFCMs were also known to be located in the pipes designed to direct steam downward to lower levels of the PSP. Although the geometry of these pipes is well

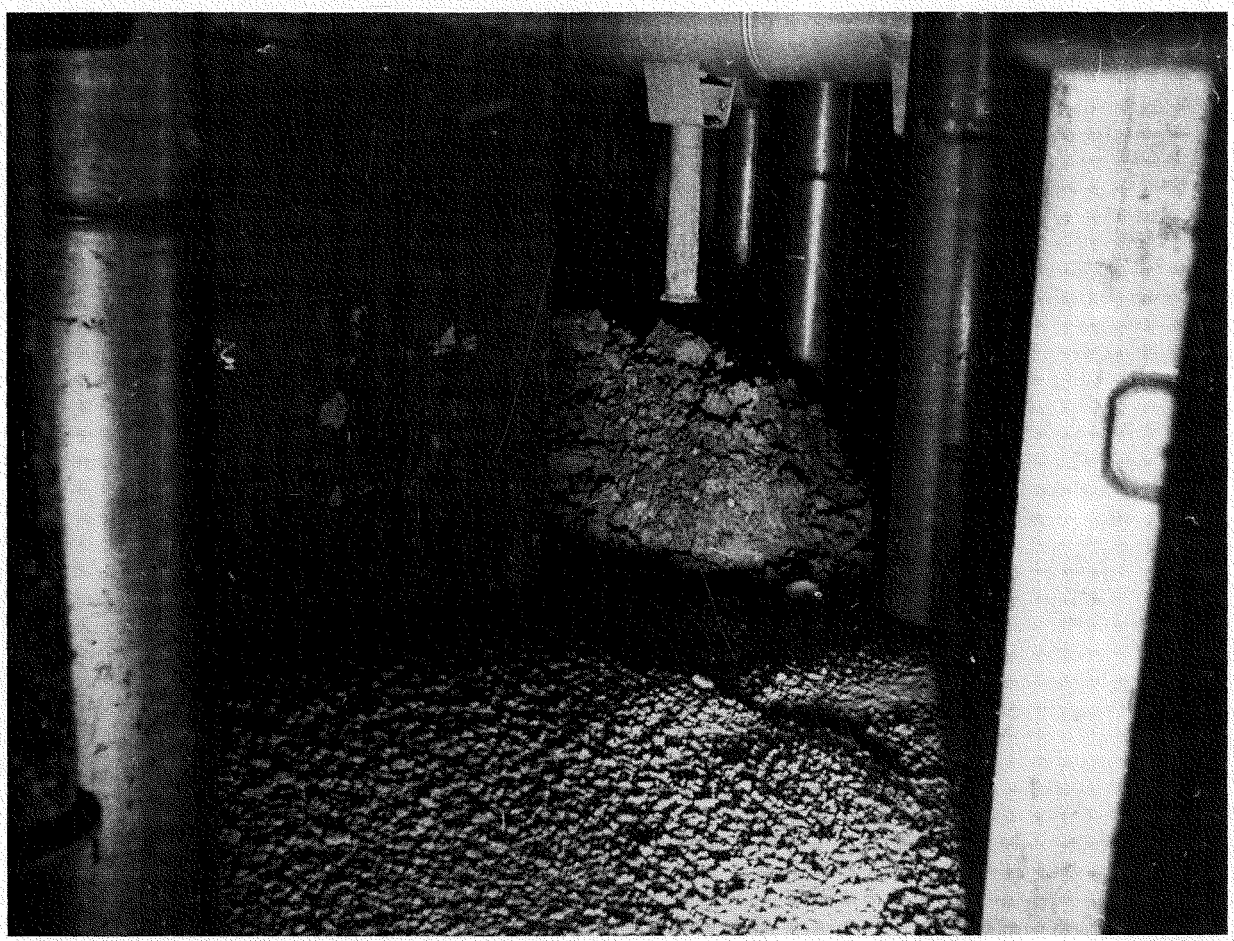

Fig. 10 Photograph taken on the second floor of the pressure suppression pool showing a pumice-like formation of nuclear fuel. Concrete poured into the reactor building during construction of the sarcophagus is visible in the foreground. (Photograph courtesy of Konstantin Pavlovich Checherov of the Inter-Branch Scientific and Technical Center "Shelter.")

known, it was not certain how and to what extent LFCMs were distributed within them. A remote-controlled collimated gamma detector was used to identify which pipes contained LFCMs along with their approximate distributions. The gamma detector also helped to define the gamma fields throughout the PSP so that dose measurements could be attributed to specific piles of LFCMs. As a result of these efforts, five pipes were identified to be the "flow paths" into LFCM piles and into rooms 012/6 and 012/14. It was also found that they were completely filled with LFCM; the total volume was 5.7 m^3. If the assumption is made that the pipes contain UO_2 in amounts similar to their associated piles, a good estimation could be made. Finally, thermography had to be used to locate and estimate the significant amount of fuel covered by concrete. The amount of fuel in the LFCMs of the PSP is estimated to be 12.5 ± 3 tonnes distributed, as shown in Table 1.

Smaller, but no less significant, quantities of LFCMs were located in various other areas. Three steam distribution headers in the steam distribution corridor (see Fig. 7) were found to contain a total of 1.8 ± 0.6 tonnes of fuel. Together with the fuel content of stalactite- and stalagmite-like LFCM formations (such as the well-known Elephant's Foot—see Figs. 11 and 12), the total amount of UO_2 located in these third-floor areas is 20 ± 5 tonnes distributed, as shown in Table 1.

The amount of fuel distributed throughout the upper levels of the reactor building is more difficult to establish,

Table 1 Chornobyl Unit 4 Fuel Distribution and Mass Balance[a]

Location and description	Fuel mass subtotal, tonne	Fuel mass total, tonne
Upper levels of the reactor building (level ≥35.5 m)		37.7 ± 5 + ?
Central hall (estimate of core fragments)	15	
Central hall (hot particles and dust)	5 ± 2	
Central hall (under pile of materials thrown from helicopters)	?	
Core fragments attached to UBS	5 ± 3	
Steam separator drum areas	2 ± 1	
Other areas above reactor	5	
Fragments within the cascade wall of the sarcophagus	1.9	
Turbogenerator hall (estimate of core fragments)	1.9	
Fuel fragments beyond reactor building but under concrete	1.9	
4th floor—subreactor region (level 9.0 m)		95.7 ± 26
Core fragments scattered upon the LBS	0.5 ± 0.2	
Subreactor region (room 305/2)	75 ± 25	
Room 304/3	14 ± 5	
Room 303/3	0.2 ± 0.1	
Corridor 301/5	3 ± 1	
Corridor 301/6	3 ± 1	
3rd floor—steam distribution corridor (level 6.0 m)		27 ± 8
Steam distribution headers (3 units)	1.8 ± 0.6	
Steam distribution corridor (rooms 210/5, 210/6, 210/7)	23 ± 8	
Corridor 217/2 (stalactites)	0.2 ± 0.1	
Corridor 217/2 ("Elephant's Foot")	2 ± 0.8	
1st and 2nd floors—pressure suppression (levels 0.0 and 3.0 m)		12.5 ± 3
PSP—(2nd floor)	(11 ± 3)	
Open "piles"	6 ± 1	
Piles covered by concrete or in piping	5 ± 3	
PSP—(1st floor)	(1.5 ± 0.5)	
Open piles	0.9 ± 0.2	
Piles covered by concrete or in piping	0.6 ± 0.5	
Total fuel contained within reactor building		172.9 ± 28 (?)
Fuel released beyond the Chornobyl station (3.5 ± 0.5%)		6.7 ± 1
Total core load at time of accident		190.3
Fuel unaccounted for		>10.7 (?)

[a]Source: Ref. 4, pp. 12-17, 37-42; Ref. 15, pp. 12-17.

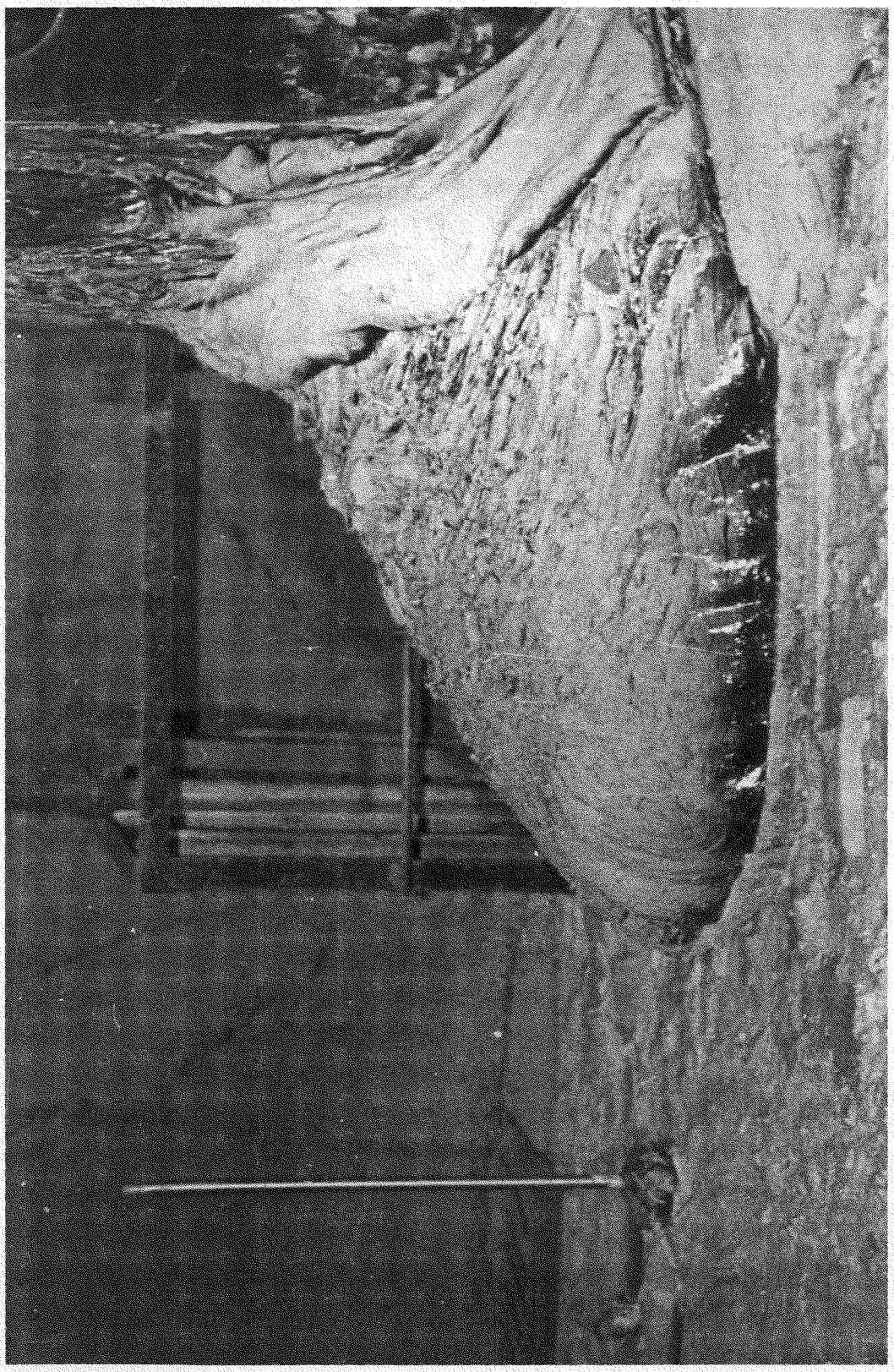

Fig. 11 Photograph of the 2-tonne accumulation of melted nuclear fuel dubbed the "Elephant's Foot." (Photograph courtesy of Aleksandr Aleksandrovich Borovoi of the Inter-Branch Scientific and Technical Center "Shelter.")

Fig. 12 Photograph of a nuclear fuel stalactite located near the southern end of Corridor 217/2. (Photograph courtesy of Aleksandr Aleksandrovich Borovoi of the Inter-Branch Scientific and Technical Center "Shelter.")

although attempts have been made; for example, the amount of fuel contained in hot particles impregnated in walls and other materials or that eventually settled out throughout the building was estimated roughly by taking swipe-samples in various locations of the reactor building (to determine the amount of fuel deposition per unit area) and multiplying by an estimate of the total amount of area available for deposition. Core fragments (graphite blocks and fuel assemblies) were counted from photographs taken before the cleanup efforts began. It is clear that, because researchers could not enter the extremely hazardous environment of the destroyed reactor building to locate more precisely fragments of the core, these estimates introduce large errors into the mass balance.

The core mass balance shown in Table 1 also presents another problem. If we assume that the Soviet value of $3.5 \pm 0.5\%$ of the core's 190.3-tonne fuel load at the time of the accident (or 6.7 ± 1 tonne) was released beyond the bounds of the station, this leaves approximately 11 tonnes of the core UO_2 fuel mass unaccounted for. Because of the rather imprecise mass estimates in Table 1, however, the "missing" fuel falls well within the total estimate's error margin. Another possibility is that the fuel could be located under the pile of debris thrown from the helicopters during the first 6 days of the accident.[a] To date, researchers have not been able to verify what may be under the material pile in the central hall because the extreme radiation environment and building structural debris make this area inaccessible for drilling equipment.[b] A final possibility is that part of the fuel may have been jammed upward through the UCCs into the upper biological shield (UBS) by the initial explosions. With the use of a finely collimated gamma spectrometer to survey the central hall in 1990, researchers noted a large source in the center of the UBS—leading them to speculate that LFCMs may be within it; however, significant plateout on the surface of the UBS during the active phase could also give rise to the observed source.

Several lower-bound estimates of the amount of fuel located in the lower regions of the reactor building have been made. [Recall that Table 1 shows that 135.2 ± 27.4 tonnes of fuel are located below the nominal core position (i.e., in the lower regions of the reactor building).] A rather rough lower-bound estimate of 90 tonnes is obtained by considering that 35% of the initial core inventory of Cs-137 remains within the fuel in the lower regions of the sarcophagus.[18] Another rough lower-bound estimate of 60 tonnes considers the amount of magnesium initially contained within the LBS (as part of the mineral serpentine) that was taken up by the corium lava as it melted through the LBS.[18,19] Finally, a group of researchers attempted to estimate the amount of fuel in the lower regions of the reactor building by using density measurements and *visually* estimating the volume of lava; however, their estimate of 22.8 to 32.7 tonnes[20] has been convincingly refuted by other researchers at Chornobyl who point to the wide range of LFCM densities (from 0.14 g/cm^3 for the pumice-like form of the corium to 3.2 g/cm^3 for ceramic glass-like forms), to the fact that "chunks" of graphite blocks and fuel assemblies are found in some accumulations of the lava, which drastically alters density estimates, and to the incorrect volume estimates of the very significant lava accumulations located under fresh concrete.[18,21–23]

Classification of the LFCMs. This section provides summarized information and data pertinent to the current discussion and for the next article in this series. For a more detailed and rigorous account of the chemistry of the LFCMs, see Ref. 24. Part of the fuel, having melted from a combination of decay heat and chemical interactions with surrounding materials, formed peculiar lava-like flows that entered various areas of the reactor building beneath the core. Figure 13 is a flow schematic for the LFCMs located in the lower regions of the reactor building that includes the locations and mass transfer mechanisms thought to be responsible for the current configuration. These LFCMs were studied for their chemical, isotopic, and mineral content along with the fraction of fuel contained and burnup. As solid, heterogeneous solutions in a silicate glass-like matrix, they may be classified into four distinct types.

---

[a]The material thrown from the helicopters was aimed at a "red, glowing mass" obscured by smoke and debris (i.e., it was never positively identified what could be "burning" at that location—although it was assumed that part of the core graphite was responsible for the glow). Because the roof of Unit 4 was covered with a large amount of tar, an argument has been put forth that it wasn't graphite that was seen burning (producing the red glow) but rather a large quantity of tar (bitumen) that collapsed into the central hall together with the roof. However, considering the fact that the building's roof and high bay walls were swept outward with the explosion's pressure wave, this hypothesis appears less plausible.

[b]Sharovarov states, "From the existing balance we know that the full quantity of fuel which remains within Shelter accounts for 96.5% [~183.6 te ?] of the original load [of 190.3 te], in other words 180 t of heavy metal. Our appraisals of visible accumulations of FCM gives 150 t. The remaining 30 t could be found in the Central Hall (~15 t), under the northern Cascade Wall, and also in a number of as yet uninvestigated areas of the upper parts of Unit-4" (from Ref. 4, p. 25).

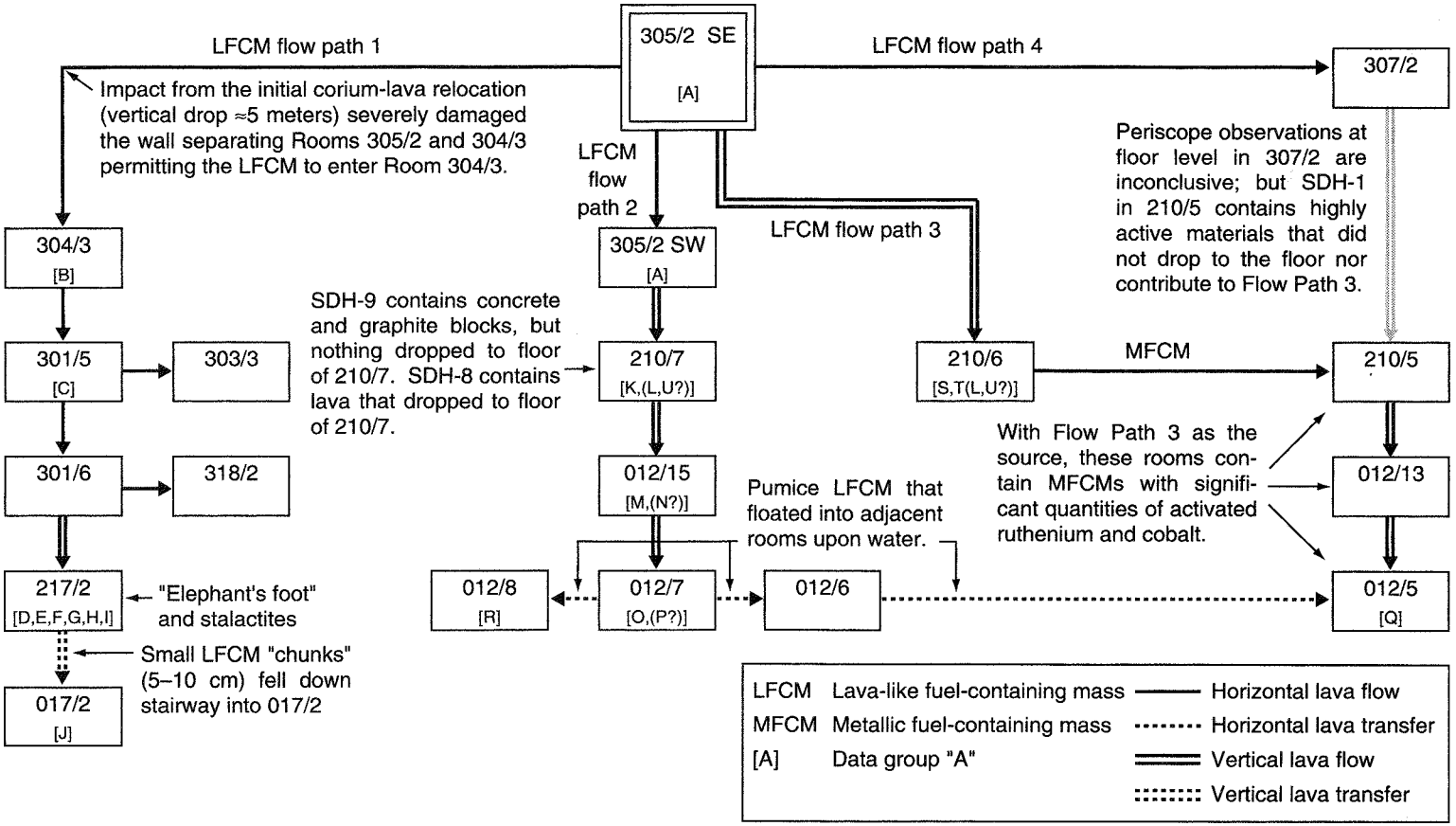

Fig. 13 Lava-like fuel-containing material flow schematic. SW is southwest and SE is southeast.

1. *LFCM1.* LFCM1 is a chocolate-brown or anthracite-black ceramic (glass-like) having a density of 2.2 to 2.3 g/cm^3 and represented by stalactite-like and stalagmite-like formations in corridor 217/2 (including the Elephant's Foot) or by accumulations in the steam distribution corridor and in the subreactor region (room 305/2). The optical refractive index is in the range of 1.45 to 1.6, and the melting temperature is approximately 1200 °C.

The chocolate-brown ceramic [mainly located along Flow Path 2 (see Fig. 12)] is brittle and at least at the surface contains many pores of varying diameters. It also contains large quantities of miniature metallic spheres, which give it its characteristic color. (At the microscopic level, the silicate matrix is transparent with a smoky–yellowish tint.) The surface is mainly lustrous, although some samples have a more matted shade of brown. It is found in all cases as an upper layer over a thin layer of previously melted and highly active metal—somewhat resembling a thick layer of impurities in high-temperature metallurgical smelting processes.

The anthracite-black ceramic (mainly located along Flow Path 1) in most cases has a matted hue with a great quantity of rather large voids averaging 1500 cm^3 in volume, which make its bulk density low. At the microscopic level, its silicate matrix is transparent with a dark "bottle-green" tint. This form of LFCM1 is most often observed near the southeast quadrant of the subreactor region (room 305/2) and in room 304/3 and resembles coke from a steel smelting process. In a fewer number of cases that are located significantly far from room 305/2 (in the form of stalactites and the Elephant's Foot in Corridor 217/2), the surface of this ceramic has a lustrous hue.

2. *LFCM2.* LFCM2 is a gray–brown, crumbly, pumice-like material discovered in the PSP area of the reactor building almost directly below the nominal position of the core. It is assumed that this material was formed when the high-temperature lava contacted the remaining water in the PSP. Interestingly, adhering to the walls and pipes of the first floor of the PSP about 30 to 40 cm above the floor are several "bathtub ring" formations of this type of the LFCM. It is presumed that, because of its low density (varying tightly around 0.14 g/cm^3), it was at one time floating on the surface of the water and was thus transported away from the main pile in room 012/7.[a]

3. *LFCM3.* LFCM3 is a red–brown or flat-black slag-like material (an intermediate formation between a ceramic and a pumice), some of which is found in the subreactor region but mainly in the PSP, where its has formed piles of corium characteristic of that area of the reactor building.

4. *LFCM4.* LFCM4 is melted metal discovered in two forms: (l) as a lower layer beneath the chocolate-brown LFCM1 in the subreactor region and (2) in the form of small (from 1 μm to several millimeters) droplets distributed in all other LFCM forms. (Strictly speaking, the first form is not considered an LFCM because it does not seem to contain a significant amount of fuel but does contain enough fission products to make it highly radioactive.)

Analyses of the LFCMs. According to Table 1, the total amount of fuel contained within the LFCMs currently located below Component OR is approximately 135 ± 30 tonnes. The corresponding mass of the LFCMs is 1370 ± 300 tonnes.[b,17] On the macroscopic or bulk level, the LFCMs are quite varied in their morphologies and densities—the density of a given LFCM is a strong function of the void content within the solid solution. The density of the solid solution also varies greatly, depending on the type of LFCM and its location with the reactor building; for example, the matte-black LFCM1 found in room 304/3 (reaching a thickness of 1 m) varies even throughout the bulk of the material and thus forms three layers based on density and void content (Table 2).

The chemical compositions of the LFCMs also varied, depending on their type and locations. There were also variations within the matrix as well as in the dissolved constituents; for example, visual examination with a

[a]Water remained on the first level of the PSP (even though the PSP was emptied before the end of the active phase) because the openings to the drain pipes are located on the walls about 30 cm above the floor. The pool, therefore, could not be completely drained.

[b]According to Pantikov et al.,[17] of this, 137 ± 30 tonnes is attributed to core structural materials (stainless steel and zirconium); 266 ± 60 tonnes is serpentine from Component OR, including the thermal compensator region; and 350 ± 50 tonnes is concrete from the floor of room 305/2, which interacted with the lava just before it solidified. The balance (442 ± 130 tonnes) could be materials dumped during accident mitigation efforts (including the construction of the sarcophagus). However, this does not make sense given that few, if any, of the materials thrown onto the core during the active phase made it into the core. Moreover, during the construction of the sarcophagus, it is difficult to imagine any interaction of the solidified corium with concrete and other structural materials. If true, however, the 442 tonnes would still represent less than 9% of the materials dumped from the helicopters—and this is not in agreement with the results of radiochemical analyses of the corium, which appear to indicate not more than 1% of the dumped materials may have entered the reactor shaft to cover the core.

Table 2 Density Variation of LFCMs in Several Locations[a]

LFCM type	Location	Room	Density, g/cm³
Black ceramic—upper layer	Level 9m	304/3	0.7 to 0.9
Black ceramic—middle layer	Level 9m	304/3	0.9 to 1.8
Black ceramic—lower layer	Level 9m	304/3	1.8 to 2.4
Brown ceramic	Steam distribution corridor	210/7	Up to 3.15
Black ceramic	Steam distribution corridor	210/7	1.6 to 2.8
Black ceramic	Steam distribution corridor	210/6	Up to 2.9
Black ceramic	Steam distribution corridor	210/6	2.0 ± 0.2
Black ceramic	PSP-2	012/15	2.1 ± 0.2
Pumice	PSP-1	012/7	0.14 to 0.18

[a]Source: Ref. 18, p. 6.

light-microscope shows that the matrix of the chocolate-brown or anthracite-black ceramic LFCM1s and the slag-like LFCM3s are a silicate-like glass with complex morphological features filled with inclusions of varied size. A scanning electron microscope reveals that the solid-phase inclusions are on the average 0.5 μm in diameter; ultrasonic microanalysis provided the chemical makeup of the silicates and inclusions. The colors of the lavas are defined by the varying amounts of inclusion dispersed throughout (primarily by thinly dispersed yellow–brown inclusions) as well as by the amount of iron contained in the matrix. Table 3 shows the silicate matrix chemical composition (average) of several forms of LFCM1; Table 4 shows the bulk chemical composition (average) of LFCM1-3 along with various ratios for comparison.

The fuel content in these materials varies from a few weight percent to approximately 18 wt %, and the average is around 7 wt % (Table 5). Fuel burnup in the LFCMs varies from 7.5 to 14.7 MWd/kgU; the average is 11.7 MWd/kgU. The burnup values are distributed evenly over all forms and locations of the LFCMs, which appears to indicate that *there was intense and thorough mixing of core materials* sometime before the lava flowed into the lower regions of the reactor building to cool and solidify. (This is an important conclusion when, in an upcoming article, a scenario is hypothesized for the active phase.) Tables 5 and 6 (following the flow distribution scheme of Fig. 12) summarize the results of radiochemical analyses of 118 samples of the LFCMs from various locations, whereas Table 7 presents a summary comparison of another approximately 110 samples showing the ratios of Cs-137 and Ru-106 to Ce-144.

DISCUSSION AND CONCLUSIONS

The consequences of the accident were intimately related to the specific design features of the second-generation RBMK-1000 represented by Chornobyl Unit 4 and to surrounding conditions in the vicinity of the core

Table 3 Chemical Compound Composition of the LFCM1 Silicate Matrix[a,b] (Weight Percent of Total)

LFCM type	K_2O	CaO	MgO	Al_2O_3	ZrO_2	Fe_2O_3	U	Sum	[SiO_2 + O]
LFCM from 210/7 chocolate-brown ceramic	1.5	6.8	5.8	5.2	3.2	—	2.4	24.9	[75.1]
LFCM from 210/6 coal-black ceramic	1.7	7.2	4.9	5.3	2.8	8.6	2.1	32.6	[67.4]
LFCM from 217/2 "Elephant's Foot" ceramic	1.7	7.2	1.9	5.1	4.5	—	4.0	24.4	[75.6]
Average	1.6	7.1	4.2	5.2	3.5	(8.6)	2.8	(27.3)	[(72.7)]

[a]Source: Ref. 18, p. 14.

[b]Uranium content is given for all its oxide forms minus the oxygen. Note the lack of boron, carbon, or lead. In addition, although not reflected in the tables, the silicate matrix also contains small (diameter, <0.1 mm) granules of graphite.

Table 4 Elemental Composition of Bulk LFCMs (Weight Percent of 75 Samples, 15 to 20% Error)[a]

	LFCM type	B (5)	Na (11)	Mg (12)	Al (13)	Si (14)	Ca (20)	Ti (22)	Cr (24)	Mn (25)	Fe (26)	Ni (28)	Cu (29)	Zr (40)	Ba (56)	Pb (82)	Sum[b]
1	LFCM1 coal-black ceramic	0.041	4.2	2.4	4.8	29.8	5.5	0.11	0.18	0.32	1.40	0.14	0.0045	3.2	0.12	0.0065	52.22
2	LFCM1 chocolate-brown ceramic	0.072	4.0	4.0	3.5	30.9	4.7	0.11	0.20	0.52	0.84	0.18	0.0018	4.8	0.18	0.0012	54.01
3	LFCM2 suppression pool pumice	0.073	1.4	4.6	2.8	35.6	4.8	0.19	0.18	0.50	1.20	0.30	0.0018	3.3	0.15	0.012	55.11
4	LFCM3 suppression pool slag	0.052	1.5	6.2	3.4	32.3	4.0	0.14	0.18	0.38	0.82	0.26	0.0015	4.5	0.15	0.11	54.00
5	LFCM3 chocolate-brown ceramic (intermediate)	0.068	—	5.0	3.3	32.7	4.5	0.15	0.22	0.46	0.83	0.27	—	4.3	0.16	—	51.96
	Overall average	0.061	2.8	4.4	3.6	32.3	4.7	0.14	0.19	0.44	1.02	0.23	0.0024	4.0	0.15	0.032	54.07
	Row 1/Row 2	0.57	1.1	0.60	1.4	0.96	1.2	1.00	0.90	0.62	1.7	0.78	2.5	0.67	0.67	5.4	0.97
	Row 1/Row 3	0.56	3.0	0.52	1.7	0.84	1.1	0.58	1.0	0.64	1.2	0.47	2.5	0.97	0.80	0.54	0.95
	Row 1/Row 4	0.79	2.8	0.39	1.4	0.92	1.4	0.79	1.0	0.84	1.7	0.54	3.0	0.71	0.80	0.059	0.97
	Row 1/Row 5	0.60	—	0.48	1.5	0.91	1.2	0.73	0.82	0.70	1.7	0.52	—	0.74	0.75	—	1.01

[a]Source: Ref. 18, pp. 8-11.

[b]The content of these elements is given without the oxygen of their associated oxide forms [i.e., oxygen accounts for the approximately 45% (weight) balance].

Table 5 Statistical Summary of FCM Radiochemical Data (Total of 118 Samples, Corrected to End of Active Phase—May 6, 1986)

Data group	Number of samples	Location	Burnup, MWd/kgU	Calculated UO_2, w/o	Measured UO_2, w/o	Ratio of measured to calculated		Cs-134/Cs-137
						Cs-137 A_m/A_c	Ru-106 A_m/A_c	
A.1	3	Subreactor region (305/2)	11.89 ± 0.48	5.15 ± 0.97	5.26 ± 0.88	0.28 ± 0.13	0.087 ± 0.053	0.57 ± 0.02
B.1	23	Room 304/3	11.37 ± 0.39	4.01 ± 0.64	4.44 ± 0.50	0.34 ± 0.10	0.033 ± 0.022	0.55 ± 0.02
C.1	11	Corridor 301/5	11.55 ± 0.38	3.49 ± 0.59	4.20 ± 0.99	0.36 ± 0.06	0.038 ± 0.017	0.56 ± 0.02
D.1	1	Corridor 217/2 (undefined)	12.02 ± 3.47	4.26 ± 2.06	4.30 ± 2.07	0.33 ± 0.58	0.050 ± 0.224	0.58 ± 0.76
E.1	2	Corridor 217/2 (Elephant's 1)	10.57 ± 0.38	5.00 ± 0.31	5.33 ± 0.03	0.42 ± 0.04	0.040 ± 0.010	0.52 ± 0.02
F.1	9	Corridor 217/2 (stalactite 1)	11.70 ± 0.32	4.67 ± 0.36	4.66 ± 0.31	0.35 ± 0.06	0.040 ± 0.023	0.56 ± 0.01
G.1	5	Corridor 217/2 (stalactite 2)	11.62 ± 0.45	4.74 ± 0.39	4.78 ± 0.39	0.43 ± 0.05	0.038 ± 0.029	0.56 ± 0.02
H.1	2	Corridor 217/2 (Elephant's 2)	11.99 ± 0.61	4.48 ± 0.69	4.61 ± 0.22	0.35 ± 0.06	0.035 ± 0.015	0.58 ± 0.03
I.1	2	Corridor 217/2 (undefined)	11.32 ± 0.05	3.99 ± 0.03	4.38 ± 0.19	0.41 ± 0.01	0.020 ± 0.000	0.55 ± 0.00
J.1	3	Corridor 017/2	11.77 ± 0.44	4.96 ± 0.18	5.00 ± 0.18	0.34 ± 0.05	0.020 ± 0.008	0.57 ± 0.02
K.1	20	Steam distribution corridor (210/7)	11.82 ± 0.67	10.2 ± 1.10	9.86 ± 1.05	0.32 ± 0.11	0.042 ± 0.028	0.57 ± 0.03
L.1	1	Steam distribution corridor (undefined)	11.77 ± 3.43	5.12 ± 2.26	7.49 ± 2.74	0.68 ± 0.83	0.360 ± 0.600	0.57 ± 0.76
M.1	8	PSP 2 (012/15)	11.68 ± 0.35	9.59 ± 1.38	9.93 ± 1.15	0.35 ± 0.09	0.045 ± 0.026	0.56 ± 0.02
N.1	2	PSP 2 (undefined)	12.84 ± 0.38	11.5 ± 1.78	11.25 ± 0.25	0.34 ± 0.01	0.040 ± 0.000	0.62 ± 0.02
O.1	8	PSP 1 (012/7)	11.85 ± 0.34	9.75 ± 0.83	9.93 ± 0.76	0.32 ± 0.03	0.040 ± 0.019	0.57 ± 0.02
P.1	2	PSP 1 (undefined)	11.38 ± 0.41	10.20 ± 0.30	14.20 ± 4.20	0.31 ± 0.00	0.040 ± 0.010	0.55 ± 0.02
Q.1	1	PSP 1 (012/5)	11.53 ± 3.40	10.44 ± 3.23	8.90 ± 2.98	0.18 ± 0.42	0.030 ± 0.173	0.56 ± 0.75
R.1	1	PSP 1 (012/8)	11.59 ± 3.40	10.14 ± 3.18	8.16 ± 2.86	0.23 ± 0.48	0.030 ± 0.173	0.56 ± 0.75
S.1	10	Steam distribution corridor (210/6)	12.16 ± 0.49	6.26 ± 1.54	6.39 ± 1.30	0.48 ± 0.11	0.107 ± 0.041	0.58 ± 0.02
T.1	1	PSP 1 (012/6)	10.98 ± 3.31	9.05 ± 3.01	8.61 ± 2.93	0.16 ± 0.40	0.030 ± 0.173	0.53 ± 0.73
U.1	3	Steam distribution corridor (undefined)	11.08 ± 0.73	6.90 ± 1.38	5.81 ± 0.48	0.26 ± 0.06	0.053 ± 0.037	0.54 ± 0.03
$\langle x \rangle \pm s$			11.66 ± 0.65	6.59 ± 2.88	6.78 ± 2.81	0.35 ± 0.11	0.049 ± 0.046	0.56 ± 0.024

Table 6 Statistical Summary of FCM Radiochemical Data (Total of 118 Samples, corrected to End of Active Phase—May 6, 1986)

	α (specific activity)					γ (specific activity)						β (specific activity)
Data group	Pu-238, Bq/g × 10^5	Pu-239+240, Bq/g × 10^5	Am-241, Bq/g × 10^5	Cm-242, Bq/g × 10^7	Cm-244, Bq/g × 10^5	Ce-144, Bq/g × 10^9	Cs-137, Bq/g × 10^7	Cs-134, Bq/g × 10^7	Eu-155, Bq/g × 10^6	Ru-106, Bq/g × 10^7	Sb-125, Bq/g × 10^6	Sr-90, Bq/g × 10^7
A.2	3.84 ± 0.58	7.29 ± 0.65	1.25 ± 0.17	1.72 ± 0.27	0.98 ± 0.17	1.34 ± 0.25	2.52 ± 0.14	1.44 ± 0.81	2.69 ± 0.66	3.72 ± 2.48	0.16 ± 0.40	
B.2	3.82 ± 0.77	7.92 ± 1.93	2.56 ± 1.71	1.77 ± 0.76	1.17 ± 0.32	1.06 ± 0.15	2.26 ± 0.68	1.24 ± 0.37	3.40 ± 1.39	1.11 ± 0.87	1.46 ± 1.44	7.59 ± 0.84
C.2	4.14 ± 0.77	7.82 ± 1.46	2.98 ± 2.02	3.48 ± 1.76	1.73 ± 1.66	0.90 ± 0.15	2.06 ± 0.55	1.15 ± 0.30	1.64 ± 0.01	0.95 ± 0.50		5.64 ± 1.96
D.2	4.72 ± 0.01	7.84 ± 0.01	1.11 ± 0.01	2.58 ± 0.01	0.77 ± 0.01	1.11 ± 0.01	2.30 ± 0.01	1.33 ± 0.01		1.67 ± 0.01		
E.2	5.30 ± 0.01	9.70 ± 0.01	1.44 ± 0.01	1.90 ± 0.01	1.20 ± 0.01	1.27 ± 0.09	3.27 ± 0.07	1.68 ± 0.02	1.91 ± 0.01	1.43 ± 0.47		
F.2	3.93 ± 0.71	9.38 ± 2.12	1.34 ± 0.16	0.99 ± 0.40	1.22 ± 0.24	1.21 ± 0.09	2.64 ± 0.44	1.48 ± 0.23	1.96 ± 0.30	1.38 ± 0.67	3.80 ± 1.01	
G.2	4.26 ± 0.70	9.34 ± 1.99	1.35 ± 0.21	1.19 ± 0.67	1.06 ± 0.17	1.23 ± 0.11	3.32 ± 0.64	1.87 ± 0.43	2.41 ± 0.52	1.40 ± 1.19	4.00 ± 0.25	
H.2	4.38 ± 0.31	7.23 ± 0.63	0.60 ± 0.27	1.75 ± 0.13	0.81 ± 0.05	1.17 ± 0.19	2.45 ± 0.01	1.41 ± 0.07		1.18 ± 0.71		5.93 ± 0.52
I.2	4.76 ± 0.75	7.18 ± 0.52	0.67 ± 0.04	1.99 ± 0.04	0.74 ± 0.09	1.03 ± 0.01	2.59 ± 0.01	1.42 ± 0.00		0.56 ± 0.06		
J.2	4.31 ± 0.89	13.28 ± 3.02	1.43 ± 0.09	1.20 ± 0.36	1.47 ± 0.11	1.29 ± 0.05	2.72 ± 0.41	1.55 ± 0.27	2.68 ± 0.28	0.75 ± 0.26	4.52 ± 1.21	
K.2	9.02 ± 1.30	20.80 ± 4.56	2.98 ± 1.01	3.11 ± 0.92	1.87 ± 0.97	2.65 ± 0.31	5.20 ± 1.83	2.98 ± 1.11	5.67 ± 2.57	2.98 ± 1.06	5.49 ± 3.19	8.15 ± 0.91
L.2	6.28 ± 0.01	11.29 ± 0.01	1.35 ± 0.01	3.51 ± 0.01	1.49 ± 0.01	1.33 ± 0.01	5.60 ± 0.01	3.17 ± 0.01		14.26 ± 0.01		
M.2	8.95 ± 0.88	19.46 ± 5.61	4.79 ± 3.03	4.43 ± 2.40	2.18 ± 0.83	2.49 ± 0.36	5.26 ± 1.01	2.96 ± 0.57	4.21 ± 0.50	3.05 ± 1.26	7.55 ± 2.18	15.20 ± 1.66
N.2		13.30 ± 0.01			4.42 ± 0.01	3.02 ± 0.46	6.32 ± 0.83	3.85 ± 0.41		3.19 ± 0.51		
O.2	9.02 ± 1.33	19.61 ± 4.06	4.30 ± 2.96	4.04 ± 1.81	2.40 ± 0.50	2.54 ± 0.22	5.06 ± 0.62	2.89 ± 0.37	4.30 ± 0.31	3.02 ± 1.27	6.53 ± 0.87	15.30 ± 1.14
P.2	9.08 ± 0.01	17.52 ± 0.01		2.92 ± 0.01	2.11 ± 0.01	2.64 ± 0.01	5.06 ± 0.18	2.79 ± 0.19		3.16 ± 0.54		
Q.2	8.28 ± 0.01	15.38 ± 0.01	3.24 ± 0.01	3.62 ± 0.01	1.64 ± 0.01	2.71 ± 0.01	3.07 ± 0.01	1.71 ± 0.01	16.63 ± 0.01	2.11 ± 0.01	0.54 ± 0.01	
R.2	8.34 ± 0.01	15.62 ± 0.01	4.35 ± 0.01	3.75 ± 0.01	2.04 ± 0.01	2.63 ± 0.01	3.78 ± 0.01	2.11 ± 0.01	15.09 ± 0.01	2.45 ± 0.01	0.58 ± 0.01	
S.2	6.73 ± 1.51	11.55 ± 2.45	2.95 ± 1.04	3.05 ± 1.22	1.06 ± 0.67	1.64 ± 0.40	4.80 ± 1.27	2.81 ± 0.75	5.70 ± 2.00	4.87 ± 1.84	0.77 ± 0.11	8.09 ± 1.21
T.2	7.49 ± 0.01	14.06 ± 0.01	3.38 ± 0.01	3.40 ± 0.01	1.73 ± 0.01	2.32 ± 0.01	2.31 ± 0.01	1.23 ± 0.01	12.77 ± 0.01	1.88 ± 0.01	0.44 ± 0.01	
U.2	5.61 ± 1.16	10.04 ± 1.94	1.87 ± 0.75	1.82 ± 0.31	1.10 ± 0.18	1.77 ± 0.36	2.72 ± 0.44	1.47 ± 0.33	6.86 ± 3.06	2.78 ± 2.24	0.23 ± 0.04	
x ± s	6.02 ± 2.47	12.69 ± 6.16	2.68 ± 1.93	2.55 ± 1.59	1.49 ± 0.89	1.72 ± 0.75	3.64 ± 1.70	2.06 ± 1.01	4.56 ± 3.14	2.42 ± 2.19	3.71 ± 2.93	8.23 ± 3.19

Table 7 Comparison of Measured-to-Calculated Relative Quantities[a] of Cs-137, Ru-106, and Ce-144

Lava type	Measured Cs-137/ Ce-144	Calculated Cs-137/ Ce-144	Cs-137 measured/ calculated	Measured R-106/ Ce-144	Calculated R-106/ Ce-144	Ru-106 measured/ calculated
LFCM1 (≈50 samples) brown ceramic vertical flow	0.0216	0.0631	0.34	0.00978	0.295	0.033
LFCM1 (≈60 samples) black ceramic horizontal flow	0.0239	0.0631	0.38	0.0144	0.295	0.049
Average	0.0228	0.0631	0.36	0.012	0.295	0.041

[a]Reference 18, pg. 8.

during the active phase. Because the reactor had no containment, the release of fission products included an important component from the direct ejection of fuel by the explosion(s), whereas the chemical aspects of the later releases were determined by a chemically oxidizing environment dominated by the graphite fire.

Unfortunately, although 9 years have passed since the accident, relatively little quantifiable data are available on the state of the melted fuel remaining within the Chornobyl Unit 4 sarcophagus.[a] Some radiochemical data are available (parts of which are presented here), but much more need to be gathered to gain a clearer understanding of the processes that occurred during the active phase and, more important, to properly quantify the source term. Despite these challenges, however, some conclusions may be drawn from the data available.

The almost complete lack of lead and boron[b] in the radiochemical data strongly indicates that few, if any, of the bags of materials (thrown into the reactor building to smother the graphite fire)[25] made it into the core region. In the approximately 71% of the core's initial fuel load (135 tonnes) that flowed into the lower regions of the reactor building, approximately 0.01 wt % lead (averaged over the entire LFCMs volume) was found in the corium. This is very roughly 1 tonne (out of 2400 tonnes dumped from the helicopters), or about 0.1 m^3 of lead that may have entered the reactor shaft and reached the corium. Additionally, the fact that only trace amounts of carbon–graphite and no carbon compounds are found in the LFCMs seems to indicate not only that complete oxidation of the pulverized graphite moderator and reflector took place (at least the graphite that made up the remains of the core that settled to the bottom of the

[a]Until the dissolution of the U.S.S.R., the Soviet government was not particularly interested in a thorough scientific investigation of the active phase of the accident. Rather, its main concerns were to locate all the fuel within the sarcophagus; to ensure that criticality could not be reestablished under any plausible circumstances; to ensure that the other three operating units and their personnel were not affected significantly by Unit 4; and to monitor air, water, and soil samples in the region to ensure that the fuel (at least that contained within the sarcophagus) was not migrating into the environment. (It is interesting that the U.S. Department of Energy took a similar position with regard to detailed study of debris from the Three Mile Island core.) These concerns are evidenced mainly by the relatively little information available on the state of the fuel and of the sarcophagus and, surprisingly, by the fact that before myself no Western nuclear engineers or scientists were permitted to investigate the accident or have access to what little data were available. The Ukrainian government is struggling with a severe economic crisis that precludes substantial funding for basic scientific research at the site (most of the money goes toward maintenance, cleanup, and monitoring). In fact, Ukraine has yet to establish a concrete policy regarding the 30-km zone—its main concern is to attract international aid to construct a second more reliable sarcophagus and to help clean up the surroundings. To better grasp the conditions in which the handful of researchers at Chornobyl conduct their work, during my year-and-a-half stint at Chornobyl, when necessary I had to drive 120 km to Kyyiv to photocopy material relevant to my research—which was due as much to a lack of paper as to the lack of a working photocopier.

[b]In the highly oxidizing conditions at Chornobyl, the boron carbide of the control rods (or what little may have been thrown in from the helicopters) would have turned into the highly volatile B_2O_3 (melting point, 450 °C; boiling point, ≈1800 °C) by either of the following reactions:

$$B_4C + 4O_2 \rightarrow CO_2 + 2B_2O_3$$

$$B_4C + 8H_2O \rightarrow CO_2 + 2B_2O_3 + 8H_2$$

The oxide melt of the fuel–serpentine mixture, however, would tend to partially retain this product.

reactor shaft) but also that little if any carburization took place.[26] Finally, it appears clear upon comparing the data from Tables 3 and 4 with the chemical compositions of Soviet concretes and specialty stainless steels (Ref. 12, Appendix B) that the major componential contributor to the LFCMs is the LBS.

The current configuration of the LFCMs located in a thick layer above the lower layer of solidified metal on the floor of the steam distribution corridor seems to indicate that, before melting through the LBS [whose center appears to be approximately about the coordinates (K, 46 + 3 m)], the molten debris had separated into two distinct layers—a lower molten metal-containing layer consisting of structural metal and metallic fission products and an upper ceramic layer consisting of molten $(U,Zr)O_2$ and oxidation-resistant metals. (Fission-product release from the ceramic "pool" during the active phase before the melt-through would be determined by bubble dynamics and the oxygen potential.) During the initial period of contact between the molten debris and the serpentine contained within the LBS, it is expected that the gas release from the serpentine was very vigorous,[a] and in most cases the oxides and the metals in the debris became well mixed. Later, depending on the initial melt temperature, the oxide phase would have detrained from the metal phase forming layers; in general, a metal phase will be more dense and will be the lower layer in such a situation.

Of vital interest to a source-term analysis is the almost complete lack of ruthenium in the LFCMs and the high activity of Ru-103 and Ru-106 in the MFCMs.[b,27] Ruthenium metal (generally thought to be in the low volatility group) would be expected to remain in the molten debris and be drawn into the lower metal layer now observed at Chornobyl;[28] however, the high loss of ruthenium from the ceramic layer seems consistent if it were exposed to a highly oxidizing atmosphere at high temperatures during the active phase. The very high volatility of RuO_3 and RuO_4 would then appear to indicate a high release of ruthenium to the environment. In fact, although the Soviets stated that only 2.9% of the core inventory of ruthenium was released during the accident, there is some inconsistency in the activity release data presented in Vienna that seems to indicate that ruthenium may have been released in greater quantities. This conjecture, in fact, may be at least partially supported by findings in Sweden, where some hot particles deposited there as a result of the accident were found to be nearly pure ruthenium.[29]

One would expect a more complex elemental composition of hot particles if the release mechanism from the fuel was mechanical in nature. Demin and Khodakovsky have noted that hot particles analyzed in the immediate vicinity of Unit 4 (on the grounds of the power station) are greatly enriched in the nonvolatiles barium and cerium and that ruthenium was "fractionating" as tellurium and iodine.[30,31] Indeed, one of the great puzzles of the Chornobyl source term is how to explain the simultaneous release of relatively large fractions of ruthenium, barium, and cerium. Oxidating environments enhance the release of ruthenium but suppress the release of barium and cerium. Similarly, reducing conditions enhance releases of barium and cerium but suppress the release of ruthenium.[32] A strong interaction of fuel with serpentine—an unsaturated silicate—should suppress the release of barium, and it might also suppress the release of cesium (see the following).

The results of the analyses also show that within the 135 tonnes of fuel (≈71% of initial core load) now located in the lower regions of the reactor building in the form of LFCMs, approximately 35% of the calculated inventory of Cs-137 remains. This implies that $65 \times 71\%$, or 46% of the initial 7.0 MCi inventory (3.2 MCi), may have been released to the environment from the LFCMs. If one also considers the remaining 29% of the core (in the form of fragments or chunks ejected beyond the bounds of the reactor building or now located under the pile of materials on the floor of the central hall) and what contribution to the overall release it may have had, it is clear that the releases of volatile radioisotopes were substantially greater than those reported by the Soviets in Vienna. This also corroborates Warman's release estimates of 30 to 50% radiocesium and 40 to 60% radioiodine into the environment[33] and thus may help to explain why a very significant increase in childrens'

[a]For serpentine, a hydrous magnesium silicate, $3MgO\ 2SiO_2\ 2H_2O$ or $Mg_6\ [Si_4O_{10}][OH]_8$, the water of crystalization present in the mineral is retained at temperatures as high as 450 to 500 °C—as opposed to ordinary concrete, in which roughly half the water content is lost because of vaporization at a temperature of 100 °C. A major feature of serpentinite concrete is that its water content is relatively higher than that of ordinary concrete—implying that a direct interaction with corium would release more gases for sparging effects.

[b]The behavior of ruthenium during the Chornobyl accident is important for two reasons: (1) the toxicity of the volatile ruthenium oxides (RuO_3 and RuO_4) and the radiation hazards of Ru-103 and Ru-104 should be considered in a reevaluation of the Chornobyl source term and its effect on the local population; and (2) ruthenium characteristics in oxidizing environments are distinctive enough to make an understanding of the kinetic behavior of ruthenium releases very useful for postaccident source-term analyses.

thyroid cancers are now appearing in Belarus and Ukraine. (Note that the Soviets reported a 13% release of Cs-137 and 20% release of I-131 in Vienna.) Unfortunately, no I-129 data appear to be available to further strengthen this conjecture. Determining the fraction of I-129 remaining in the Chornobyl fuel is crucial to any credible source-term estimate.[a,34]

Regarding an estimate of the source term, two things remain unknown in the findings. The first is whether there was significant plateout along the release path and into the environment. By all indications the reactor shaft was partially blocked by the UBS, some of its highly damaged MCCs along the periphery, part of the UCCs, and several larger fragments of the central hall wall from above the 35.5-m (floor) level. Although certainly the release was open to the atmosphere, it had what is usually termed a torturous path, which made plateout quite likely; however, during the active phase the UBS and other fragments were probably being heated by the molten corium (convective heating by hot updrafts, radiative heating, and self-heating from deposited fission products). In this case, revaporization (the release to the environment of volatile fission products previously deposited on surfaces along the release path) would be a very likely release mechanism for volatiles such as cesium and iodine.

The second and more enigmatic finding is that, although more radiocesium and radioiodine were released from Unit 4 than previously thought, a considerable amount of Cs-137 (35%) remains within the solidified remnants of the core. In fact, the amount of Cs-137 retained in the LFCMs (on the average) is *significantly higher* than that retained at TMI-2 in the molten ceramic lower plenum debris (average of 3% retained) or in the upper plenum debris (average of 19% retained).[35,36] This is particularly unexpected given the long (9-day) duration of the active phase, the oxidizing environment to which the core was exposed, the thorough mixing of the core, and the apparent high volatility of cesium. It seems to suggest that some of the cesium may be in an involatile chemical form stable at high temperatures,[b,28,37] or if a significant crust did form above the corium, it may have presented a very formidable barrier to volatile fission-product releases. Cesium retention could also be explained by the interaction of the melted fuel with serpentine and the formation of fairly refractory cesium silicates.

Obviously, much remains to be investigated at Chornobyl because the findings are as yet too sketchy to provide an accurate account of the active phase. Radiochemical analyses and a quantification of large core chunks ejected beyond the building are needed as well as more detailed analyses of LFCMs and MFCMs. Moreover, a more precise material balance of the FCMs located within the sarcophagus is required to account for all the fuel. (It is imperative, for example, to identify what is lying under the pile of materials, dumped by the helicopters, located on the floor of the central hall.) Western experts, who have considerable degraded-core experimental and accident experience, should explore opportunities with the Ukrainians for joint severe-accident research at Chornobyl.

Although the design of RBMK reactors differs clearly from that of Western LWRs and the accident sequence is a special case not directly comparable to Western severe accident models, any observations that may be of generic interest should be evaluated for the benefit of improving the knowledge of severe accidents. More important, given that 15 RBMKs continue to operate in Lithuania, Russia, and Ukraine, safety analyses of these reactors would clearly benefit from a revisitation of the consequences of the Chornobyl accident.

REFERENCES

1. A. A. Borovoi, Fission Product and Transuranic Element Release During [the] Chornobyl Accident (preprint), presented at *The International Conference "The Fission of Nuclei—50 Years," Leningrad, USSR, October 16–20, 1989*, p. 2, Chornobyl, Ukraine: The Chornobyl Complex Expedition of the I. V. Kurchatov Institute of Atomic Energy, 1990.
2. T. S. Kress et al., Chornobyl Accident Sequence, *Nucl. Saf.*, 28(1): 1-9 (January–March 1987). Actually, the Chornobyl Unit 4 had no containment to speak of so far as the West defines a containment. The "containment" in RBMKs is compartmentalized to minimize the spread of radioactivity in the event of a design-basis accident (i.e., the compartment is designed to withstand the rupture of the largest pipe in the compartment). Common-mode rupture of several pipes is a beyond-design-basis accident. The reactor central hall for Unit 4 (the region above the upper shielding cover plates of the reactor with dimensions of approximately 24 m wide by 80 m long by 35 m high) is constructed of reinforced 1.5-m-thick concrete walls for

[a]Fission-product source terms should not necessarily assume highly volatile forms of iodine. Because iodine and cesium tend to form condensable species that form aerosols during transport away from a hot or molten core (at least in the steam environment of a Western LWR), aerosol behavior must be considered for volatile fission-product analysis.

[b]Interestingly, it is thought that "chemical and/or physical phenomena cause *retention of 5 to 15%* iodine and *cesium* for extended periods in molten corium"[34] (emphasis added).

the lower bay and a steel frame roof with precast concrete panel sheathing for the walls of the high bay.

3. U.S. Nuclear Regulatory Commission (Comp.), *Report on the Accident at the Chornobyl Nuclear Power Station,* Report NUREG-1250, pp. 2-13, 1987. The central hall is designed to withstand only normal building structural loads. Compare this with a modern PWR "dry" containment's rated design-basis accident pressure of approximately 65 psig (0.44 MPa)—although actual failure will occur at two to three times this pressure [i.e., not below 140 psig (0.95 MPa)]. (Note, however, a Western ice-condenser containment PWR is *much* weaker than a dry containment.) The *first* containment in the Soviet Union was constructed for the VVER-1000 Unit 5 at the Novovoronezh Nuclear Power Station in 1980.
4. G. A. Sharovarov, *Technical Substantiation for the Nuclear Safety of Object "Shelter" on the Basis of the Investigation of the Accident Dynamics: Characteristics of "Shelter"—Its Physical and Mathematical Models*, p. 36, The Academy of Sciences of the Belarusian SSR, The Institute of Nuclear Energy, Minsk, Belarus, 1990.
5. V. A. Kurnosov, V. M. Bagryanskii, and I. K. Moiseev, Entombment of Chornobyl Unit 4, *At. Energy,* 64(4): 299-306 (April 1988).
6. "According to Nikolai Shteinberg, former chairman of Ukraine's State Oversight Committee for Nuclear and Radiation Safety, *DerzhAtomNahljad,* who was chief engineer at Chornobyl for the first 10 months after the accident: 'From an engineering standpoint, no one can tell you what will happen to the sarcophagus in the next half-hour.' " Chrystia Freeland, Waiting for the Next Chornobyl, *The Financial Times of London,* No. 32,043, Week 16: 20 (April 21, 1993).
7. Since coming under the administrative jurisdiction of the nuclear power plant, repair work on the sarcophagus has picked up slightly. During 1993–1994, for example, 246 m^2 of openings in the roof were covered over, and an anticorrosive paint was applied to some of the external walls. The Ukrainian State Committee for the Utilization of Nuclear Energy and the Ukrainian Inter-Branch Scientific and Technical Center "Shelter," *The Encasement "Ukryttja" State and Its Safety Problems,* p. 12, report presented to the International Symposium "'Ukryttja'-94 Safety" Chornobyl, Ukraine, 1993. By late 1994–early 1995, the remaining openings in the sarcophagus had been sealed.
8. Concrete Pumps for Chornobyl, *Nucl. Eng. Int.*: 3 (December 1986).
9. Because little reliable information is available on the integrity of the sarcophagus (built upon the remains of the reactor building), much speculation (often unsubstantiated) surrounds the issue as to how much of a danger the sarcophagus poses if a postulated collapse of some of the supporting structures were to occur. Inspection of the sarcophagus and strengthening work continues; but it is unclear whether this will lead to significant improvement, given the inaccessibility of some of the supporting members and the dangerous working conditions. The European Commission has awarded a feasibility study contract to a French and German "Alliance" consortium to independently assess the state of the sarcophagus and to determine whether it is practical to erect a second, more structurally sound sarcophagus. Decommissioning work could then be conducted on the destroyed reactor within this second sarcophagus. The study is expected to be completed by September 1995. Alliance Wins Chornobyl Sarcophagus Study, *Nucl. Eng. Int.*: 13 (September 1994).
10. For a summarized account of remote methods employed to investigate Unit 4, see A. A. Borovoi, A. I. Ivanov, and A. R. Sich, Use of Robotic Technologies and Remote Systems for Diagnostics and Research Within the Chornobyl Sarcophagus, in *Proceedings of the ANS Fifth Topical Meeting on Robotics and Remote Systems, Knoxville, Tennessee, April 25–30, 1993.*
11. See also A. A. Borovoi, A. I. Ivanov, and Yu. A. Myshchenko, *Diagnostic Robots at the 4th Unit of the Chornobyl Nuclear Power Plant,* Ukrainian Academy of Science's Inter-Branch Scientific and Technical Center "Shelter" and the V. M. Hlushkov Institute of Cybernetics, Preprint 94-5, 1994.
12. For a significantly more detailed description of the remains of the reactor shaft, surrounding areas, the nuclear fuel, and further references, see A. R. Sich, *The Chornobyl Accident Revisited: Source Term Analysis and Reconstruction of Events During the Active Phase,* Chapter V, Nuclear Engineering Ph.D. Dissertation, Massachusetts Institute of Technology, January 7, 1994.
13. Private communication with several Kurchatov Institute researchers, September 1992. At 10 days, 1 month, and 3 months after the accident, the decay heat was calculated to be 42 kWt/t U, 24 kWt/t U, and 12 kWt/t U, respectively. One can certainly assume that the explosions must have, to some extent, weakened Component S.
14. At this point, it seems odd that the Soviets came to the following conclusion in August 1986 at Vienna: "The lower slab of the reactor shaft [LBS] had been preserved and fuel was localized mainly (roughly 96%) in the reactor shaft an[d] in compartments of steam water and lower steam service lines [lower coolant channels]." U.S.S.R. State Committee on the Utilization of Atomic Energy (Comp.), *The Accident at the Chornobyl Nuclear Power Plant and Its Consequences; Part 1: General Material,* presented at the International Atomic Energy Agency Expert's Meeting, Vienna, August 25–29, 1986, Report NP-6901809 (CONF-8608143), 1986.
15. E. B. Anderson et al., *Lava-Like Fuel-Containing Masses of the "Shelter" Encasement,* Ukrainian Academy of Science's Inter-Branch Scientific and Technical Center "Shelter" and the V. M. Hlushkov Institute of Cybernetics, Preprint 94-4, Kyyiv, 1994.
16. *Technical Basis for the Radiation Safety of Object "Shelter,"* pp. 50-59, Chornobyl, Ukraine and Minsk, Belarus: The I. V. Kurchatov Institute's Complex Expedition and the Belarusian Academy of Science's Institute of Ecological Problems, 1992.
17. Yu. S. Panitkov et al., *Reconstruction of the Dynamics of the Destruction of the 4th Unit of the ChNPP on the Basis of Physico-Mathematical Modeling: Working Out of a Physical Model of the Chornobyl Catastrophe,* pp. 108-114, Minsk, Belarus: The Belarusian Academy of Sciences, 1991.
18. E. B. Anderson et al., *Lava-Like Fuel-Containing Masses of the "Shelter" Encasement,* Ukrainian Academy of Science's Inter-Branch Scientific and Technological Center "Shelter" and the V. M. Hlushkov Institute of Cybernetics, Preprint 93-17, pp. 24-25, Kyyiv, 1993.
19. It was later found that the authors had underestimated the amount of serpentine in the LBS because they had not

considered its peripheral thermal expansion zone, which contained substantial amounts of the mineral. This produced a new lower-bound estimate of approximately 100 tonnes. A. R. Sich and A. A. Borovoi, private communication.

20. A. N. Kiselyov, A. Yu. Nenaglyadov, A. I. Surin, and K. P. Checherov, *Experimental Research of the Lava-Like Fuel-Containing Masses at the 4th Unit of the Chornobyl NPP*, Moscow, Russia, Kurchatov Russian Research Institute, Preprint IAE-5533/3, p. 96, 1992.
21. *Preparation and Consummation of TOYaRB of Object "Shelter" on the Basis of Assessed Data Bases of the Object and Its Impact on the Surrounding Environment*, Chornobyl, pp. 17-20, Ukraine, Ukrainian Academy of Science's Inter-Branch Scientific and Technical Center "Shelter," December 23, 1993.
22. Unfortunately, along with allegations of impropriety, the technical competence of the leader of the group conducting *visual* inspections of the LFCMs, Konstantin Checherov, has been questioned. For a sobering account of the work of the scientists at Chornobyl, see S. Benkleman, Dealing with Chornobyl: Eight Years After the Accident, Big Potential Risks Remain, *Newsday*, 55(80) (November 21, 1994), and S. Benkleman, Learning to Love a Disaster: Study of Chornobyl Enthralls Scientists, *Newsday*, 55(81) (November 22, 1994).
23. In a cursory report that presents apparently contradictory information, Edward Purvis attempts to present an alternate account of the accident. (Purvis, Edward E., "The Chornobyl Accident Sequence: April 1995," report to the Ukrainian Academy of Sciences, April 6, 1995.) By its own admission, much of what the report concludes is based primarily on *visual* (photographic and video) investigations of LFCMs not covered by "fresh" concrete. The theories of Konstantin Checherov, a Chornobyl researcher who led these visual investigations and who is cited extensively in the report, are rejected as "fantasy" by other senior scientists at Chornobyl—something the executive summary of the report fails to mention.
24. Edvard M. Pazukhin, Lava-Like Fuel-Containing Materials of Chornobyl Unit 4: Topography, Physico-Chemical Properties, and Formation Scenario, *Radiochemistry* (Moscow): 36(2): 97-142 (1994).
25. A. R. Sich, Chornobyl Accident Management Action, *Nucl. Saf.*, 35(1): 1-24 (January–June 1994).
26. D. A. Powers has argued for carburization as a possible mechanism for activity releases during the active phase. Powers provides excellent background information and an hypothesis. Unfortunately, this analysis is based on the dubious Soviet accounts of the core's being covered with materials thrown from helicopters to smother the graphite fire. Moreover, no carbon compounds are observed in the LFCMs—in particular, uranium carbide; however, if carburization did take place, after 7 to 8 years all evidence would have been erased by the continued exposure of hot material to air—at least those LFCMs not covered by fresh concrete. D. A. Powers, Carburization as a Mechanism for the Release of Radionuclides During the Chornobyl Accident, in *Proceedings of the First International Workshop on Past Severe Accidents and Their Consequences, October 30–November 3, 1989*, pp. 113-125, E. P. Velikhov and L. A. Bolshov (Eds.), Nauka, Moscow.
27. F. C. Inglesias, C. E. L. Hunt, F. Garisto, and D. S. Cox, Ruthenium Release Kinetics from Uranium Oxides, presented at the International Seminar *Fission Product Transport Processes in Reactor Accidents, Dubrovnik, Yugoslavia, May 22–26, 1989*, Hemisphere Publishing, New York, 1990.
28. Richard Hobbins expects that, because of its very high oxygen potential, ruthenium should exist in its elemental form under severe accident conditions, and very small releases are expected on the basis of the low volatility of the metal. He also points out that large releases from the fuel (but negligible releases from the core) were observed for ruthenium in the TMI-2 accident and that ruthenium is retained in molten metallic materials, which is in agreement with that observed at Chornobyl (albeit more qualitatively than quantitatively) and Western out-of-pile meltdown studies. R. R. Hobbins, D. A. Petti, and D. L. Hagrman, Fission Product Release from Fuel Under Severe Accident Conditions, *Nucl. Technol.*, 101(3): 270–281 (March 1993). In general, medium- to low-volatility fission products can be retained in large fractions by the chemistry of ceramic melts with metallic inclusions.
29. L. Devell, H. Tovedal, U. Bergstrom, A. Applegren, J. Chyssler, and L. Andersson, Initial Observations of Fallout from the Reactor Accident at Chornobyl, *Nature*, 321 (6067): 192-193 (May 15, 1986) as reported in Ref. 26.
30. V. F. Demin and I. L. Khodakovsky, Released Radioactive Material During the Chornobyl Accident, as Appendix 10 in *USNRC Workshop on the Chemical Reactions and Processes in Severe Reactor Accidents* (November 1987), pp. 140 and 141. Demin's findings that more ruthenium may have been released is disputed by Aleksandr Borovoi of the Chornobyl research group. He points out that the very volatile oxides RuO_3 (which decomposes at low temperatures) and RuO_4 (with a melting point of 25.5° C and which decomposes at 108° C) were released from the surfaces of the LFCMs after the active phase in the elevated temperatures of the particularly hot summer of 1986 in addition to the decay heat generated in the remains of the fuel—thus artificially enriching hot-particle releases. Borovoi bases his argument on analyses of ejected fuel fragments (as yet unavailable), which indicate that ruthenium as well as other middle and nonvolatiles left as "fuel chunk aerosols." He could not, however, explain the apparently higher release of cerium and Ba-140.
31. Private communication with A. Borovoi, August 12, 1993. It is unfortunate that Demin and Khodakovsky did not present much new information beyond that reported by the Soviets at Vienna in August 1986.
32. F. Garisto, F. C. Iglesias, and C. E. L. Hunt, A Thermodynamic/Mass-Transport Model for the Release of Ruthenium from Irradiated Fuel, presented at the International Seminar *Fission Product Transport Processes in Reactor Accidents, Dubrovnik, Yugoslavia, May 22–26, 1989*, Hemisphere Publishing, New York, 1990.
33. E. A. Warman, Soviet and Far-Field Radiation Measurements and an Inferred Source Term from Chornobyl, presented at the *New York Chapter Health Physics Society Symposium on the Effects of the Nuclear Reactor Accident at Chornobyl, April 3, 1987, Brookhaven National Laboratory*. Because iodine is one of the most hazardous fission products, its chemical forms and behavior after releases are particularly important.
34. R. R. Hobbins, D. A. Petti, D. J. Osetek, and D. L. Hagrman, Review of Experimental Results on Light Water Reactor Core Melt Progression, *Nucl. Technol.*, 95(3): 287–307 (September 1991).

35. D. A. Petti, J. P. Adams, J. L. Anderson, and R. R. Hobbins, Analysis of Fission Product Release Behavior from the Three Mile Island Unit 2 Core, *Nucl. Technol.,* 87(1): 243–263 (August 1989). According to Ref. 28, 12% of the Cs-137 inventory is retained in the lower plenum, whereas 20% is retained in the upper debris. An earlier study concluded that more Cs-137 was retained at TMI (although still less than at Chornobyl): 9 to 22% (average 16%) in the lower plenum debris and 6 to 32% (average 21%) in the upper plenum.
36. D. W. Akers, R. R. Hobbins, S. Langer, J. P. Adams, and S. J. Niemczyk, Fission Product Behavior in the TMI-2 Core: Preliminary Evaluation of Transport and Chemistry, in *Proceedings of the Symposium on Chemical Phenomena Associated with Radioactivity Releases During Severe Nuclear Plant Accidents,* Report NUREG/CP-0078 (CONF-860911-Pt. 1), June 1987.
37. Even quite recent experiments that simulate fission-product releases for severe accident conditions conclude that cesium retention is low: "The results [of the investigations] for the volatile species show clearly that the release rates for the rare gases, the halides, and the alkali metals all are very high and are similar for LWR fuel in the temperature range 1700 to 2700 K." M. F. Osborne and R. A. Lorenz, ORNL Studies of Fission Product Release Under LWR Severe Accident Conditions, *Nucl. Saf.,* 33(3): 344-365 (July–September 1992).

General Safety Considerations

Edited by G. T. Mays

Nuclear Power Safety in Central and Eastern Europe

By R. Wilson[a]

Abstract: *The Chernobyl accident showed the weaknesses in the Soviet approach to safety, particularly of nuclear reactors. Until recently, Western governments, scientists, and engineers did not understand how to help their Russian colleagues make a safer society. This article discusses the two main types of Soviet reactors, their safety problems, and the help Westerners are giving to make them safer.*

Before the Chernobyl accident, few people in the Western world knew or cared about reactors in the former U.S.S.R., although the RBMK (light-water-cooled, graphite-moderated multichannel reactor) had been described in English.[1] It took analysts in the United States less than a week to realize two weak points about the design: the positive void coefficient and the inability to protect against the simultaneous failures of several channel tubes.

For many years after Chernobyl, there were few sympathetic government responses to the Soviet problems. Westerners took the paternalistic position that the Soviets had to shut down their nuclear facilities because they were unsafe, but Westerners did not provide an alternative. This position can only be called an arrogant conversation stopper.

As always, there is the question, "How safe is safe enough?" Several analysts have compared the risks to health and life from different methods of electricity generation. On average, we are spending too much, both in the United States and Russia, on risks involved in nuclear safety compared with what we spend on the risks (especially air pollution prevention) of other electricity technologies. I would rather live next to an RBMK than to any coal-fired power plant, I would rather live next to a VVER than to an RBMK, and I would rather live next to any Western reactor than to a VVER.[2] The effects of coal burning are as bad each year as those of the single Chernobyl accident.[3] This view depends on the belief that particulate pollution is bad for health at low doses. Recent data suggesting this may be found in Ref. 4.

According to this logic, the West's demand that Russians close down their unsafe power plants should apply first to their coal-fired power plants, a view many Russian specialists still hold. Russians made such calculations in 1985.[5] The specialists are not wrong, but they do not reflect the way most people think, especially those not knowledgeable about nuclear energy.

For about 5 years after Chernobyl, specialists in the West felt that another accident of that severity would destroy the world's nuclear power industry. The specialists believed that another accident must not happen, and therefore it was essential for the West to shut down all the RBMK reactors and the older VVER-440/230 power plants. That approach is unrealistic because no financially viable alternative was offered. It would cost more than $30 billion for a Western country to replace these power plants with safer nuclear ones; the United States was willing to spend only a few *million* dollars a year—too little by a factor of more than 1000. The sum has increased in 1994, but it is still less than a hundred million.

[a]Mallinckrodt Professor of Physics, Department of Physics, Harvard University, Cambridge, MA 02138.

A turning point in the thinking of professional engineers occurred at a meeting[6] where the theme was that it is our duty to help the Russians and other owner/operators of Russian-designed nuclear power plants to help themselves. They alone must make the decisions whether to operate on the basis of the circumstances in their countries. The general approach now is to give modest help to upgrade the RBMKs and the VVER-440/230s but not enough to encourage them to keep going *all* their originally planned lives.

The change of thinking is emphasized by recent World Bank studies of the energy needs of eastern and central European countries that suggest that shutting these reactors down would cost more than upgrading them to reasonable standards and operating them till the end of their plant lives.[7] The enthusiasm for doing so, however, was clearly less for the older RBMK reactors and for the VVER-440/230s.

TYPES OF REACTORS

Russia has designed two main types of reactors for electric power generation (Fig. 1).[8] The first is a graphite-moderated, light-water-cooled multichannel reactor (RBMK) developed from the early plutonium production reactors. The RBMK reactor was never sold to a satellite country of eastern Europe (Lithuania was considered an

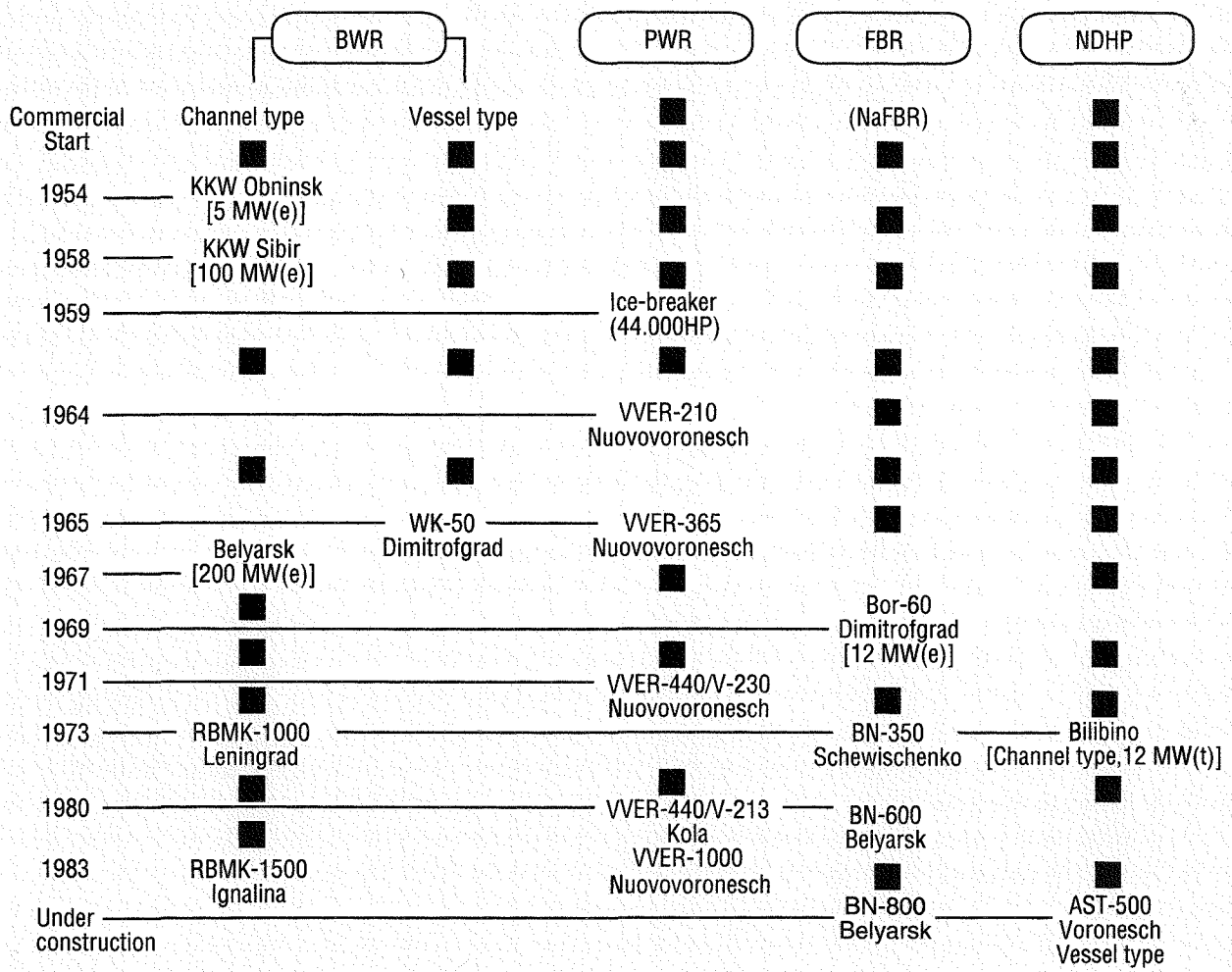

Fig. 1 Historical overview of nuclear power plant development in the former USSR. BWR is boiling-water reactor, PWR is pressurized-water reactor, FBR is fast breeder reactor, and NDHP is heat producing reactor.

integral part of the U.S.S.R.). It is widely assumed that this is because these reactors can easily be operated to produce weapons-grade plutonium (with only a small amount of ^{240}Pu).

The second type of reactor, a water-cooled, pressurized-water reactor, was also designed in Moscow (ITEP). These are now the VVER-440/230; a later development, the VVER-440/213; and a larger type, the VVER-1000. The locations and construction times of these are shown in Tables 1 and 2.[8]

SAFETY OF THE RBMK

Although in August 1986 Professor V. A. Legasov stressed operator error as the principal cause of the Chernobyl accident,[9] the West was unwilling to be so dogmatic. One committee stated, "There is need to shift the balance of perception so as to emphasize more the deficiencies in the safety features of the design and to recognize the problems conferred by the framework within which the plant operation was carried out."[10]

The 100 or so safety improvements the Russians have made since Chernobyl[11] fall into two main categories: the neutronics of the core and the hydraulics of the pressure tubes.[12] The neutronics of the core include three subheads: the positive void coefficient, the control-rod tip design, and the control-rod insertion speed.

The void coefficient was listed in the papers of Dollezhal and Emylianov[1] as 2×10^{-4} per percentage void. Taken literally, this means that reactivity would increase 2% if all the pressure tubes were initially filled with water, which would then be converted to steam. This reactivity increase exceeds the fraction of delayed neutrons so that it will be prompt with a time constant comparable to the time to slow down the neutrons (about 1 ms). This reactivity increase (unless compensated) leads at once to a power increase; the power increase will, in turn, lead to a temperature increase and evaporation of more water. This becomes a runaway reaction that is not possible to control, as occurred at Chernobyl. In the laconic words of Academician Valerii Legasov,[9] the reactor had no choice but to "rearrange itself," which Unit 4 at Chernobyl did.

Several possibilities exist to reduce the void coefficient. The best is to reduce the amount of graphite in the moderator. This leads to an "undermoderated" core, and the water is necessary to complete the slowing down of the neutrons. This can be done only in initial design, however; a backfit to the existing reactors would be hard. Other possibilities are to insist on absorbers in the core at all times. This was the normal operating procedure for the RBMK with a requirement that 25 control rods be in the core at all times. Under such circumstances, immediate movement of the control rods can have an immediate effect on reactivity and power level and compensate any positive reactivity coefficients as they occur and before they exceed the fraction of delayed neutrons. This requirement was not backed up by interlocks or even by the education of operators concerning the necessity of such a rule. This requirement has now been changed to demand that 80 control rods be in the core at all times. Although it is evident that operators are now made abundantly clear of the need for this, it seems that no interlock exists. Many people have asked why. The question was raised at the American Nuclear Society workshop, for example,[6] but the answers were vague. One Soviet reactor expert who is "out of the loop" has suggested building absorber into the fuel assembly to prevent its easy removal.[13] The absence of a definite interlock seems to provide potential for serious problems. To allow for the increased absorption and increase the fuel-to-moderator ratio, the enrichment of the uranium in the core has been increased as fuel has been changed in all RBMKs.[11] The void coefficient is still $+(0.5 \pm 0.2)$ beta.[14] The quoted error seems to be a variation among plants. Although this void coefficient is less than one-fourth of what it was before and below unity so that prompt criticality would be impossible, other reports suggest that the void coefficient at Chernobyl is still 1% and positive.

A second weakness is the fact that each control rod had on its tip a 1-m rod of carbon. When fully inserted, this carbon matched the carbon in the moderator at the bottom of the core. But when inserted from the top, this carbon produced a large positive reactivity insertion, which was fatal to an unstable reactor. It is widely believed that the proximate cause of the Chernobyl accident was the pressing of the scram button by the operator at 1:23 and 40 seconds on that fateful morning of April 26, 1986: "The scram just before the sharp rise in power that destroyed the reactor may well have been the decisive contributing factor."[10] Many Westerners have asked many Russians many times why this stupid design was ever allowed to be built. I know of no satisfactory answer except that it was a result of a centralized planning system with inadequate review. It remains unclear whether this has been changed in all RBMK reactors. No American has seen a publicly available list of all reactors and the dates the safety improvements were made to each one. This leads to a suspicion that on most reactors they have *not* been made.

Table 1 Reactors Connected to the Grid[a]

Country	Reactor		Type and model	Capacity, MW(e)		Operator	NSSS supplier	Construction start	Grid connection	Commercial operation	CF % to 1990	EAF % to 1990
	Code (IAEA)	Name		Net	Gross							
Bulgaria	BG-1	Kozloduy-1	VVER-440/230	408	440	EEE	AEE	1970–04	1974–07	1974–07	72.0	77.3
	BG-2	Kozloduy-2	VVER-440/230	408	440	EEE	AEE	1970–04	1975–10	1975–11	76.0	83.2
	BG-3	Kozloduy-3	VVER-440/230	408	440	EEE	AEE	1973–10	1980–12	1981–01	78.8	84.8
	BG-4	Kozloduy-4	VVER-440/230	408	440	EEE	AEE	1973–10	1982–05	1982–06	82.8	88.4
	BG-5	Kozloduy-5	VVER-1000	953	1000	EEE	AEE	1980–07	1987–11	1988–09	43.3	52.0
	BG-6	Kozloduy-6	VVER-1000	408	1000	EEE	AEE	1984–07	1991–03	1991	(1)	(1)
Slovakia	CS-2	Bohunice-1	VVER-440/230	408	430	EBO	AEE	1974–04	1978–12	1981–06	73.2	74.0
	CS-3	Bohunice-2	VVER-440/230	408	430	EBO	AEE	1974–04	1980–03	1981–01	77.3	78.1
	CS-13	Bohunice-3	VVER-440/213	408	430	EBO	SKODA	1976–12	1984–08	1985–02	74.5	74.6
	CS-14	Bohunice-4	VVER-440/213	408	430	EBO	SKODA	1976–12	1985–08	1985–12	80.9	81.0
Czechoslovakia Republic	CS-4	Dukovany-1	VVER-440/213	408	440	EDU	SKODA	1978–07	1985–02	1985–08	77.0	77.0
	CS-5	Dukovany-2	VVER-440/213	408	440	EDU	SKODA	1980–12	1986–01	1986–09	79.4	76.9
	CS-8	Dukovany-3	VVER-440/213	408	440	EDU	SKODA	1978–07	1986–11	1987–05	82.8	79.3
	CS-9	Dukovany-4	VVER-440/213	408	440	EDU	SKODA	1978–07	1987–06	1987–12	81.5	78.1
Russia	SU-96	Balakovo-1	VVER-1000	950	1000	MAEP		1980–12	1985–12	1986–05	48.6	51.0
	SU-97	Balakovo-2	VVER-1000	950	1000	MAEP		1981–08	1987–10	1988–01	74.8	78.2
	SU-98	Balakovo-3	VVER-1000	950	1000	MAEP		1982–11	1988–12	1989–04	75.5	75.4
	SU-21	Belyoarsk-3	BN-600 (FBR)	560	600	MAEP		1966	1980–04	1981–11	72.8	74.0
	SU-14A	Bilibino-A	LWGR	11	12	MAEP		1970	1974–01	1974–04	77.0	86.5
	SU-14B	Bilibino-B	LWGR	11	12	MAEP		1970	1974–12	1975–02	78.8	88.9
	SU-14C	Bilibino-C	LWGR	11	12	MAEP		1970	1975–12	1976–02	79.5	89.7
	SU-14D	Bilibino-C	LWGR	11	12	MAEP		1970	1976–12	1977–01	80.6	90.1
	SU-30	Kalinin-1	VVER-1000	950	1000	MAEP		1977–02	1984–05	1985–06	71.3	70.7
	SU-31	Kalinin-2	VVER-1000	950	1000	MAEP		1982–02	1986–12	1987–03	76.9	78.3
	SU-12	Kola-1	VVER-440/213	411	440	MAEP		1970–05	1973–06	1973–12	79.1	80.1
	SU-13	Kola-2	VVER-440/213	411	440	MAEP		1973–01	1974–12	1975–02	78.7	79.6
	SU-32	Kola-3	VVER-440/213	411	440	MAEP		1977–04	1981–03	1982–12	83.3	83.3
	SU-33	Kola-4	VVER-440/213	411	440	MAEP		1976–08	1984–10	1984–12	85.3	84.1
	SU-17	Kursk-1	RBMK	925	1000	MAEP		1972–06	1976–12	1977–10	74.0	74.7
	SU-22	Kursk-2	RBMK	925	1000	MAEP		1973–01	1979–01	1979–08	72.2	73.8
	SU-38	Kursk-3	RBMK	925	1000	MAEP		1978–04	1983–10	1984–03	75.4	77.5
	SU-39	Kursk-4	RBMK	925	1000	MAEP		1981–05	1985–12	1986–02	75.6	75.8
	SU-15	Leningrad-1	RBMK	925	1000	MAEP		1970–03	1973–12	1974–11	58.4	58.3
	SU-16	Leningrad-2	RBMK	925	1000	MAEP		1970–06	1975–07	1976–02	79.0	79.4
	SU-34	Leningrad-3	RBMK	925	1000	MAEP		1970–12	1979–12	1980–06	82.9	83.3
	SU-35	Leningrad-4	RBMK	925	1000	MAEP		1975–02	1981–02	1981–08	86.3	86.4

Table 1 (Continued)

Country	Reactor		Type and model	Capacity, MW(e)		Operator	NSSS supplier	Construction start	Grid connection	Commercial operation	CF % to 1990	EAF % to 1990
	Code (IAEA)	Name		Net	Gross							
Russia	SU-9	Novovoronezh-3	VVER-440/230	385	417	MAEP		1967–07	1971–12	1972–06	72.4	76.8
	SU-11	Novovoronezh-4	VVER-440/230	385	417	MAEP		1967–07	1972–12	1973–03	78.0	83.1
	SU-20	Novovoronezh-5	VVER-1000	950	1000	MAEP		1974–03	1980–05	1981–02	51.2	52.1
	SU-23	Smolensk-1	RBMK	925	1000	MAEP		1975–10	1982–12	1983–09	81.2	81.1
	SU-24	Smolensk-2	RBMK	925	1000	MAEP		1976–06	1985–05	1985–07	80.0	80.4
	SU-67	Smolensk-3	RBMK	925	1000	MAEP		1984–05	1990–06		59.1	60.4
Ukraine	SU-25	Chernobyl-1	RBMK	925	1000	MAEP		1972–06	1977–09	1978–05	70.5	72.0
	SU-42	Chernobyl-3	RBMK	925	1000	MAEP		1977–05	1981–11	1982–06	58.6	58.9
	SU-40	Khmelnitski-1	VVER-1000	950	1000	MAEP		1981–11	1987–12	1988–08	73.3	73.8
	SU-27	Rovno-1	VVER-440/213	361	392	MAEP		1976–08	1980–12	1981–09	85.8	85.3
	SU-28	Rovno-2	VVER-440/213	384	416	MAEP		1977–10	1981–12	1982–07	83.3	85.4
	SU-29	Rovno-3	VVER-1000	950	1000	MAEP		1981–02	1986–12	1987–05	70.9	75.4
	SU-44	So. Ukraine-1	VVER-1000	950	1000	MAEP		1977–03	1982–12	1983–10	60.8	62.0
	SU-45	So. Ukraine-2	VVER-1000	950	1000	MAEP		1979–10	1985–01	1985–04	37.6	38.7
	SU-48	So. Ukraine-3	VVER-1000	950	1000	MAEP		1985–02	1989–09	1989–12	68.4	69.4
	SU-54	Zaporozhe-1	VVER-1000	950	1000	MAEP		1980–04	1984–12	1985–04	49.1	51.5
	SU-56	Zaporozhe-2	VVER-1000	950	1000	MAEP		1981–04	1985–07	1985–10	50.6	56.4
	SU-78	Zaporozhe-3	VVER-1000	950	1000	MAEP		1982–04	1986–12	1987–01	76.8	80.2
	SU-79	Zaporozhe-4	VVER-1000	950	1000	MAEP		1984–01	1987–12	1988–01	77.8	79.9
	SU-126	Zaporozhe-5	VVER-1000	950	1000	MAEP		1985–07	1989–08	1989–10	69.0	69.4
Lithuania	SU-46	Ignalina-1	RBMK	1380	1500	MAEP		1977–05	1983–12	1985–05	54.4	64.3
	SU-47	Ignalina-2	RBMK	1380	1500	MAEP		1978	1987–08	1987–08	60.4	68.6
Finland	FI-1	Loviisa-1	VVER-440/213	445	465	IVO	AEE	1971–05	1977–02	1977–05	82.4	83.1
	FI-2	Loviisa-2	VVER-440/213	445	465	IVO	AEE	1972–08	1980–11	1981–01	86.9	88.0
	FI-3	Ivo-1	BUR	710	735	IVO	ASEA	1974–02	1978–09	1979–10	86.4	87.5
	FI-4	Ivo-2	BUR	710	735	IVO	ASEA	1975–08	1980–02	1982–07	90.3	91.0
Hungary	HU-1	Paks-1	VVER-440/213	410	440	MVMT	AEE	1974–08	1982–12	1983–08	83.5	84.2
	HU-2	Paks-2	VVER-440/213	415	440	MVMT	AEE	1974–08	1984–09	1984–11	87.5	86.0
	HU-3	Paks-3	VVER-440/213	410	440	MVMT	AEE	1979–10	1986–09	1986–12	87.8	85.8
	HU-4	Paks-4	VVER-440/213	410	440	MVMT	AEE	1979–10	1987–08	1987–11	87.7	84.3

[a]Modified from International Atomic Energy Agency tables.

Table 2 Reactors Under Construction[a]

Country	Reactor Code (IAEA)	Reactor Name	Type and model	Capacity, MW(e) Net	Capacity, MW(e) Gross	Operator	NSSS supplier	Construction start	First criticality	Date of estimate	Percent completion (12/93)
Slovakia	C5-6	Mochovce-1	VVER-440/213	388	432	EMO	SKODA	1983–10	1994		90
	C5-7	Mochovce-2	VVER-440/213	388	432	EMO	SKODA	1983–10	1995		90
	C5-10	Mochovce-3	VVER-440/213	388	432	EMO	SKODA	1985	1995		50
	C5-11	Mochovce-4	VVER-440/213	388	432	EMO	SKODA	1983–10	1996		30
Czechoslovakia Republic	C5-23	Temelin-1	VVER-1000	892	972	ETE	SKODA	1984	1992–05		50
	C5-24	Temelin-1	VVER-1000	892	972	ETE	SKODA	1985	1994–01		10
Russia	SU-99	Balakovo-4	VVER-1000	950	1000	MAEP		1984–04	1994	5/93	
	SU-114	Balakovo-5	VVER-1000	950	1000	MAEP		1987–04	1996		
	SU-115	Balakovo-6	VVER-1000	950	1000	MAEP		1988–05	2001		
	SU-60	Bashkir-1	VVER-1000	950	1000	MAEP		1983			
	SU-85	Bashkir-2	VVER-1000	950	1000	MAEP		1983–12			
	SU-130	Gorky	(heat only)		500	MAEP	1982				
	SU-36	Kalinin-3	VVER-1000	950	1000	MAEP	1985-10	1995	5/93	10	
	SU-120	Kursk-5	RMBK	925	1000	MAEP	1985-12	1995	5/93	60	
	SU-59	Rostov-1	VVER-1000	950	1000	MAEP	1981-09	Restart	5/93		
	SU-62	Rostov-2	VVER-1000	950	1000	MAEP	1983-05	Restart	5/93		
	SU-63	Rostov-3	VVER-1000	950	1000	MAEP	1989-01	Restart	5/93	60	
	SU-92	Tatar-1 (Kama)	VVER-1000	950	1000	MAEP	1987-04				
	SU-93	Tatar-2 (Kama)	VVER-1000	950	1000	MAEP	1988-05				
	SU-131	Voronezh	(heat only)-1		500	MAEP	1983-09				
	SU-135	Voronezh	(heat only)-2		500	MAEP	1985-05				
Ukraine	SU-41	Khmelnitski-2	VVER-1000	950	1000	MAEP		1985–02	1995	6/94	80
	SU-51	Khmelnitski-3	VVER-1000	950	1000	MAEP		1986–03	1997	6/94	50
	SU-52	Khmelnitski-4	VVER-1000	950	1000	MAEP		1987–02	1997	6/94	50
	SU-69	Rovno-4	RMBK	950	1000	MAEP		1986–08	1996	6/94	
	SU-49	South Ukraine	VVER-1000	950	1000	MAEP		1987–01			50
	SU-127	Zaporozhe-6	VVER-1000	950	1000	MAEP		1986–04	1994	7/94	95
Romania	R0-1	Cernovoda-1	CANDU	625	700	MME	AECL	1980–09	1994		
	R0-2	Cernovoda-2	CANDU	625	700	MME	AECL	1982	1995		
	R0-3	Cernovoda-3	CANDU	625	700	MME	AECL	1984	1997		
	R0-4	Cernovoda-4	CANDU	625	700	MME	AECL	1985	1998		
	R0-5	Cernovoda-5	CANDU	625	700	MME	AECL	1986	1999		

[a]Modified from International Atomic Energy Agency tables.

A third, less serious problem with neutronics was the slow speed of insertion of the shutdown rods. They were allowed to fall in, not with an acceleration caused by gravity of *"g"* but with the slowness resulting from having to unwind from a drum and also with the magnetic inertia of the control-rod motor. It took 20 seconds to insert them. Now a new and, I believe, additional shutdown system has been installed in *all* RBMK reactors that inserts the rods in 2 seconds.

Under hydraulics of the pressure tubes are two subheads: the effect of simultaneous rupture of several pressure tubes, which has been called the Achilles' heel of these reactors,[15] and methods to avoid simultaneous rupture of pressure tubes. Above the core of the RBMK is a small cavity, or upper plenum, covered by the 2000-ton reactor cover, which spans the 30 ft of the reactor itself. If the pressure rises to 40 psi or above in this cavity, the cover plate will lift and thus break *all* the pressure tubes and lift out *all* the absorbing control rods. At Chernobyl the cover plate was lifted, almost intact. A stereoscopic photograph taken from a helicopter at the time[16] shows it by the side of the reactor, although more recent examination from inside the sarcophagus suggests that it is at an angle above the reactor.[17]

A small pressure release tube slowly released steam from this cavity to the large pressure suppression pool below. A simple calculation shows that if three tubes break simultaneously, the pressure will rise enough to lift the plate. This is being changed in two reactors (Leningrad 1 and Smolensk 3) by adding a larger tube to release pressure faster.[11] This should be enough to protect the reactor if 12 tubes fail simultaneously. Other units will be fitted when long shutdowns occur to permit it. But this still leaves a dozen RBMK reactors unfitted.

The probability that two tubes fail simultaneously has been variously set at less than 10^{-6} per year[18] and 10^{-4} per year.[19] There are only three cases of *one* tube rupturing during operation, although leaks are common (about 100 cases). At Chernobyl Unit 2 in 1992 a tube ruptured when an operator inadvertently closed a valve at the coolant inlet. In March 1992 in Leningrad a tube ruptured as a result of a partial failure of the inlet valve. In neither case did a neighboring channel actually rupture, although serious damage occurred in one. This gives considerable reassurance. Some engineers have written that "reactor scram and ECCS [emergency core cooling system] appear to be adequate to preclude multiple tube rupture."[20] If the problem of tube rupture is decisively resolved, the major professional concern about the RBMKs will evaporate.

During 1993 and 1994, 100 man-years of Western European experts and an equivalent number from Russia were spent on detailed safety analyses of the RBMK—using Ignalina 3 and Smolensk 2 as reference plants. These included a probabilistic risk assessment (PRA). Fourteen key recommendations were made to improve safety (Table 3). These would, if implemented, reduce the core-melt frequency to a number comparable to that of Western plants.[21] Reference 21 states, "Eastern members noted with satisfaction that Western members have discovered no fundamental safety issue that would justify a call for the premature closure of RBMK reactors." There is still no containment, however, and a core melt is likely to be catastrophic in an RBMK, unlike the core melt at Three Mile Island (TMI), which was contained in the reactor vessel. Western safety experts still argue, therefore, that RBMKs should be replaced as soon as possible.

SAFETY OF THE VVER SERIES

The VVER does not possess some safety features common in Western reactors, but it has some inherent positive features, such as a large water inventory and low power density. Safety analyses show that the most probable cause of disaster in an American pressurized-water reactor (PWR) or boiling-water reactor (BWR) is "station blackout" during some malfunction when the reactor has scrammed. The core of an American or western European reactor might start to melt after 1.5 hours of such isolation. In contrast, Soviet reactors have survived without apparent damage for 8 hours under these conditions. Although only a detailed analysis can show what the safety margins actually are for any particular power plant, the following design deficiencies of the VVER-440/230 are compared with those of the Western PWRs.[22–24]

1. Absence of containment for pipe breaks above 100 cm in diameter [written as 100 cm in one of the above references] compared with 200 cm for Western plants.
2. No substantial ECCS.
3. Failure to separate critical electric and fuel systems, which makes them sensitive to common-mode failures.
4. Inadequate fire protection.

These deficiencies can be discussed only on a case-by-case basis because many reactor owners have installed additional features that reduce these design deficiencies.

Table 3 The Most Important Key Recommendations for RBMK Safety[21]

1. Perform plant-specific safety reviews and develop plant-specific safety analysis reports for all nuclear units.
2. Develop and install a diverse scram system.
3. Install full-scope emergency core cooling systems (ECCSs) on all first-generation units.
4. Ensure introduction of advanced absorber rods to eliminate the void reactivity effect connected with the loss of water in the containment purge system (CPS) channels.
5. Upgrade the control and protection system to enhance its reliability and efficiency as well as to minimize the consequences of human errors.
6. Provide equipment for improving in-service metal inspection of the primary circuit.
7. Perform verification and validation of the transient thermal–hydraulic and neutronic codes on the basis of comparison with experimental data and other applicable codes.
8. Investigate and solve the problem of multiple pressure tube ruptures.
9. Equip all RBMK reactors with filtered ventilation systems designed to prevent radioactive releases during major accidents.
10. Develop methods for using operational experience and create a centralized data base on RBMK operation.
11. Make design changes to protect safety systems (CPS, ECCS, and emergency power supply) against common-mode failures like fire.
12. Provide plant-specific simulators for regular personnel training, recovery of the skills, development of procedures, etc.
13. Review the safety management system and implement the safety culture enhancement measures.
14. Legalize regulatory regime in Russia by adopting the Nuclear Energy Law.

In Finland, for example, a Western-style containment vessel has been installed, which has led some humorists to call them the "Eastinghouse" reactors. The absence of a Western-style containment is the most important feature that leads Western countries to urge early replacement of the VVER-230s.

The VVER-440/213 reactor is more modern than the VVER-440/230. It has some degree of containment with a bubbler suppression and a large volume inside the partial containment. The containment has never been tested, however, so it is unclear what range of accidents will be contained. The Czechs and the Hungarians argue that they will run the reactors no matter what the outcome of such a test, so why bother about the test? But this is a narrow view of a test program. A test might suggest small modifications that will greatly enhance the range of accidents that are contained. Therefore Western help has been provided for such tests, which are proceeding.

West German experts made recommendations for safety improvements at the four East German VVER-440/230 reactors at Lubmin Nord.[24] Because at that particular moment there was an excess of generating capacity in West Germany, it was decided to shut them down (together with a VVER-440/213) rather than to upgrade them. Three other VVER-440/213 reactors under construction at Lubmin Nord and two VVER-1000 at Stendal were canceled at the same time.

All experts seem to agree that the four VVER-440/213 reactors at Paks in Hungary are operated well. This seems to be appropriate for a country that gave birth to Von Neuman, Teller, Wigner, and Szilard. Furthermore, two VVER-440/230 reactors at Bohunice in the Czech Republic and 6 VVER-440/213 reactors at Bohunice and Dukovany also seem to be well run. The reactor vessels made at the Skoda works in Slovakia are of a higher quality than those originally made in Russia, although the pressure vessels at Bohunice still needed the annealing that the early Russian reactors demanded to avoid radiation damage. There is, however, considerable concern about the two older VVER-440/230 reactors in Bulgaria, particularly because the earthquake hazard in Bulgaria is not negligible.[25] The two VVER-1000s in Bulgaria have a good containment but a poor availability record. This seems to be due to xenon oscillations, which arise because of the tall, narrow core design. It should not be a fundamental or expensive task to fix the xenon oscillations because the Russians and Ukrainians seem to have overcome the problems. If they can be fixed,

enough additional electricity could be generated to equal the output of two VVER-440 reactors and thereby bring a shutdown of these less-safe reactors somewhat closer.

SAFETY ASSISTANCE FROM THE UNITED STATES

Safety assistance to the former U.S.S.R. and eastern Europe comes in three ways: (1) through the International Atomic Energy Agency (IAEA) by participation and membership of its committees; (2) through formal U.S./U.S.S.R. cooperative agreements, which set up a Joint Coordinating Committee for Civilian Nuclear Reactor Safety (JCCCNRS) on April 26, 1988; and (3) through industry and private initiatives.

The joint U.S./U.S.S.R. efforts have been extended for another 5 years with two separate agreements between the United States and the Russian federation and between the United States and the Republic of the Ukraine. Joint agreements have been negotiated with Hungary, Czechoslovakia, and Poland.

A budget of $21.9 million was available in FY 1992 for JCCCNRS activities. Funds rose rapidly in late 1993 and in 1994 to nearly $100 million. Although the American government personnel working in JCCCNRS seem to consider central European countries as part of their domain because the reactors are similar, this is not a part of the two agreements mentioned previously, and in 1992 only about $3 million was spent specifically on assistance to central European countries (defined here as countries other than Russia and the Ukraine). Again, this assistance is increasing fast.

The two committees met jointly at the end of March 1993 and again in May 1994.[26] The reports, however, are not very complete.

In respect to industry and private initiatives, the Institute of Nuclear Power Operations (INPO) in Atlanta has sent personnel and been involved with many meetings between Russians and Americans. The ANS has been arranging meetings. Private foundations, and in particular the Andrei Sakharov Foundation, the Soros Foundation, and the Macarthur Foundation, have arranged conferences, provided equipment, or aided information transfer. Individuals such as Dr. Milton Levinson, formerly of Bechtel Corporation; Dr. Robert Budnitz of Future Resources Associates; Professor Fred Mettler of the University of New Mexico; and me have become involved directly on an individual basis. Although at first this direct involvement often confused the Russians who were used to an authoritarian structure, they have now come to appreciate the alternative methods of information transfer and cooperate fully.

These are extensive funds from western Europe to help in various aspects of reactor safety. The European Community PHARE program in contrast allocated $11.5 million ECU (about $13.2 million) in 1991 for Bulgarian assistance. European assistance is also increasing. For the Ukraine alone, the G7 Summit approved $200 million in grants and as much as $600 million in loans, but this so far is on paper and subject to a commitment to shut down Chernobyl.

As usual, there is reciprocal criticism. U.S. experts complain that the assistance from European countries is uncoordinated—but Europeans complain that the U.S. effort is uncoordinated!

OPERATION

Although Western experts did not agree with the Russian emphasis on operator error as the principal cause of the Chernobyl accident, they did agree on its importance, and much of the Western help has been directed to improving operation. The most important contribution is the establishment of a safety culture.

All operators and staff members should think about safety in all their actions, knowing that their supervisors will encourage and support them. This is particularly hard in such societies as Russia, India, and China, where safety is not a feature of everyday life. Helping them to develop a safety culture needs patience and understanding. In Ref. 21, for example, the definition of *safety culture* in Russian regulations is more restricted than the IAEA definitions.

Designers should design a reactor so that even bad operation cannot lead to a serious accident, and operators should operate a reactor so that even a bad design is safe. The opposite seems to have been the approach in the U.S.S.R.! Even today Russians find it hard to understand why interlocks are necessary to prevent operators from breaking the rules about withdrawing too many control rods: "No good operator will violate this rule."[27]

Two large, full-scope simulators (costing $8 million each), one for a VVER-1000 and the other for a RBMK, were constructed in the INPO in Moscow with U.S. funds and help. They have been shipped to Zaparodze and Smolensk, respectively. A third simulator for a VVER-440, paid for by Japan, is now being built to be sent to Kola. The Russians have also widely praised the

visits of Russian and Ukrainian operators to U.S. power plants and reciprocal visits of U.S. operators to Russia and the Ukraine (jointly arranged by INPO and JCCCNRS).

FIRE SAFETY

At Vienna[9] the general in charge of the fire brigade described in great detail the major shortcomings of fire protection in the plant. The shortcomings were many and varied, from the absence of fire extinguishers to the presence of materials that were supposed to be inflammable but nonetheless burned readily.

The first U.S. visitors to Chernobyl after the accident[3,28] emphasized that the most important accident initiators for U.S. reactors are reactor trips with station blackout so that pumps cannot operate and fire, which can simultaneously destroy redundant systems. We were very cognizant of the Brown's Ferry fire in 1975, which resulted in the inability to operate coolant pumps for some time. Fire has been common in the nuclear reactors of the U.S.S.R. The Armenian reactor in about 1983 and a Ukrainian one in 1985 both suffered fire and blackout. Fortunately in the VVER-440, as mentioned previously, the large water inventory enabled them to sit for 8 hours without a problem. This contrasts with the situation for a U.S. reactor, in which the core is predicted to melt after 1.5 hours. At least a part of the difference is due to the large core inventory of the U.S. reactors. In 1988 at Ignalina (Lithuania) there was a fire in the cable room of an RBMK that could have been very serious. Less fortunate was Chernobyl Unit 2, which a turbine fire destroyed in 1990.

An important component of U.S. assistance has consequently been fire protection. The major part of this has been "walk-throughs" by U.S. personnel. Numerous recommendations for upgrades have been made and some executed. Steel fire doors are in Smolensk Unit 1, but it appears that the fire doors were replaced by wood (presumably because of cost or unavailability) in Units 2 and 3. This is being changed. Many millions are now being spent on such equipment for Russia and the Ukraine.

EVACUATION EXPERIENCE

After Chernobyl, everyone had a lot to learn from the Soviet experience in handling the accident. What was actually done and who did what? In retrospect was it sensible, or would those responsible do something different if the accident happened again? What procedural steps should be taken to ensure a better response in the future? How would such procedures depend on the particular cultural and political system? Unless one can understand the past, one is condemned to repeat it. At the August 1986 meeting many Russians said: "We will be preparing a full report within the next few months." The only report of use is that by Medvedev[29] (who was not at the 1986 meeting!). We still do not know who did what and when at the end of April and the beginning of May 1986, nor do we have a list of names and job descriptions of the 31 persons who died as a direct result of the Chernobyl accident. Were these brave individuals mostly fire fighters, as some maintain, or were they mostly reactor staff? What were they doing?

Chernobyl is being used as a political weapon in the post-U.S.S.R. political discussions; truth goes out the window, and those who had the misfortune of the awesome responsibility of coping with the accident are frantically defending their reputations, and perhaps even their personal freedom.[30] In the absence of careful reports by those concerned, there are many reports by other organizations. One strongly criticizes the authorities for not evacuating children and others from Kiev in May 1986.[31] Yet the data available to me at the time, and further data available now, suggest that, although preparations for an evacuation were appropriate and were made, actual evacuation would have been wrong. If the Russians and Ukrainians who were responsible can be persuaded to write these reports at long last, it will do more than anything else to reassure the public that any future emergency will be properly handled—and perhaps to reburnish their reputations.

SAFETY ANALYSIS

Russian mathematicians are probably the best in the world, and Russian theoretical physicists and statisticians can hold their own. Therefore it might have been expected that Russians would be good at theoretical reactor safety analyses. This is not the case. In particular, they are slow to adopt a systems approach.

This change from merely considering a design basis accident (and designing an engineered system to prevent or mitigate it) to performing a full PRA started with the Reactor Safety Study[32] but only took hold after TMI. The Russians are only just beginning to understand the importance of this change.

Before 1986, Russians were welcomed at conferences where safety matters were discussed, but they usually remained silent. Even as late as 1991, Russian safety experts would take refuge in an "official" view. This changed in 1991,[33] where at a conference Russian experts started arguing among themselves. But they are still not routinely considering the problems of successive failures.[8]

Until 1993 the international assistance from IAEA seemed to be addressed only to *design basis accidents*, which do not seem, for example, to include the simultaneous failures of several pressure tubes in an RBMK.

New Reactors Coming on Line[11,34]

After Chernobyl, a few reactors were completed, but construction and planning for many others were stopped (Table 4). Now that energy problems have become apparent, various Soviet authorities have announced that construction will be resumed.[11] It is always hard to understand the approval processes of another country, so it is unclear when an approval is final.

Russia. Balakovo Unit 4 (VVER-1000) (PWR) should be finished in 1994, Kalinin Unit 3 (VVER-1000) (PWR) should be finished in 1995, Kursk Unit 5 (RBMK) should be finished in 1995, and Rostov (two units) (VVER-1000) (PWR) will finally be started and perhaps finished before the year 2000.

Ukraine. The following will probably be completed, and Western help to finish them and bring them to Western safety standards was discussed:[35] Zaparozhe Unit 6 (VVER-1000) (PWR) should be finished in 1995, Khmelnitski Unit 2 (VVER-1000) (PWR) should be finished in 1996, Rovno Unit 4 should be finished in 1997, and two units in South Ukraine (VVER-1000) should be finished by the year 2000.

Belarus. Belarus is discussing whether to build its own nuclear power plant.

Czech and Slovak Republics. In the Czech and Slovak republics, four more VVER-440/213s are under construction at Mochovce and two VVER-1000s at Temelin. Citibank of New York has made a $300 million loan to complete the Temelin reactors, and Westinghouse has been awarded the contract to complete them..

Armenia. Armenia has two VVER-440/230 reactors, which operated through 1989, even during the 1988 earthquake. Somewhat more than 2 million people live within 30 miles of these uncontained reactors. They were shut down soon after the earthquake in response to influential opposition; however, the present energy crisis in Armenia, caused by unfriendly neighbors, encouraged the government in 1992 to propose their reopening. The complete process of recommissioning will take 12 to 18 months. The Armenian government made the decision in April 1994, and the Russian government agreed to help provided that the Armenian government pays. The restart of Unit 2 is anticipated in 1995 and of Unit 1 in 1996. A safety review committee of the European Bank for Construction and Development is expected to visit in June 1995. The major public concern is not from inside out but from outside in. Because there is no containment, an Azeri mortar shell might set off a serious accident.

Two VVER-440/213 reactors under construction at Zarnowic in Poland and two VVER-1000 reactors at Paks in Hungary were canceled after Chernobyl. No restart of construction has been announced.

PROPOSED NEW RUSSIAN REACTOR DESIGNS

Beyond the year 2000 there are three projects for new safer reactors: the NP500, the NP1000, and the MKR900.[11] The NP500 is to be an evolution of the VVER-440 reactors. It will have six primary coolant loops. The following safety features will be in the NP500 design:

- Double containment systems.
- As large a margin of water as in the VVER-440 four systems of safety (shutdown).
- Estimated probability of core melt of 10^{-5}.

This reactor will look somewhat like the U.S. project, the AP600. It is interesting that the Russians are adding U.S. safety features to the VVER-400, and the United States is reducing the power density and increasing the water inventory in the AP600, which makes it more like the VVER-400! Both countries are incorporating the good features of each design. The NP1000 will be a larger version of NP600.

The MKR900 is a liquid-metal-cooled reactor (a fast breeder that is also usable as a plutonium burner). This is being designed by Professor Adamov. The plan is to locate it in the Urals, perhaps near Belyoarsk. It would be convenient for getting rid of the actinides in the nuclear wastes in the Urals as well as the stocks of military plutonium.

Table 4 Reactors Shut Down as of Dec. 31, 1991

Country	Reactor Code (IAEA)	Reactor Name	Type and model	Capacity, MW(e) Net	Capacity, MW(e) Gross	Operator	NSSS supplier	Construction start	First criticality	Grid connection	Commercial operation	Shutdown
Armenia	SU-18	Armenia-1 (restart 1996)	VVER-440/230	376	408	MAEP		1973–01	1976–12	1976–12	1979–10	1989–02
	SU-19	Armenia-2 (restart 1997)	VVER-440/230	376	408	MAEP		1975–07	1979–12	1979–12	1980–05	1989–03
Czchslvk	CS-1	A-1 Bouhunice	HWGCR	110	144	EBO	SKODA	1958	1972	1972–10	1972–12	1979–05
Germany	DE-502	Greifswald-1	VVER-440/230	408	440	VE	AEE	1970–03	1973–11	1973–12	1974–07	1990–12
	DE-503	Greifswald-2	VVER-440/230	408	440	VE	AEE	1970–03	1974–12	1974–12	1975–04	1990–02
	DE-504	Greifswald-3	VVER-440/230	408	440	VE	AEE	1972–10	1977–10	1977–11	1978–05	1990–02
	DE-505	Greifswald-4	VVER-440/230	408	440	VE	AEE	1972–10	1979–07	1979–08	1979–11	1990–06
	DE-506	Greifswald-5	VVER-440/213	408	440	VE	AEE	1976–12	1989–03	1989–04	1989–11	1990–11
	DE-	Greifswald-6	VVER-440/213	408	440	VE	AEE		Stopped			1990
	DE-	Greifswald-7	VVER-440/213	408	440	VE	AEE		Stopped			1990
	DE-	Greifswald-8	VVER-440/213	408	440	VE	AEE		Stopped			1990
	DE-	Stendhal-1	VVER-1000						Stopped			1990
	DE-	Stendhal-2	VVER-1000						Stopped			1990
Hungary	HU-	Paks-5	VVER-1000						Stopped			1990
	HU-	Paks-6	VVER-1000						Stopped			1990
Lithuania	SU-72	Ignalina-3	RMBK	1380	1500	MAEP		1985–06	Stopped	5/93		
Poland		Zarnowici-1	VVER-1000						Stopped			1987
		Zarnowici-2	VVER-1000						Stopped			1987
Russia	SU-3	Beloyarsky-1	RBMK	102	108	MAEP		1958–06	1963–09	1964–04	1964	1983
	SU-6	Beloyarsky-2	RBMK	146	160	MAEP		1956	1967–10	1967–12	1969–12	1990–01
	SU-37	Kalinin-4	VVER-1000	950	1000	MAEP		1986–08	Stopped			
	SU-121	Kursk-6	RMBK	925	1000	MAEP		1986–08	Stopped			
	SU-4	Novovoronezh-1	VVER-440/230	197	210	MAEP		1957–07	1963–12	1964–09	1964–12	1988–02
	SU-8	Novovoronezh-2	VVER-440/230	336	365	MAEP		1964–07	1969–12	1969–12	1970–04	1980–08
	SU-68	Smolensk-4	RMBK	925	1000	MAEP		1984–10	Stopped			
Ukraine	SU-26	Chernobyl-2 (fire)	RBMK	925	1000	MAEP		1973–02		1978–12	1979–05	1992
	SU-43	Chernobyl-4 (explosion)	RBMK	925	1000	MAEP		1979–04	1983–12	1983–12	1984–03	1986–04

There is another project, the VPBR600, which Professor Musibkov is working on (my notes are not clear on the name spelling) from Nishni Novgorod. This would not be an evolutionary reactor but a *revolutionary* reactor that follows some features of the RBMK but with a containment and passive cooling after shutdown.

A joint venture has recently been set up for the design of a high-temperature, gas-cooled reactor together with General Atomic in the United States. This would use a gas turbine to generate electricity.

It is clear that these reactors cannot all be built, but no priority has been set.

CONCLUSIONS

The worldwide interest in ensuring the safety of nuclear reactors in eastern Europe and the former Soviet Union is only just bearing fruit. The Russians have had problems understanding the importance of a safety culture in their society, and the West has had problems understanding that each country must make its own decisions and all the West can do is to offer help. The present political instability in Russia and the Ukraine makes it essential that the West continue to approach these problems with understanding, patience, and a true spirit of cooperation—especially since the financial aid that can be given is limited and is still a small fraction of the replacement cost of the less safe reactors the West would like to see shut down.

ACKNOWLEDGMENTS

This report would not have been possible without the free and open cooperation of a large number of scientists who have provided me with information. They come from various organizations in Russia, Ukraine, Belarus, central and western Europe, and Japan as well as the United States. In some cases I have quoted their opinions directly; in others they have provided reports. To all of them I express my thanks.

REFERENCES

1. N. A. Dollezhal and Emylianov, Graphite-Water Steam-Generating Reactor in the USSR, *Nucl. Energy,* 20(5): 385-390 (1981).
2. R. Wilson, What Really Went Wrong? *Nature,* 323: 29 (Sept. 4, 1986).
3. R. Wilson, Visit to Chernobyl, *Science,* 236: 1636-1640 (June 26, 1987).
4. D. W. Dockery, C. A. Pope, X. Xu, J. D. Spengler, J. H. Ware, M. E. Fay, B. G. Ferris, and F. E. Speizer, *New Engl. J. Med.,* 329:1753-1759 (1993) and references therein.
5. V. F. Demin, V. A. Legasov, and Y. V. Shevalev, Is it Necessary to Know the Extent of Safety Provisions? *Energiya* (1984) (Russian). See an unfavorable comment on this by V. N. Soifer, A Collision Course in Catastrophe, *Chicago Tribune,* 2 May 1987, Sec. 1, p. 13. For a Western approach, see D. Okrent, *Science,* 236: 296 (1987).
6. American Nuclear Society, Workshop on Safety of Soviet-Designed Nuclear Power Plants, Chicago, Ill., Nov. 21–22, 1992, compilation of papers. Available from Dr. Edward Warman, Stone and Webster Corp., Boston, Mass., 1992.
7. World Bank reports on energy problems in Lithuania, Ukraine, Bulgaria, Slovakia, and Armenia, 1993.
8. A. Birkhofer, presentation at retirement symposium for Professor N. F. Rasmussen, Massachusetts Institute of Technology, 1993.
9. V. A. Legasov, in IAEA Report of Russian delegation to IAEA experts meeting, August 1986.
10. International Atomic Energy Agency, Report of the INSAG 7 Committee, 1986.
11. A. Abagyan, Extensive private discussions with Professor Armen Abagyan of the Institute of Nuclear Power Operations, 1993.
12. Valerii Legasov, in *Safety Assessment of Proposed Improvements to RBMK Nuclear Power Plants,* IAEA TECDOC-694, International Atomic Energy Agency, 1993.
13. Y. Petrov, Petersburg Nuclear Physics Laboratory, Gatchina, Leningrad District.
14. Burlakov and Krayushkin, Report IAEATC-805, International Atomic Energy Agency, 1992.
15. M. Levinson, reports at many scientific meetings, 1986.
16. E. Velikhov, shown at a meeting in Rome in November 1985.
17. A. Sich, Thesis, Nuclear Engineering Department, Massachusetts Institute of Technology, 1994.
18. Voronin, Deputy Director, Institute of Nuclear Power Operations, Moscow, private communication, 1993.
19. Comment by Professor Adamov, Director of the Russian Development Institute for Power Engineering (NTEC), which designed the RBMK, 1993.
20. Minutes of IAEA Review Meeting in Smolensk, June 1993.
21. "Safety" of Design Solutions and Operation of the NPP with RBMK Reactors RBMK/CMC/FR, Issue 1, presented in Brussels, Belgium, June 10, 1994.
22. International Atomic Energy Agency, *Ranking of Safety Issues for VVER-440 Model 230 Nuclear Power Plants: Report of the IAEA Extra Budgetary Programme,* IAEA TECDOC-640, 1992.
23. U.S. Department of Energy, *Department of Energy's Team Analyses of Soviet Designed VVERs,* USDOE Assistant Secretary for Nuclear Energy, Report DOE/NE-0086-Rev 1, September 1989.
24. Gesellschaft fur Reaktorsicherheit, *Safety Assessment of the Greifswald Nuclear Power Plant Units 1 to 4,* Report GRS-78, 1991.
25. M. J. Griffin, L. J. Brogagnolo, and P. I. Yanev, 1992, *The December 7th 1988 Armenia Earthquake,* Report EPRI-NP-7359-M, 1991.
26. JCCCNRS, Record of the First Joint Meeting of the US–Russian and US–Ukraine Joint Coordinating Committees for Civilian

Nuclear Reactor Safety, March 30–31, 1993, at Kiev in Ukraine, USNRC Report SECY-93-094, 1993. Report of second meeting, Moscow, May 16–17, 1994.
27. Two senior reactor operators from CIS privately expressing puzzlement (at a meeting in the USA) that an interlock is necessary, 1993.
28. F. Bernthal, private report of official visit of NRC Commissioner, 1987.
29. G. Medvedev, *Novy Mir* (translated by Basic Books), 1990.
30. Senior members of both the Russian Government and the Belarus Government orally expressed to me the view that "Professor X and Professor Y" (names quoted, but withheld here) should go to jail, 1993.
31. Report of Independent Lawyers Committee on the Effects of the Chernobyl Accident, Kiev, 1993.
32. N. F. Rasmussen et al., *The Reactor Safety Study,* AEC Report WASH-1400, 1985.
33. A. Birkhofer, Report of Workshop on "What Happened," First International Sakharov Conference on Peace Progress and Human Rights, Moscow, May 21, 1991.
34. A. Abagyan, private communication, May 21, 1994.
35. Newspaper reports and various working papers for the G7 Summit Meeting, July 1994.

Safety of Nuclear Power Reactors in the Former Eastern European Countries

By S. Chakraborty[a]

Abstract: *This article discusses the safety of nuclear power plants in the former Eastern European countries (including the former Soviet Union). The current international design, fabrication, construction, operation, safety, regulatory standards and practices, and ways to resolve plant problems are addressed in light of experience with the Western nuclear power development programs.*

The investigation after the accident at the Chernobyl nuclear power plant reaffirmed that the design, operating procedures, and regulatory safety principles of Soviet-designed and -constructed nuclear power plants are afflicted with intractable problems that emanate from sociological, economic, and political problems of the closed, state-controlled societies.

The changing political and economic landscape in Eastern Europe and the countries of the former Soviet Union (FSU) has heightened the concerns about the safety of nuclear power plants currently operating in these countries. The situation is compounded with the economic, social, and political problems that have ensued since the breakup of FSU-dominated Eastern Europe. Reviews performed by several international organizations, including those of the International Atomic Energy Agency (IAEA),[1] the Organization for Economic Cooperation and Development (OECD) countries, and several other countries, have identified many concerns related to design, siting (i.e., plant sites near major tectonic faults), operation, maintenance, management, safety culture, and regulatory mechanisms in the nuclear power industries of the FSU and the former Eastern Bloc countries.

The largest barrier to solving these problems and implementing the needed improvements is economically based. Another problem is that the universe of safety concerns keeps growing not only because of the shortcomings in design and operations but also because of the lack of available information.[1]

Severe electricity shortages, an increased demand for electricity, and the large dependence on nuclear power reduce the likelihood of taking some of these power plants out of operation.[1–3] Today 57 nuclear power reactors are operating in Eastern Europe and countries of the FSU. Collectively, these operating plants generate a substantial portion of electricity in the region: nearly 60% in Lithuania, 51% in Hungary, 36% in Bulgaria, 29% in Czech and Slovak republics, 25% in the Ukraine, 12% in the Russian Federation, and 12% in Kazakhstan.[1] If the decision is made to restart the shutdown reactors in Armenia to overcome critical shortages there, the reactors could account for 25% of that country's total electricity supply.

The objective of this article is to discuss the safety concerns with the Eastern nuclear power plants and ways to address the problems on the basis of the experience with the Western nuclear power development programs and current international design, fabrication, construction, operation, safety, and regulatory standards and practices.

[a]Swiss Federal Nuclear Safety Inspectorate, Ch-5232 Villigen-HSK, Switzerland.

PROBLEMS WITH SOVIET-TYPE NUCLEAR POWER PLANTS

The problems that have surfaced since the Chernobyl accident and since the breakup of the countries under the former Soviet sphere of influence result from several factors, including inadequate designs, substandard fabrication, faulty construction practices, insufficient resources, neglected safety culture, inadequate regulatory mechanisms, lack of access to modern mathematical models/analysis tools, and lack of sufficient information and understanding of design and safety issues peculiar to Soviet-designed reactors.[3–5]

Currently, 57 nuclear power plants are in operation and 13 are under construction in Eastern Europe and the Commonwealth of Independent States (CIS). These plants consist of 10 VVER-440 Model 230s, 14 VVER-440 Model 213s, 19 VVER-1000s, and 14 Chernobyl-type graphite-moderated reactors (RBMKs). The 10 first-generation VVER-440 MW Model 230 units have the most serious design deficiencies. Two units in Armenia and four in Eastern Germany have already been shut down. Some of the more pressing design deficiencies of the 14 second-generation VVER-440 MW Model 213s have already been remedied.

The VVER-1000 is the most modern Soviet-designed nuclear power plant in service. These units are similar in concept to the Western-designed pressurized-water reactors (PWRs), which feature a reactor surrounded by a full containment structure and are used worldwide. These power plants have the least serious safety deficiencies; nevertheless, there are concerns related to instrumentation and control systems, performance of steam generators, and reactor power stability.

There are 15 operational RBMKs of three design generations: 2 1500-MW units (the world's largest nuclear power reactors) in Lithuania, 11 1000-MW units in Russia, and 2 at Chernobyl in Ukraine. One unit is under construction in Russia.[5]

In general, the design and construction inadequacies result from a lack of a consistent design basis, failure to account for adequate separation and system redundancies, and insufficient fire protection and seismic support systems. Resource constraints are particularly evident in all aspects of power plant maintenance and support. Plant layouts and piping and flow diagrams are not always available and consistent with the as-built facility. Safety studies are not comprehensive and lack adequate and full documentation. Basic spare parts and components, such as valves, pumps, and instrumentation, are in short supply. This supply problem is even more severe in the countries outside the Russian Federation. Most of these countries lack the economic means to acquire Russian-made components and spare parts.[4]

The problem of inadequate resources is also affecting personnel training at all levels of nuclear power plant operation. A large number of experienced scientists, engineers, and technicians are leaving their posts for better financial rewards elsewhere. This economic and industrial stagnation is also affecting the morale of the power-plant engineers and support personnel. Daily economic chores detract attention from a worker's normal responsibilities and duties.[4]

Conditions are even worse for the nuclear regulatory side of the industry. Rampant inflation; the government's inability to meet workers' needs; the lack of adequate controls, a proper mandate, and a clear sense of direction; and limited authority for oversight have led many to leave their posts. The lack of a clear government policy for nuclear regulation compounds this morale problem.

Little attention has been paid to nuclear safety culture in the former Eastern Bloc countries. Inadequacies in nuclear safety culture seriously affect the safe operation of the nuclear power plants in these countries. Recent reviews reveal that inadequacies exist in all aspects of nuclear power development, including system design practices, selection of sites, construction habits, operating procedures, training, maintenance practices, and accident response procedures.

Lack of adequate attention to the details of industrial safety practices by nuclear plant operators, together with inadequate regulatory requirements, resource constraints, and a clear national nuclear safety policy, is hindering implementation of many of the safety improvements that have been proposed through many international programs. This is perhaps the most significant hindrance to nuclear safety within the former Eastern Bloc nuclear industries. Even if design deficiencies, regulatory shortcomings, and operating procedures are corrected, without very serious attention to safety culture, a measured improvement in the nuclear power safety in these countries could not be achieved.

WESTERN NUCLEAR SAFETY PRACTICES

Since the early days of nuclear power development in the West, safety has always been given the first and foremost attention. This includes consideration of measures for accident prevention and accident mitigation within the design basis. Stringent codes and standards

were set for the design, fabrication, and construction of nuclear power reactors, and regulations were promulgated at the national level to ensure the safe operation of nuclear power facilities (Fig. 1).

Consistent with the defense-in-depth philosophy (Fig. 2), the evolution of the Western nuclear power reactor technology has always relied on multilayers of protection consisting of a fuel matrix structure, reactor-coolant-system boundaries, and a containment building for inhibiting radiological releases to plant workers, the general public, and the environment during potential malfunctions. Traditionally, the licensing process for Western nuclear power plants has focused on the concept of design basis accident (DBA), which excluded accidents that involved severe core damage. The nuclear power plants were assessed on the basis of a deterministic framework for a predetermined spectrum of accidents that were assumed to be limited by design to prevent potential core damage and to comply with the required radiation protection standards.[6] This approach was based on the premise that severe reactor accidents that involve multiple failures of emergency systems and protection barriers were of very low likelihood and could therefore be excluded from the DBA envelope. Following the accident at the American Three Mile Island Nuclear Station Unit 2 (TMI-2) in 1979, however, and as a result of extensive probabilistic and deterministic studies dealing with the evolution of severe accidents, considerable changes are taking place in the approach to employee training and the operation, maintenance, and regulation of nuclear power plants. Consideration of accidents beyond the traditional DBA envelope has become an integral part of the safety decision-making process. Figure 3 displays the underlying advanced safety concept.

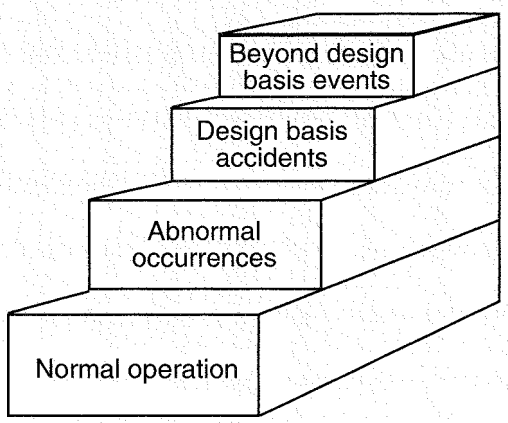

Safety stairs

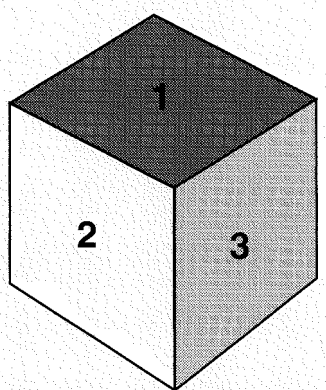

1: Retention of core melt in containment
2: Maintaining short- and long-term containment functions
3: Assurance of long-term decay heat removal

Fig. 1 Typical western safety concept.

Plant-specific probabilistic safety analyses (PSAs) are being used to determine specific plant and containment-system vulnerabilities. These studies attempted to realistically address the potential likelihood of multiple failures leading to loss of core cooling and ultimately core damage. Results of human reliability and PSA studies are being used to modify operating procedures, upgrade control-room designs, and improve human–machine interfaces. PSA is a powerful technique for providing a numerical assessment of safety. An inevitable mathematical consequence of considering the PSA is that there is no such thing as zero risk—the probability simply gets smaller and smaller as more is done to reduce it.

Safety has become an integral element of management, organization, and operational maintenance. It is practically impossible to economically design systems to exclude all potential accidents; therefore the defense-in-depth concept is being extended to cope with accidents beyond the DBA envelope. Severe accidents, even highly unlikely, should be dealt with within the current design of the plant and containment systems. Therefore accident management programs are being implemented to extend emergency operating procedures to deal with accidents beyond the traditional design bases, including core damage scenarios. These, together with sometimes overly zealous regulatory oversight, have led to an ever-improving operational record for the Western commercial nuclear power industry. The Western nuclear power experience shows that the most important factor of safe operation of the nuclear power industry is the

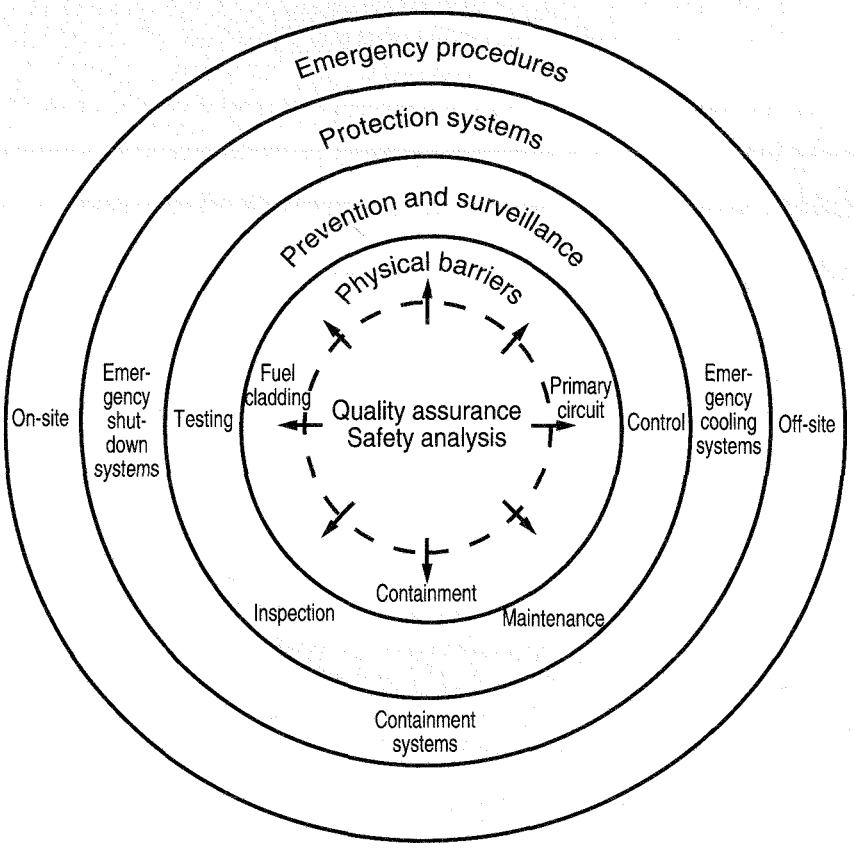

Fig. 2 The concept of defense-in-depth. (Source: Achieving Nuclear Safety, OECD/NEA, 1993.)

Objectives	General nuclear safety objective	Radiation protection objective	Technical safety objective				
Fundamental management principles	Safety culture	Responsibility of operating organization	Regulatory control and verification				
Defense-in-depth principles	Defense in depth	Accident prevention	Accident mitigation				
General technical principles	Proven engineering practices	Quality assurance	Human factors	Safety assessment and verification	Radiation protection	Operating experience and safety research	
Specific principles	Siting	Design	Manufacturing and construction	Commissioning	Operation	Accident manage-ment	Emergency prepared-ness

Fig. 3 INSAF safety objectives and principles for nuclear power plants. (Source: Basic Safety Principles for Nuclear Power Plants, Safety Series 75-INSAG-3, International Atomic Energy Agency, 1988.)

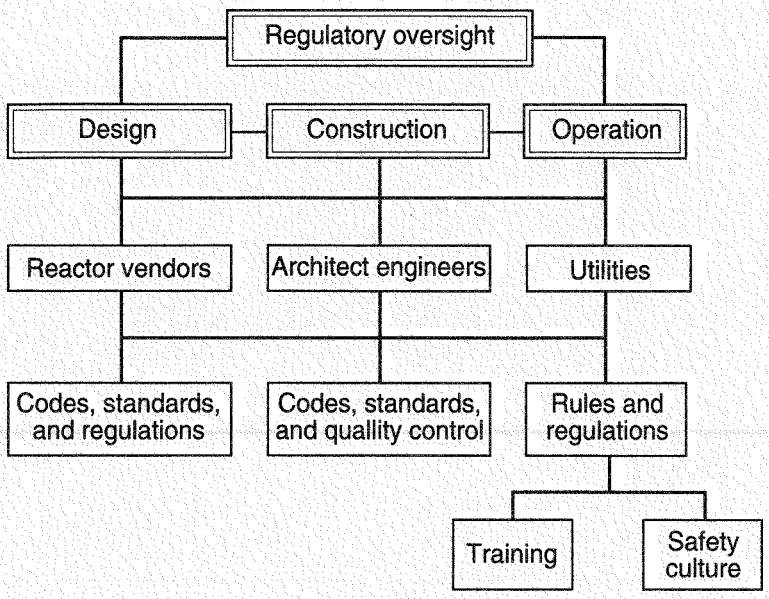

Fig. 4 Interplay of regulations and nuclear power.

implementation of safety culture within the operating and management environment of nuclear plant operators and their oversight/regulatory bodies. Figure 4 shows the interplay of regulatory oversight on the design, construction, and operation of modern nuclear power reactors.

Typically, regulatory oversight is exercised at all levels of design, construction, and operation. The design process is strongly tied to top-level safety requirements and is also governed by applicable codes, standards, and regulatory criteria. Applicable codes and high construction standards govern the construction of Western nuclear power plants. The existing national and international regulations are strictly enforced by the nuclear operators; however, the ultimate responsibility for plant safety falls under the operating utility management organization. Safety is a culture and cannot be imported, purchased, or imposed through regulations alone.

Before power operation is permitted, all operational power plants in European Community countries are subject to comprehensive and detailed reviews of the safety of their design, construction, commissioning, and proposed operating regime. In addition, the operating staff and the regulatory staff, who, in general, have previous relevant operating or regulatory experience, receive adequate training. The operating staff familiarize themselves with the plant in the design, construction, and commissioning phases. During operation, the operating regime of every nuclear power plant is constantly subject to inspection and assessment by the national regulatory body.[6]

As the Western nuclear industry has matured, its safety standards and practices have changed as a result of operational experience, new concepts in safety, and better analytical methods. One consequence has been a growing uncertainty regarding the extent or need for operational plants to satisfy the safety standards and practices being applied to new power plants. The demand for high safety standards can be satisfied in several ways. Experience in the regulation of nuclear safety in the European Community caused regulators in the Western countries to consider that the high safety standards required of the operating nuclear power plants needed supplementation to the existing regulatory arrangements through occasional Periodic Safety Reviews (PSRs). Regulators in some other countries prefer alternative arrangements, such as occasional generic reviews of specific safety issues and full clearance of new problems or changes in standards and practices as they arise.[6]

APPROACH TO SAFETY ENHANCEMENT

In this section the approach to improving the safety of nuclear power reactors in the former Eastern Bloc countries is proposed on the basis of the lessons learned from Western nuclear power development, construction, and operation over the past 40 years.

A multipronged safety resolution approach consisting of the following is needed:

1. A rehabilitation of safety culture within the Eastern nuclear operations and regulatory process.
2. Development of a comprehensive nuclear regulatory process and safety acceptability criteria.
3. Assessment of plant vulnerabilities and the most cost-effective ways of plant modifications.
4. Development of programs for operational training, testing procedures, and maintenance.
5. Development of revised design standards and licensing procedures for the modernization of the Eastern nuclear power industries.

Safety is a culture of no limits. Nuclear safety is an evolving field. Operational experience with the various reactor types is growing, and the unresolved safety issues are slowly being addressed through international nuclear safety research programs. One of the major lessons of the TMI accident in 1979 was the relevance of the "human" element in the progression and evolution of the accident. The importance of the operator/human element was quickly recognized within the international nuclear safety community. In most cases control rooms were redesigned, operator training procedures were modified, operational environments were changed, and, above all, incentives for operational readiness and good practices were created. This important issue was reinforced in the 1980s by several other industrial catastrophes that clearly involved human errors of commission, including Chernobyl, Bhopal, and the Challenger explosion. Another major issue that surfaced after these catastrophes was the importance of management and organizational factors, which are all within the purview of safety culture and the human factors.

This issue is echoed by the latest update of the IAEA's International Nuclear Safety Advisory Group (INSAG) report on Chernobyl, which concluded that the lack of safety culture was at the heart of the problem in the FSU. The INSAG report states that there was a "... lack of safety culture, not only at the Chernobyl plant, but throughout the Soviet nuclear establishment at the time. Chernobyl like many other major disasters resulted from a fundamental failure of the institutions, in which it was embedded, to deal satisfactorily with safety." Therefore the human and organizational safety culture element is at the heart of the problem in achieving safety in the former Eastern Bloc countries. We must recognize the importance of the role of the human element from the initial design through the fabrication and construction, testing, operation, maintenance, and regulation of nuclear power plants throughout the world, in particular, the former Eastern Bloc countries.

The regulatory bodies must be reshaped with substantial outside assistance from IAEA and Western nuclear power nations. This can involve both financial and technical support and training. Modern computational methods, computers, and staff training in their use must also be made available to Eastern regulatory bodies for a slow development of modern licensing bases and standards. Recently, several countries have begun initiatives to help in building the necessary organizational structures for independent regulatory organizations in the various Eastern Bloc countries and countries of the FSU.

Economics and financial incentives must also be provided, at least in this initial transition period, to ensure maintenance of the necessary technical competence and quality for nuclear power oversight. Examples include the provision of temporary staff positions within the Western nuclear regulatory community (e.g., industry, utilities, regulatory bodies, and research centers) as a means of encouraging retention of nuclear safety expertise, indirect financial assistance to competent engineers, and direct transfer of Western know-how. Here again programs are just starting through various bilateral and multilateral initiatives.

Technical assistance must also be provided for development of a modern licensing process based on the most up-to-date research information. Assistance must also be provided to better understand the unique problems associated with RBMK-type reactors[7] for which relatively little technical information is available outside the FSU.

It is unlikely that the older generation of reactors (i.e., RBMKs and VVER-230s) will be totally upgraded, both for economic and technical reasons. Nevertheless, their immediate shutdown is not a viable option for many of these economically stranded nations; therefore, as a minimum, obvious deficiencies in design and operational procedures must be resolved immediately through direct Western assistance to avoid another catastrophe with wide-ranging implications for Western nuclear programs. The eventual decommissioning of some of these older reactors cannot be avoided, however.

Conversely, for the newer generation of power reactors (i.e., VVER-1000s) with a substantial life expectancy, a comprehensive safety reassessment is needed to identify the following:

Category 1: Crucial "short-term" obvious safety problems needing immediate attention.

Category 2: Less crucial "long-term" safety problems that either are not clearly obvious or are of lower priority than those in the first category.

Category 1 problems should be corrected as soon as possible with direct outside assistance and know-how, whereas Category 2 problems can be deferred to a longer-term safety resolution program that is best handled by operator countries with assistance, on an as-needed basis, from Western countries. The longer term Western assistance is probably more efficient if it is coordinated and a systematic program is developed. This program can include technical training, hardware, equipment, spare parts, and other support.

During the 1980s, the development and application of qualitative and quantitative safety criteria within the PSA framework took place. Considerable advances were made in the development of PSA methodology and its application for identification of plant vulnerabilities and in the resolution of a host of outstanding safety-related issues. Shutdown heat removal and reliability of a-c power represent just two important examples. The accident precursor studies represented an important new application of PSA methodology. The lessons learned from all incidents must be fully implemented everywhere. Continuous verification of a plant's operational safety level by performance indicators, specific probabilistic safety evaluations, internal audits, and peer reviews should be introduced as an early warning system for possible safety degradation and to help prevent any serious incident. The Swedish program is an excellent example. In this program the daily operating information from the 12 operating plants is entered into their living PSAs to observe trends among the plants and determine their effect on potential failures.[8]

The safety improvements that are a prerequisite for a reliable nuclear power industry encompass not only reduction of risk from severe accidents but also reduction of economic risk (which could threaten the fragile national economy of Eastern Europe and CIS) and improvements in operational reliability. International bodies such as IAEA can help by enabling access to experts and by establishing objective measures of safety. International reviews of regulatory programs are useful to ensure that the structure is effective and credible. For public confidence at the international level, Western researchers must join with their Eastern colleagues to help the former Eastern countries address these pressing problems.

The longer term safety enhancement should include several important elements, such as the following. Operation and maintenance procedures should be reassessed, and to the extent possible, symptom-based plant-specific Emergency Operating Procedures should be devised and plant operators should be trained to follow them. Training simulator centers should be built with outside assistance to upgrade the training of the Eastern nuclear operators. A clear line of authority should be established at the power-plant organizations to be able to deal correctly with potential mishaps and accident conditions. A comprehensive operating data collection process is also needed for Soviet-designed reactors to improve future trending and PSA studies to support reactor operations. Maintenance procedures that consider the realities of Soviet-designed power plants should also be devised.

Plant-specific accident-management and accident-mitigation procedures should also be developed to deal with severe accidents. One phase of accident management covers the actions taken during the course of an accident by the plant operating and technical staff to prevent or minimize off-site radiation releases, gain control, and return the plant to a safe shutdown state. Inherent in accomplishing these goals is obtaining a clear picture of the nature of the accident and plant status. A systematic evaluation of accident-management information sources and their application is the right path to control the potential risk of operating plants in Eastern Europe and CIS.

Rigorous attention must be paid to the safety of plants while they are shut down for refueling and maintenance. Outage Risk Management Guidelines are under development in various Western countries. Similar guidelines should be developed and implemented for Eastern plants.

Finally, on a much longer time frame, researchers should work to harmonize and develop revised nuclear power-plant design standards[9] and licensing procedures for modernization of the international nuclear power industries. These design and safety standards require consistency with state-of-the-art understanding of the existing power-plant operations, and the potential for new reactor development activities in worldwide nuclear safety research will guide future nuclear power development.

REFERENCES

1. V. Gillen (Ed.), *International Assistance to Upgrade the Safety of Soviet-Designed Nuclear Power Plants, An Overview*, Report INIS-mf-13818, December 1993.
2. N. Steinberg, Nuclear Power in Ukraine: Status and Problems, paper presented at the Fourth International Topical Meeting on

Nuclear Thermal Hydraulics, Operations and Safety, Taipei, Taiwan, April 5–9, 1994.
3. International Atomic Energy Agency, Vienna, Austria, *The Safety of WWER and RBMK Nuclear Power Plants: Progress Report of the IAEA Extra Budgetary Programme on the Safety of WWER and RBMK Nuclear Power Plants, 1992–1994,* Report IAEA-TECDOC-773, November 1994..
4. W. C. Potter, The Future of Nuclear Power and Nuclear Safety in the Former Soviet Union, *Nucl. News,* 36(3): 61-67 (March 1993).
5. L. Lederman, *IAEA Programmes Related to Nuclear Power Plant Safety in Eastern Europe and the Commonwealth of Independent States,* International Atomic Energy Agency, Vienna, Austria, September 1994.
6. Periodic Safety Review of Nuclear Power Plants in EC Member States, Finland, Sweden and Switzerland: A Review of Current Practices, prepared for the Nuclear Safety and Nuclear Regulatory Working Groups by a CEC Task Force and the Services of Consultant Dr. D. Goodison, Report OECD/CSNI/NEA, February 1993.
7. E. Adamov, Channel-Type Reactors: Nuclear Safety Upgrading, paper presented at the Fourth International Topical Meeting on Nuclear Thermal Hydraulics, Operations and Safety, Taipei, Taiwan, April 5–9, 1994.
8. Swedish Regulators May Monitor Units Through PSA, *Nucleonics Week* (July 22, 1993).
9. A. Birkhofer, Safety of Soviet-Designed Nuclear Power Plants—Safety Standards and Principles, in *Workshop on Safety of Soviet-Designed Nuclear Power Plants,* American Nuclear Society, Chicago, Illinois, November 20–21, 1992.

Technical Note: On the Definition of Common-Cause Failures

By Henrique Paula[a]

Abstract: *Common-cause failure (CCF) events have occurred in virtually all complex technological systems that use redundancy to help achieve high reliability. In particular, industry experience and the results of probabilistic risk assessments (PRAs) have indicated that CCFs are major contributors to the risk posed by nuclear power-plant operation. Although significant efforts are typically devoted to analyzing and preventing CCFs, no standard definition exists for CCFs—CCF means different things to different people. PRA analysts attempt to identify and treat most types of dependencies (sources of CCFs) explicitly in their PRA models; the types that are not treated explicitly are addressed in a separate CCF analysis task. Therefore, for the purpose of PRA applications, CCFs are dependent failures resulting from causes that are not explicitly modeled in the PRA.*

Most safety-related systems at nuclear power plants are designed with redundant trains of equipment. As a result of this practice, accidents cannot usually occur unless more than one component fails to perform its design functions. Multiple component failures can occur as a result of the independent failure of each component involved; however, operational experience shows that this type of system failure is rare. This may be understood with the following simple, numerical example: Consider a low-pressure injection system (LPIS) that consists of three redundant trains of equipment (A, B, and C), each train having a dedicated pump, valves, piping, and controls. In this example, each train can perform the system's safety function by itself. The probability that each train will fail on demand, P{•}, is assumed constant with respect to time and is equal to 0.01. If it is further assumed that failures of these three trains are independent, then the probability that the system will fail on demand, P{S}, is given by the following equation:

$$P\{S\} = P\{A\} \cdot P\{B\} \cdot P\{C\} = (10^{-2})^3 = 10^{-6}$$

The system is expected to fail from multiple independent failures only once in every one million demands. It is clear in this example that the assumption that the three trains are independent resulted in a very low estimate for the probability of system failure. This is typical of probabilistic risk assessment (PRA) evaluations, and it can lead to very low estimates of the frequency of core damage accidents at nuclear power plants if other factors (discussed next) are not considered.

[a]JBF Associates, Inc., Knoxville, TN 37932-3353.

Design engineers and reliability specialists have long recognized that system failures can also occur as a result of a single event that renders multiple components unavailable (a dependent failure event); for example, Epler discussed many common-mode failure events (the original term for certain types of dependent failure events) in some of his publications in the 1960s (e.g., Ref. 1). Because dependent failure events can typically be attributed to a single cause of failure (e.g., fire, design deficiency, and maintenance-related error), they are often called common-cause failures (CCFs).

In fact, operational experience,[2–4] as well as the results of PRAs,[5–9] indicates that CCF events are usually major contributors to the risk posed by nuclear power-plant operations. These events have occurred in a variety of plant types (e.g., boiling-water reactors and pressurized-water reactors from different vendors) in the United States and abroad.[2,3] Also, these occurrences have involved most types of components in nuclear power plants (e.g., diesel generator, pump, and valve). Indeed, CCF events have been reported in virtually all complex technological systems that use redundancy to help achieve high reliability;[4] for example, Stephenson discusses two recent, unrelated air tragedies (a Japan Air Lines Boeing 747 and a United Airlines DC-10) that resulted from the complete loss of redundant hydraulic systems caused by severing of the redundant hydraulic lines in the rudder of each aircraft, where, on both aircraft, all hydraulic lines were close together.[10]

Although the generic data support the contention that CCFs are potentially major contributors to the unavailability of safety-related systems and should be addressed in PRAs, there are generally not enough data from a particular plant to perform a plant-specific CCF analysis and to estimate plant-specific CCF probabilities. Therefore generic, industry-wide data must be used for these purposes; these data will supplement (or sometimes substitute for) plant-specific data. The use of information from a variety of plants in a plant-specific CCF analysis requires (1) interpreting previous failure occurrences to identify the mechanisms involved in these events and (2) reinterpreting these occurrences in light of the design and operational features of a specific plant.[11–14]

One of the most widely used sources of generic data is the Licensee Event Report (LER) submitted to the U.S. Nuclear Regulatory Commission by nuclear power-plant licensees in accordance with U.S. Government regulations.[15] The Sequence Coding and Search System (SCSS) is a data base used for storing and retrieving experience data from LERs.[16] The SCSS data base contains LER information that has been analyzed and coded by experienced nuclear engineers on the SCSS staff. The SCSS has powerful search and screening capabilities that allow users to retrieve useful information without having to review every event in the data base; however, the SCSS has no formal search scheme for CCF events. The first step toward developing such a scheme is to clearly define CCF events.

Thus this technical note presents many characteristics of CCF events and discusses many aspects of CCF definitions in support of the development of an SCSS search scheme for CCF events. The objective is to develop a CCF search scheme for the SCSS data base with the following features: (1) a powerful screening capability that will reduce the number of events for detailed review and (2) a reliable search scheme to ensure that no significant event is left out.

CCF DEFINITION—STILL A DILEMMA

In 1980, Smith and Watson identified a broad spectrum of CCF definitions used by various authors.[17] Many authors have even used different terminology to describe this class of events, including "cross-linked failure," "systematic failure," "common disaster," "common mode failure," "common cause failure," and "dependent failure." In the 1980s, the terms "common cause failure" and "dependent failure" gained popularity and are now generally accepted within the nuclear industry; however, there is still no consensus on the definition of CCFs.

The nature of the CCF dilemma lies in the nature of CCF events themselves: A CCF (or a dependent failure) is not a unique physical phenomenon but a coupling in the failure times of different components (these failures are caused by or associated with underlying component defects, hardware and/or human-related errors, or destructive chemical or physical phenomenon).

The available literature shows many causes of CCF events that are generally no different from those of single, independent failures—except for the addition of a condition(s) or coupling factor(s) that is the same for all components that failed. The coupling factor(s) is responsible for the occurrence of multiple instead of single failures; for example, the spurious operation of a deluge system can result in the (single) failure of an electronic component (A) in a certain location of the plant. The same deluge system failure would probably have resulted in the failure of both redundant components (A and B)

if they were in the same location. The cause of component failure is the same in both cases; coupling (same location in this example) is what separates CCF events from single failure events. Other coupling factors include same design, same hardware, same installation/maintenance/operations staff, same written procedures, and same environment. Therefore some authors (justifiably) define CCFs very broadly; for example, Ref. 17 offers the following example of an all-inclusive definition of CCFs: "Multiple failures, potential or real, attributable to a common cause."

Such a broad definition can be useful in general discussions of CCFs; for example, the Browns Ferry Nuclear Power Station fire[18] has been quoted as a CCF event in the risk assessment literature for the chemical process industry (CPI).[19] This well-known and well-publicized incident can alert (or remind) the CPI and other industries to the general issue of CCFs and thereby help reduce the potential for CCFs in many facilities.

A broad definition often includes too many and too different types of failure mechanisms and physical phenomena to be of any use in several applications in the nuclear industry. Many of the events that are CCFs under a broad definition show more differences than similarities between themselves; for example, the analysis of multiple failures caused by energetic harsh environments (e.g., seismic, fire, and flood) is significantly different from the analysis of multiple failures caused by a maintenance crew overtightening the packing in redundant motor-operated valves. The methodology, analysis techniques, and expertise required in these two types of analyses are different. Additionally, the defenses and corrective actions that can be taken to prevent these events are different. Therefore other authors (also justifiably) define CCFs narrowly and focus on specific failures of interest. The following is an example of a narrow definition of CCFs:

> Multiple failures of identical, redundant components, failed in the same mode, failed within a critical time period, resulting in complete system failure, accompanied by a challenge, resulting in consequential damage beyond the original multiple failures, all attributable to a common cause other than energetic harsh environments, which fails each of the multiple components directly.

Neither of the two example CCF definitions presented is wrong, nor are any of the other few dozen or so definitions found in the available literature. They can each be useful in particular applications or specific uses. But there is obviously the potential for confusion and misunderstanding, particularly if the quantitative data and qualitative insights derived under one definition are used and implemented with another definition in mind.

CCF DEFINITION FOR PRA APPLICATIONS

There are many causes of dependent failures, and analysts performing nuclear power-plant PRAs generally try to treat a large fraction of these causes explicitly in their event tree/fault tree models; for example, functional dependencies of frontline systems on support systems (such as emergency electric power or service water) are usually included in the logic models.[20] Cascading failures, such as two pumps that fail because a valve in a common suction line was mistakenly closed, are also covered explicitly in these models. In addition, certain operator errors are among other causes of dependency that analysts will tend to treat explicitly in their models. Typically, these actions are described in the plant emergency operating procedures, such as the failure to manually realign a safety-related system from the injection to the recirculation mode.

PRA studies also treat external events [e.g., seismic, external fire, external flood, and high wind (tornado and hurricane)] explicitly because these events require methodologies, analysis techniques, and analysis models (e.g., event tree/fault tree) that are often different from those used in the analysis of internal events.[21] For the same reasons, some of the internally initiated energetic harsh environments (internal fire and internal flood) are often addressed in separate PRA tasks.

There are several other important causes of dependent failures, but these are generally not explicitly addressed in the reliability models. These causes have been associated with many multiple-component failure events at nuclear power plants, and they include inadequate design, manufacturing deficiencies, installation and commissioning errors, operations- and maintenance-related errors, and environmental stresses (e.g., excessive moisture, corrosion, or contamination).[13,22] Rather than being explicitly addressed, many of these causes are lumped together into basic events in the models that represent multiple-component failures that result from any of these several causes. *In general, for the purpose of PRA applications, CCFs are dependent failures resulting from causes that are not explicitly modeled.*[11,12,23,24] (Because, under this definition, the scope of the CCF analysis includes only the residual sources of dependency, the terminology "residual dependent failures" or "residual CCFs" is actually more appropriate

Table 1 Summary of Dependent or Common-Cause Failures and Their Treatment in PRAs

Dependency	Typical treatment in PRAs	Typically within the scope of the residual CCF analysis in PRA applications
Functional dependency (e.g., dependency of frontline systems on support systems)	Included explicitly in the event tree/fault tree models	No
Cascading failure and failure of multiple components because of the failure of a shared component or piece-part	Included explicitly in the event tree/fault tree models	No
Inadequate design	Often not treated separately	Yes
Manufacturing deficiency	Often not treated separately	Yes
Installation and commissioning error	Often not treated separately	Yes
Operator error associated with actions described in the emergency operating procedures	Included explicitly in the event tree/fault tree models	No
Other operator errors (e.g., those associated with recovery actions)	Included explicitly in the event tree/fault tree models or in a separate recovery analysis	No, but specific events may have to be reviewed to ensure that they are addressed explicitly
Maintenance-related error	Often not treated separately	Yes
Environmental stress (e.g., excessive moisture, corrosion, or contamination; high/low temperature; and vibration)	Often not treated separately	Yes
External harsh environment (earthquake, external fire, external flood, hurricane, tornado, etc.)	Analyzed in a separate PRA task	No
Internal harsh environment:		
Fire and flood	Analyzed in a separate PRA task	No
Missile impact, pipe whip, etc.	Often not treated separately	Yes

for PRA applications, but it is not widely used.) Table 1 summarizes many types of dependencies and shows how they are typically addressed in PRA studies. The last column in the table indicates whether these dependencies are inside or outside the scope of a "residual" CCF analysis for PRA applications, and it provides a basis for the SCSS CCF search scheme for PRA applications.

Table 1 provides some guidance for developing a SCSS search scheme for CCF events. The two key characteristics of a CCF event are (1) the coupling in the failure times of multiple components and (2) the common root cause of the failures. The type of failure cause is also an important feature for the SCSS search scheme because, as summarized in Table 1, several types of CCFs are treated in separate PRA tasks and are therefore beyond the scope of a typical CCF analysis. All types of dependency in Table 1 are treated in PRAs, however, and SCSS search schemes for the types that are beyond the scope of a CCF analysis may be very useful in other PRA tasks.

Most CCFs that have occurred at nuclear power plants have involved identical, redundant, active components within the same system, which were operated and maintained in the same way (same testing scheme, same preventive maintenance, same operating procedures, etc.). Therefore many PRA studies do not consider CCFs of passive components or dissimilar components. Also, many PRA studies consider CCFs of components within the same system only (intrasystem CCFs); intersystem CCFs are often assumed negligible. However, the limited scope of many PRAs does not imply that a SCSS search scheme for CCFs should be restricted to identical, redundant, active components within the same system. In fact, it is crucial that the SCSS data base be examined for CCF events involving passive components, dissimilar components, or components within different systems.

Such a search can help justify and support the assumptions in current PRAs and thereby add credibility to these studies.

Finally, many failure occurrences at nuclear power plants involve partial failure of a redundant system (e.g., failure of two trains in a four-train redundant system) and/or incipient or degraded failures (e.g., four redundant pumps that delivered slightly less than the design flow rate during testing because of partially plugged strainers). These partial and/or degraded failure events can be of great value in a CCF analysis by providing (1) qualitative insights about CCF events and (2) supplemental data for the quantification of CCF events.[11–14] (In fact, some analysts argue that even single failure events can provide useful qualitative insights and supplemental data.)[12,14,22] Therefore events involving partial failures and/or events involving incipient or degraded conditions should not necessarily be screened out when compiling data for a CCF analysis.

REFERENCES

1. E. P. Epler, Common Mode Failure Considerations in the Design of Systems for Protection and Control, *Nucl. Saf.*, 10(1): 38-45 (January–February 1969).
2. H. M. Paula and D. J. Campbell, *Analysis of Dependent Failure Events and Failure Events Caused by Harsh Environmental Conditions*, Report JBFA-LR-111-85, August 1985.
3. K. N. Fleming, A. Mosleh, and D. L. Acey, *Classification and Analysis of Reactor Operating Experience Involving Dependent Events*, Report EPRI NP-3967, June 1985.
4. G. T. Edwards and I. A. Watson, *A Study of Common-Mode Failures*, Report SRD-R-146, July 1979.
5. A. M. Kolaczkowski et al., *Analysis of Core Damage Frequency: Peach Bottom, Unit 2, Internal Events*, Report NUREG/CR-4550-Vol. 4-Rev. 1-Pt. 1 (SAND-86-2084, Vol. 4-Rev. 1-Pt. 1), August 1988.
6. H. M. Paula, A Probabilistic Dependent Failure Analysis of a D-C Electric Power System in a Nuclear Power Plant, *Nucl. Saf.*, 29(2): 196-208 (April–June 1988).
7. A. Poucet, A. Amendola, and P. C. Cacciabue, *CCF-RBE Common Cause Failure Reliability Benchmark Exercise*, Report EUR-11054, 1987.
8. *Seabrook Station Probabilistic Safety Assessment*, Report PB-84-186949 (PLG-0300), December 1983.
9. *Ringhals 2 Probabilistic Risk Assessment*, Report NUS-4635, May 1983.
10. J. Stephenson, *System Safety 2000: A Practical Guide for Planning, Managing, and Conducting System Safety Programs*, Van Nostrand Reinhold, New York, N.Y., 1991.
11. A. Mosleh, K. N. Fleming, G. W. Parry, H. M. Paula, D. H. Worledge, and D. M. Rasmuson, *Procedures for Treating Common Cause Failures in Safety and Reliability Studies: Volume I, Procedural Framework and Examples*, Report NUREG/CR-4780 (EPRI-NP-5613), January 1988.
12. H. M. Paula, Data Base Features that are Needed to Support Common Cause Failure Analysis and Prevention: An Analyst's Perspective, *Nucl. Saf.*, 31(2): 159-173 (April–June 1990).
13. H. M. Paula, D. J. Campbell, and D. M. Rasmuson, Qualitative Cause-Defense Matrices: Engineering Tools to Support the Analysis and Prevention of Common Cause Failures, *Reliab. Eng. Syst. Saf.*, 34(3): 389-415 (1991).
14. A. Mosleh, Common Cause Failures: An Analysis Methodology and Examples, *Reliab. Eng. Syst. Saf.*, 34(3): 249-292 (1991).
15. Licensee Event Report System, 10 CFR 50, *Fed. Regist.*, 50(73) (1987).
16. N. M. Greene, G. T. Mays, and M. P. Johnson, *Sequence Coding and Search System for Licensee Event Reports: User's Guide*, Report NUREG/CR-3905-Vol. 1-Rev. 1 (ORNL/NSIC-223, Vol. 1, Rev. 1), April 1985.
17. A. M. Smith and I. A. Watson, Common Cause Failures—A Dilemma in Perspective, in *1980 Proceedings of the Annual Reliability and Maintainability Symposium, San Francisco, Calif.*, January 1980.
18. *Report to the Congress on Abnormal Occurrences, January–June 1975*, Report NUREG-75/090 (PB-245404), October 1975.
19. Center for Chemical Process Safety, AIChE, New York, N.Y., *Guidelines for Chemical Process Quantitative Risk Analysis*, 1989.
20. M. V. Frank and K. N. Fleming, Risk-Significant Functional Dependencies in Pressurized Water Reactors, *Reliab. Eng. Syst. Saf.*, 34(3): 293-308 (1991).
21. R. J. Budnitz, External Initiators in Probabilistic Reactor Accident Analyses—Earthquakes, Fires, Floods, Winds, *Risk Anal.*, 4(4) (December 1984).
22. D. M. Rasmuson, Some Practical Considerations in Treating Dependencies in PRAs, *Reliab. Eng. Syst. Saf.*, 34(3): 327-344 (1991).
23. S. Hirschberg, Experiences from Dependent Failure Analysis in Nordic Countries, *Reliab. Eng. Syst. Saf.*, 34(3): 355-388 (1991).
24. G. W. Parry, Common Cause Failure Analysis: A Critique and Some Suggestions, *Reliab. Eng. Syst. Saf.*, 34(3): 309-326 (1991).

Accident Analysis

Edited by R. P. Taleyarkhan

Modeling and Analysis of Core-Debris Recriticality During Hypothetical Severe Accidents in the Advanced Neutron Source Reactor

By S.-H. Kim, V. Georgevich, D. B. Simpson, C. O. Slater, and R. P. Taleyarkhan[a]

Abstract: *This article discusses salient aspects of severe-accident-related recriticality modeling and analysis in the Advanced Neutron Source (ANS) reactor. The development of an analytical capability that uses the KENO5A-SCALE system is described, including evaluation of suitable nuclear cross-section sets to account for the effects of system geometry, mixture temperature, material dispersion, and other thermal–hydraulic conditions. Benchmarking and validation efforts conducted with KENO5-SCALE and other neutronic codes and compared with critical experiment data are described. Potential deviations and biases resulting from the use of the 16-group Hansen–Roach library are shown. A comprehensive test matrix of calculations to determine the reactivity of various hypothetical configurations that might arise, along with the effects of various parameters on that reactivity, is described. Strong dependencies on geometry, material constituents, and thermal–hydraulic conditions are also discussed as well as the introduction of designed mitigative features.*

Oak Ridge National Laboratory's (ORNL's) Advanced Neutron Source (ANS) reactor will be a new user facility[1,2] for all kinds of neutron research centered on a research reactor of unprecedented ($\sim 10^{20}$ $m^{-2} \cdot s^{-1}$) neutron flux available to the beam tubes. A defense-in-depth philosophy has been adopted to improve system vulnerability to severe accidents by incorporating design fixes and developing an effective accident management strategy during the early stage of ANS design. In response to this commitment, ANS project management has initiated severe accident analysis and related technology development early in the design phase to aid in the design of a sufficiently robust containment for the retention and controlled release of radionuclides in the event of an accident. This step also provides a means for satisfying on- and off-site regulatory requirements and evaluating the accident-related dose exposures. Containment response and source-term best-estimate analyses for the Levels 2 and 3 Probabilistic Risk Analyses (PRAs) are to be provided. Moreover, the analyses will provide the best possible understanding of ANS under severe-accident conditions and consequently will provide insights for the development of strategies and design philosophies for accident mitigation, management, and emergency preparedness efforts.

This article describes salient aspects of the work done to date on addressing a potentially important severe-accident issue dealing with recriticality during hypothetical severe accidents.

ANS SYSTEM DESIGN

The ANS is currently in the conceptual design stage. As such, design features of the containment and reactor system are evolving on the basis of insights from ongoing

[a]Oak Ridge National Laboratory, Oak Ridge, TN 37831.

studies. Table 1 summarizes the current principal design features of ANS from a severe-accident perspective compared with those of ORNL's High-Flux Isotope Reactor[3] (HFIR) and a commercial light-water reactor (LWR). As shown in Table 1, high-power-density research reactors can give rise to significantly different severe-accident issues. Specifically, the ANS reactor will use about 15 kg of highly enriched (~93 m/o ^{235}U) uranium silicide fuel in an aluminum matrix with a plate-type geometry and a total core mass of 100 kg. About 13 g of B^{10} burnable poison is provided in the end caps of fuel plates to reduce excess reactivity at the beginning of cycle (BOC) and to help shape the power distribution. Heavy water (D_2O) is used as a moderator and coolant. The power density of the ANS will be about 50 to 100 times as high as that of a large LWR. Figure 1 shows a schematic representation of the reactor and cooling circuit. The reactor core is enclosed within a core pressure boundary tube and enveloped in a reflector tank. Four inlet pipes deliver D_2O coolant upward into the core at a high velocity (~27 m/s), and D_2O then enters a large stainless steel pipe before branching into several pipes leading to heat exchangers. Much of the coolant-system piping is submerged in light-water pools.

IMPORTANCE OF THE RECRITICALITY ISSUE FOR ANS

A disrupted reactor core during severe accidents could lead to an undesirable fuel configuration and thus result in uncontrollable nuclear fission reactions. Such a configuration may become critical again. Such a recriticality event could lead to damaging steam explosion loads.

Table 1 Severe Accident Characteristics of the ANS[a] and Other Reactor Systems

Parameter	Commercial LWR[b]	HFIR[c]	ANS
Power, MW(t)	2600	85	300
Fuel	UO_2	U_3O_8–Al	U_3Si_2–Al
Enrichment, m/o	2 to 5	93	93
Fuel cladding	Zircaloy	Al	Al
Coolant–moderator	H_2O	H_2O	D_2O
Coolant outlet temperature, °C	318	69	8.5
Average power density, MW/L	<0.1	1.7	4.5
Clad melting temperature, °C	1850	580	580
Hydrogen generation potential, kg	850	10	12

[a]ANS, Advanced Neutron Source.
[b]LWR, light-water reactor.
[c]HFIR, High-Flux Isotope Reactor.

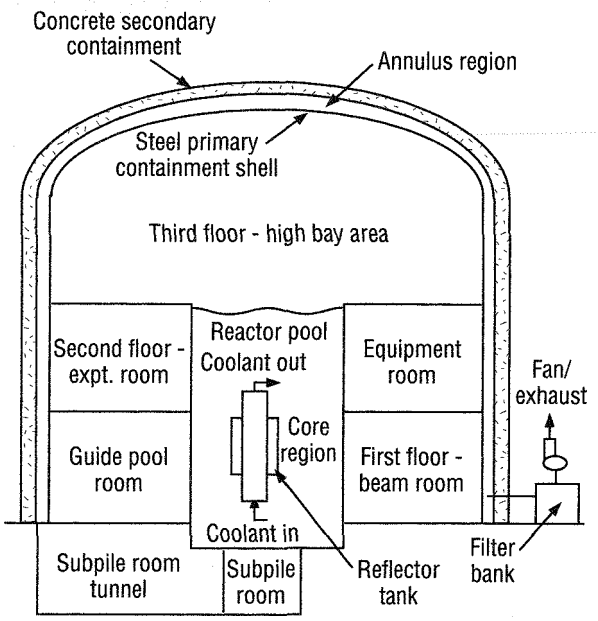

Fig. 1 Schematic representation of Advanced Neutron Source reactor and containment.

Additional fission-product generation and high-energy bursts of radiation are also undesirable by-products. The scoping study of recriticality in ANS under hypothetical severe accidents was motivated by the need to gage the potential for such an occurrence and by the need to consider designed mitigative features early in the design process.

MODELING AND PROBLEM FORMULATION FOR ANS RECRITICALITY ANALYSIS

During hypothetical severe accidents in ANS, fuel-plate melting may occur either with or without a flowing medium adjacent to the melting plates. Hypothetical accident conditions, such as core inlet flow blockages or large-pipe loss-of-coolant accidents (LOCAs), may provide such conditions. Under such circumstances, and if a steam explosion does not occur, the core mass may slump and agglomerate downward into the primary coolant-system piping regions. Again, experiments[4] with melting aluminum tubes in the presence of flowing media show that, depending on the destabilizing surface forces caused by flowing media, debris dispersal and entrainment in the flowing medium may occur. Debris dispersal also may occur in the presence of steam explosions. Such dispersion

mechanisms can cause fragmented core debris to be swept into the coolant outlet piping. Hence, for ANS severe-accident analysis, lumped and dispersed configurations need to be analyzed for gaging recriticality potential.

The process of modeling and analysis for recriticality under severe-accident conditions for ANS involves several steps. First, a modeling capability was developed to account for ANS debris in various configurations and surrounded with various geometries and materials. The modeling framework was benchmarked and validated against known critical experiments. Next, the potential for recriticality in ANS under severe-accident conditions was analyzed. Because of the absence of a mechanistic core-melt-progression capability, the various geometries and thermal–hydraulic conditions were postulated and analyzed parametrically. Again, the time-dependent behavior of the system following a recriticality event would require the development of a transient modeling capability, which was considered beyond the scope of this simplified study. Hence a wide range of parametric studies was conducted to gage the behavior of the system under various conditions of temperature and void fraction. Finally, evaluations were made for the incorporation of designed mitigative features to prevent recriticality. Salient aspects of these various steps are subsequently described.

Modeling Framework Development, Benchmarking, and Validation

Because of its versatility, the well-known KENO5A-SCALE[5] neutronic code system was the modeling framework of choice for evaluating the recriticality potential of ANS core debris. A series of experiments was researched to gage the applicability of this system to ANS-debris lumped or dispersed geometries. These experiments considered lumped and dispersed fuel configurations in the presence of light and heavy water. In addition to using KENO5A for evaluating k_{eff}, transport-theory-based (viz., XSDRNPM[5] and TORT[6]) calculations also were conducted to provide a basis for bias determination and for evaluating the appropriateness of using the 39- and 99-group ANSL-V cross-section libraries.[7] Several details of the comparison are omitted because of space considerations. An abstract of the benchmarking and validation exercises is presented.

Table 2 provides the results of KENO5A and XSDRNPM calculations for k_{eff} against the well-known GODIVA[8] bare enriched-uranium–metal sphere experiment. Note that criticality is evaluated within one standard deviation of the experiment. This forms an important benchmark for the cross-section libraries used in the analysis of ANS reactor lumped-core cases. Thereafter ancillary calculations were performed with XSDRNPM and KENO5A for three H_2O-reflected spheres and five D_2O-reflected spheres. The results of XSDRNPM and KENO5A agreed within one standard deviation of individual calculations, which represents excellent comparisons.

Five ORNL critical spheres,[9] consisting of enriched uranyl nitrate in water in one of two spheres of radius 345.98 or 610.108 mm (the first four spheres having the smaller radius), were analyzed. The first and fifth spheres (ORNL-1 and ORNL-10, respectively) contain the critical concentrations for unpoisoned solutions within the two spheres.

Table 2 Comparison of Code Predictions with Critical Experiment Data

		k_{eff} calculation results			
Experiment	Measurement, k_{eff}	XSDRNPM (39-group)	Calculations (99-group)	KENO calculations (39-group)	Notes
GODIVA	1.00 ± 0.003	0.9990	0.9979	0.9965	Bare sphere (^{235}U mass = 49.1 kg) of radius = 87.401 mm.
ORNL-1	1.00 ± 0.0025	1.0025	1.0012	1.0046	ORNL uranyl nitrate–water solution unreflected critical spheres of different diameters.
ORNL-10	1.00 ± 0.0025	1.0013		1.0031	
L7	1.0000	1.0090	1.0076		ORNL uranyl fluoride light-water critical spheres of different shell thicknesses, radii, and ^{235}U masses.
L8	1.0004	1.0103	1.0090		
L9	1.0000	1.0068	1.0056		
L10	1.0000	1.0069	1.0057		
L11	0.9999	1.0069	1.0054		

In the other three, criticality is maintained by counterbalancing increases in the uranium concentration with increases in the natural boron concentration of the solution. KENO5A calculations were performed for the first and fifth critical spheres. Table 2 shows selected results. The results of computations are within 0.25% uncertainty of the experiments, and again excellent agreement is seen between predictions and experiment and between XSDRNPM and KENO5A calculations. Also, with the use of 39- and 99-group cross sections, almost identical results were obtained. Separately, additional comparisons with the use of XSDRNPM and DORT also were made with six D_2O-reflected spheres[10] and five bare cylinders filled with uranyl fluoride in D_2O. Excellent agreement was obtained between predictions and experiments. Separately, five supplemental ORNL-reflected and bare critical spheres consisting of enriched uranyl fluoride in water were analyzed. These experiments supplemented the earlier uranyl nitrate sphere comparisons in that a wider range of $H/^{235}U$ ratios was introduced and reflected spheres were included.

Predictions were made with both the ANSL-V 39- and 99-group cross-section libraries in the SCALE system and with XSDRNPM to perform k-calculations. As noted in Table 2, calculated results were in excellent agreement with experimental data and confirm the applicability of the ANSL-V cross-section libraries in the SCALE system. Together, the previously mentioned comparisons provide reasonable confidence in the use of the KENO5A-SCALE system for evaluation of k_{eff} values for ANS core debris in either lumped or dispersed configurations.

The KENO5A-SCALE system was ported to work on an IBM/RISC-6000 workstation platform. Twenty-five benchmark calculations were executed with the use of the integrated system. Table 3 compares the k_{eff} value calculated on the workstation with both the supplied random number generator and an alternate generator with the reported value for each case. Excellent agreement was obtained between KENO5A-SCALE on the ORNL mainframe and that on the workstation computers.

Table 3 KENO5A Sample Problem Results

	Reported		Supplied generator		Alternate generator	
Problem	k_{eff}	Deviation	k_{eff}	Deviation	k_{eff}	Deviation
1	0.9998	0.0041	1.0145	0.0035	0.9993	0.0040
2	0.9998	0.0041	1.0145	0.0035	0.9993	0.0040
3	1.0105	0.0055	1.0121	0.0054	1.0172	0.0050
4	1.0117	0.0046	1.0161	0.0058	1.0116	0.0050
5	1.0244	0.0038	1.0238	0.0035	1.0274	0.0036
6	0.7562	0.0031	0.7451	0.0037	0.7515	0.0039
7	1.0032	0.0044	1.0081	0.0043	1.0093	0.0040
8	0.9436	0.0037	0.9446	0.0042	0.9440	0.0036
9	2.3092	0.0067	2.3022	0.0081	2.3018	0.0049
10	0.9998	0.0041	1.0145	0.0035	0.9993	0.0040
11	0.9998	0.0041	1.0145	0.0035	1.0085	0.0040
12	1.0065	0.0048	1.0127	0.0051	1.0199	0.0056
13	1.0057	0.0042	1.0067	0.0044	0.9956	0.0044
14	0.9990	0.0039	1.0070	0.0042	0.9916	0.0042
15	1.0059	0.0049	1.0066	0.0042	1.0070	0.0043
16	0.9901	0.0027	0.9977	0.0027	0.9937	0.0026
17	0.9921	0.0158	1.0359	0.0176	1.0007	0.0185
18	1.0067	0.0071	1.0385	0.0065	1.0282	0.0079
19	1.0115	0.0051	1.0064	0.0048	1.0203	0.0057
20	1.0063	0.0063	1.0119	0.0055	0.9975	0.0054
21	0.9891	0.0033	0.9893	0.0037	0.9888	0.0033
22	1.0026	0.0039	1.0145	0.0035	0.9994	0.0043
23	0.9987	0.0041	1.0144	0.0035	1.0030	0.0042
24	1.0068	0.0042	1.0062	0.0044	1.0014	0.0038
25	1.0071	0.0041	1.0102	0.0042	1.0017	0.0038

Establishing a Bias for the Calculated k_{eff}

Because for a critical system $k_{eff} = 1.0$, deviations of the calculated values from unity indicate some bias in the calculational methods and/or data. For subcriticality of the ANS core debris, the calculated k_{eff} values should be below established limits. The established limits are set at $k_{avg} - 3\sigma - 0.02$ (where 0.02 has been subtracted for extra shutdown margin). From a comparison of the SCALE system results for k_{eff} for both lumped and dispersed configurations, one arrives at bias k_{eff}'s of 0.965 for lumped and dispersed geometries. Thus any configuration with a calculated k_{eff} greater than 0.965 would be considered critical.

ANS DEBRIS RECRITICALITY MODELING AND ANALYSIS

The ANS system is being developed. Previous core designs consisted of about 24 kg of ^{235}U, which now has been reduced to 15 kg. Calculations for k_{eff} with the larger fuel loading also have been conducted and are reported. For the evaluation of the threat of a recriticality event under different conditions, several different configurations and thermal–hydraulic conditions needed to be analyzed. The development of a suitable test matrix and analysis results are subsequently described.

Test Matrix Development and Modeling

Tables 4 and 5 show the test matrix of calculations. Calculations for k_{eff} were conducted with lumped and dispersed core-debris materials in a stainless steel pipe filled with D_2O and reflected on the outside by H_2O. The lumped configurations were analyzed first and were found to be relatively unimportant. Because of the importance of dispersed configurations, most parametric calculations were conducted in dispersed geometries. As mentioned previously, lumped configurations are studied in a smaller diameter pipe [approximating the core inlet piping, which has a 488-mm(19-in.) inner diameter and is 10 mm thick]. Dispersed configurations are studied for debris dispersal in the 610-mm(24-in.) schedule 20 outlet piping. If a room temperature was not specifically indicated, for conservatism, an assumption was used for the calculations. Again, unless otherwise indicated, the core debris is assumed to be contained in a pipe volume extending more than 3 m. Dispersed configurations are assumed to be nominally distributed over a length of 1 m unless otherwise stated in Table 5.

A typical geometry for dispersed debris recriticality calculations is shown in Fig. 2. As shown, the modeled regions are divided into four material zones. Zone 1 comprises the fueled zone. Fuel is assumed to be homogeneously mixed with coolant in Zone 1. A reflecting boundary (Zone 2) extends to a distance of 1 m from both ends of the mixing or fuel zone. The 1-m length was calculated essentially to provide infinite reflection of neutrons. The stainless steel piping constitutes Zone 3. Finally, the H_2O outside the primary coolant piping is represented as Zone 4.

As mentioned previously, lumped fuel calculations (even with 26 kg of ^{235}U) gave rise to significantly subcritical values of k_{eff}. This was not true for dispersed geometries. A detailed test matrix thus was developed for parametrically evaluating the effects of changes in important variables (Table 5). The base case was developed in which coolant temperature is set at 50 °C to

Table 4 Criticality Calculations for Lumped and Dispersed Geometries

Case	Configuration and debris constitution	k_{eff} calculation results		
		KENO5[a]	KENO5[b]	DORT, TORT
1	Lumped: 220-m-diameter sphere of U_3Si_2–Al at bottom of D_2O-filled steel pipe submerged in H_2O (pipe ID, 488 mm); 24 kg ^{235}U	0.873	0.850	0.866
2	Dispersed: U_3Si_2 mass uniformly suspended in a 1-m-long section of D_2O-filled steel submerged in H_2O (pipe ID, 488 mm); 15 kg ^{235}U	1.070	1.030	

[a]These calculations were done with the 39-group cross-section library in the SCALE system.
[b]These calculations used the 16-group Hansen–Roach cross-section library.

Table 5 Test Matrix of Recriticality Calculations for ANS with Dispersed Configuration

Case No.	H_2O mole fraction	Void fraction	Dispersion length, m	Aluminum content, kg	Temperature, °C	k_{eff}	Standard deviation	Notes
1	0.002	0	1	40	50	1.0392	0.0034	Base-case[a] light-
2	0.1	0	1	40	50	1.1803	0.0039	water contamina-
3	0.5	0	1	40	50	1.3397	0.0035	tion cases
4	1	0	1	40	50	1.3171	0.0031	
5	0.002	0.2	1	40	660[b]	0.8855	0.0036	Void fraction
6	0.002	0.4	1	40	660[b]	0.7262	0.0035	variation cases
7	0.002	0.6	1	40	660[b]	0.5722	0.0030	
8	0.002	0	0.25	40	50	0.8776	0.0033	Dispersion length
9	0.002	0	0.5	40	50	0.9707	0.0035	variation cases
10	0.002	0	1.5	40	50	1.0522	0.0035	
11	0.002	0	2	40	50	1.0438	0.0039	
12	0.002	0	3	40	50	1.0230	0.0035	Aluminum mass
13	0.002	0	1	0	50	1.0767	0.0038	variation cases
14	0.002	0	1	60	50	1.0211	0.0036	
15	0.002	0	1	87	50	0.9919	0.0036	Mixture temperature
16	0.002	0	1	40	72	1.0334	0.0040	variation cases
17	0.002	0	1	40	100	1.0140	0.0037	
18[c]	0.002	0	1	40	50	1.1082	0.0042	Fuel depletion
19[c]	0.002	0	1	40	50	1.0914	0.0040	cases

[a]For the base case, the fuel contains 13 g of B^{10}.

[b]This temperature is only for U_3Si_2, aluminum, and boron. Coolant temperature for this case is 50 °C.

[c]These cases are the same as the base case but with ^{235}U depletion (30% for Case 18 and 40% for Case 19) and 100% boron depletion. Note: 40% ^{235}U depletion corresponds to end of cycle.

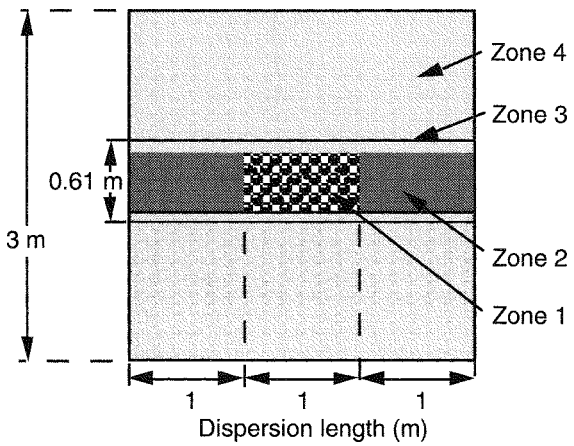

Fig. 2 Schematic representation of dispersed core-debris configuration in Advanced Neutron Source outlet pipe for recriticality evaluations.

represent a nominal coolant outlet temperature of the ANS core under normal operation (instead of assuming room temperature). The BOC inventory of fuel is assumed for the base case, coupled with all the 13 g of B^{10} burnable poison. The assumption was made that, upon fuel melting-cum-dispersion, only the aluminum in the fuel-melt section would accompany the fuel. Hence about 40 kg of aluminum is associated with the recriticality calculations of base-case debris in Table 5. Further, the assumption was made that the fuel debris would cool down to 50 °C by the time the 1-m-length dispersion occurs in the outlet piping. On the basis of ANS Technical Specifications, the amount of H_2O contamination in the D_2O is specified to a mole fraction of 0.002 [i.e., if there is no influx of reactor pool H_2O in the reactor coolant system (RCS)].

Under certain circumstances, it is conceivable that the H_2O fraction in the primary coolant circuit may increase (e.g., LOCA or in-leakage). An increase in H_2O content in the primary circuit will significantly change the neutronic characteristics associated with debris recriticality. This is caused by the significantly enhanced moderation

by H_2O compared with D_2O. However, this increased moderation characteristic is compensated by higher absorption. For such interactions, several mole fractions of H_2O are included in the test matrix.

An important parameter that can significantly affect reactivity is the degree of voiding generated in the coolant. Such voiding may initiate in a previously cold system that has become critical, whereby the fuel material heats up to cause coolant boiling. For purposes of modeling, voids are assumed to be homogeneously distributed in Zone 1 (i.e., with fuel, D_2O, and H_2O). As is well known, increased voiding can provide negative reactivity feedback, which then may shut down the criticality escalation. Several KENO5-SCALE calculations are included in the test matrix. For these calculations, the fuel mixture (i.e., uranium, silicon, boron, and aluminum) is assumed to be at the aluminum melting temperature of 660 °C. Herein a conservative assumption is made that heat from the core debris goes toward only the changing phase in the coolant. The coolant temperature also may increase, however. Therefore additional calculations are included in the test matrix, and Zone 1 contents are equilibrated at 72 °C (i.e., perfect mixing of fuel at melting temperature with 281 kg of D_2O). An additional case considered the entire mixture at 100 °C. This was done to represent a possible situation wherein molten core debris may have superheated above the aluminum melting temperature and then mixed with the D_2O coolant to reach boiling conditions at atmospheric pressure.

These calculations evaluate the effect of temperature on reactivity. The effect of temperature on fuel arises mainly from Doppler broadening. Hence mainly resonance absorption determines the fuel temperature coefficient of reactivity. Because moderator density decreases with increasing temperature, the moderator coefficient of reactivity may be attributed to the change in thermal utilization.[11] For these calculations, densities of D_2O and H_2O are suitably changed with temperature to account for the appropriate reduction in number densities of hydrogen, deuterium, and oxygen atoms. Densities of other materials are assumed to remain unchanged.

As mentioned previously, the 1-m length of the fuel debris mixture (i.e., Zone 1) was chosen arbitrarily. Clearly, a change in this length will cause the deuterium/uranium ratio to change. Therefore system criticality also can be significantly affected. Hence parametric studies are conducted for different dispersion lengths.

Different amounts of aluminum may accompany the fuel debris in a severe accident. Hence calculations are conducted to account for this effect.

Also, a severe-accident-induced debris recriticality may occur at the end of the cycle (EOC), when about 30 to 40% of the ^{235}U and all the B^{10} are depleted. These cases also are studied conservatively; the absence of fission-product poisoning is assumed. Note that the EOC case with about 40% of the ^{235}U depleted would also tend to represent a case in which only the unirradiated outer fuel element undergoes a hypothetical severe-accident-induced core-debris dispersion (albeit without any burnable poison).

Analysis Results

Specific KENO5 models for the various cases in Tables 4 and 5 were set up and executed. The results of the k_{eff} calculations are summarized in the tables and are shown graphically in Figs. 3 to 8. Unless otherwise stated, all calculations were conducted with the KENO5-SCALE system using the 39-group cross-section library.

As noted in Table 4, even if the U_3Si_2–Al mixture consisting of 24 kg of ^{235}U were to form a lump in the inlet pipe region, the system remains significantly subcritical (i.e., k_{eff} = 0.873). For the same pipe geometry, a dispersed configuration also was evaluated. The dispersed geometry leads to a k_{eff} value significantly greater than 1.0. These same calculations also were conducted with the well-known Hansen–Roach library[12] [with suitable adjustments for selecting the resonance self-shielding cross sections (s_p), as recommended in Ref. 13]. As shown in Table 4, although the predicted k_{eff} values are in the general vicinity of those predicted with the use of the 39-group library, use of the 16-group

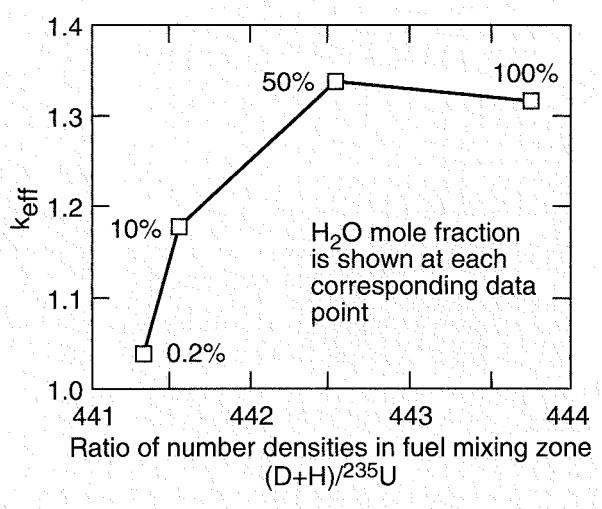

Fig. 3 Effect of light-water contamination on k_{eff}.

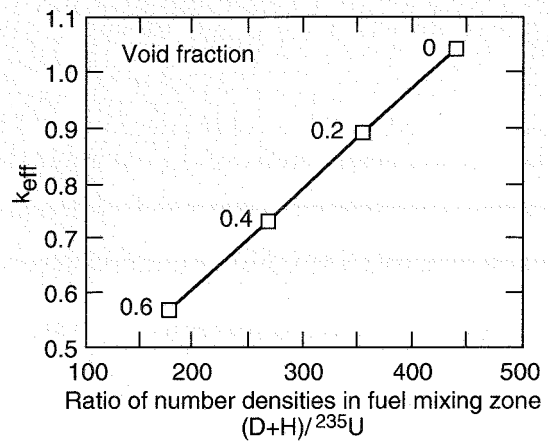

Fig. 4 Effect of void fraction on k_{eff}.

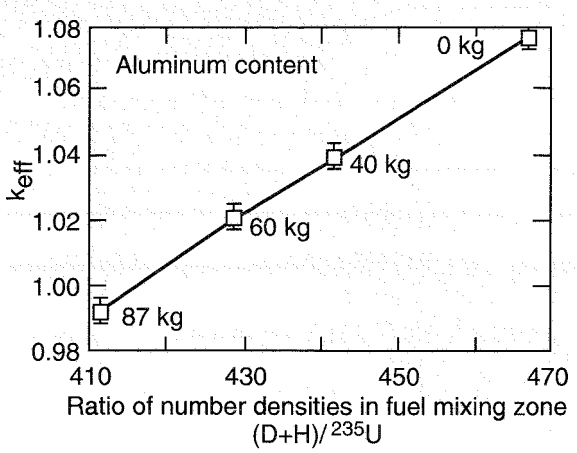

Fig. 7 Effect of aluminum content on k_{eff}.

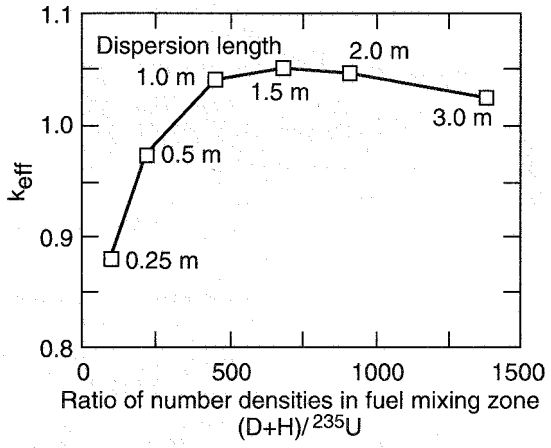

Fig. 5 Effect of dispersion length on k_{eff}.

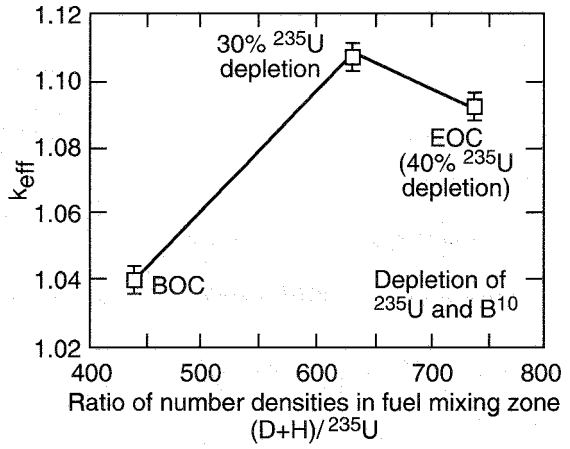

Fig. 8 Effect of fuel depletion on k_{eff}.

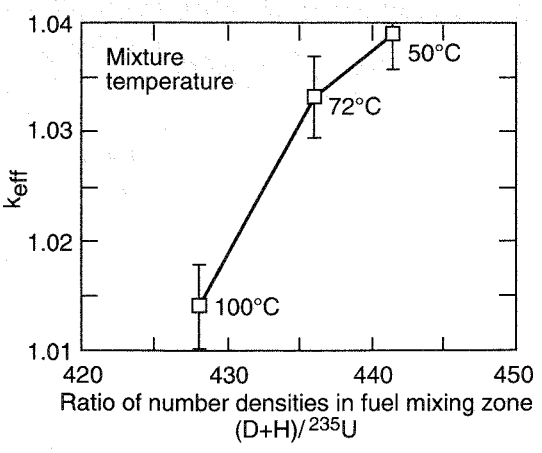

Fig. 6 Effect of fuel temperature on k_{eff}.

Hansen–Roach cross-section library (at least under these conditions) can lead to significant underprediction of k_{eff}. Because the ANS fuel mass is critical in the core region, it can be surmised that the significantly reduced value for k_{eff} in lumped configurations results from the poisoning effect of the stainless steel piping. This aspect was confirmed through additional calculations wherein the steel pipe was modified to be made with aluminum. Significantly higher values by more than 7% were noted for k_{eff}.

Because the lumped core-debris configuration with 24 kg of ^{235}U remained significantly subcritical, the decision was made that lumped configurations in the ANS reactor coolant system (RCS) would not lead to a recriticality threat. Therefore only dispersed configurations were studied

further with the current fuel loading in the ANS core (viz., 15 kg of ^{235}U, as shown in Table 1). The results for individual cases are tabulated in Table 5. Figures 3 to 8 show k_{eff} variation with the $(D+H)/^{235}U$ atom ratio in the core-debris mixing zone.

Figure 3 indicates that H_2O contamination in the RCS can significantly increase k_{eff} values because of enhanced moderation. The effect tapers off beyond 50% H_2O mole fraction, however, and then starts to decrease because of enhanced neutron absorption. These calculations demonstrate the need to keep H_2O out of the RCS. Note that, for nonsevere accident conditions, recriticality from incoming H_2O is prevented by design. Under such circumstances, control rods immediately insert to counter a reactivity addition from light-water entry into the RCS or into the reflector tank.

A linear decrease in k_{eff} is shown in Fig. 4, and increasing void fraction occurs in the debris zone. With only 20% void fraction, the system k_{eff} drops from 1.04 to 0.89 (viz., a 15% decrease). The variation with increased void fraction also tends to indicate that a strong mechanism exists for limiting a reactivity excursion event.

A strong variation also is shown with dispersion length in Fig. 5. A reduction in dispersion length causes a lumped mass-type geometry and decreases k_{eff}. As shown in Fig. 5, k_{eff} values do not increase significantly beyond a 1-m dispersion length. Only a relatively mild variation with mixture temperature was noted. Figure 6 shows that a k_{eff} decreases from 1.0392 at 50 °C to 1.014 at 100 °C (about 7 to 8 cents/°C). This result indicates that a resonance absorption caused by Doppler broadening would provide enough negative feedback to compensate for positive reactivity insertion from increased thermal use by the fuel as the temperature increases. Overall, these variations demonstrate the significance and importance of properly modeling thermal–hydraulic conditions during severe accidents.

Figure 7 shows that the amount of aluminum accompanying the core debris also can have a significant effect on system criticality. The variation of k_{eff} with aluminum mass is almost linear. It is not so strong as that with variation with void fraction. It is significant, however, and demonstrates the importance of proper core-melt-progression modeling.

Finally, Fig. 8 demonstrates the importance of B^{10} in the fuel mixture. Under EOC-type conditions when approximately 30 to 40% of the ^{235}U and all the B^{10} are depleted, the k_{eff} value goes up significantly from 1.04 to about 1.11 and then starts declining. Obviously, this variation with burnup is predicated on the accompaniment of the B^{10} with the fuel debris at BOC conditions in the first place.

Prevention and Mitigation of Debris Recriticality Loads in ANS

An important by-product of the results shown in Fig. 8 deals with a possible approach for mitigation of recriticality. It demonstrates that the incorporation of borated pipe regions in strategic locations could play a very important role in preventing recriticality. A preliminary calculation was conducted to demonstrate this aspect wherein a previously supercritical configuration was made significantly subcritical by borating the ANS outlet pipe. This result is currently being studied.

Overall, it is clear that debris recriticality in the ANS RCS can be effectively prevented if dispersed configurations are avoided. These evaluations demonstrate, to the extent that they represent expected conditions, that a mechanism should be found that prevents dispersion of a large enough portion of core debris during severe accidents. If fuel dispersion is inevitable, it is clearly preferable to introduce design features that allow only small portions to disperse. Clearly, the need for prevention of debris dispersion must be balanced with the need for maintaining debris coolability (which is enhanced with dispersion). Thus research efforts are to be focused toward analytical quantification of melt-progression aspects with the potential for leading to recriticality coupled with qualification through scaled experimentation.

All in all, this is a clear case in which a design fix that will prevent recriticality is far preferable to an extensive research program that may solve the problem because not much is known on modeling and analysis of "transient" debris recriticality events.

SUMMARY AND CONCLUSIONS

This article has described salient aspects of benchmarking and validation of the KENO-SCALE neutronic code system for the evaluation of system criticality wherein lumped and dispersed core-debris configurations may arise during hypothetical severe accidents in the ANS. Benchmarking and validation were done against data from a series of critical experiments and between various codes. These comparisons demonstrated the suitability of using the KENO-SCALE code system in conjunction with the 39-group cross-section library. A detailed test matrix of calculations was developed for evaluating the potential of recriticality in

the ANS RCS during severe accidents. The evaluations indicated that lumped configurations in the RCS would not pose a recriticality threat; however, significant potential exists for recriticality from dispersed debris configurations. Strong dependencies were noted on key thermal–hydraulic parameters, such as mixture void fraction, H_2O contamination, aluminum content in debris, and dispersion length. A relatively weak dependence on mixture temperature was noted. Mixture void fraction was determined to be the single most important parameter affecting recriticality. These calculations indicated the importance of proper core-melt progression and thermal–hydraulic modeling. It was determined that prevention of recriticality in the ANS RCS may be achieved through limitation of debris dispersion coupled with strategic positioning of borated regions in the RCS piping. Alternative choices may also be possible (e.g., thickening of pipe walls for increased parasitic absorption or modifying pipe diameters to stay away from optimum $D/^{235}U$ ratio regions).

REFERENCES

1. C. D. West, The Advanced Neutron Source: A New Reactor-Based Facility for Neutron Research, *Trans. Am. Nucl. Soc.*, 61: 375-376 (June 1990).
2. Oak Ridge National Laboratory, *Advanced Neutron Source Plant Design Requirements,* Report ORNL/TM-11625, 1990.
3. F. T. Binford and E. N. Cramer, *The High Flux Isotope Reactor, A Functional Description,* Report ORNL-3572 (Rev. 2), June 1968.
4. J. P. Morin and M. L. Hyder, The Reaction of Molten SRP Reactor Fuel with Water, in *ANS Workshop on the Safety of U–Al Fueled Reactors, Idaho Falls, Idaho, March 15, 1990,* Report CONF-890378-6 (DP-MS-89-53), 1989.
5. L. M. Petrie and N. F. Landers, KENO5A—An Improved Monte Carlo Criticality Program with Supergrouping, Vol. 2, Sec. F11, in *SCALE: A Modular Code System for Performing Standardized Computer Analyses for Licensing Evaluation,* Report NUREG/CR-0200-Vol. 2 (ORNL/NUREG/CSD-2/Vol. 2), December 1984.
6. W. A. Rhoades and R. L. Childs, *Updated Version of DOT 4 One- and Two-Dimensional Neutron/Photon Transport Code,* Report ORNL-5851, Oak Ridge National Laboratory, July 1982.
7. J. W. Arwood et al., *Preparation and Benchmarking of ANSL-V Cross Sections for Advanced Neutron Source Reactor Studies,* Report CONF-871101-83, 1987.
8. G. E. Hansen and H. C. Paxton, *Reevaluated Critical Specifications of Some Los Alamos Fast-Neutron Systems,* Report LA-4208, Los Alamos National Laboratory, September 1969.
9. A. Staub, D. R. Harris, and M. Goldsmith, Analysis of a Set of Critical Homogeneous U–H_2O Spheres, *Nucl. Sci. Eng.*, 34: 263-274 (1968).
10. R. N. Olcott, Homogeneous Heavy Water Moderated Critical Assemblies, Part 1. Experimental, *Nucl. Sci. Eng.*, 1: 327-341 (1956).
11. S. Glasstone and M. C. Edlund, *The Elements of Nuclear Reactor Theory,* D. Van Nostrand, Inc., 1952.
12. G. E. Hansen and W. H. Roach, *Six and Sixteen Group Cross Sections for Fast and Intermediate Critical Assemblies,* Report LAMS-2543, Los Alamos National Laboratory, December 1961.
13. C. M. Hopper and J. P. Renier, Expanded and Applied Sixteen Neutron-Energy Group Cross-Section Library, *Trans. Am. Nucl. Soc.*, 61 (June 1990).

Ignitability of Hydrogen/Oxygen/Diluent Mixtures in the Presence of Hot Surfaces

By R. K. Kumar and G. W. Koroll[a]

Abstract: *In the licensing process for CANDU[b] nuclear power stations it is necessary to demonstrate tolerance to a wide range of low-probability accidents. These include loss of moderator accidents that may lead to the formation of flammable mixtures of deuterium, oxygen, helium, and steam in the reactor calandria vessel. Uncovered adjuster or control rods are considered as possible sources of ignition when a flammable mixture is present. A knowledge of the minimum hot-surface temperature required for ignition is important in assessing the reactor safety. These hot surface temperatures were measured using electrically heated adjuster rod simulators in a large spherical vessel (2.3-m internal diameter). Whereas the effects of geometry on ignition temperature were studied in the large-scale apparatus, some of the effects, such as those produced by a strong radiation field, were studied using a small-scale apparatus.*

Investigations carried out over a range of hydrogen and diluent concentrations indicated that, although the ignition temperatures were fairly insensitive to the hydrogen concentration, they were strongly affected by the presence of steam. The addition of 30% steam to a dry combustible mixture increased the minimum surface temperature required for ignition by approximately 100 °C. Of the diluents investigated, steam had the most effect on ignition. The effect of initial temperature of the mixture on the ignition temperature was small, whereas the effect of initial pressure was significant. The effect of substituting deuterium for hydrogen on ignition temperature was small. The effect of a high-intensity gamma-radiation field on the minimum hot-surface temperature required for ignition was investigated using a 2-dm^3 ignition vessel placed in a linear accelerator. Radiation had no measurable effect on ignition temperature. The results presented in this article will be of use in the safety analyses of other reactors or in industrial environments where a combustible mixture of hydrogen/air or hydrogen/oxygen/diluent is present.

INTRODUCTION

In the licensing process for CANDU® nuclear power stations it is necessary to demonstrate tolerance to a wide range of low-probability accidents. One of the postulated accidents in a CANDU reactor involves the loss of moderator (heavy water) resulting from a pipe break in the moderator circuit, leading to a rapid loss of the moderator from the reactor calandria vessel. During normal operation the moderator is exposed to a high radiation field present in the calandria, which causes the radiolytically produced deuterium and oxygen to be released continuously into the cover-gas space containing helium. The D_2 and O_2 so released are circulated through a catalytic recombiner where they are recombined to form heavy water and introduced back into the calandria vessel. In this way, radiolytic gases dissolved in the moderator are maintained at low concentrations during the normal operation of the reactor. In an accident, the moderator is assumed to drain from the calandria vessel and cause the pressure in the vessel to drop. If it is further postulated that this is concurrent with abnormal moderator chemistry, resulting in increased radiolytic yields of D_2 and O_2 and hence abnormally high dissolved gas concentrations, the decreasing pressure in the vessel would lead to a supersaturated condition and prompt release of the dissolved gases into the cover-gas space. If the release rates exceed the capacity of the recombiner, it is possible that a flammable deuterium/oxygen/helium/steam mixture could occur in the calandria vessel. Should ignition occur, a deflagration wave may develop and propagate in the mixture. While the calandria vessel can withstand any foreseeable combustion pressures, ignition and deflagration in a reactor calandria are undesirable because of potential damage to internal hardware.

A combustion threat requires a source of ignition as well as a flammable mixture. In the cover-gas space, there are no obvious sources of ignition but a possible source of ignition is the uncovered adjuster or control

[a]AECL Research, Whiteshell Laboratories, Pinawa, Manitoba, Canada R0E 1L0.

[b]CANDU (CANada Deuterium Uranium) is a registered trade name of AECL.

rod. The temperature of an uncovered adjuster/control rod will increase because of gamma heating. There may be other hot surfaces as well, such as uncovered calandria tubes within the calandria vessel. However, calculations show that the control rod surfaces are expected to attain the highest temperatures. Figure 1 shows a schematic of the cross section of a typical CANDU reactor calandria. The reactor calandria contains a large number of horizontal parallel flow channels. The control and adjuster rods are introduced into the reactor core vertically. Ignition and combustion of the combustible gas can be ruled out if the maximum adjuster rod temperature attainable is lower than the minimum surface temperatures required for ignition. The margin between the measured (or calculated using a suitable model) ignition temperature and the estimated rod temperature is the margin of safety.

Ignition at a hot surface is a complex process involving heat transfer from the hot surface to the adjacent gas, formation of the chain-branching radical species, and the exothermic runaway chemical reactions in the gas phase. In this connection it is important to note that for ignition to occur the temperature of a flammable mixture should be raised to a value known as the autoignition temperature (AIT). For hydrogen/air mixtures at 100 kPa, this value is approximately 580 °C (Ref. 1). Below this value the rate of production of the radical species responsible for chain branching and the rate of energy release are not sufficient to overcome the losses, and only a slow oxidation will result. Above this temperature the reactions become explosive and lead to a spontaneous ignition.

Ignition at a hot surface is essentially an autoignition; however, because of the steep temperature and concentration gradients prevailing at or near the hot surface, there is a high rate of loss of energy and active species from the hotter to the cooler gases. To overcome these losses and to allow the ignition reactions to proceed, the hot surface should be maintained at a temperature above the AIT. Below this temperature no ignition is possible unless the gases are contained in an adiabatic enclosure.

Hot surface ignition temperatures for hydrogen/air mixtures were reported[2] as early as 1937. Since then, experiments have been carried out by many investigators[1,3–5] using surfaces of different shapes and sizes. The reported values for ignition temperatures range from approximately 600 °C to more than 800 °C. Experiments performed with thin wires and cylindrical rods ranging from 0.025 mm in radius to several centimeters in diameter demonstrate that the ignition temperature depends strongly on the size of the ignition source and that it decreases sharply as the surface-to-volume ratio decreases. Below a certain surface-to-volume ratio, the ignition temperature becomes nearly independent of this ratio. Ignition experiments performed in a 17-dm^3 vessel with a 6-mm-diameter glow plug (4-cm^2 surface area) and a coil type of igniter (TAYCO®) with a large surface area corroborate these observations.[3,4] Although the observed ignition temperatures for mixtures containing 4 to 75% hydrogen ranged from 700 to 800 °C for the glow plug igniter, they were in the range of 650 to 750 °C for the coil type of igniter.

For realistic analyses, it is important that the ignition temperature be determined as a function of the thermodynamic state of the mixture and the igniter geometry. Experiments were therefore performed in a large, 2.3-m-diameter spherical vessel with simulated CANDU adjuster rod geometries to determine the ignition temperatures.[6] A CANDU adjuster rod is several meters long, and a complete simulation is therefore not possible. Because the adjuster rods are generally made up of many segments of identical geometry, however, simulation with the use of one segment is adequate to obtain ignition temperatures representative of those in an actual calandria.

Another important aspect of the reactor that cannot be simulated in a large-scale apparatus is the radiation field. As mentioned earlier, the high-intensity radiation field present in a reactor calandria may have a significant effect on the ignition process. The radiation field is expected to contribute to the pool of radical species required for the chain-branching reactions. Intuitively, such an increased radical concentration would lead to a lower ignition temperature. Conversely, the rates of gas-phase reactions have an exponential dependence on the temperature, and a small increase in the concentration of radicals may not produce a measurable change in ignition temperature. Also, because the gases are poor absorbers of radiation, it is not clear whether the ignition process in an actual reactor is significantly affected by the radiation field. It is possible, however, to establish the effects of radiation theoretically if a reliable theoretical ignition model can be constructed. Though detailed chemical kinetic models have been constructed to determine the AITs in hydrogen/oxygen mixtures,[7] no such models exist for ignition at a hot surface.

Most of the work reported to date deals with either two-dimensional (2-D) steady-state or one-dimensional (1-D) transient ignition models with global kinetics;[5,8,9] i.e., a simple one-step chemical reaction of the form [fuel] + [oxygen] → [product]. Although such models can explain the observed ignition behavior qualitatively,

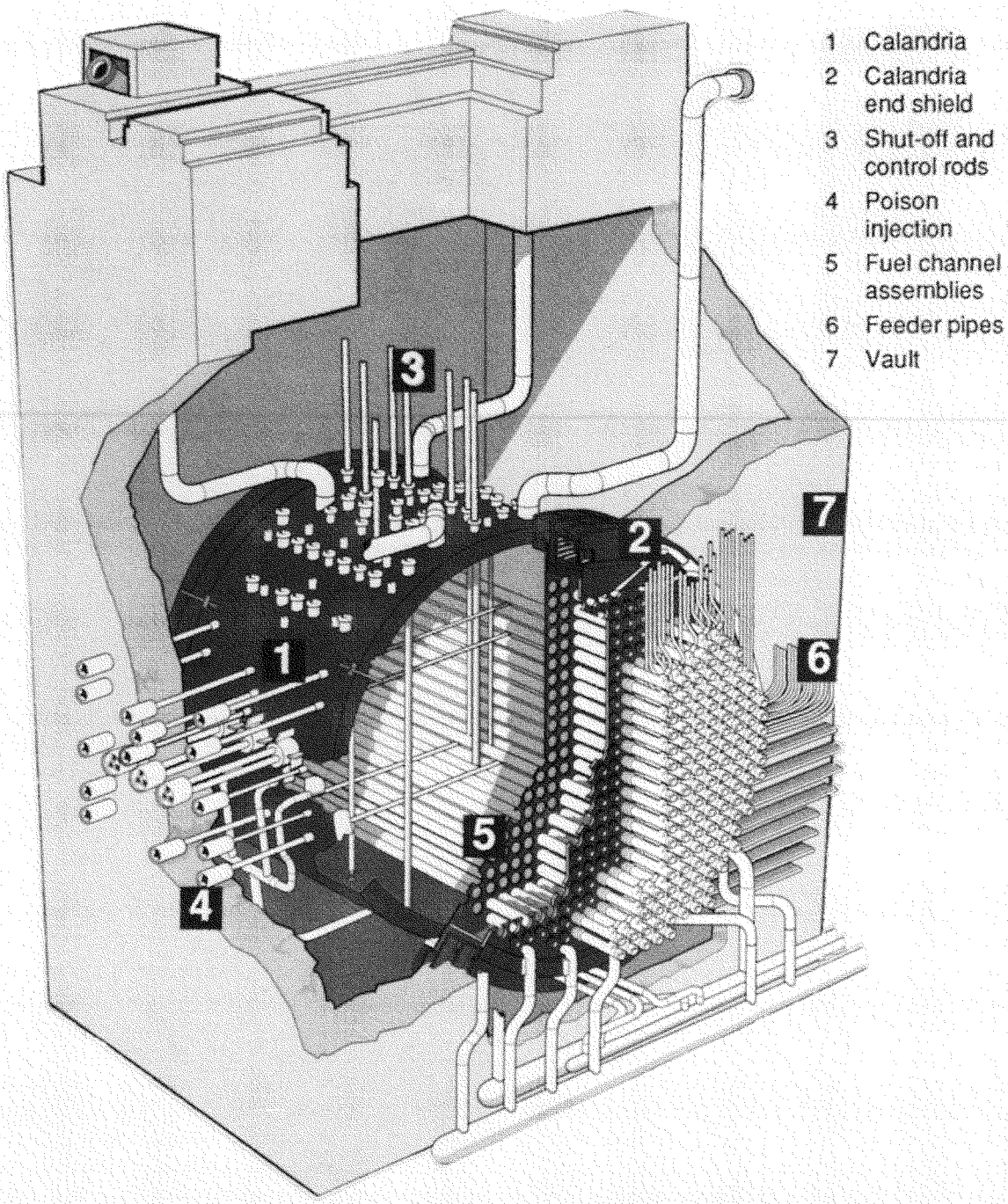

Fig. 1 Cutaway sectional view of a typical CANDU reactor calandria.

they cannot be used for quantitative predictions. These shortcomings led to the development of a mathematical model[6] that could explain the observed ignition behavior in the absence of a radiation field. The model was then modified to incorporate the effects of radiation and was used to determine the ignition temperatures in the presence of ionizing radiation. The model predicted that even for the most intense radiation field that can exist within a reactor core the effect of radiation on ignition was insignificant. Such a null-effect prediction, from the

reactor safety and licensing point of view, requires an experimental verification. Because radiation fields of the magnitude that exist in a reactor core can be obtained only in an accelerator, a small-scale (2-m^3) ignition apparatus was constructed, and the ignition temperatures were determined in a high-intensity gamma field produced by a linear accelerator. This article describes the experimental determination of the ignition temperatures in a simulated CANDU cover-gas environment with simulated adjuster rod configurations, the development of a theoretical ignition model, and its validation.

EXPERIMENTAL DETAILS

The experiments were performed in apparatuses of two different sizes—a bench-scale (2-dm^3) nearly cylindrical vessel and a large spherical vessel (2.3-m internal diameter). The bench-scale apparatus was used to study the isotope, diluent substitution, and radiation effects on ignition. Also, as mentioned earlier, determination of the ignition temperatures in an accelerator required a small-scale apparatus because of the size limitations. Moreover, comparison of the results of ignition experiments performed in two different size apparatuses provides useful information on the effects of scale on the ignition behavior.

Description of the Bench-Scale Apparatus

Figure 2 shows a schematic of the small-scale apparatus and its instrumentation. It consisted of an upright cylindrical vessel with an internal diameter of 5 cm and a volume of 2 dm^3. The vessel was trace-heated by hot

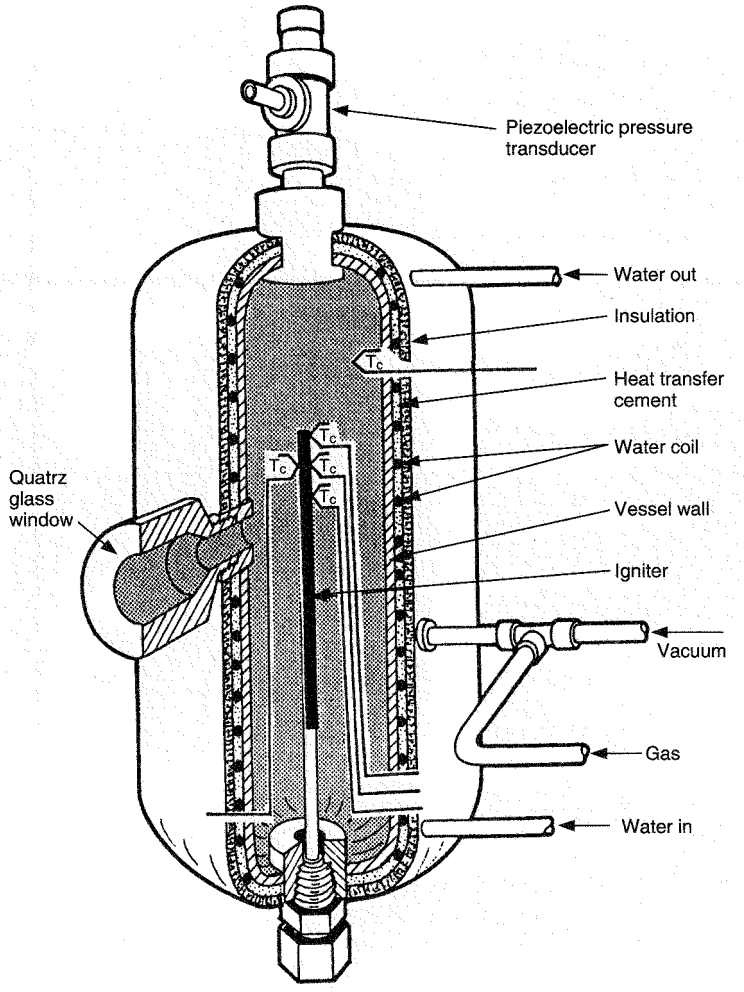

Fig. 2 Schematic of 2-dm^3 small-scale vessel used in ignition tests. T_c is thermocouple.

water and insulated to maintain a steady wall temperature. The vessel was equipped with two quartz windows for viewing the igniter and the surrounding volume. The igniter was a commercial stainless steel resistance heater with an outer diameter of 0.7 mm and a length of 10 cm. The 3-cm-long heated section of the igniter was instrumented with four K-type thermocouples spot-welded to the surface. The rod temperature was controlled by a programmable temperature controller, and the feedback to the controller was provided by one of the thermocouples welded to the rod. Pressure development in the vessel during ignition and subsequent combustion was measured by a piezoelectric transducer (see Fig. 2).

The experimental procedure consisted of evacuating the vessel and adding the required gases sequentially into the vessel with the use of the method of partial pressures. Analyses of gas mixtures in large- and small-scale apparatuses with the use of mass spectroscopy and a hydrogen gas analyzer (commercial type) have established that the partial pressure method of gas addition is accurate and reliable. The precision of gas additions was ±0.05 kPa. The gases in the vessel were mixed by circulating them through a pump for several minutes. Ignition was achieved by ramping the rod temperature over a period of 2 to 3 min. The instant of ignition was detected by an abrupt pressure rise in the vessel, and the rod surface temperature corresponding to the instant of ignition was taken to be the ignition temperature.

Description of the Large-Scale Apparatus

Figure 3 shows a view of the large-scale experimental apparatus used in the ignition experiments. The apparatus consists of an insulated spherical steel vessel with a 2.3-m internal diameter trace-heated by steam to maintain a desired vessel temperature. The vessel is designed to withstand internal pressures of up to 10 MPa. The vessel

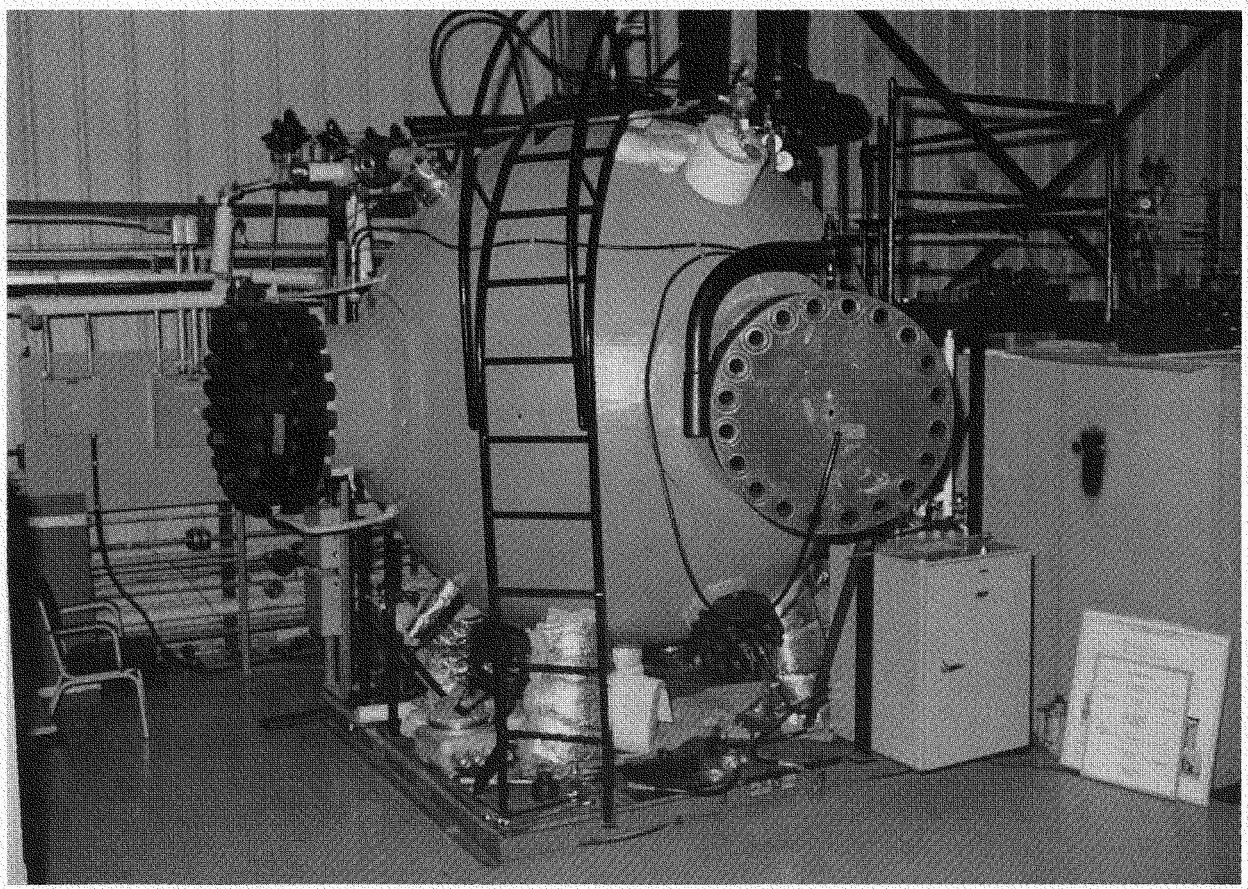

Fig. 3 A view of the large-scale test facility.

has several large penetrations to allow personnel to enter it to install the required equipment (fans, igniter, probes, etc.). Several small penetrations are provided to allow for the installation of pressure transducers, the removal of cables and thermocouple lead wires, gas addition, and gas sampling. Two 45-cm fans were placed in the vessel diametrically opposite each other to mix the gases.

Several different igniter geometries were investigated. Two of the igniter geometries used simulated segments of four-pin (adjuster rods used in Pickering reactors) and annular (adjuster rods used in Darlington reactors) CANDU adjuster rods. These have been identified as the possible sources of ignition. In some investigations a resistance-heated circular flat plate mounted horizontally or vertically at the center of the vessel was used.

The Four-Pin Adjuster Rod Simulator

Figure 4 shows a schematic of the four-pin igniter arrangement simulating a segment of the Pickering CANDU adjuster/control rod and its instrumentation. The igniter consists of four 8-mm-diameter stainless steel/Inconel igniter rods mounted vertically inside a stainless steel tube around a central support rod. In some experiments a perforated tube was used to simulate the adjuster rod configuration during a postulated accident. With the perforated tube, a convective upward flow prevails over the igniter surface so that effects of convection can be studied.

Three fine-wire (0.15-mm-diameter), type-K thermocouples were spot-welded to the surface of each of the igniter rods (T_1 to T_{12} in Fig. 4). Because the heating

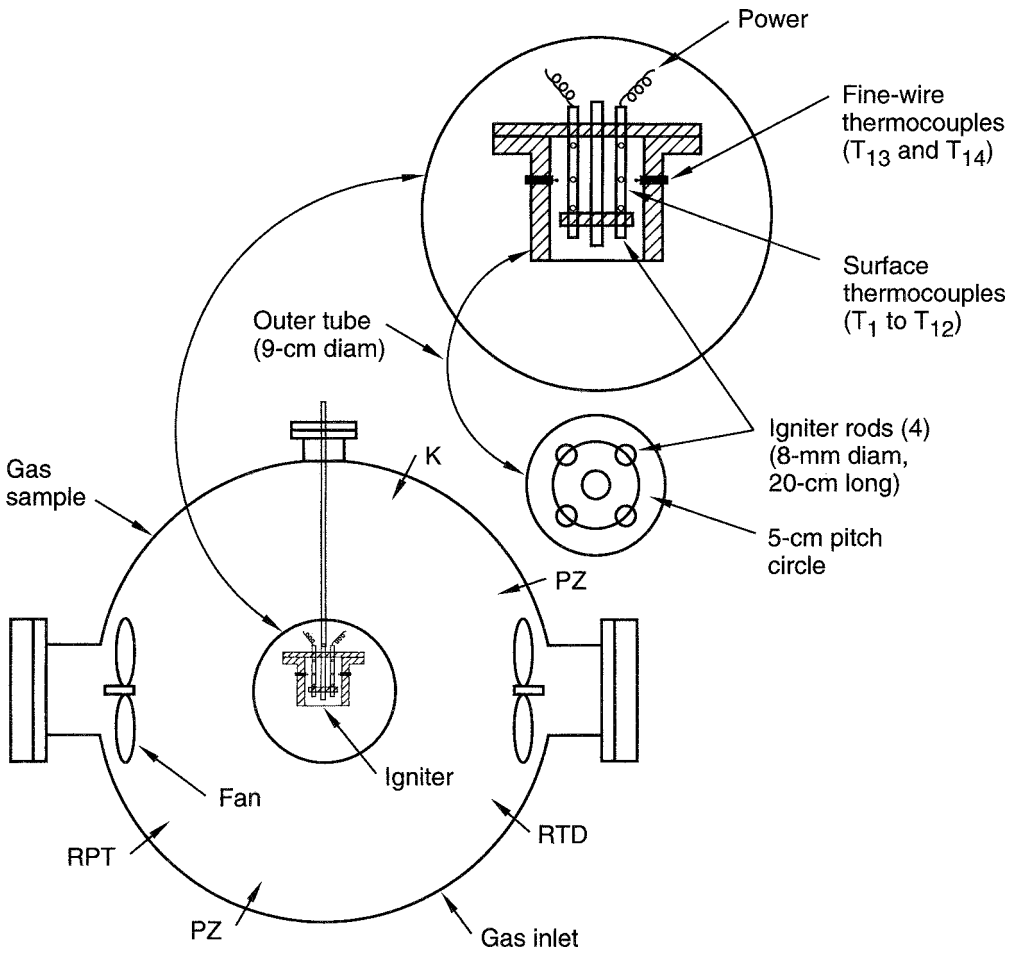

Fig. 4 Schematic of the igniter arrangement and instrumentation in the vessel. K is Kulite transducer, RPT is Rosemount pressure transmitter, PZ is piezoelectric pressure transducer, and RTD is resistance temperature detector.

rates were generally low, on the order of 5 °C/s, the thermocouple response was assumed to be adequate to determine the surface temperature at the instant of ignition. The thermocouples were equispaced, with a thermocouple located at the mid-length of the igniter rod. Two fine-wire (0.075-mm-diameter), type-S thermocouples (T_{13} and T_{14}) were installed in the gas space between the igniter and the steel pipe, as shown. The whole igniter assembly was suspended in the vessel by a vertical rod. All the chromel/alumel thermocouples were standard commercial type and were expected to be accurate to ±1.0% of the reading (approximately ±7 °C). Most of the experiments were reproducible within this range of accuracy.

The temperature along the length of the igniter pin was not uniform. The maximum pin temperature occurred close to the mid-region; temperature at either end of the rod was 20 to 40 °C lower. Since ignition occurs at the location of the highest surface temperature, the thermocouples located in the mid-region of the pins were used to determine the ignition temperature.

The igniter pins (or heaters) were connected in series so that all of them were heated at nearly the same rate. Figure 5 shows the assembled view of the igniter as installed.

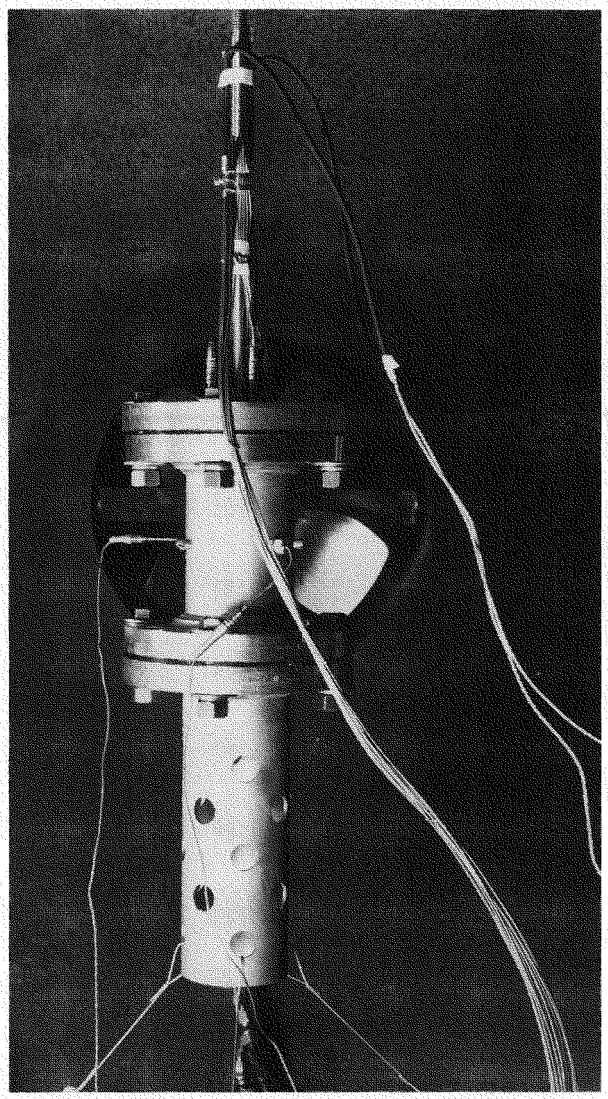

Fig. 5 Assembled view of the four-pin (Pickering-type) igniter.

The Annular Adjuster Rod Simulator

Figure 6 shows a schematic of the annular rod-type igniter that simulates the Darlington or CANDU 600 adjuster rod. It consists of a central (shim) rod surrounded by a steel (adjuster) tube and an outer perforated guide tube (not shown). Because the entire length of the adjuster could not be simulated, only a 25-cm length of the adjuster was simulated. The effect of length was studied by repeating some experiments with a 50-cm adjuster rod simulator.

In the annular type of igniter, both the central rod (inner heater) and the steel tube (outer heater) were heated simultaneously, and the central rod was at the higher temperature. The guide tube was unheated. Thus, in the experiments, ignition would occur at the surface of the central rod. In the four-pin adjuster rod, the gases were contained between the hot igniter surface and a relatively much cooler outer shroud, whereas in the annular rod geometry the gases in the ignition volume were heated by the inner shim rod and the outer adjuster tube.

The central igniter rod was a commercial (Incaloy 800-clad) 350-W heater rod. The adjuster tube was built from two concentric stainless steel cylindrical shells with a coil of 1.58-mm steel-clad heater wire between the cylinders. The annular gap between the inner and outer adjuster tube shells was sealed off at the ends. The central rod and the adjuster tubes were heated independently. The power to each heater was adjusted to simulate the differential heatup rate of the uncovered adjuster surfaces during accident conditions.

The igniter instrumentation consisted of fine-wire, type-K thermocouples spot-welded at two vertical locations on the shim rod and the adjuster tube. Two thermocouples were installed in the annular gas space between the shim rod and the adjuster tube to measure the temperature of the gases.

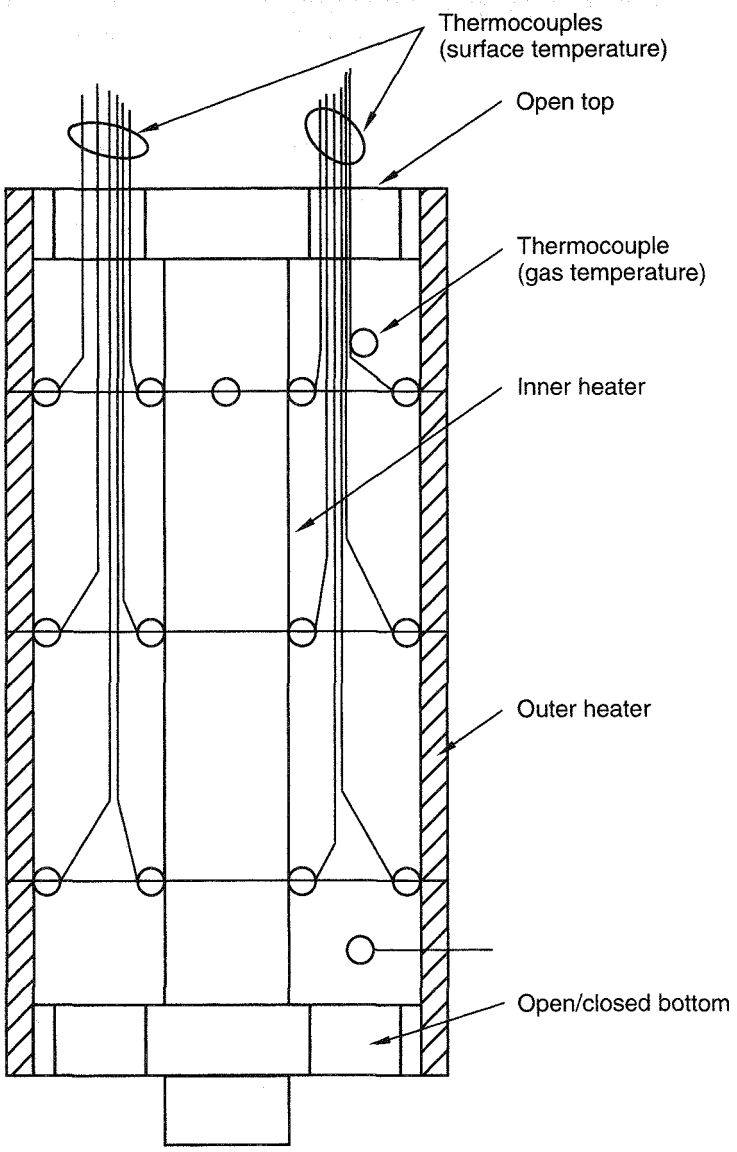

Fig. 6 Schematic of the instrumentation of the annular rod simulator.

Hot-Plate Igniter

Although it is assumed that adjuster rods are the likely sources of ignition in a reactor calandria, a general understanding of the geometrical factors that affect ignition is important. To gain this understanding, experiments were performed in different orientations with a circular heated plate as the igniter. Figure 7 shows a schematic of the hot-plate igniter and its instrumentation.

The hot plate was constructed from two circular stainless steel flat plates with a flat coil of heater sandwiched between them. The heater coil was made of 3-mm-diameter, type-K stainless steel sheathed thermocouple wire. One of the plates was hollowed to make room for a copper plate and the heater coil. The copper plate was installed to distribute heat evenly to the ignition surface and thus make the surface temperature almost uniform. Thermocouple measurements have indicated that a circular area of approximately 100 cm^2 around the center of the plate was almost uniformly heated. Figure 6 shows the location of the thermocouples on the hot plate. Six fine-wire thermocouples were welded in the ignition side

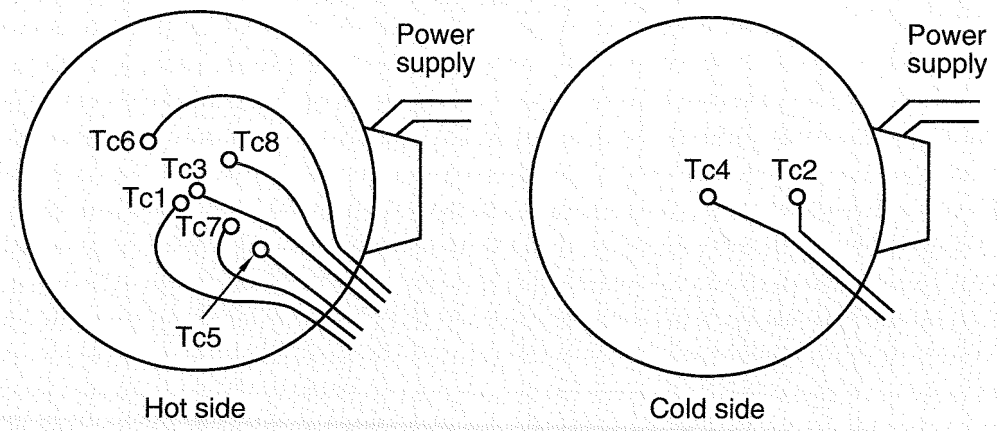

Thermocouple	Location
Tc1	90 mm
Tc2	45 mm
Tc3	Centre
Tc4	Centre
Tc5	60 mm
Tc6	70 mm
Tc7	80 mm
Tc8	65 mm

All measurements taken from outside edge

Fig. 7 Schematic of the instrumentation of the flat plate.

(hot side) and two on the bottom side (cold side), as shown.

Instrumentation of the Large-Scale Apparatus

Apart from the specific instrumentation provided for measuring the igniter surface temperatures for each igniter geometry, instrumentation was also provided to monitor the pressure of the gases in the vessel during gas addition, vessel gas temperature, and combustion pressures. A Rosemount pressure transmitter with a response time of 0.2 second and a strain gauge transducer (Data Instruments, Model AB) were used to monitor the pressure during the addition of gases to the vessel. The rapidly rising postignition pressure in the vessel was measured by several piezoelectric transducers and a Kulite pressure transducer mounted flush with the vessel wall. A schematic of the instrumentation of the vessel is shown in Fig. 4. The signals from the thermocouples and pressure transducers, after amplification, were digitized and stored in high-speed transient recorders for further processing.

Experimental Procedure (Large-Scale Apparatus)

The vessel was evacuated to below 10 kPa and filled to atmospheric pressure with the required diluent gas—air for hydrogen/air mixtures and helium for hydrogen/oxygen/helium/steam mixtures. In all cases, the vessel was purged with the diluent gas at least twice so that gases from the previous experiment were completely expelled. The diluent gas was pumped out until the desired pressure was reached in the vessel. Hydrogen, oxygen, and any other required gases were then added in the desired amounts (by the partial pressure method) and were mixed by fans for 2 to 3 min. For dry hydrogen/air mixtures, a commercial hydrogen and oxygen analyzer was used to carry out on-line gas analysis. For other dry mixtures, such as those containing helium or carbon dioxide, gas samples were collected and sent to mass-spectrographic analysis. For mixtures containing steam, the addition of gases by the method of partial pressures produced adequate accuracy. After the samples were drawn, the igniter voltage was set to a predetermined

value, and the power to the igniter was turned on. The power was turned off when the combustion was over.

RESULTS AND DISCUSSION

Experimental Conditions

The experimental conditions for both small- and large-scale apparatuses included a range of initial temperatures from 25 to 100 °C, initial pressures from 25 to 150 kPa, hydrogen concentrations from 10 to 50%, and a variety of diluents, such as helium, argon, nitrogen, carbon dioxide, and steam. Although the mixture of interest in a CANDU reactor calandria vessel during a postulated loss-of-moderator accident consists of hydrogen (deuterium), oxygen, helium, and steam with hydrogen and oxygen occurring in stoichiometric proportions, diluents other than helium and steam were used for the sake of completeness and to aid in model development.

SMALL-SCALE EXPERIMENTS

The purpose of the small-scale experiments was to investigate the effects that could not be investigated in a large-scale apparatus because of either practical reasons or cost (for example, radiation experiments in a large-scale apparatus would be impractical). Experiments in a large-scale apparatus where deuterium is substituted for hydrogen (and heavy water steam for light water steam), though feasible, would be expensive, especially if a large number of experiments were performed. Conversely, small-scale experiments, though highly economical and easy to perform, have some drawbacks. Because of their small size and volume, effects caused by proximity of the igniter to the wall and preoxidation at the igniter surface become important and affect the measured ignition temperatures. Thus the ignition temperatures determined in a small-scale apparatus would be different from those expected in a large-scale apparatus. Nevertheless, the relative ignition behavior, for example, of diluent substitution (or substituting deuterium for hydrogen) is expected to be the same in both large- and small-scale apparatuses. The effects of some of the physical and chemical parameters that affect ignition are discussed in the following text.

Effect of Diluent Substitution

The addition of a diluent to a stoichiometric hydrogen/oxygen mixture is expected to significantly influence the ignition temperatures. The extent to which the ignition temperature is affected depends on the diluent type (i.e., its physical and chemical properties). The physical and chemical properties that affect the ignition temperature are the thermal conductivity, mass diffusivity, specific heat, and third-body effectiveness of the diluent. Figure 8 shows the effect of diluent type and diluent concentration on the measured ignition temperature for a stoichiometric hydrogen/oxygen mixture. For most diluents (except steam), the ignition temperature decreases as the diluent concentration increases. In view of the fact that a stoichiometric hydrogen/oxygen mixture is the most reactive of all hydrogen/oxygen/diluent mixtures, this result is somewhat surprising; however, calculations performed with the use of the ignition model indicate that the ignition temperature is not sensitive to the mixture stoichiometry. Physical properties of the combustible mixture appear to be more important in determining the ignition temperature.

Dilution with argon results in the lowest ignition temperatures, whereas dilution with steam produces the highest ignition temperatures. Carbon dioxide and argon have similar thermal conductivities and mass diffusivities. The specific heat of carbon dioxide, being a

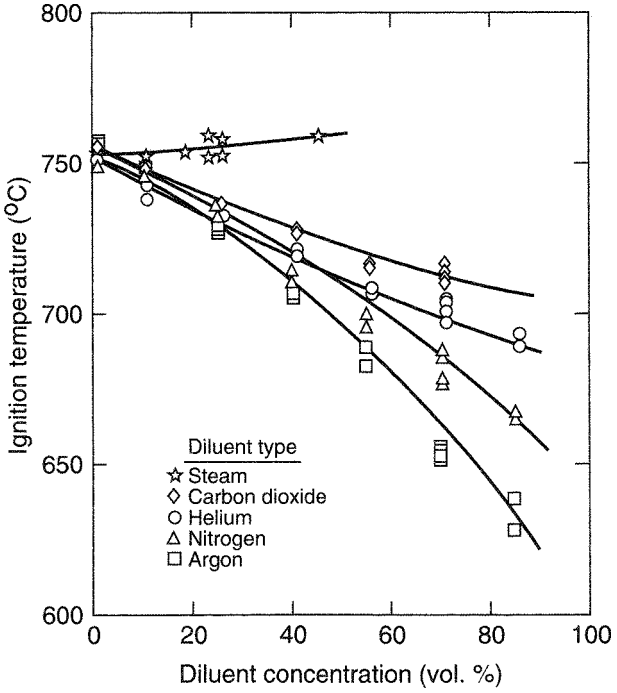

Fig. 8 Variation of the hot-surface ignition temperature with diluent concentration for various diluents.

triatomic gas, is much higher than that of argon. Thus, for a given heat release, the gas temperature in an argon-diluted mixture is higher than that with carbon dioxide and thereby results in shorter induction times or ignition delays. As will be shown later, any chemical or physical property that results in a shorter induction time also leads to a lower ignition temperature.

Both helium and argon are inert gases and have the same specific heats; however, because helium has much higher thermal and mass diffusivities than argon, with helium heat and active species are lost from the reaction zone at a much faster rate than with argon. This increases the ignition delay and thus the ignition temperature.

Although steam and carbon dioxide have similar molar specific heats and thermal conductivities, the ignition temperatures with steam are much higher than those with carbon dioxide. This, as will be explained later, is mainly because of third-body effectiveness of steam. Whereas most diluent gases have third-body effectiveness near that of hydrogen (~1), the third-body effectiveness of steam is 6.5.

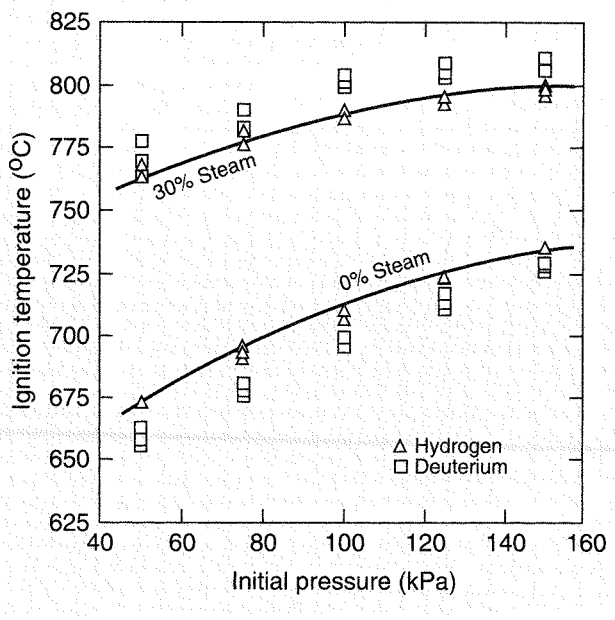

Fig. 9 Effect of isotope substitution on ignition temperatures in the small-scale apparatus.

Isotope Effects

Because the moderator used in a CANDU reactor is heavy water, in a postulated accident the calandria vessel is assumed to contain a mixture of deuterium, oxygen, helium, and heavy steam. Although many of the combustion characteristics, such as flammability limit and burning velocity of deuterium/oxygen mixtures, can be deduced from the known values for hydrogen/oxygen mixtures with the use of simple correlations,[10] no such correlations exist for deducing the ignition temperatures. A series of experiments was therefore performed in the 2-dm^3 vessel; deuterium was substituted for hydrogen, and heavy water was substituted for light water. Figure 9 shows the measured ignition temperature as a function of initial pressure. For dry mixtures, the substitution of D_2 for H_2 results in a slight reduction (approximately 10 °C) in the measured ignition temperatures. This is probably due to changes in the physical properties of the mixture. Because D_2 has lower thermal and mass diffusivities than H_2, the energy losses from the reaction zone with D_2 are correspondingly less, which results in lower ignition temperatures. For wet mixtures, however, the substitution of D_2O for H_2O results in a slightly higher ignition temperature. This is probably due to an increased third-body effectiveness of the mixture when D_2O is substituted for H_2O. In any case, the effect of replacing H_2 with D_2 is small for all practical purposes.

Preoxidation Effects

Although most of the ignition reactions occur in the gas phase, and for practical purposes the igniter surface can be considered as a passive source of heat, in reality, reactions do occur at the surface. The effect of such surface reactions on ignition temperature depends strongly on the nature of the surface (i.e., whether the surface is mildly or strongly catalytic). Experiments were therefore performed with two igniters—stainless steel and nickel—widely differing in their surface reactivities. Nickel has a much higher surface reactivity than untarnished stainless steel. Figure 10 shows the ignition temperatures with nickel and stainless steel igniters plotted as a function of the initial gas pressure. At lower pressures, the ignition temperatures with nickel are much higher than those with stainless steel. As the pressure increases, the differences between ignition temperatures of the two igniters decrease, and at approximately 150 kPa, both surfaces exhibit nearly the same ignition temperature. Because the mass and thermal diffusivities of a combustible mixture are inversely proportional to its pressure, it is expected that there would be a rapid exchange of reactants and products at the surface at low pressures. This depletes the reactants close to the surface, and the runaway ignition reactions therefore have to occur at a considerably greater distance from the hot surface. Since for a given mixture the reactants have to

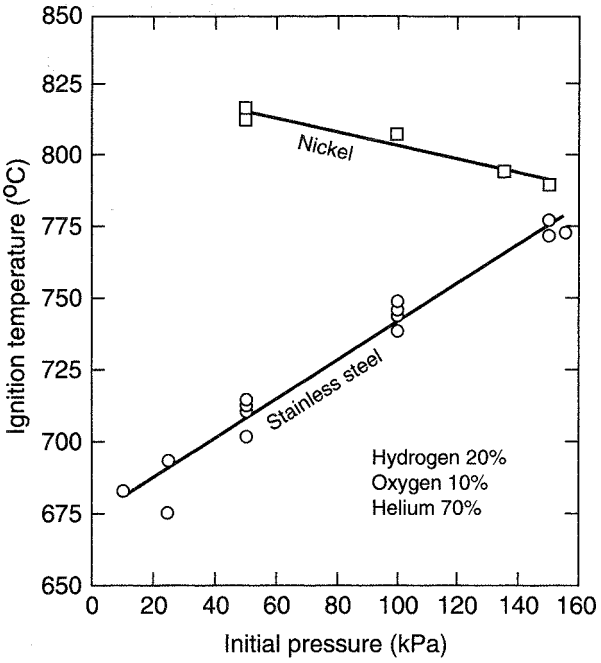

Fig. 10 Effect of igniter material on ignition temperatures.

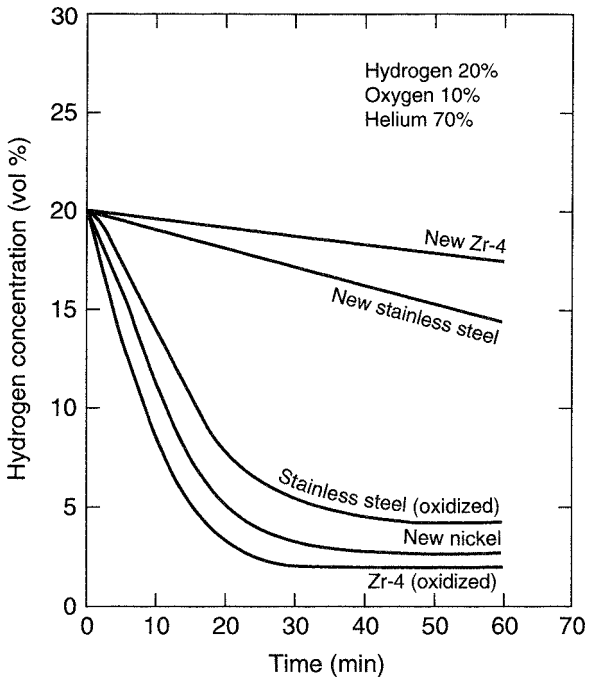

Fig. 11 Variation of hydrogen concentration with time for various igniter surfaces.

be raised to their ignition temperature no matter where the reactions occur, the surface with a larger reactivity should be maintained at a higher temperature. The extent to which the surface temperature is required to be raised depends on the reactivity of the surface; the higher the reactivity, the higher the surface temperature. Note, however, that there is an upper limit to the reactivity of the surface beyond which ignition occurs spontaneously at all surface temperatures, as is the case with catalysts. In the case of a catalyst, the surface reactivity is extremely large, several orders of magnitude larger than that of a normal surface, and ignition occurs almost instantly even at room temperatures. Figure 11 shows the variation of hydrogen concentration in the vessel as a function of time for various surfaces. Oxidized surfaces exhibit a high degree of surface reactivity; for this reason, the behavior of oxidized zirconium-4 and oxidized stainless steel surfaces is similar to that of the nickel. The surface ignition properties of materials (control/adjuster rods and calandria pipes) used in the CANDU reactor calandria change with time, and a knowledge of the state of the surfaces is required before an assessment of the ignition temperature can be made. Because of the continued presence of oxygen in the reactor calandria, most of the surfaces to which the gases are exposed can be assumed to be oxidized. For reactor safety analyses, however, if a fresh, noncatalytic surface is assumed, conservative estimates of the ignition temperatures can be made.

LARGE-SCALE EXPERIMENTS

Small-scale experiments are important in obtaining a clear understanding of the effects of various fundamental physical and chemical properties of the combustible gas mixture and of the igniter surface on the ignition temperature; however, for a definite assessment of the ignitability of a gas mixture in the reactor calandria, an experimental simulation of the ignition surface in a large-scale apparatus is essential.

FOUR-PIN CONTROL/ADJUSTER ROD SIMULATOR

Effect of Hydrogen and Steam Concentrations

Figure 12 shows the ignition temperatures with the four-pin adjuster rod simulator plotted as a function of the initial gas pressure for several hydrogen and steam

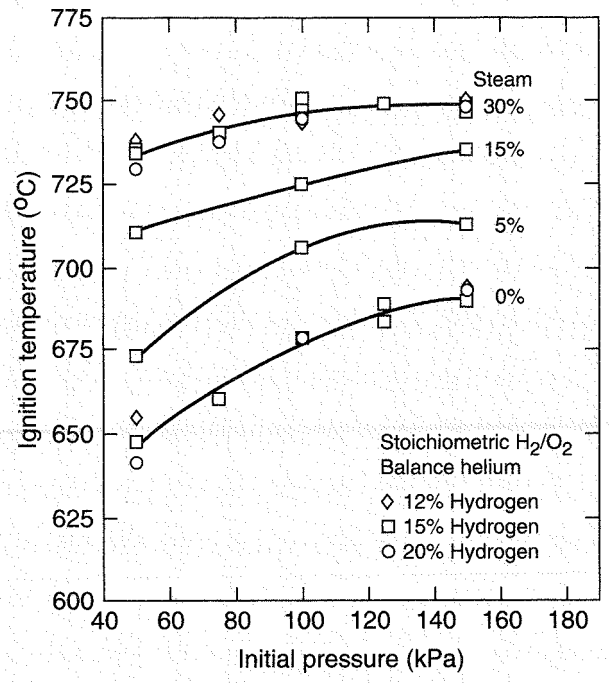

Fig. 12 Effect of steam on ignition temperature in the large-scale apparatus for the four-pin simulator.

concentrations. For the reasons mentioned earlier, only stoichiometric hydrogen/oxygen/diluent mixtures were investigated. It is apparent that, over the range of hydrogen concentrations investigated, the effect of hydrogen on ignition temperatures is small; however, the effect of steam is large (even small amounts of water vapor significantly change the ignition temperature). The presence of 5% water vapor, for example, increases the ignition temperature by 25 °C, and a 30% water vapor produces an increase of 60 to 100 °C. These results are consistent with previous findings.[6]

Effect of Initial Gas Temperature and Pressure

Tests performed over an initial temperature range of 25 to 100°C did not reveal any significant changes in the measured ignition temperatures. This was also confirmed from the small-scale tests. Intuitively, it is expected that, as the initial temperature of the flammable mixture increases, the ignition temperature should decrease because, as the initial temperature increases, the concentrations of the radical species responsible for chain-branching reactions increase and thus reduce the ignition delay. As will be shown later, the ignition temperature can be directly related to the ignition delay; however, the production of the radical species will not be significant for initial gas temperatures below the AITs, and thus for gas temperatures of 150 °C or less, no significant effect of initial temperature on ignition is expected.

In contrast to the effect of initial temperature, the effect of initial pressure on ignition is significant. As shown in Fig. 12, for dry mixtures an increase in the initial gas pressure from 50 to 150 kPa increases the ignition temperature by approximately 40 °C. For wet mixtures the increase is not significant. Because hot-surface ignition is essentially an autoignition, the factors affecting hot-surface ignition are the same as those that affect autoignition. Since the reaction rate for elementary reactions such as $O + H_2 \rightarrow OH + H$ and $H_2 + M \rightarrow H + H + M$, where M stands for the third body (a third body is an inert or a stable gas molecule such as N_2, O_2, H_2, or H_2O that imparts or absorbs energy from other colliding species during an encounter), increases as the square of the initial pressure (approximately p^2), the rate of production of the active species from these reactions also increases; however, the third-order chain-terminating reactions such as $O + O + M \rightarrow O_2 + M$, $O + OH + M \rightarrow HO_2$, $H + H + M \rightarrow H_2 + M$, and $H + O_2 + M \rightarrow HO_2 + M$ increase more rapidly with pressure (approximately p^3). The net result is that as the pressure increases the ignition temperature also increases.

Effect of Convection

In CANDU reactors the guide-tube sections immersed in the moderator water have perforations to enable free circulation of the moderator over the control rod surface for cooling purposes. These perforations enable circulation of the gases when the control rods are uncovered by the rapidly decreasing moderator level in the calandria. Figure 13 shows the effect of perforations on ignition temperature. Because perforations allow free convection over the igniter surface, a free-convection boundary layer is established over the hot surface, and one would expect the temperature distribution with convection, close to the hot surface, to be significantly different from that without convection, which would affect ignition; however, as shown in Fig. 13, the effect of convection is only marginal. The ignition temperature decreases by approximately 10 °C when convection is present. This is discussed further in the theory section.

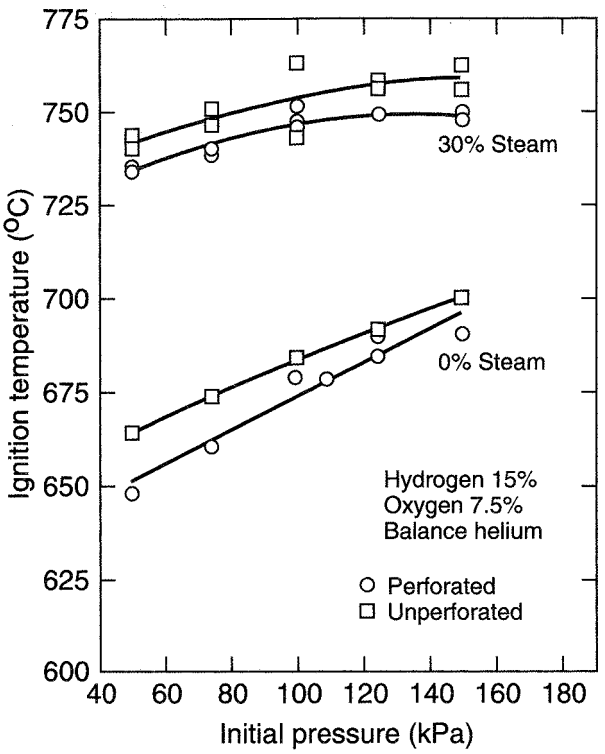

Fig. 13 Effect of convection on ignition temperature (four-pin igniter).

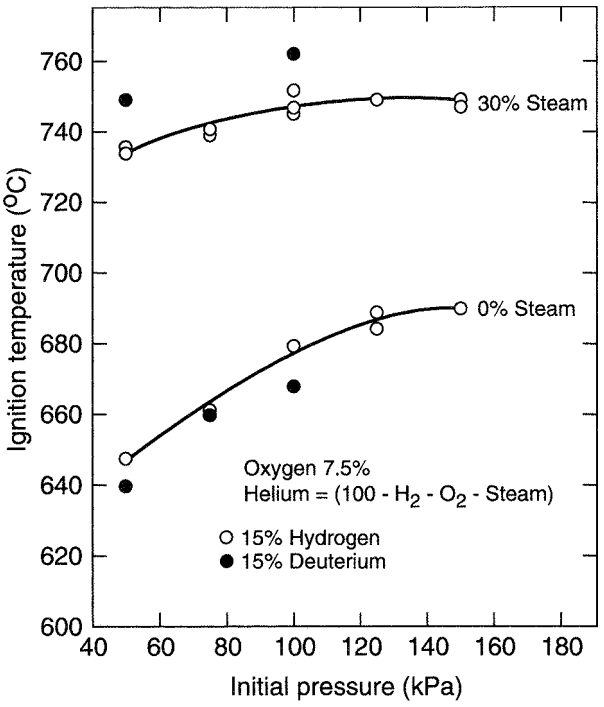

Fig. 14 Effect of isotope substitution in the large-scale apparatus (four-pin igniter).

Isotope Effects

Because deuterium and heavy water are expensive, a few selected tests were carried out with deuterium to confirm the results of small-scale experiments. Figure 14 shows the effect of deuterium. For dry mixtures, deuterium results in slightly lower ignition temperatures (approximately 10 to 15 °C) than hydrogen. For wet mixtures, the ignition temperature in deuterium is generally higher than that in hydrogen by 10 to 20 °C. These are consistent with the findings in the small-scale apparatus.

Effect of Mixture Stoichiometry

Deuterium and oxygen originate from the radiolysis of heavy water in the reactor calandria. For this reason, most of the tests were carried out with stoichiometric hydrogen/oxygen mixtures; however, mechanisms are proposed to exist whereby oxygen is preferentially retained in the moderator in the form of peroxides.[11] The cover-gas mixture may thus be hydrogen-rich. Small-scale experiments indicated that rates of recombination in hydrogen-rich mixtures are much higher than in hydrogen-lean and stoichiometric mixtures. The ignition temperatures in such mixtures may be severely affected by the rapid depletion of oxygen. A series of tests with hydrogen-rich mixtures was therefore performed to determine the effects of surface recombination. Tests were performed in both perforated and unperforated guide tube geometries. As found in the unperforated guide-tube geometry, rich mixtures with hydrogen/oxygen ratios of 3.6 or higher did not ignite. These mixtures may have been rendered nonflammable by oxygen depletion. With a perforated guide tube, ignition readily occurred even for a hydrogen/oxygen ratio of 3.6.

The preceding observations can be readily explained. With an unperforated guide tube, the depleted oxygen is not readily replaced; the reaction products, hydrogen, and water vapor (along with the cover gas, helium) collect in the ignition cavity and thus form an inert mixture. With a perforated guide tube, fresh reactants are constantly recirculated over the igniter surface by convection, so oxygen depletion has no significant effect. In any case, when ignition occurred, the ignition temperatures were nearly independent of the guide tube and were not significantly different from those for stoichiometric mixtures.

ANNULAR ADJUSTER ROD SIMULATOR

The annular adjuster rod consists of a single shim rod surrounded by a movable adjuster tube enclosed in a perforated guide tube. The gases exposed to the shim rod are contained in the annular gap between the shim rod and the adjuster tube. The annular gap is open at the top. The bottom may be open or closed, depending on the moderator level.

The shim rod and the adjuster tube are continually heated by the neutron bombardment and gamma radiation present in the reactor calandria. To simulate this heating, the shim rod and the adjuster tube were heated independently. The relative power applied to each heater was adjusted to approximate the calculated differential heatup rate of the uncovered adjuster surfaces under accident conditions. Typically, at the time of ignition, the shim rod temperature would be approximately 650 to 750 °C and that of the adjuster would be approximately 500 °C.

Because both large- and small-scale experiments indicated that ignition temperature was not sensitive to the hydrogen concentration, only one hydrogen concentration (15%) with stoichiometric amounts of oxygen was chosen for detailed investigations. The range of investigation included as much as 30% steam and initial pressures as great as 150 kPa.

Figure 15 shows the ignition temperature plotted as a function of pressure for the annular igniter. Although the ignition temperatures appear to be similar to those for the four-pin igniters, the variation with pressure is steeper for the annular igniter. Because the gases contained in the annular region are heated by both the adjuster and shim-rod surfaces, the situation is similar to that of ignition occurring in a preheated gas. Because of this, the ignition temperatures are generally lower than those with the four-pin igniter by 20 to 50 °C, especially at pressures less than 100 kPa. For pressures greater than 100 kPa, the ignition temperatures with the annular adjuster are similar to those with the four-pin adjuster.

As noted earlier, catalytic surface reactions affect the ignition temperature significantly if the surface recombination rates are high. Experiments performed with igniters made of two different igniter materials—Incaloy 800 and stainless steel (type 304)—showed no significant difference in the ignition behavior.

Effect of Igniter Length

A long heated length would increase or decrease the ignition temperature, depending on which of the two mechanisms—preoxidation or preheating—prevailed.

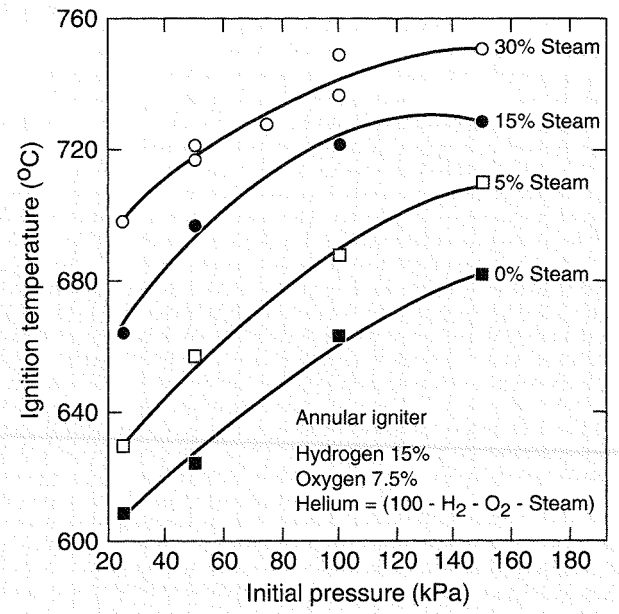

Fig. 15 Ignition temperature with the annular adjuster simulator.

The adjuster rods in a nuclear reactor are long, on the order of 10 m, and the whole length of the control/adjuster rod could not be simulated; however, the effect of the heated length on ignition was determined with 25- and 50-cm simulators. Figure 16 compares the ignition temperatures for the two igniters. The figure indicates no significant difference in the ignition temperatures. Further increase beyond approximately 50 mm in the igniter length (determined from small-scale experiments) will have no significant effect on ignition.

Effect of Covered- and Open-Bottom Annular Gap

The free inflow and outflow of the gases in the annular gap between the shim rod and the adjuster tube in a reactor calandria depend on the moderator level. For a study of the effects of a covered bottom, the perforated bottom cover was replaced by a blanking plate.

With a covered bottom the mixtures would stagnate within the annulus and would thus be prone to preoxidation effects. Because preoxidation effects strongly depend on the hydrogen/oxygen ratio, experiments were carried out over a range of H_2/O_2 ratios. Also, to ascertain that the mixture inside the annulus was the same as the surrounding mixture, a slight modification to the procedure was made: after addition and mixing of the constituent gases and before ignition, several liters of the

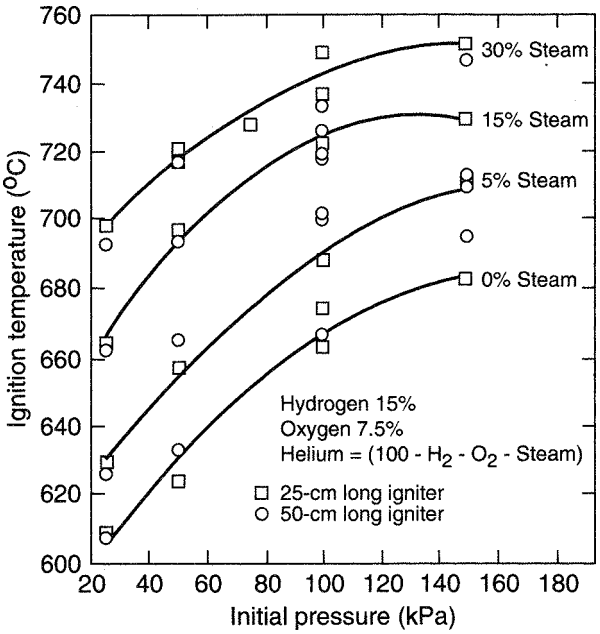

Fig. 16 Effect of igniter length on ignition temperature.

gas mixture were drawn through the annulus with a pump attached to a special fitting at the bottom of the simulator.

The ignition temperatures with the covered-bottom simulator were generally lower than those with the open bottom; extreme lean mixtures ignited at temperatures 30 °C lower. This is probably due to the preheating of the gases within the annulus. Whether extreme lean mixtures can be realized in a nuclear reactor calandria is not clear.

Flat-Plate Igniter

Whereas the four-pin and annular adjuster rod simulators are specific to Pickering and Darlington reactors, respectively, and are likely to achieve the highest temperatures, a flat-plate igniter describes a generic hot surface that may be present in any reactor calandria.

The experimental procedure for determining the ignition temperature with the heated flat plate is similar to that for other geometries with one exception: the heat-up time for the flat plate, because of its mass, is much longer than heat-up times for other igniters; however, as discussed earlier, the heat-up time has no significant effect on the measured ignition temperature for a freely ventilated surface.

The orientation of the igniter is an important parameter that affects ignition. Although the adjuster rod orientation has invariably been vertical, a flat surface present in the reactor calandria may have any orientation. The effect of igniter orientation (of a flat plate) was determined by measuring the ignition temperatures of hydrogen/oxygen/helium/steam mixtures with the hot plate in four different orientations: (1) horizontal with hot side down, (2) horizontal with hot side up, (3) shrouded horizontal plate with hot side down, and (4) hot side vertical.

Figure 17 shows the ignition temperature plotted as a function of the initial pressure for various plate orientations and indicates that the ignition temperature is a strong function of the orientation. The highest ignition temperatures are observed when the plate is vertical with natural circulation over the surface; the ignition temperatures are not significantly different for the horizontal hot surface with the hot side facing down.

A significant decrease in the ignition temperature is observed when the plate is horizontal with the hot side facing up. In this orientation, the ignition temperatures are approximately 100 °C lower than those for other orientations. Because severe convective flows with strong recirculation zones that normally lead to higher ignition temperatures exist on the upper surface, this result is surprising; however, a closer examination of the temperature distribution in the gases in the vicinity of the upper and lower surfaces indicates that the experimentally observed behavior is reasonable. Figure 18 shows typical temperature distribution in the gas around the hot plate,

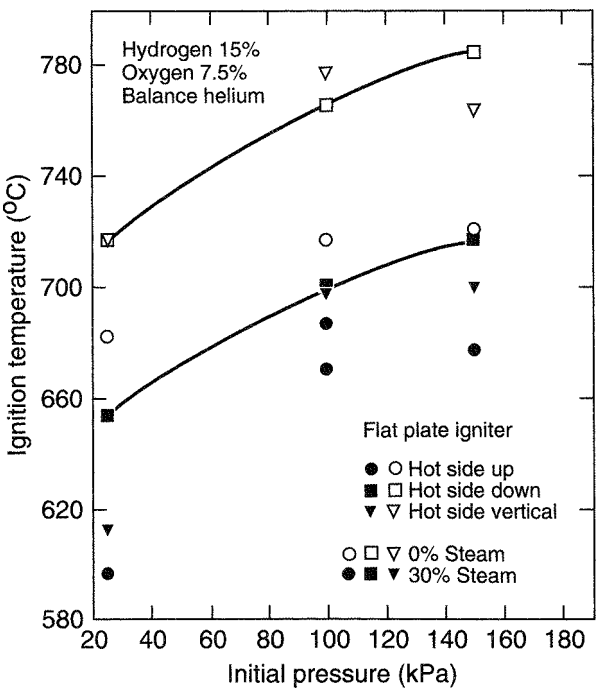

Fig. 17 Ignition temperatures for the hot-plate igniter.

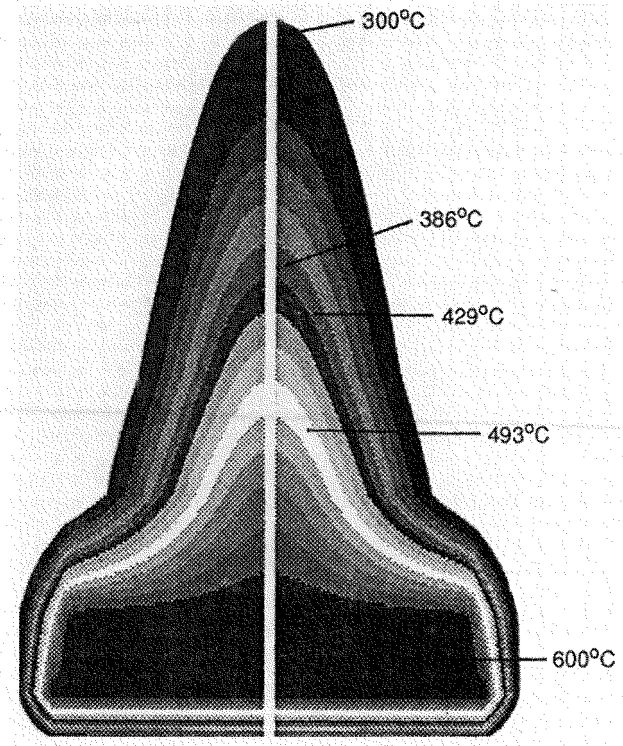

Fig. 18 Typical temperature distribution around a hot plate.

which is maintained at 600 °C. On the lower side of the plate the temperature gradient is steep, and on the upper side it is small. In fact, a layer of gas that is several centimeters thick and heated to high temperatures (approximately 400 to 500 °C) is on the top surface. This situation is similar to the one in which ignition occurs in a preheated gas. It has been shown theoretically (in the theory section) that the ignition temperature decreases as the initial gas temperature increases.

On the lower side of the plate, the preheated gas layer is thin, and a strong temperature gradient is across the layer. This causes the heat and radical species to be lost from the reaction zone at a much higher rate than when the plate is horizontal with the hot side up. The ignition behavior in this case would be similar to that of a vertical plate or a rod.

THEORETICAL ANALYSIS

The Physical Model

Figure 19 shows a schematic of the hot-surface ignition model. The assumption is made that the flammable mixture is suddenly exposed to a hot surface.

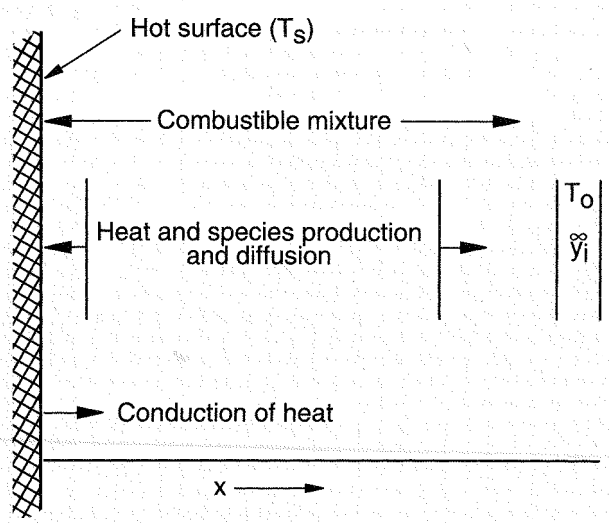

Fig. 19 Schematic of the ignition model. T_s is the temperature of the hot surface (k); T is the gas temperature (k), where $T_0 = T(0,x) = T(t,\infty)$; and y_i is the species mass fraction, where $y_i(0,x) = y_i(t,\infty) = y_i^{\infty}$.

Heat is transferred from the hot surface to the adjacent gases by conduction. This raises the temperature of the gases close to the hot surface to a high enough temperature to cause exothermic chemical reactions in the gas phase. Whether an ignition can occur depends on the net rate of active species and heat generation, which is the difference between the production rate of the active species and heat by chemical reactions and their loss to the cooler gas by diffusion and conduction. The reactions occur through several elementary steps. The following assumptions are made in developing the model:

1. The diffusion of species and energy is one-dimensional.
2. The temperature of the hot surface remains constant and uniform, independent of time.
3. The pressure in the gas phase remains uniform and constant.
4. The ignition surface is noncatalytic (i.e., inert) and does not participate in the chemical reactions.

Although some of the assumptions appear to be unrealistic at first glance, they are not limiting. If the ignition surface is vertical, for example, a buoyant flow is induced over the hot surface, and the flow will be two-dimensional; however, because the gases heat up as they move upward, and ignition is essentially confined to a thin boundary layer where the connective velocities are low, the heat transfer to the gases occurs essentially by

conduction. Intuitively, a convective flow can be visualized as a thin one-dimensional slab of gases in contact with the hot surface moving vertically (i.e., a series of thin one-dimensional slabs at consecutive instants of time stacked on top of one another). In this situation, the one-dimensional model adequately describes the ignition phenomenon. The most severe assumption is the one involving the nature of the ignition surface. Most surfaces are catalytic and promote surface reactions by reducing the effective activation energy of the reactions. A reaction that has a high activation energy requires a high temperature if it has to occur in the gas phase; however, a reaction can proceed at an appreciable rate in the presence of a catalyst. Most surfaces normally encountered in practice, including those which are used in nuclear reactors, are only mildly catalytic and do not significantly affect the reaction rates. In the case of a mildly catalytic surface, the slow catalytic reactions gradually consume the combustible mixture to form products. The effect of such a surface becomes significant only when the volume of the combustible gas is small, such as in a small-scale apparatus. Thus, when ignition is modeled in a small enclosure, the effect of surface reactions and reactant depletion should be included.

In contrast to experiments, a uniform and constant surface temperature is assumed in the model. As will be described later, in the experiments the surface temperature was ramped, and the ignition temperature was reached only slowly (~120 seconds). Such a slow ramping would result in some preoxidation and consumption of the reactants; however, as has been demonstrated by experiments, the oxidation reactions become significant only above a certain minimum surface temperature. When ignition occurs, the reactions become explosive within a fraction of a second (<100 milliseconds), and the ramp rate has no influence on the measured ignition temperature. The assumption of constant pressure is generally valid because there is no combustion until ignition occurs.

As mentioned earlier, although the overall reaction between hydrogen and oxygen can be represented by the simple stoichiometric relationship,

$$2H_2 + O_2 \rightarrow 2H_2O$$

the actual reaction mechanism is very complex. Direct collisions between hydrogen and oxygen molecules are generally not successful. In fact, for the reactions to occur at an appreciable rate, active radical species such as [H], [O], [OH], or [HO_2] should be present in the mixture. An ignition device such as a glow plug or spark plug will act as an initial source of radicals. Once appreciable quantities of radical or atomic species are produced, the reactions become self-sustaining and proceed as follows:[12]

$$H + O_2 \leftrightarrow OH + O$$

$$O + H_2 \leftrightarrow OH + H$$

$$H + O_2 \leftrightarrow HO_2$$

and so on.

The Mathematical Model

These equations describe the ignition:

Overall continuity

$$\partial\rho/\partial t + \partial(\rho u)/\partial x = 0 \qquad (1)$$

Species conservation

$$(\rho\partial y_i/\partial t) + (\rho u \partial y_i/\partial x) = \partial[\rho D_i M_m^{-1}\, \partial(y_i M_m)/\partial x]/\partial x + w_i \qquad (2)$$

Conservation of Energy

$$(\rho\partial h/\partial t) + (\rho u \partial h/\partial x) = [\partial(\lambda \partial T/\partial x)/\partial x] + \{\partial[\rho D_i h_i M_m^{-1}\, \partial(y_i M_m)/\partial x]\}/\partial x \qquad (3)$$

where D_i = diffusion coefficient of species, i
y_i = species mass fraction
T = gas temperature (absolute)
ρ = mixture density

The thermal conductivity λ of the mixture can be approximated by

$$\lambda = \frac{\left[\sum(\lambda_i X_i) + \dfrac{1}{\Sigma(X_i/\lambda_i)}\right]}{2}$$

where X_i is the species mole fraction and λ_i is the species thermal conductivity.[13] The dependence of thermal conductivity on temperature is assumed to be of the form $\lambda_i = \lambda_{io}(T/T_o)^n$. The mixture molecular weight, M_m, is defined as $M_m = (\sum y_i/M_i)^{-1}$. The net rate of production,

w_i, of the ith species is given by $w_i = \sum w_{i,k}$, where $w_{i,k}$ is the production rate of the species (i) in the kth reaction $\sum \nu'_{i,k} A_i \rightarrow \sum \nu''_{i,k} A_i$ and is given by $w_{i,k} = M_i\left(\nu''_{i,k} - \nu'_{i,k}\right)\omega_k$. The reaction rate of the kth reaction is given by $\omega_k = k_{b,k} \Pi c_i^{\nu''_{i,k}} - k_{f,k} \Pi c_i^{\nu'_{i,k}}$, where $k_{f,k}$ and $k_{b,k}$ are the rate constants for the forward and reverse reactions, respectively. The mixture enthalpy, h, is defined as $h = \Sigma h_i y_i$, where $h_i = h_{io} + \int C_{pi}\, dT$ and h_{io} is the heat of formation of the species i.

The preceding equations are solved with the following initial and boundary conditions:

$$\begin{aligned} y_i(0,x) &= y_i(t,\infty) = y_i^{\infty} \\ T(0,x) &= T(t,\infty) = T_o \\ T(t,0) &= T_s \text{ for } t > 0 \\ v(t,0) &= v(0,x) = 0 \\ \partial y_i / \partial x &= 0 \text{ at } x = 0 \text{ and} \\ v(t,\infty) &= 0 \end{aligned} \qquad (4)$$

Numerical Solutions

Equations 1 to 4 were solved numerically with the use of the forward-difference technique. The forward-difference scheme is stable for $D(T)\Delta t/\Delta x^2 \leq 0.5$; for reasonable accuracy, both time and space step sizes, Δt and Δx, should be kept small. In the computations, Δx was maintained constant, whereas Δt was reduced or increased as dictated by stability. The time step size ranged from approximately 10^{-6} second initially to $<10^{-8}$ second as ignition was approached. The space step size selected was on the order of 0.05 to 0.1 mm.

The model considered a total of nine species—[H], [OH], [O], [HO_2], [H_2O_2], [H_2], [O_2], [H_2O], and a diluent, such as nitrogen, helium, carbon dioxide, or argon. The assumption was made that these diluents do not participate in the reactions; however, they act as third bodies that absorb or give up energy during collisions, for example, in the following reactions:

$$\begin{aligned} H + H + M &\leftrightarrow H_2 + M \\ H + OH + M &\leftrightarrow H_2O + M \end{aligned} \qquad (5)$$

where M stands for [He], [CO_2], [N_2], or [Ar]. The third bodies absorb energy and terminate the chain-branching reactions. The definition of the third body includes stable molecules of reactants and products, such as [H_2], [O_2], and [H_2O] also. The third-body effectiveness of various diluents differs, with steam having the highest effectiveness of 6.5 relative to hydrogen. The third-body effectiveness of other molecules is close to that of hydrogen, which is unity. The detailed kinetic scheme[6] used is extracted from Burks and Oran[7] and Kailasanath et al.[14]

Ignition Event and Ignition Temperature

The definition of the ignition event is important when determining the ignition temperature. Experimentally, once ignition occurs, a combustion wave propagates rapidly through the unburned mixture, and there is an attendant increase of pressure in the vessel. For most mixtures investigated, combustion was complete in less than a second. Experimentally, the instant of ignition is easily discernible from the pressure trace, and the temperature corresponding to this instant can be read from the temperature trace. In practice, the instant of ignition was determined by first scanning the pressure data file on the computer. The igniter surface temperature is determined by scanning the temperature data corresponding to this instant. For the four-pin igniter, the average of the temperature readings of the four mid-location thermocouples was used. For other igniters, the highest igniter surface temperature recorded at the instant of ignition is taken as the ignition temperature.

Theoretically, the definition of an ignition event is complex and somewhat arbitrary. It may be defined as either the instant at which the heat generated at any point in the gas exceeds the heat losses from that point or the instant at which the temperature at any point in the gas exceeds the temperature of the hot surface. In the present work, the latter definition is used to define the ignition event. Criteria based on concentrations of the intermediate species, such as [H], [OH], and [HO_2], or their rate of change may also be used to define ignition.

The definition of ignition as the achievement of a certain gas temperature in excess of the hot-surface temperature is arbitrary; different ignition times would result for different excess gas temperatures; however, once the thermal runaway begins, the temperature rise in the gas is so rapid that almost all ignition criteria produce the same ignition delay.[6]

Minimum Surface Temperature Required for Ignition

Theoretically, an adiabatic system can be considered ignited at all temperatures. The heat generated by the

reactions gradually increases the temperature of the gases until runaway occurs; however, in practice, this does not occur. The heat generated at room temperatures is not sufficient to accelerate the reactions, and the reactions are suppressed by the loss of heat and active species. It has been observed that a definite minimum hot-surface temperature is required to achieve ignition. Below this minimum temperature ignition will not occur no matter how long the gases remain in contact with the igniter surface; above this temperature ignition occurs within a few milliseconds. The minimum surface ignition temperature (MSIT) is closely related to the AIT of the flammable mixture. This is the minimum temperature to which a uniform mixture of a flammable gas should be raised to achieve ignition. The AIT is lower than the MSIT by approximately 100 °C. Theoretically, ignition will result if a slab of a combustible mixture, equal to the laminar flame thickness, is raised to its AIT; however, because of loss of heat and active species from the reaction zone, the thickness of the slab of gas that should be raised to AIT is much larger. Typically, a slab of 5 to 10 times the laminar flame thickness is required. To maintain a slab of this thickness at or above AIT requires a surface temperature considerably in excess of the AIT.

The eventual outcome (i.e., ignition or no ignition) of exposing a combustible gas mixture to a hot surface is related to the ignition delay or the induction time. Figure 20 shows the computed ignition delay as a function of the hot-surface temperature for several hydrogen/air mixtures, initially at 300 K and 100 kPa. The ignition delay is short for a high-surface temperature and rises exponentially as the surface temperature decreases. Below 1000 K, the ignition delay shows a sharp increase.

Ignition is assumed to occur when the induction time (or ignition delay) is small, on the order of a few milliseconds. When the induction time is large, on the order of seconds, there is ample time for active species to diffuse out of the reaction zone, and ignition may not occur. Theoretically, no ignition will correspond to infinite ignition delay. It has been shown[6] that, for a given hydrogen/oxygen/diluent mixture, the ignition delay (t^*) at any surface temperature (T_s) is related to the hot-surface temperature for infinite ignition delay ($T_{s\infty}$) by the relationship

$$T_s = T_{s\infty}\, e^{A/t^*} \qquad (6)$$

From Eq. 6 it is clear that as $t^* \to \infty$, $T_s \to T_{s\infty}$, and that for $T_s \to \infty$, $t^* \to 0$. These are in agreement with the experimentally observed facts of limiting surface temperatures required for ignition.

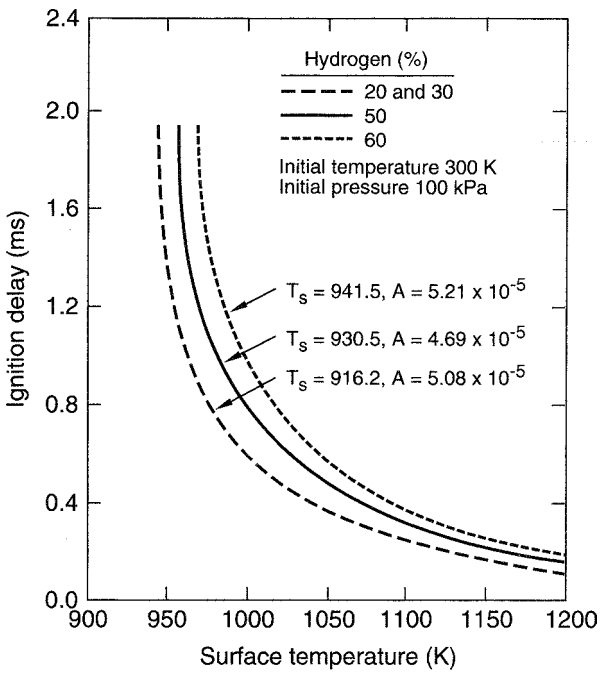

Fig. 20 Variation of induction time with surface temperature for hydrogen/air mixtures. T_s is the temperature of the hot surface (k) and A is the characteristic time constant (seconds).

When the t^* vs. T_s curves were drawn in Fig. 20, the induction times were calculated by solving Eqs. 1 to 4 numerically for each hot-surface temperature. From the calculated values of t^*, the unknown quantities $T_{s\infty}$ and A were evaluated. Note that only two values of t^* are required to deduce these unknown quantities; however, both $T_{s\infty}$ and A converge to their final values as induction times become larger and larger. The quantity $T_{s\infty}$ is the desired minimum hot-surface ignition temperature, and the parameter A depends on the mixture stoichiometry.

With the use of the preceding procedure, the minimum ignition temperatures were calculated for a range of hydrogen/air mixtures and are shown in Fig. 21. For comparison, the experimentally measured ignition temperatures in the 2.3-m-diameter sphere with the four-pin hot-surface igniter[6] are also shown. The heater/igniter surfaces are prone to aging, and with time the surfaces become oxidized and acquire catalytic properties; thus an experiment repeated after a considerable lapse of time may indicate a slightly different ignition temperature. Some of the scatter of the ignition temperature data in Fig. 21 may have resulted from this. The agreement between the measured and calculated MSITs is good.

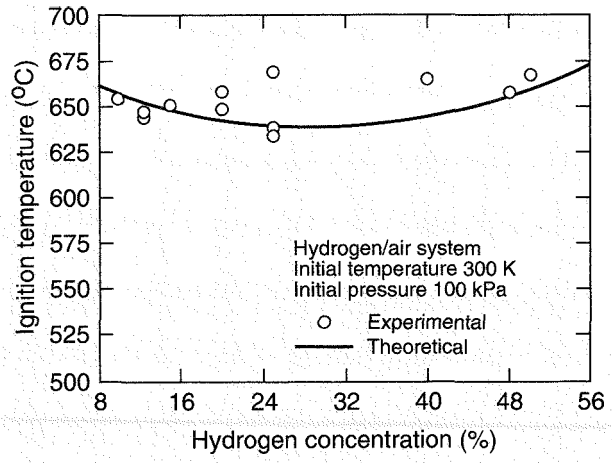

Fig. 21 Comparison of measured and calculated minimum ignition temperatures for hydrogen/air mixtures.

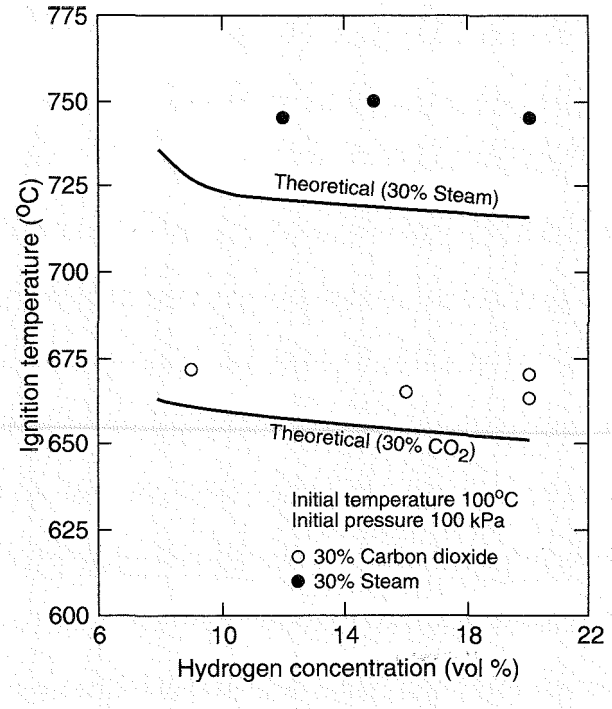

Fig. 22 Comparison of measured and calculated minimum surface ignition temperatures for stoichiometric hydrogen/oxygen/helium mixtures containing 30% steam.

Although a good agreement between the calculated and predicted MSITs is an indication of the validity of the model for hydrogen/air mixtures, the mixtures encountered in the reactor calandria vessel, as mentioned previously, consist of deuterium, oxygen, helium, and steam with deuterium and oxygen existing in stoichiometric proportions. Thus it is important to establish the validity of the model for a range of cover-gas mixtures. Experiments were therefore performed in our 2.3-m-diameter vessel with mixtures representative of those in the reactor calandria. Figure 22 shows the measured and calculated MSITs for stoichiometric hydrogen/oxygen/helium mixtures containing 30% steam. The measured temperatures are higher than the calculated values by approximately 25 °C. Earlier experiments with these mixtures had indicated that the calculated values were approximately 10 to 15 °C higher than those measured.[6] In view of the assumptions made in formulating the model, the agreement is reasonably good.

Figure 22 also shows the measured and calculated MSITs for the carbon dioxide diluent. As with steam, the measured ignition temperatures are slightly higher than the calculated values; however, the discrepancy in this case is not large (~10 °C) and is attributable to approximations made in the model. In the model the assumption has been made that carbon dioxide is inert and acts only as a heat sink. If all the reactions involving carbon dioxide were included in the calculations, a better agreement may result.

Effect of Initial Temperature on MSIT

As explained earlier, as the initial temperature increases, one would expect the MSIT to decrease. Most of the experiments reported here were performed at initial temperatures in the range of 25 to 125 °C. At these temperatures the radicals responsible for runaway chemical reactions are not formed at a rate sufficient to influence the ignition behavior. At low and moderate initial temperatures, the rates of reverse reactions in which the radicals recombine to form stable species are much faster than the forward reaction rates in which the radicals are produced, which offers a qualitative explanation of the observed insensitivity of the MSIT to initial gas temperatures. Theoretical investigations indicate no significant change in the induction times for initial temperatures up to 500 K. Because ignition temperatures are related to the induction times, as in Eq. 6, it can be concluded that the effect of initial temperatures up to 500 K on MSIT is not significant.

It is clear from the preceding discussion that the present one-dimensional model adequately describes the ignition behavior, and the model can be used with

reasonable confidence to predict the ignition behavior in CANDU cover-gas mixtures.

IGNITION IN AN IONIZING RADIATION FIELD

The gases in a reactor calandria are exposed to very high intensity ionizing gamma-radiation fields. These radiation fields, upon interaction with gas molecules, cause the gases to dissociate. The products of dissociation are the atoms and free radicals, such as [H], [OH], and [O]. Because explosive chemical reactions occur via chain-branching reactions involving atoms and radical species, it is reasonable to expect that high-intensity gamma radiation present within the reactor calandria will significantly affect the ignition process. Experimental work on the effect of radicals on ignition and flame propagation is scant. Some work has been done in the area of photochemical ignition xenon lamps and excimer lasers by Lavid and Stevens,[15] Lavid and Blair,[16] Lucas et al.,[17] and Forch and Miziolek.[18] Some studies by Ward and Wu[19] and Ward[20] with microwave/flame-plasma interactions indicate that significant flame-speed enhancement occurs in the presence of radiation. No experiment has ever been performed in a gamma field to determine behavior.

Equations 1 to 6 remain valid for hot-surface ignition of a combustible mixture in a radiation field; only a slight modification to the source terms of the species and energy is required. When a stable species such as oxygen is subjected to radiation, it undergoes the following excitation process:[21]

$$\begin{aligned} O_2 &= O + O^* \\ O_2 &= O_2(a^1\Delta g) \\ O_2 &= O_2(b^1\ \Sigma_g^+) \\ O_2 &= O_2(A^3\ \Sigma_u^+) \\ O_2 &= O_2(B^3\ \Sigma_u^-) \end{aligned} \qquad (7)$$

which dissociates to $O(^3P) + O(^1D)$.

The overall yield of radical species and atoms from the primary excitation process of the gaseous species is characterized by the G-value of the process (G = 100/W, where W is the mean energy in electron volts required to produce an ion pair). The G-values for dissociation of O_2 and water vapor are approximately 3 and 7, respectively.[21,22] The radiolysis of water vapor results in the formation of H, OH, O, and H_2. The primary yields of O and H_2 (1.08 and 0.45, respectively) are small compared with those of H and OH (7.4 and 6.2, respectively), and it is therefore assumed in the present calculations that the primary products of water vapor radiolysis are H and OH.

The energy absorbed by the gaseous species depends, to a good approximation, on its electron stopping power (S_i) and concentration (ξ_i). The stopping powers of helium, steam, and oxygen relative to hydrogen are 0.951, 4.331, and 6.767, respectively,[23] and the major absorbers of radiation are water vapor and oxygen. It was therefore assumed in the model that no radiation was absorbed by hydrogen. The fraction of the total energy absorbed by each species (α_i) was calculated as $\alpha_i = \xi_i S_i / \sum \xi_i S_i$.

Gases are generally poor absorbers of radiation, and they typically absorb approximately 0.01 to 1% of the incident radiation. In the region of 100 MeV, the absorption is mainly due to ion-pair production. For water exposed to gamma rays with energies on the order of 10 to 100 MeV, the mass absorption coefficient is approximately 0.02 cm^2/g, which is nearly independent of the incident photon energy.[24] The absorbed energy can be calculated from the relationship

$$I = I_o\, e^{-\rho d_i \varepsilon} \qquad (8)$$

where I_o is the incident radiation, d_i is the optical path length, and ε is the extinction coefficient. For typical values of ρ, ε, and d_i, Eq. 8 indicates that the energy absorbed is approximately 0.01% of the incident energy. Because the total energy absorbed by the gases is not known precisely, the present calculations were carried out over a range of absorbed dose rates. Thus an absorbed dose rate of 10^7 Gy/h corresponds to an incident radiation of 10^9 Gy/h with 1% absorption and 10^{11} Gy/h with 0.01% absorption.

In a continuous radiation field, near-steady-state conditions are expected to prevail. The H, O, and OH radicals produced by the dissociation of water vapor and oxygen molecules react with other species and produce other radical species; for example, H, O, and OH produce HO_2 and H_2O_2 in the following reactions:

$$\begin{aligned} H + O_2 &\rightarrow O + OH \\ H + O_2 &\rightarrow HO_2 \\ OH + OH + M &\rightarrow H_2O_2 + M \\ O + OH + M &\rightarrow HO_2 + M \end{aligned} \qquad (9)$$

Thus an ionizing radiation field alone will yield all the radicals that are normally present in a flame. For an

evaluation of the ignition behavior in the presence of a radiation field, it is necessary to first calculate the steady-state species concentration in the gas caused by radiation and then introduce the hot surface.

With radiation-induced dissociation, the production rates (i.e., source terms) for H_2O, O_2, H, O, and OH are calculated as

$$w_i = \Sigma\, w_{i,k} \pm \sigma_i k_i c_i M_i, \quad k_i = \alpha_i k_i'' R \qquad (10)$$

where k_i (mol • g^{-1} • s^{-1}) = dissociation rate (the values of k_i'' are 2.9×10^{-13} and 0.97×10^{-13} for water vapor and oxygen, respectively)
c_i = mass concentration of species i
R = absorbed dose rate
$w_{i,k}$ = production rate of species in the elementary reaction step k
subscript i = H_2O, O_2, H, O, or OH
σ_i = stoichiometric coefficient, which is unity for H_2O, H, OH, and O_2 and two for O-atom production

The sign of the last term in Eq. 10 is negative for $i = H_2O$ and O_2 and positive for i = H, O, or OH. The absorbed radiation dose rate is assumed to be proportional to the mass concentration of the species absorbing it.

At the moderate initial temperatures considered in this work, the radical species have a short life span and readily react to form water and other stable species. During computation of near-steady-state concentration of species in a radiation field, it was observed that the gas temperature increased, although only slightly, in response to energy released by the species recombination process. As mentioned previously, the effect of moderate increases in the initial gas temperature on ignition is small, and the effect of slight preheating of the gases caused by radiation can be neglected.

Note that the ignition path or sequence assumed in the present analysis may not be identical to the one that may occur in the reactor vessel. In reality, radical buildup and surface heating occur simultaneously, and the calculated MSIT may be different from the actual; however, because the radical equilibration times are much shorter (~10^{-3} second) than the surface heatup time (~100 seconds), ignition occurs in an initially steady concentration field. It is therefore expected that the assumptions made in the present analysis may produce minimum surface ignition temperatures near the actual values.

Figure 23 shows the ignition delay plotted as a function of the hot-surface temperature for various absorbed dose rates. There is no change in the computed ignition delays for absorbed dose rates below 10^7 Gy/h. The figure clearly shows that, as the dose rate increases, the induction time decreases, even if only slightly. If the minimum surface temperature at ignition ($T_{s\infty}$) is computed with the use of the procedure outlined previously (see Eq. 6), the curve in Fig. 24 is obtained. As the radiation field increases, the calculated MSIT decreases; the decrease, however, is small (~20 °C) over the range of absorbed dose rates (0 to 10^9 Gy/h). The effect is negligible for radiation fields of interest in nuclear reactor safety analysis.

So that the validity of the model could be tested, experiments were performed in the 2-dm^3 instrumented vessel, described earlier, placed in an accelerator. The glass windows on the vessel were replaced by two 0.3-mm-thick, 3-cm-diameter aluminum windows capable of withstanding the combustion overpressures and placed diametrically opposite each other, which

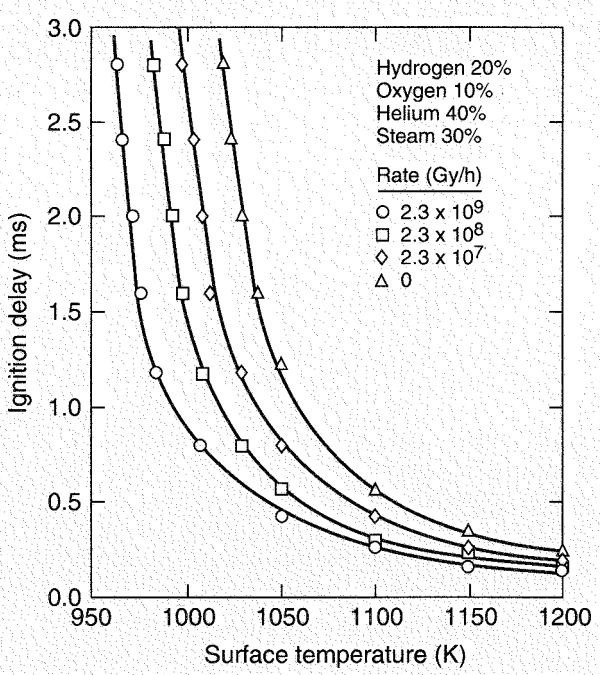

Fig. 23 Effect of absorbed radiation dose rate on calculated induction times.

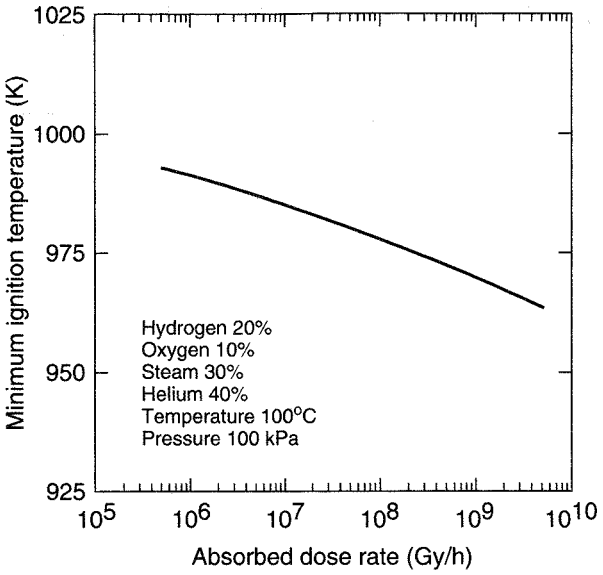

Fig. 24 Effect of absorbed dose rate on calculated ignition temperatures.

provided a path of minimum resistance to the gamma rays. The desired gas mixture in the vessel was obtained by adding component gases to the required partial pressures. Dry steam was added through heated lines from a small pot boiler. The experiments were performed from a remote control room situated approximately 50 m from the target area.

The source of radiation for the tests was a 300-MeV linear accelerator with a pulse stretcher ring at the University of Saskatchewan.[25] The unit produced a continuous beam of 10 to 100 MeV gamma photons of fluxes up to 5×10^{13} MeV • cm^{-2} • s^{-1} ($\sim 5 \times 10^6$ Gy/h) and a pulsed beam of much higher peak intensity (10^{16} MeV • cm^{-2} • s^{-1}) with a beam diameter of 2 cm.

Experiments were performed over a range of initial pressures from 27 to 100 kPa with stoichiometric hydrogen/deuterium/oxygen/helium/steam mixtures with 20% hydrogen and 30% steam at an initial temperature of 100 °C. The tests were carried out in both pulsed- and continuous-beam modes. In both cases the radiation beam was a broad spectrum of bremsstrahlung photons from 150-MeV electrons impacting on a metal target.

In the pulsed mode, the pulse duration was 1.3 μs delivered at 10 Hz. The peak gamma flux during the pulse was estimated to be 10^{16} MeV • cm^{-2} • s^{-1}. No effect on ignition temperature attributable to the radiation field was observed. Calculations with the model indicate that a pulse duration much shorter than the ignition delay should not affect the overall ignition behavior because of the short lifetime of the radical species at moderate temperatures. Unless the radiation is sustained, radicals produced by radiolysis decay within a few microseconds. Typical induction times for test mixtures at surface temperatures close to MSIT are calculated to be on the order of 5 to 10 milliseconds. Therefore a shortening of the ignition delay by at least two orders of magnitude by radiation sensitization would be required if the radiation pulse is to produce an effect on MSIT. The presence of radiolytically produced radical species shortens the ignition delay approximately by a factor of 2 for a tenfold increase in the dose rate. Unless the peak of the pulse is sufficient to produce an ignition delay of the same order as the lifetime of the species, no effect can be expected. For the peak-incident radiation intensities used in the present experiments, the ignition delay is still far greater than the lifetime of the species. That no change was observed in the experimentally measured MSIT is an indication that the short pulse duration was too short to affect the ignition behavior, which is in agreement with theoretical predictions. Lavid, Stevens, and Westbrook[26] showed that a 100-μs-wide pulse produced an oxygen atom mole fraction of 10^{-8} and caused autoignition. A radiation pulse of similar width and a dose rate of the order of 10^{12} Gy/h is required to observe autoignition in our experiments.

Table 1 summarizes the results of experiments performed with the accelerator in the continuous beam mode. No effect of radiation was observed on the ignition temperature. The highest incident beam intensity obtainable in the continuous mode was approximately 5×10^6 Gy/h (the intensity of interest in nuclear reactors is on the order of 10^7 Gy/h). Theoretical calculations, shown in Fig. 23, indicate that the lowest absorbed dose rate at which a measurable change (~10 °C) in MSIT could be observed is greater than 10^7 Gy/h. That an incident dose rate of 5×10^6 Gy/h ($\sim 5 \times 10^2$ Gy/h absorbed) did not show any reduction in the measured MSIT is therefore not surprising.

Because the ignition delay (and thus MSIT) depends on the lifetime of the species, experiments were performed at low initial pressures (the lifetime of the species increases as the pressure decreases); however, as the pressure decreases, the absorption of radiation decreases and thereby reduces the concentration of the active species. The net result was that, once again, no effect was observed. Experimental investigations carried out with hydrogen-rich mixtures and tests in which hydrogen was replaced by deuterium also showed no measurable effect on MSIT.

Table 1 Summary of Hot-Surface Ignition Tests in Continuous Beam Radiation Field: Photon Flux >10^{13} MeV · cm^{-2} · s^{-1}

Mixture composition, %				Pressure,	Number	MSIT,[a]	Beam
H_2	O_2	He	Steam	kPa	of tests	°C	on/off
20	10	40	30	100	14	789 ± 1	Off
20	10	40	30	100	3	789 ± 1	On
20	40	10	30	100	2	770 ± 2	Off
20	40	10	30	100	2	771 ± 3	On
20	10	40	30	50	4	768 ± 5	Off
20	10	40	30	50	3	771 ± 4	On
20	10	40	30	27	2	765 ± 3	Off
20	10	40	30	27	1	765	On
20	10	70	0	50	1	677	Off
20	10	70	0	50	1	676	On
60	10	0	30	100	2	785 ± 2	Off
60	10	0	30	100	1	786	On
20 D_2	10	40	30	100	1	806	Off
20 D_2	10	40	30	100	1	806	On
2:1 H_2–air			30	100	1	794	Off
2:1 H_2–air			30	100	1	794	On

[a]MSIT, minimum surface ignition temperature.

Conservative estimates of the maximum control rod/adjuster rod surface temperatures achievable (~588 °C) in a CANDU reactor calandria during a postulated loss-of-moderator accident show a considerable safety margin.[27]

CONCLUSIONS

Extensive small- and large-scale experiments have been carried out to determine the ignition temperatures in flammable hydrogen/oxygen/diluent mixtures likely to be present in the CANDU reactor calandria vessel during a postulated loss-of-moderator accident. Electrically heated igniters simulating the CANDU absorber/control rods were used to ignite the mixtures. It was found that ignition temperatures were not sensitive to the hydrogen concentration and the initial temperature over the range of investigation. Pressure, however, had a significant effect. The effect of diluent on ignition temperature was found to depend on the diluent type and its concentration. Because of the third-body effectiveness, the ignition temperatures with steam were much higher than those with any other diluent. The addition of 30% steam to a hydrogen/oxygen/helium mixture increased the ignition temperature by approximately 100 °C. Experiments have also indicated that the effect of catalytic preoxidation (recombination) has no significant effect on ignition temperature at low and moderate rates of preoxidation. For surfaces (and certain mixture compositions) exhibiting high rates of preoxidation, a significant increase in the ignition temperature was observed. A one-dimensional ignition model was found to adequately describe the hot-surface ignition process. For the cases analyzed, the agreement between theoretical and experimental ignition temperatures was good.

Theoretical analysis of ignition in a radiation field showed that an absorbed dose rate in excess of 10^7 Gy/h is required to produce a perceptible reduction in MSIT. A change in the absorbed dose rate from 10^7 to 10^{10} Gy/h is predicted to change the MSIT by approximately 20 °C.

Experiments performed in an accelerator with pulsed and continuous radiation beams with incident gamma fields of 10^{16} and 5×10^{13} MeV · cm^{-2} · s^{-1}, respectively (corresponding to 10^9 Gy/h and 5×10^6 Gy/h), showed no change in MSIT. For radiation fields of interest in nuclear reactors, the effect of ionizing radiation on MSIT is small.

Considerable safety margin exists between the maximum estimated control rod temperature and the required ignition temperature in a CANDU reactor calandria.

ACKNOWLEDGMENTS

Funding for this work was provided by the CANDU Owners Group, consisting of Atomic Energy of Canada Limited, Ontario Hydro, Hydro Quebec, and NB Power.

REFERENCES

1. J. M. Kuchta, R. J. Cato, and M. G. Zabetakis, Comparison of Hot Surface and Hot Gas Ignition Temperatures, *Combust. Flame,* 8 (4): 348-349 (December 1964).
2. R. R. Silver, *Phil. Mag.*, 23: 633-657 (1937).
3. H. Tamm, R. McFarlane, and D. D. S. Liu, *Effectiveness of Thermal Ignition Devices in Lean Hydrogen–Air–Steam Mixtures*, Report EPRI NP-2956 (AECL-7820), 1985.
4. H. Tamm, M. Ungurian, and R. K. Kumar, *Effectiveness of Thermal Ignition Devices in Lean Hydrogen–Air–Steam Mixtures: Final Report*, Report EPRI NP-5254 (AECL-8363), 1987.
5. D. C. Bull, L. R. Cairnie, A. J. Harrison, and P. A. Morgan, The Influence of Natural Convection on the Critical Conditions for Hot Surface Autoignition, paper presented at the 3rd International Symposium on Loss Prevention and Safety Promotion in the Process Industries, Basle, Switzerland, September 15–19, 1980.
6. R. K. Kumar, Ignition of Hydrogen–Oxygen–Diluent Mixtures Adjacent to a Hot, Nonreactive Surface, *Combust. Flame*, 75(2): 197-215 (1989).
7. T. L. Burks and E. S. Oran, *A Computational Study of the Chemical Kinetics of Hydrogen Combustion*, Report NRL-MR-4446 (AD-A-094348), 1981.
8. D. Wang, Z. Yafu, Z. Huifu, and R. Aifeng, *Eng. Thermophys. China*, 1: 367-383 (1981).
9. L. D. Chen and G. M. Faeth, *Combust. Flame*, 42: 77-92 (1981).
10. G. W. Koroll and R. K. Kumar, *Combust. Flame*, 84: 154-159 (1991).
11. R. S. Dixon, Dissociation of Water Vapor by Photolytic, Radiolytic, and Electron Impact Methods, *Radiat. Res. Rev.*, 2(3–4): 237-296 (1970).
12. B. Lewis and G. von Elbe, *Combustion, Flames and Explosions of Gases*, Third Edition, Academic Press, Inc., Orlando, Florida, 1987.
13. R. J. Kee, J. Warnatz, and J. A. Miller, *FORTRAN Computer-Code Package for the Evaluation of Gas-Phase Viscosities, Conductivities, and Diffusion Coefficients*, Report SAND-83-8209, 1983.
14. K. Kailasanath, E. S. Oran, and J. P. Boris, A Theoretical Study of the Ignition of Premixed Gases, *Combust. Flame*, 47(2): 173-190 (1982).
15. M. Lavid and J. G. Stevens, Photochemical Ignition of Premixed Hydrogen/Oxidizer Mixtures with Excimer Lasers, *Combust. Flame*, 60(2): 195-202 (1985).
16. M. Lavid and D. W. Blair, Experimental and Analytical Results of Radiative Ignition in Premixed Hydrogen–Air Flows, paper presented at the Eastern Section Technical Meeting of the Combustion Institute, Paper 64 in *Chem. Phys. Processes Combust.*, 1985.
17. D. Lucas, D. Dunn-Rankin, K. Hom, and N. J. Brown, *Ignition by Excimer Laser Photolysis of Ozone,* Report LBL-20871 (CONF-8610180-2), 1986.
18. B. E. Forch and A. W. Miziolek, Oxygen-Atom Two-Photon Resonance Effects in Multiphoton Photochemical Ignition of Premixed Molecular Hydrogen/Molecular Oxygen Flows, *Opt. Lett.*, 11(3): 129-131 (1986).
19. M. A. V. Ward and T. T. Wu, Theoretical Study of the Microwave Heating of a Cylindrical Shell, Flame-Front Electron Plasma in an Internal Combustion Engine, *Combust. Flame,* 32(1): 57-71 (1978).
20. M. A. V. Ward, Microwave Stimulated Combustion, *J. Microwave Power,* 15(3): 193-202 (1980).
21. C. Willis and A. W. Boyd, Excitation in the Radiation Chemistry of Inorganic Gases, *Int. J. Radiat. Phys. Chem.*, 8(1–2): 71-111 (1976).
22. D. A. Armstrong, The Radiation Chemistry of Gases, in *Radiation Chemistry: Principle and Applications*, Farhatziz and M. A. J. Rodgers (Eds.), pp. 263-320, VCH Publishers, Inc., New York, 1987.
23. D. W. Huyton and T. W. Woodward, Ionisation Measurements and Some Ionic Reactions in Gas Phase Radiolysis, *Radiat. Res. Rev.*, 2: 205-234 (March 1970).
24. A. J. Swallow, *Radiation Chemistry: An Introduction*, Longman Group Limited, London, 1973.
25. D. M. Skopik, The First Experimental Results from EROS, invited paper presented at the Workshop on Nuclear Physics with Real Photons Below Pion Threshold, Gent, Belgium, May 25–26, 1989.
26. M. Lavid, J. G. Stevens, and C. K. Westbrook, Analytical Modeling of Enhancement of Premixed H_2/Air Flames With Photochemically Produced Radicals, in *ASME/JSME/ISES Solar Energy Conference, Honolulu, Hawaii*, Report CONF-870307-19, Vol. 1, pp. 241-248, 1987.
27. K. K. Fung and W. I. Midvidy, Methodology for Calculation of Temperature of Uncovered In-Core Reactivity Mechanisms, paper presented at the 12th Annual Conference, Canadian Nuclear Society, Suskatoon, Saskatchewan, Canada, June 9–12, 1991, pp. 321-330.

Coupled RELAP5 and CONTAIN Accident Analysis Using PVM

By K. A. Smith,[a] A. J. Baratta,[b] and G. E. Robinson[b]

Abstract: *This article describes the development of an integrated accident analysis capability considering both reactor vessel and containment system responses. This integrated package, which uses the RELAP5 and CONTAIN computer codes, provides the user with greater accuracy and modeling flexibility when compared with accident analyses using these codes separately. Multiprocessing, together with message-passing-based data transfer, enables these concurrent RELAP5 and CONTAIN calculations. The data transfer facilitates the coupling between the reactor vessel and containment portions of the calculation. The Parallel Virtual Machine software system running on a network of IBM RISC System/6000 workstations provided the multiprocessing capabilities required for this work. The results of an anticipated-transient-without-scram scenario for a boiling-water reactor nuclear power plant are provided. For the scenario analyzed, the containment temperatures and pressures that were predicted on the basis of the stand-alone codes and standard analysis methods were lower (i.e., less conservative) than those predicted with the use of the integrated code package.*

For a detailed analysis of a nuclear power plant for accident conditions, separate calculations are currently performed on the reactor vessel and containment system. These separate calculations are necessary because most of the detailed accident analysis codes in use today concentrate on either the reactor vessel and primary system (in-vessel) or the containment system (ex-vessel) portion of the calculation. When calculations are performed with the use of separate codes, the coupling between the in-vessel and ex-vessel phenomena is not precisely modeled. In practice, this coupling is provided by using the results of the in-vessel calculation to drive the ex-vessel calculation, often without regard to the fact that containment conditions can influence in-vessel conditions. For certain transients, such as an anticipated-transient-without-scram (ATWS) scenario at a boiling-water reactor (BWR) plant, the coupled system and containment response can be important. The analyses of the current Advanced Light-Water Reactor (ALWR) concepts, which by design couple the reactor and containment systems, also require an integrated analysis capability to accurately predict plant behavior. The ideal solution to this problem would be to integrate the in-vessel and ex-vessel code calculations without significantly increasing computation time.

Such codes as the Transient Reactor Analysis Code (TRAC)[1,2] and the Reactor Loss-of-Coolant Analysis Program (RELAP)[3] were developed to accurately model the thermal–hydraulic behavior of the reactor primary system during normal operating and transient conditions. The CONTAIN[4] code was developed to predict the performance of containment systems during design basis and severe accidents. Such codes as MELCOR[5] provide the capability to perform both in-vessel and ex-vessel analysis; however, the analyses performed are not intended to be best-estimate.

This article outlines the development of an integrated accident analysis capability to simulate the response of the entire reactor system using the RELAP5 and CONTAIN computer codes. This integrated code system provides the user with the capability of performing integrated calculations using the current best-estimate in-vessel and ex-vessel analysis codes endorsed by the Nuclear Regulatory Commission (NRC). The multiprocessing platform chosen for the implementation of this integrated calculation is a network of UNIX-based IBM RISC System/6000 workstation computers using the Parallel Virtual Machine (PVM) software system.[6]

PVM SOFTWARE SYSTEM

This section outlines the function and syntax of the PVM Version 2.3 constructs used in the integration of RELAP5 and CONTAIN calculations. The PVM User's Guide contains more detailed information on these routines and the syntax of their invocation.[7]

[a]Oak Ridge National Laboratory, Oak Ridge, Tennessee 37831-6392.

[b]The Pennsylvania State University, University Park, Pennsylvania 16802.

Overview

The PVM software, which was designed to provide multiprocessing capabilities on a loosely coupled network of diverse computer systems, is divided into two separate pieces: the first is a daemon process that can be installed by any user, and the second is a user interface library that contains routines for process management, interprocess communication, and synchronization. A key concept used in the PVM system is that of a *component.* Under PVM, application programs are divided into components; each component represents a relatively independent portion of the original program. For the purposes of this work, the RELAP5 and CONTAIN codes can be considered components.

User Interface Routines

The PVM user interface routines were originally developed with the use of C programming language. For access to PVM routines from FORTRAN programs, FORTRAN to C interface routines are provided. These FORTRAN to C interface routines were used because both RELAP5 and CONTAIN are written in FORTRAN. The routines of interest can be divided into two distinct areas, process management and data transfer. What follows is a brief description of selected user interface routines to introduce the reader to some of the capabilities of the PVM system. The PVM User's Guide contains detailed description of all the PVM user interface routines and the syntax for their use.[7]

Process Management. The first set of routines presented deals with process initiation and control. In PVM terminology, a *process* is any executing portion of a component. Each process is identified by the component name and a positive instance number. Before any of the PVM user interface routines are invoked, a process must call the "fenroll" routine, which enrolls the component as a PVM client process. Conversely, the "fleave" routine is used to notify PVM that a process has completed execution and is leaving.

To initiate a process, the "finitiate" routine is used with a component name as an argument. PVM will then initiate the specified component and return the instance number of the process to the user. PVM provides several different modes for process initiation with the use of variations of the "finitiate" command. The "finitiate" command initiates a component on a machine of the specified architecture. If the "finitiate" command is used with the architecture set to NULL, PVM chooses the location for component initiation. The "finitiatem" command is used to initiate a component on a specific machine.

Data Transfer. Because the PVM system was designed to run on a network using different computer architectures, the data transfer between different machines must be accomplished in a machine-independent manner. In the PVM system a message destination is specified by a (component–name, instance–number) pair because the location of a process is by design unknown to the user program. The following example illustrates the use of selected PVM data transfer routines.

First, "finitsend" is used to initiate the send buffer. Following initiation of the send buffer, the message is composed by placing data into the send buffer; for example, "fputnint" places an integer array into the send buffer, whereas the "fputndfloat" places a double-precision array into the send buffer. After the message is complete, "fsnd" sends the message to a specific instance of a component using the supplied message type. The "frcv" routine receives a message of the specified type. Extraction of the data from the message requires the use of the companion routines to those used to compose the message. The "fgetnint" and "fgetndfloat" extract the integer and floating point data placed in the message buffer by the "fputn[int,dfloat]" constructs.

RELAP5/CONTAIN INTERFACE

The SCDAP/RELAP5/MOD3/7AF code package[8] developed at Idaho National Engineering Laboratory (INEL) for the NRC is used to perform the in-vessel portions of the calculation. This code was developed as a best-estimate transient analysis program for scenarios involving light-water-reactor power-plant accident scenarios. The RELAP5 code models the thermal–hydraulic behavior of the reactor coolant system and the core during normal operational transients and accident sequences with an intact core. RELAP5 is based on a nonequilibrium, nonhomogeneous model of a two-phase system. The hydrodynamics of the two-phase steam–water mixture present inside the reactor coolant system are modeled with the use of a one-dimensional (1-D), transient, two-fluid representation, which is modified to account for the presence of noncondensible gases in each phase. The RELAP5 code package includes generic component models that can be used to model a variety of physical systems. These component models include pumps, pipes, valves, jet pumps, turbines, separators, and control system components. Special process models are also available for the treatment of the following effects: flow branching, boron tracking, choked flow, and the

transport of noncondensible gases. RELAP5 also has a reactor kinetics capability to predict the power behavior of the nuclear reactor. The CONTAIN Version 1.12 (Refs. 9 and 10) computer code developed at the Sandia National Laboratories (SNL) for the NRC is used to perform the ex-vessel portion of the calculation. The code was developed for best-estimate calculations of containment performance during severe accident conditions. CONTAIN includes mechanistic models for a wide variety of the physical, chemical, and radiological processes occurring inside containment during a severe accident situation. The processes treated by the CONTAIN code system can be grouped into the following phenomenological areas: thermal–hydraulics, fission products, and aerosols.

Calculation Coupling

For the facilitation of integrated reactor-containment accident analysis calculations, an interface was developed that coupled the RELAP5 and CONTAIN calculations at some user-selected time interval. This interface controls the execution of the RELAP5 and CONTAIN computer codes while providing the data needed by each code to couple the reactor and containment portions of the calculation. The development of this interface routine proceeded along two separate lines, one dealing with program execution and the other with calculation coupling.

The execution control portion of the interface routine controls the execution of the integrated code calculation. This routine, "srlcon" (see Fig. 1), is responsible for the

```
      program srlcon
c     Host program to execute SCDAP/RELAP5/MOD3 V7af
c     and CONTAIN 1.12 concurrently under the PVM system
      integer info,mynum,inst
      character*8 arch
      character*12 nodename
c     enroll host in PVM
      call fenroll("srlcon\0",mynum)
      if( mynum .lt. 0) then
            print *,'failure in fenroll on host'
            stop
      endif
c     set ARCH to any available machine
      arch ="RIOS\0"
c     Initiate contain node program on psunuke
c     call finitiate("contain\0",arch,inst)
      call finitiatem("contain\0","psunuke\0",inst)
      if( inst .lt. 0) then
            print *,'failure to initiate'
            stop
      endif
c     Initiate relap node program on mongo
c     call finitiate("selap\0",arch,inst)
      call finitiatem("selap\0","mongo\0",inst)
      if( inst .lt. 0) then
            print *,'failure to initiate'
            stop
      endif
c     leave PVM
      call fleave()
      stop
      end
```

Fig. 1 RELAP5/CONTAIN execution control program.

execution of the RELAP5 and CONTAIN programs under the PVM system. As shown in Fig. 1, the "srlcon" program first calls "fenroll," which allows access to the PVM system and enables interprocessor communication. Following successful enrollment in PVM, the "srlcon" program initiates the *contain* and *selap* node programs. As their names suggest, the *contain* node program is the CONTAIN code portion of the calculation, whereas the RELAP5 calculations are performed in *selap*.

The "srlcon" program has no responsibility regarding the synchronization between the *contain* and *selap* node programs. The synchronization of these calculations is handled by the calculation coupling routines incorporated into the *selap* and *contain* node programs. This configuration is chosen to reduce interprocess communication in an effort to minimize execution time.

For effective coupling of the calculations performed by RELAP5 and CONTAIN, routines were developed to accurately transfer data between the *selap* and *contain* node programs. This data transfer, coupled with code changes to receive and process these data, allows the integration of the separate code calculations. The necessary coupling data can be identified by examining the boundary conditions commonly used during the execution of RELAP5 and CONTAIN for accident sequences.

The conditions inside containment are required by RELAP5 when quantities such as heat losses from the reactor vessel or primary system piping are to be calculated. CONTAIN also performs heat-transfer calculations between structures exposed to cell atmospheric conditions. In this case, both codes have the ability to predict heat losses off structures. The ideal solution to this problem would be to have both codes model one-half of the desired heat structure coupled through heat flux data, which would allow both codes to accurately predict structure surface conditions. This scheme would require either a one-to-one correspondence between RELAP5 and CONTAIN structures or the development of a scheme to connect multiple RELAP5 heat structures to a single CONTAIN structure. Because, invariably, the nodalization used to model the primary system with RELAP5 is finer than that used to model the containment with the use of CONTAIN, a larger number of heat structures are considered in the RELAP5 calculation. Because this approach was considered undesirable, the decision was made to calculate structural heat losses with the use of RELAP5 and pass the data to CONTAIN, acknowledging that this approach neglects surface phenomena calculated by CONTAIN.

Along with heat-transfer calculations, the atmosphere thermal–hydraulic models must also be coupled. Accident calculations usually model a break somewhere in the primary system of the reactor. For an accurate prediction of the pressure response of the reactor and containment systems, the atmosphere thermal–hydraulic models of each code must be coupled through break mass and energy flows.

Another important aspect of an accident calculation that must be addressed is the transfer of water between the reactor and containment systems by safety systems. For existing pressurized-water-reactor (PWR) and BWR containment systems (and the proposed ALWR concepts), the sources of water for the reactor safety injection systems are inside containment. This type of scenario necessitates the implementation of a capability of transferring water between the RELAP5 and CONTAIN calculations.

As stated earlier, the calculation coupling routines are responsible for the synchronization of the integrated code calculations. To accomplish this, the coupling routines must have access to transient control variables. These transient control variables include calculation start and end times, current calculation time, calculation time step, sending PVM message data time interval, and receiving PVM message data time interval. Not only must these routines have access to these quantities locally (i.e., within their respective node program) but also they must have the ability to access these quantities inside another node program.

During the development of the calculation coupling routines it was decided that the ex-vessel conditions predicted by the CONTAIN code would be incorporated into the RELAP5 calculation with the use of time-dependent volume data. With the use of these ex-vessel conditions, the RELAP5 calculation would then determine the mass and energy flows between the reactor and containment systems. These sources would then be incorporated into the CONTAIN calculation to generate updated containment conditions to be passed back to the RELAP5 calculation.

This decision was reached after considering the form of the system equations for the RELAP5 and CONTAIN codes. The governing equations for the RELAP5 and CONTAIN code systems upon which the integrated analysis capability will be based are summarized in Tables 1 to 6. The conservation equations for the CONTAIN[9] code (Tables 1 to 3) are ordinary differential equations, whereas those for the RELAP5[3] code (Tables 4 to 6) are partial differential equations. The basic

Table 1 CONTAIN Conservation of Momentum Equation for Flow Between Cell i and Cell j

$$\frac{dW_{ij}}{dt} = \left[\Delta P_{ij} - C_{FC}\frac{|W_{ij}|W_{ij}}{\rho_{ij}A_{ij}^2}\right]\frac{A_{ij}}{L_{ij}}$$

with

$$\Delta P_{ij} = P_i - P_j + \Delta P_{ij,g}$$

$$\Delta P_{ij,g} = g\left[\rho_i(H_i - H_1) + \rho_a(H_1 - H_2) - (H_j - H_2)\right]$$

and for the suppression pool flow path

$$\Delta P_{ij} = P_w - P_d$$

where W_{ij} = flow path mass flow rate
t = time
ΔP_{ij} = pressure drop between cells
C_{FC} = irreversible flow loss coefficient
ρ_{ij} = flow path gas density
A_{ij} = area of flow path ij
L_{ij} = inertial length of flow path ij
P_i, P_j = pressure in cell i and cell j
$\Delta P_{ij,g}$ = pressure effects due to gravity
g = acceleration due to gravity
ρ_i, ρ_j = gas density in cell i and cell j
H_i = elevation of cell i center
H_1 = elevation of flow path in cell i
ρ_a = average gas density of cells i and j
H_2 = elevation of flow path in cell j
H_j = elevation of cell j center
P_d, P_w = pressure in drywell and wetwell

Table 2 CONTAIN Conservation of Mass Equation for Gas k in Cell i

$$\frac{dm_{i,k}}{dt} = \dot{m}_{\text{in}} - \dot{m}_{\text{out}} + \dot{m}_{ex,so} - \dot{m}_{ex,si} + \dot{m}_{br}$$

where $m_{i,k}$ = mass of gas component k in cell i
$\dot{m}_{\text{in}}$ = mass flow rate of gas k into cell i
$\dot{m}_{\text{out}}$ = mass flow rate of gas k leaving cell i
$\dot{m}_{ex,so}$ = source rate from explicit cell models
$\dot{m}_{ex,si}$ = depletion rate from explicit cell models
$\dot{m}_{br}$ = implicit flow boiling source rate

Table 3 CONTAIN Conservation of Energy Equation for Cell i

$$\frac{dU_i}{dt} = q_w + q_e + q_{\text{sup}} + q_{\text{boil}} + q_g + q_{LC}$$

where dU_i/dt = rate of change of cell i total energy
q_w = rate of energy transferred to cell i via flow
q_e = rate of energy transferred to cell i from explicit cell models
q_{sup} = energy transfer rate via suppression pool vent flow
q_{boil} = implicit pool boiling energy transfer rate
q_g = energy transfer rate due to work against gravity
q_{LC} = energy transfer from lower cell models

Table 4 RELAP5 Phasic Continuity Equations

Vapor phase

$$\frac{1}{V}\frac{\partial}{\partial t}\left(V\alpha_g\rho_g\right) + \frac{1}{A}\frac{\partial}{\partial x}\left(\alpha_g\rho_g v_g A\right) = \Gamma_g + \sum_{ni=1}^{N}\Gamma_{ni} - 9\Gamma_h$$

Liquid phase

$$\frac{1}{V}\frac{\partial}{\partial t}\left(V\alpha_f\rho_f\right) + \frac{1}{A}\frac{\partial}{\partial x}\left(\alpha_f\rho_f v_f A\right) = -\Gamma_g + \Gamma_{si}$$

where V = volume
t = time
α_g = vapor void fraction
ρ_g = vapor density
A = area
x = length
v_g = vapor velocity
Γ_g = vapor generation rate per unit volume
Γ_{ni} = noncondensible species generation rate per unit volume
N = total number of noncondensible species
Γ_h = hydrogen generation rate due to metal–water reactions
α_f = liquid void fraction
ρ_f = liquid density
Γ_{si} = solute generation rate per unit volume

two-fluid differential equations used in RELAP5 possess complex characteristic roots that give the system of equations a partially elliptic character. These complex roots introduce high-frequency spatial components into the solution, which necessitates a much smaller system time step when compared with the CONTAIN system of

Table 5 RELAP5 Phasic Conservation of Momentum Equations

Vapor phase

$$\alpha_g \rho_g A \frac{\partial v_g}{\partial t} + \frac{1}{2}\alpha_g \rho_g A \frac{\partial v_g^2}{\partial x} = -\alpha_g A \frac{\partial p}{\partial x} + \alpha_g \rho_g B_x A - (\alpha_g \rho_g A)\, FWG\,(v_g)$$
$$+ \Gamma_g A(v_{gI} - v_g) - (\alpha_g \rho_g A)\, FIG\,(v_g - v_f)$$
$$- C\alpha_g \alpha_f \rho A \left[\frac{\partial (v_g - v_f)}{\partial t} + v_f \frac{\partial v_g}{\partial x} - v_g \frac{\partial v_f}{\partial x}\right]$$
$$- \sum_{ni=1}^{N} \Gamma_{ni} A v_g + 9\Gamma_h A v_g$$

Liquid phase

$$\alpha_f \rho_f A \frac{\partial v_f}{\partial t} + \frac{1}{2}\alpha_f \rho_f A \frac{\partial v_f^2}{\partial x} = -\alpha_f A \frac{\partial p}{\partial x} + \alpha_f \rho_f B_x A - \left(\alpha_f \rho_f A\right) FWG\left(v_f\right)$$
$$+ \Gamma_g A\left(v_{fI} - v_f\right) - \left(\alpha_f \rho_f A\right) FIF\left(v_f - v_g\right)$$
$$- C\alpha_f \alpha_g \rho A \left[\frac{\partial \left(v_f - v_g\right)}{\partial t} + v_g \frac{\partial v_f}{\partial x} - v_f \frac{\partial v_g}{\partial x}\right]$$
$$- \Gamma_{si} A v_f$$

where B_x = body force in the x direction
FWG = vapor wall friction term
v_{gI} = vapor interface velocity
FIG = vapor interfacial friction term
C = virtual mass coefficient
FWF = liquid wall friction term
v_{fI} = liquid interfacial velocity
FIF = liquid interfacial friction term

equations. On the basis of this observation, one can conclude that the solution of the CONTAIN portion of the calculation will advance much faster than that of the RELAP5 portion.

The system time step of the RELAP5 code system is limited by the high-frequency components of the solution. To RELAP5 the change in containment conditions over a system time step is almost constant. In fact, the proposed system uses CONTAIN to supply the necessary boundary conditions for the RELAP5 calculation. With the use of these boundary conditions, RELAP5 calculates the sources required by CONTAIN to accurately predict containment response.

Another critical decision made during the development of the calculation coupling routines dealt with the incorporation of source data into the respective codes. It was decided that the incorporation of PVM source data would use the existing code architecture and process source data in a manner identical to the existing source processing routines. In other words, the addition of PVM source data (which parallels the existing source routines) would not circumvent existing error checking and time-step control loops.

On the basis of these discussions, the following four different source types (discussed later in greater detail and summarized in Table 7) are used to pass data

Table 6 RELAP5 Phasic Energy Equations

Vapor phase

$$\frac{1}{V}\frac{\partial}{\partial t}\left(V\alpha_g\rho_g U_g\right) + \frac{1}{A}\frac{\partial}{\partial x}\left(\alpha_g\rho_g U_g v_g A\right) = -P\frac{\partial\alpha_g}{\partial t} - \frac{P}{A}\frac{\partial}{\partial x}\left(\alpha_g v_g A\right)$$

$$+ Q_{wg} + Q_{ig} + \Gamma_{ig}h_g^* + \Gamma_w h_g^s + DISS_g + \sum_{ni=1}^{N}\Gamma_{ni}h_{ni} - 9\Gamma_h h_g$$

Liquid phase

$$\frac{1}{V}\frac{\partial}{\partial t}\left(V\alpha_f\rho_f U_f\right) + \frac{1}{A}\frac{\partial}{\partial x}\left(\alpha_f\rho_f U_f v_f A\right) = -P\frac{\partial\alpha_f}{\partial t} - \frac{P}{A}\frac{\partial}{\partial x}\left(\alpha_f v_f A\right)$$

$$+ Q_{wf} + Q_{if} + \Gamma_{if}h_f^* + \Gamma_w h_f^s + DISS_f + \Gamma_{si}h_{si}$$

where U_g = vapor internal energy
Q_{wg} = wall heat transfer rate
Q_{ig} = interfacial heat transfer rate
Γ_{ig} = interfacial vapor generation rate
h_g = vapor phase enthalpy
h_g^s = vapor phase saturation enthalpy
$DISS_g$ = vapor energy dissipation term
h_{ni} = enthalpy of ni-th noncondensible
U_f = liquid internal energy
Q_{wf} = liquid wall friction energy term
Q_{if} = liquid interfacial friction energy term
h_f = liquid phase enthalpy
h_f^s = liquid phase saturation enthalpy
$DISS_f$ = liquid energy dissipation term
h_{si} = solute source enthalpy

between the RELAP5 and CONTAIN code calculations: (1) the "atmos" source for primary system breaks, (2) the "srv" source for Safety Relief Valve (SRV) discharge, (3) the "pool" source to couple vessel injection systems and the suppression pool, and (4) the "rxq" source to couple reactor vessel heat loss calculations. These four general source types provide the flexibility to model various reactor-containment system configurations. The use of these source types to define the desired coupling between RELAP5 and CONTAIN will be discussed later.

RELAP5 Modifications

The modifications to the RELAP5 code are divided into three distinct areas: interaction with the PVM system, extraction and passing of requested data to CONTAIN, and receiving and processing data from CONTAIN.

The RELAP5 routine is the main program driver for the entire RELAP5 code. For access of the RELAP5 node program, *selap*, to PVM resources, a call to "fenroll" was added to routine RELAP5. RELAP5 is also responsible for reading in the data necessary to define the coupling between the RELAP5 and CONTAIN calculations. The input data needed to define this coupling for the RELAP5 calculation along with that needed for the CONTAIN calculation are discussed later.

The modifications to extract the data for the CONTAIN portion of the calculation are incorporated into subroutine TRAN. TRAN controls the advancement of all portions of the transient calculation and consequently has access to any data that are required for

Table 7 PVM RELAP5/CONTAIN Source Interface Definitions

Source type	Process modeled	Data sent to CONTAIN	Data returned to RELAP5
atmos	Break	$\dot{m}_f$, $\dot{m}_g$, h_f, h_g	Pressure and temperature of volume attached to break
srv	SRV discharge	$\dot{m}_f$, $\dot{m}_g$, h_f, h_g	Pressure and temperature of wetwell volume
pool	Vessel injection	$-\dot{m}_f$	Pool cell pressure and pool temperature
rxq	Structural heat loss	q	Temperature of volume attached to structure

the CONTAIN calculation. The current version of the coupling routine in TRAN allows the user to extract the following quantities for any junction in the RELAP5 model: liquid mass flow rate, vapor mass flow rate, liquid enthalpy, and vapor enthalpy. These quantities are not standard junction variables and therefore are calculated. The liquid and vapor mass flow rates are calculated on the basis of the junction mass flow and phasic void fraction data in the following manner:

$$mfjunc = mflowj(kjun) * voidfj(kjun)$$

$$mgjunc = mflowj(kjun) * voidgj(kjun)$$

where mfjunc = junction liquid mass flow (kg/s)
mgjunc = junction vapor mass flow (kg/s)
mflowj = junction mass flow (kg/s)
voidfj = junction liquid void fraction
voidgj = junction vapor void fraction
kjun = junction pointer

The liquid- and vapor-phase enthalpies are also calculated on the basis of liquid- and vapor-phase internal energies.

$$hfjunc = ufj(kjun) + p(kvfr)/rhofj(kjun)$$

$$hgjunc = ufg(kjun) + p(kvfr)/rhogj(kjun)$$

where hfjunc = junction liquid enthalpy (J/kg)
hgjunc = junction vapor enthalpy (J/kg)
ufj = junction liquid specific internal energy (J/kg)
ugj = junction vapor specific internal energy (J/kg)
p = donor volume pressure (Pa)
rhofj = junction fluid density (kg/m^3)
rhogj = junction vapor density (kg/m^3)
kvfr = donor volume pointer

These junction quantities are categorized by one of three possible source types: "atmos," "srv," and "pool." This categorization, in conjunction with an additional PVM input file, defines how these sources will interface with the CONTAIN model and the data to be transferred. The "atmos" source type is used to identify sources (usually breaks) to be added directly to the atmosphere of a specific CONTAIN model cell. Likewise, the "srv" source type identifies sources that are introduced into the CONTAIN model through SRV discharge into the suppression pool. Currently, the "pool" keyword can be used only to define sources (mainly vessel injection systems) to be removed from the suppression pool. All junction quantities of a like source type are summed and passed to the correct CONTAIN coupling routine for incorporation into the calculation.

Another quantity that is passed to the CONTAIN calculation is the heat-transfer rate from user-selected RELAP5 heat structures. This type of source is specified by using the "rxq" keyword. The user has the ability to specify the heat-transfer rate from either side (left or right) of a heat structure. Once again heat-transfer rate is not a standard heat structure quantity and must be calculated with available heat structure variables at the specified boundary surface. The heat-transfer rate from a heat structure surface is calculated by multiplying heat flux at the surface by the total area of the surface; for example, the heat-transfer rate from the right side of a heat structure is calculated using

$$qrhs = htsrfn(j) * htrnrn(j)$$

where qrhs is the heat-transfer rate at right surface (W), htsrfn is the area at right boundary (m^2), and htrnrn is the heat flux at right surface (W/m^2). The heat loss from all selected heat structures is summed and passed to a CONTAIN coupling routine that adds the energy to the atmosphere of the specified cell.

With the use of this mass and energy source data, CONTAIN updates conditions inside the containment and passes these conditions back to the RELAP5 TSTATE routine. The TSTATE routine is responsible for processing time-dependent volume and junction data during code execution. TSTATE receives the message data from CONTAIN and updates the conditions of the appropriate time-dependent volume. Volume numbers along with source-type keywords are once again used to distinguish between the separate data streams. The "atmos," "srv," and "pool" keywords are used to specify the conditions inside the time-dependent volumes attached to the "atmos," "srv," and "pool" junctions used to pass data to CONTAIN. The "atmos" and "srv" keywords indicate that the selected CONTAIN cell atmosphere temperature and pressure are being supplied. The data needed for a pool-type time-dependent volume are slightly different. The pool keyword indicates that cell pressure and pool temperature data are being supplied. The "rxq" keyword is used to update conditions inside a RELAP5 time-dependent volume (using data from the CONTAIN calculation) that specifies a sink temperature for calculations of reactor heat loss.

CONTAIN Modifications

The changes made to the CONTAIN code differ slightly from those incorporated into RELAP5. Once again these changes can be grouped into three distinct areas: communication with PVM, receiving and processing RELAP5 data, and sending data to RELAP5.

As with RELAP5, a call to "fenroll" was added to the main program CONTAIN. The CONTAIN routine is also responsible for reading the input data that define which cells and source types will be used for calculation coupling. These changes are identical in function to their counterparts made in the RELAP5 driver routine. CONTAIN uses a modular code design that treats each phenomenological model with a distinct set of subroutines, which results in a code structure that is different from that of RELAP5. The CONTAIN code has both global and cell-level routines, each performing a specific function; therefore several routines are needed to process the coupling data from the RELAP5 calculation. New source processing routines were created on the basis of existing CONTAIN subroutines. These new routines were renamed and altered to accept and process the incoming PVM data from RELAP5.

The "atmos" source type from RELAP5 contains the mass flow and enthalpy data for the liquid and vapor streams to be added to a specified cell atmosphere. In CONTAIN, atmospheric sources are processed in the SORATM routine, which is a cell-level routine called by the atmosphere control routine CCNTRL. A new routine called SHOVATM (based on SORATM) was created to receive and process "atmos" source data from RELAP5.

In a similar manner, the SHOVPL routine was created on the basis of the SORPL routine. The SORPL routine is the pool source routine used to introduce material into or remove material from the lower cell pool model. Unlike the SHOVATM routine, the SHOVPL routine accepts only liquid mass flow data from RELAP5. Liquid is then removed from the pool region at the rate specified by RELAP5. Because mass is being removed from the pool, the temperature of the liquid removed is set to the temperature of the pool itself.

In the unmodified CONTAIN code, the SRVSOR routine, which deals with the incorporation of SRV discharge sources into the CONTAIN calculation, loads the SRV source data into the interface array for the scrubbing model. One of the routines called by SRVSOR is once again the SORATM (atmospheric source) routine. A new routine called SHOVSRV, which uses "srv" source data from RELAP5, was created to perform the same function as SORATM. The only difference between the SHOVATM and SHOVSRV routines is the location where source data are placed.

The last routine, which accepts PVM data from RELAP5, is the R5HEAT routine. The R5HEAT routine adds the heat transfer ("rxq" source data) off the RELAP5 heat structures into the global energy array.

In addition to the new source routines, the existing CONTAIN routines responsible for calling these source routines were modified to ensure that the PVM source data were received and introduced to the correct cell.

In their present configuration, the SHOVATM, SHOVPL, SHOVSRV, and R5HEAT receive PVM data from RELAP5 at the beginning of each CONTAIN system time step. Once received, these data are stored inside each routine and assumed to remain constant over the system time step. These various source data are processed with the explicit sources shown in the conservation of mass and energy equations for CONTAIN in Tables 2 and 3. The relationship between the CONTAIN and RELAP5 system time step, along with the frequency at which data are passed between the codes, is controlled solely by user input.

A new routine, PVMO (which follows existing CONTAIN conventions for accessing data stored in

common), was added to supply updated containment conditions to the RELAP5 calculation. This new routine is called by CONTROL at every system time step to send data to the RELAP5 program.

PVM Execution Control Input

The input necessary to define the coupling between the RELAP5 and CONTAIN code calculations is provided through the use of two files, one for each code. This approach was acceptable for this preliminary work, but at some point the input defining the PVM data interface should be incorporated into the main input stream for each code. An example of the PVM input file (pvm.srelap) required by the RELAP5 code is shown in Fig. 2.

The first line of this file tells the code if an integrated PVM calculation is to be performed (t for true, f for false). The next lines specify the time interval between successive messages sent to CONTAIN (pvmint) and the amount of time RELAP5 should wait (after sending a message to CONTAIN) before receiving message data from CONTAIN (rcvint). The current value of zero implies that the code will receive CONTAIN data during the next time step.

The next input block defines the time-dependent volumes that will be updated using CONTAIN data. The data simply consists of the number of time-dependent volumes to be updated followed by [volume number, source type] pairs. Associated with each volume number is one of the four source types ("atmos," "pool," "srv," or "rxq") introduced earlier (see Table 7). For time-dependent data input, the source type informs RELAP5 what type of data will be provided for the time-dependent volume by CONTAIN.

Following the time-dependent volume input is the PVM junction input. This input defines which junctions in the model will contribute to the "atmos," "srv," or "pool" sources to be sent to CONTAIN. The format is, once again, the number of junctions to provide sources followed by [junction number, source type] pairs. For junction data input, the source type tells RELAP5 which CONTAIN coupling routine will be receiving the data. The final input block includes the [heat structure number, boundary] pairs used to define the heat structures that will be used to calculate reactor heat losses to the containment.

The format of the PVM input required by the CONTAIN code executing under PVM is illustrated by the example (pvm.contain) shown in Fig. 3. Upon examination of Figs. 2 and 3, one can see that the PVM

```
t                       * PVM execution control
0.05d0                  * PVM send interval
0.0d0                   * PVM receive interval
3                       * PVM time dependent volume data
304010000 rxq
400010000 pool
991010000 srv
2                       * PVM junction data
401000000 pool
901000000 srv
5                       * PVM heat structure data
3201001 left
3201002 left
3201003 left
3201004 left
3201005 left
```

Fig. 2 RELAP5 Parallel Virtual Machine execution input.

```
t       * PVM execution control
1       * CONTAIN cell for atmos source
3       * CONTAIN cell for srv source
3       * CONTAIN cell for pool source
2       * CONTAIN cell for rxq source
f       * PVM flag for atmos source
t       * PVM flag for srv source
t       * PVM flag for pool source
t       * PVM flag for rxq source
```

Fig. 3 CONTAIN Parallel Virtual Machine execution input.

input for CONTAIN is simpler than that for RELAP5. The first line of the input tells CONTAIN whether concurrent execution with RELAP5 under the PVM system will be performed. The next four lines specify the CONTAIN model cell numbers where the atmos, "srv," "pool," and "rxq" sources are to be placed. PVMO also uses this input to send the necessary containment conditions back to RELAP5. The last four lines of input specify which of the four source types will be received during the PVM calculation.

DEMONSTRATION TRANSIENT

This section discusses the selection of a transient to demonstrate the capability of the PVM-based RELAP5 and CONTAIN integrated code package. Implicit in this choice is the choice of a specific reactor-containment system configuration. As stated earlier, the new ALWR plants are designed to couple the response of the primary and containment systems. A transient considering one of the ALWR plants would have been an ideal choice; however, because of the proprietary nature of these designs, specific data needed to accurately model these plants are not generally available. For this reason, the analysis of an existing plant configuration was chosen.

The specific transient chosen for this analysis was a main steam isolation valve (MSIV) closure that initiated an ATWS scenario using a BWR/6 MK III reactor-containment system. The ATWS scenario involves the failure of reactor scram capabilities followed by some anticipated transient. This anticipated transient is an event that has a high probability of occurrence sometime during the operational lifetime of the plant. The anticipated transient chosen for this study is an MSIV closure.

Traditionally large thermal–hydraulic codes, such as RETRAN, RELAP, or TRAC, have been used to model the in-vessel response to such transients up to the point of fuel failure. For the accommodation of this type of modeling, certain assumptions must be made regarding the vessel injection systems. Assumptions must be made about availability (i.e., if the system has failed or not) and the temperature of the injection source. The drawback to this approach is that in the plant these systems would fail or trip on the basis of conditions present inside the containment. Because containment response cannot be accurately predicted by these codes, the modeler must decide when to trip a particular system. For the case of an injection source, the modeler must also input some assumed temperature variation with time.

The ATWS initiated by MSIV closure was chosen to maximize the interaction between the primary and containment systems. Following the MSIV closure, the only means to relieve system pressure is the venting of steam through the reactor vessel Safety Relief Valves (SRVs) into the pressure suppression pool of the containment system. The amount of steam vented to the suppression pool is a function of reactor power. Contrary to most accident scenarios, during an ATWS the reactor power level is not simply decay heat production. Implicit in the ATWS scenario is the failure to scram the reactor; therefore it is possible for the reactor to reach a condition in which power can vary anywhere between decay heat levels and several times normal power. These large

variations in core power are possible because of the influence of reactor vessel pressure, injection system flow rate, and core recirculation flow.

For the MSIV-closure-initiated ATWS, the reactor reaches this tenuous state in the following manner. Immediately following MSIV closure, the reactor primary system pressure begins to rise. The recirculation pumps will trip on high vessel pressure and thus cause the core flow to be switched from forced to natural circulation. During this transition to natural circulation, the feedwater flow into the vessel will also be lost. A BWR/6 MK III system has motor-driven feedwater pumps to avoid loss of feedwater pumping capability on loss of drive steam; however, the suction for these motor-driven pumps is taken from the hotwell of the condenser, which depends on MSIV steam flow. Upon loss of steam, the condenser hotwell has a fixed inventory that will be exhausted by full feedwater flow in several minutes. The reactor has now reached the following state: pressure controlled by SRV actuation, natural circulation inside the vessel, and injection flow governed by available safety systems and system pressure. The core power for a reactor in this state is governed by the interaction of all these factors. Increases in system pressure will collapse some of the voids in the core, which will result in an insertion of positive reactivity into the core. In contrast, a decrease in system pressure causes increased voiding and lower power through negative reactivity insertion. Changes in core recirculation rate affect core power in a similar manner. A decrease in recirculation rate will increase void production, which lowers power, whereas an increase in recirculation flow will have the opposite effect.

The vessel injection systems can affect core power production in several ways. First, the injection systems take their suction from sources that are much cooler than the reactor vessel inventory. The injection of this cooler water will result in a power increase because of lower moderator temperature and void fraction. The magnitude of the injection flow compared with that of the core steam production rate will determine if the vessel water level is increasing or decreasing. An increase in vessel water level will increase core flow, which will increase core power; the opposite occurs if the water level is decreasing.

From the preceding discussions, one can see that the accurate modeling of the magnitude and timing of the vessel injection is very important to the determination of core power level for this type of transient. In the determination of the vessel injection, the interaction between the primary and containment systems is very important. First, the vessel injection systems take suction from some source in the containment system itself. Second, the vessel pressure determines which systems are available to inject via pump shutoff head and differential pressure to containment. Finally, the initiation and tripping of the vessel injection systems is influenced by conditions inside containment; for instance, one of the initiating signals for most vessel injection systems is elevated containment pressure.

Another important factor that will influence system response to an ATWS is the automatic depressurization system (ADS). The ADS is used when the high-pressure injection systems cannot maintain an acceptable water level inside the reactor vessel. The ADS is designed to facilitate low-pressure injection by lowering system pressure with the use of several SRVs. During this depressurization, the voiding inside the core will increase, which will further reduce vessel water level and possibly uncover a large portion of the core. Once the system pressure has fallen to a level below the shutoff head of the low-pressure coolant injection (LPCI) and low-pressure core spray (LPCS) systems, low-pressure injection will commence. This situation could result in very large power spikes because of the rapid injection of cold water into a partially uncovered core. These power spikes may be large enough to cause fuel damage that, when combined with containment failure, could result in fission-product release to the environment.

RESULTS

As stated earlier, the initiating event chosen for this ATWS sequence is an MSIV closure. Following the MSIV closure, vessel pressure will begin to rise and thus cause the recirculation pumps to trip. In this state, the reactor vessel pressure will be controlled by automatic SRV actuation, and the high-pressure core spray (HPCS) and standby liquid control (SLC) systems are assumed to fail. The loss of these systems removes the capability of injecting water into a fully pressurized vessel. The loss of SLC also removes the pathway for boron injection into the core to reduce reactor power. Coupled with the loss of the high-pressure injection systems, the feedwater inventory in the condenser hotwell will be depleted (assuming full power flow) in less than 2 minutes.

The level in the reactor vessel will begin to fall because of loss of high-pressure injection and reduction of feedwater flow. Initiation of the ADS will be required to enable low-pressure vessel injection. The ADS will use seven SRVs to reduce reactor vessel pressure until the

differential pressure from the reactor vessel to the containment system is 155 psi differential. Once ADS initiation has lowered vessel pressure (reactor to containment pressure drop <325 psi differential), the LPCI system will be used to maintain vessel water inventory.

This ATWS sequence will be used to compare in-vessel and ex-vessel responses with the use of the integrated RELAP5 and CONTAIN code package and the stand-alone versions of the code.

The results of several different ATWS analyses with varying degrees of coupling between the reactor and containment system will be presented. Each of these cases was based upon the scenario described previously and has the following sequence of events:

—MSIV closure initiated at 0.0 second

—Recirculation pumps trip on high pressure at 3.9 seconds

—MSIVs fully closed at 4 seconds

—Full feedwater flow lost as a result of loss of condenser hotwell inventory at 200 seconds (flow continues at 3% of rated)

—Water level cannot be maintained, ADS timer initiated at 230 seconds

—ADS initiated after 120-second timer delay

After the initiation of the ADS at 350 seconds, the results of the individual runs start to diverge on the basis of the degree of interaction between the reactor and containment systems. The predicted containment response for several cases is presented. Reference 11 presents further details on the scenarios and their results. The first case (fully coupled) involved the complete coupling of the reactor and containment systems using the "srv," "pool," and "rxq" source types defined previously. The second case (semicoupled) is identical to the fully coupled case except that the "pool" source data from CONTAIN is not incorporated into the RELAP5 analysis. In this manner, the pressure and temperature boundary conditions for the suppression pool (which is the source of water for the LPCI pumps) remain constant at their initial values. The semicoupled case is analyzed to predict what effect the assumption of constant containment boundary conditions has on the calculation. Finally, stand-alone RELAP5 and CONTAIN calculations were also performed. Selected results of the three RELAP5 analyses are shown in Figs. 4 and 5. Figure 4 compares the integrated mass passed to the containment for each calculation, whereas Fig. 5 shows integrated energy sent to containment. The semicoupled and stand-alone responses are almost identical because the boundary

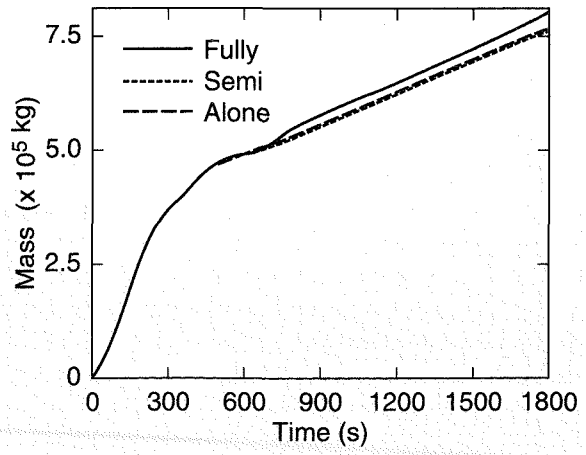

Fig. 4 Integrated Safety Relief Valve mass discharged to containment.

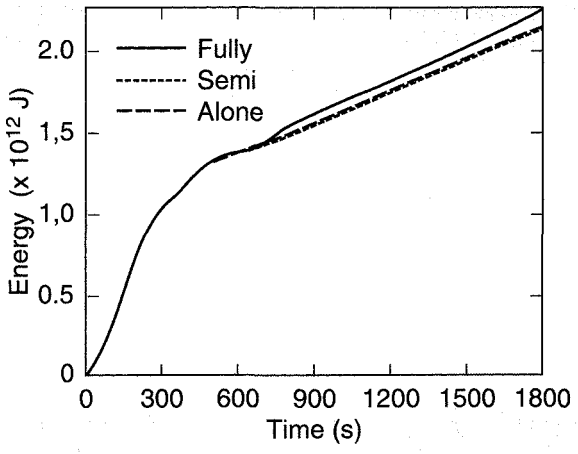

Fig. 5 Integrated Safety Relief Valve energy discharged to containment.

conditions for the wetwell of the containment is the same. The fully coupled case predicts higher LPCI injection flow rates to the vessel because of the reduction in differential head between the reactor vessel and wetwell. This increased injection generates more steam, which is passed through SRV discharge in the suppression pool. Figures 6 to 10 compare results from the various CONTAIN calculations. Figures 6 and 7 compare the fully coupled and semicoupled drywell and wetwell pressure responses. The data in Figs. 6 and 7 indicate that the containment pressures predicted by the semicoupled case are about 76 000 Pa (~11 psi) lower than those predicted by the fully coupled analysis. This is, in part, because the reduction in differential head between the

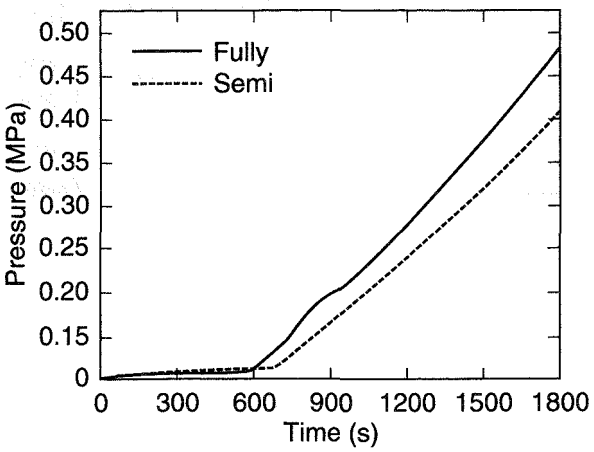

Fig. 6 Drywell atmosphere pressure comparison.

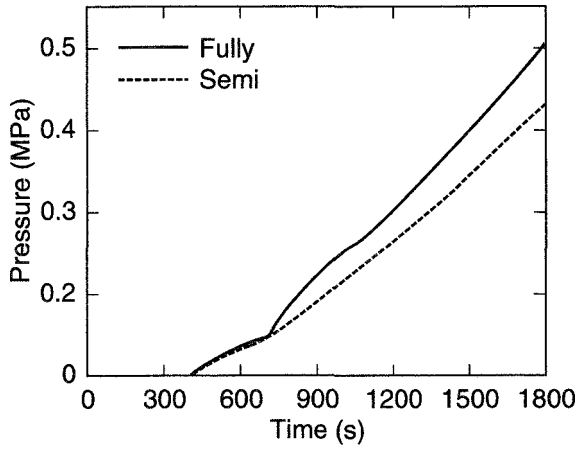

Fig. 7 Wetwell atmosphere pressure comparison.

reactor vessel and the suppression pool is not modeled in RELAP5 for the semicoupled case. For the fully coupled analysis, this reduction in differential head results in higher RELAP5 predictions for LPCI flow and thereby generates more steam, which further pressurizes the containment. The effect of this larger steam generation can also be seen in Figs. 8 and 9, which compare the suppression pool and wetwell atmosphere predictions for the fully coupled and semicoupled analyses. Figure 10 compares the drywell temperatures for all three cases. The stand-alone analysis does not predict the initial increase in drywell temperature that is due to heating from the reactor vessel. This heating is modeled by using the "rxq" source in the fully and semicoupled analyses.

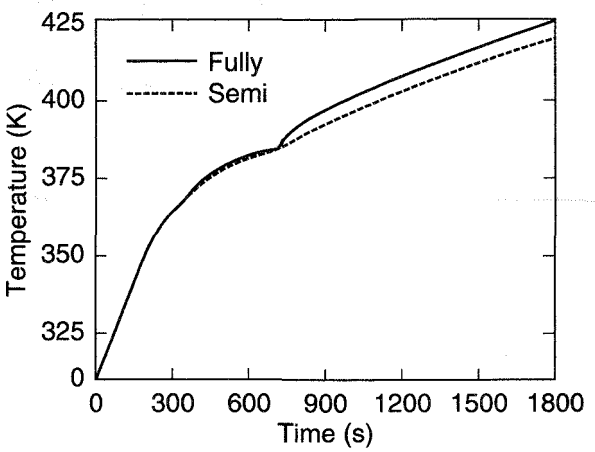

Fig. 8 Suppression pool temperature comparison.

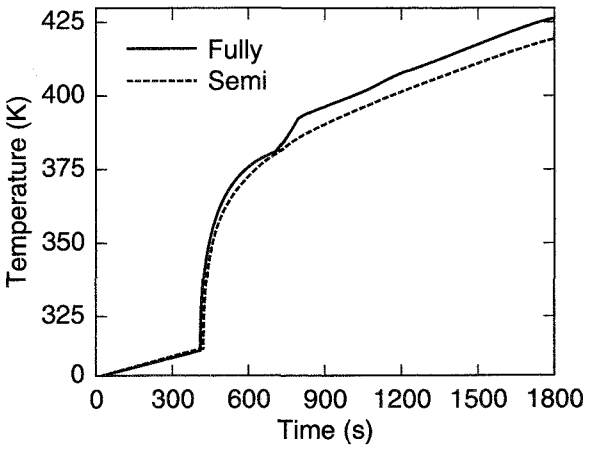

Fig. 9 Wetwell atmosphere temperature comparison.

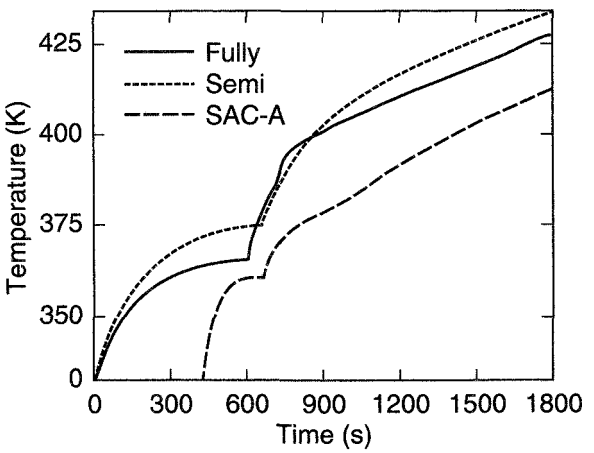

Fig. 10 Drywell atmosphere temperature comparison.

CONCLUSIONS

The results of analyses presented herein demonstrate the ability of the PVM-based RELAP5/CONTAIN code package to predict the integrated response of the reactor and containment systems during an ATWS. Not only are the results more accurate than those generated using the stand-alone codes but also the integrated analysis avoids the cumbersome data transfer required when using the codes in their stand-alone form; thus the analysis is simpler to perform. With the use of the integrated code system (executing each code on a separate processor), one can perform fully coupled RELAP5 and CONTAIN calculations in approximately the same amount of time as the bounding RELAP5 analysis. The ATWS scenario results stress the importance of accurately modeling the interaction between the reactor and containment systems during accident analysis. As illustrated by the semicoupled CONTAIN results, specifying constant containment boundary conditions is less conservative with respect to containment loading; that is, the specification of constant containment boundary conditions results in a containment temperature and pressure response that is lower (less conservative) than the fully coupled case.

The integrated RELAP5/CONTAIN analysis capability also has direct applicability to transient analysis of new advanced reactor concepts. Current advanced reactor designs open valves between the reactor and containment systems and rely extensively on passive safety systems tied to the containment, which increases the coupling between the two systems and further complicates transient analysis with the use of existing code packages. A follow-on version of the PVM-based RELAP5 and CONTAIN coupling described herein has been developed by INEL personnel for ALWR applications.[12]

ACKNOWLEDGMENTS

This work was funded by the Nuclear Engineering Department of The Pennsylvania State University. The authors would like to thank Joe Miller of Gulf States Utilities for information on the ATWS sequence analyzed, Dick Wagner at Idaho National Engineering Laboratory for information regarding RELAP5 code structure, and Ken Washington at Sandia National Laboratories for CONTAIN code structure information.

REFERENCES

1. D. Liles and J. H. Mahaffy, *TRAC-PF1/MOD1: An Advanced Best-Estimate Computer Program for Pressurized Water Reactor Thermal–Hydraulic Analysis,* Report NUREG/CR-3858, 1986.
2. D. Taylor et al., *TRAC-BD1/MOD1: An Advanced Best-Estimate Computer Program for Boiling Water Reactor Thermal Hydraulic Analysis,* Report NUREG/CR-3633, 1986.
3. C. M. Allison and E. C. Johnson (Eds.), *SCDAP/RELAP5/MOD2 Code Manual, Volume I: RELAP5 Code Structure, System Models, and Solution Methods,* Report NUREG/CR-5273-Vol. I (EGG-2555-Vol. I), 1989.
4. K. K. Murata, D. E. Carroll, K. E. Washington, F. Gelbard, G. D. Valdez, D. C. Williams, and K. D. Bergeron, *User's Manual for CONTAIN 1.1: A Computer Code for Severe Nuclear Reactor Accident Containment Analysis,* Report NUREG/CR-5026 (SAND87-2309), 1989.
5. R. M. Summers, R. K. Cole, Jr., E. A. Boucheron, M. K. Carmel, S. E. Dingman, and J. E. Kelly, *MELCOR 1.8.0: A Computer Code for Nuclear Reactor Severe Accident Source Term and Risk Assessment Analyses,* Report NUREG/CR-5531 (SAND 90-0364), 1991.
6. G. A. Geist and V. S. Sunderam, *Network Based Concurrent Computing on the PVM System,* Report ORNL/TM-11760, 1991.
7. A. Beguelin, J. Dongarra, A. Geist, R. Manchek, and V. Sunderam, *A User's Guide to PVM (Parallel Virtual Machine),* Report ORNL/TM-11826, 1991.
8. C. M. Allison and E. C. Johnson (Eds.), *SCDAP/RELAP5/MOD2 Code Manual, Volume II: SCDAP Code Structure, Models, and Solution Methods,* Report NUREG/CR-5273-Vol. II (EGG-2555-Vol. II), 1989.
9. K. E. Washington et al., *Reference Manual for the CONTAIN 1.1 Code for Containment Severe Accident Analysis,* Report NUREG/CR-5715 (SAND-91-0835), 1991.
10. K. K. Murata, D. C. Williams, R. G. Gido, R. O. Griffith, K. E. Washington, and D. Y. L. Louie, New Containment Modeling Features of the CONTAIN Code, in *Proceedings of the NRC Nineteenth Water Reactor Safety Information Meeting,* Report NUREG/CP-0119 (CONF-911079), 1992.
11. K. A. Smith, Multiprocessor Based Simulation of Degraded Core and Containment Responses, Ph.D. Thesis, The Pennsylvania State University, 1992.
12. R. P. Martin and G. W. Johnsen, Coupling of the RELAP5/MOD3 to CONTAIN for ALWR Analysis, in *Transactions of the Twenty-First Water Reactor Safety Information Meeting,* 1993.

Control and Instrumentation

Edited by C. R. Brittain

Application of Fuzzy Logic in Nuclear Reactor Control Part I: An Assessment of State-of-the-Art

By A. S. Heger,[a] N. K. Alang-Rashid,[b] and M. Jamshidi[c]

Abstract: *This article discusses the application of fuzzy logic to nuclear reactor control. The method has been suggested by many investigators in many control applications.[1–6] Reviews of the application of fuzzy logic in process control are given by Tong[7] and Sugeno.[8] Because fuzzy logic control (FLC) provides a pathway for transforming human abstractions into the numerical domain, it has the potential to assist nuclear reactor operators in the control room. With this transformation, linguistically expressed control principles can be coded into the fuzzy controller rule base. Having acquired the skill of the operators, the FLC can assist an operator in controlling the complex system. The thrust of FLC is to derive a conceptual model of the control operation, without expressing the process as mathematical equations, to assist the human operator in interpreting incoming plant variables and arriving at a proper control action.*

To introduce the concept of FLC in nuclear reactor operation, an overview of the mythology and a review of its application in both nuclear and nonnuclear control application domains are presented along with subsequent discussion of fuzzy logic controllers, their structures, and their method of information processing. The article concludes with the application of a tunable FLC to a typical reactor control problem.

[a]Chemical and Nuclear Engineering Department, University of New Mexico, Albuquerque, New Mexico, U.S.A.

[b]Malaysian Institute for Nuclear Technology Research, Kompleks PUSPATI, Bangi, Selangor, Darul Ehsan, Malaysia. This work was performed while the author was a resident at the University of New Mexico Chemical and Nuclear Engineering Department.

[c]Electrical and Computer Engineering Department, University of New Mexico, Albuquerque, New Mexico, U.S.A.

Nuclear reactor control has been the subject of extensive studies. Various control techniques, such as optimal control[9–13] and adaptive and model-reference adaptive control,[14,15] have been investigated. None of these techniques, however, can take advantage of the expertise of the reactor operators. The reactor operators cannot use the mathematical control laws that govern the behavior of the controller as a guide in predicting future actions. The operators must use the plant mathematical model and the controller mathematical formulation when estimating future control actions.

The need for on-line reactor operator support systems became obvious after the Three Mile Island Nuclear Station Unit 2 accident in 1979. Seven years later, reactor operators failed to anticipate the consequence of their actions and to diagnose the resulting abnormal reactor condition that led to the Chernobyl accident in the Ukraine. These events drew attention to the techniques of artificial intelligence, which have proved successful in other areas, as a possible method for providing operator advisers. To this end, expert systems have proliferated in many reactor operation support areas, such as alarm filtering, that do not require human motor actions.[16,17] This replacement has reduced the burden on the reactor operators and has minimized the need for a human expert being present for routine operation of the reactor.[18–20]

The use of fuzzy logic control (FLC) diametrically opposes the conventional approach of controller design, which relies on a plant model and formally derived mathematical control laws. Subsequently, the conventional

controllers require extensive computation and a precision that is not normally relevant when human operators are the controllers.

FUZZY LOGIC AND ITS APPLICATION IN NUCLEAR REACTOR CONTROL

Despite its success in other domains, the application of fuzzy logic in nuclear reactor control has been sporadic. Table 1 provides a summary of some of the current application areas that relate to nuclear engineering.

In the area of nuclear reactor control, Bubak et al. (1983)[21] use a high-temperature reactor (HTR) simulation model to study the applicability of fuzzy logic for the control of a nuclear reactor. The control objective is to follow the desired power trajectory. The researchers use the control rod velocity as the manipulated or controlled variable. Their results show that the controller can satisfy the control objective. The nagging question of how to derive the effective set of control rules, however, remains. Kinoshita et al.,[23] on the basis of the plant status and control objectives, use fuzzy logic to determine the length of control rod movements in a boiling-water reactor (BWR). Their simulations indicate that the FLC performance is comparable to that of a human operator. Terunuma et al.[24] developed an FLC test system to operate the feedwater control system of a heavy-water reactor. The control rules are derived from human experts. Terunuma and colleagues observe that the FLC has the potential to use human operator skills. Their experiments, too, are conducted with a simulation model. Akin and Altin[25] use a simulation model of the H. B. Robinson Plant pressurized-water reactor (PWR) to study the application of FLC for nuclear power plant control. Specifically, the FLC is used for maintaining the reactor power at a steady operating level. The FLC adjusts steam flow rate to maintain the desired operating level. Kuan et al.[26] also use a simulation model to control PWR steam generator water level. Actually, the FLC is used in tandem with a proportional–integral–derivative (PID) controller. Large deviation from a set point is corrected by the FLC, whereas set-point errors are adjusted by a PID controller.

Table 1 Application of Fuzzy Logic in Nuclear Engineering

Area	Researcher
Control	Bubak et al. (1983)[21]
	Bernard (1988)[22]
	Kinoshita et al. (1988)[23]
	Terunuma et al. (1988)[24]
	Akin and Altin (1991)[25]
	Kuan et al. (1992)[26]
	Alang-Rashid (1992)[27]
Diagnosis	Kitowski and Bargiel (1986)[28]
	Guth (1989)[18]
	Hassberger (1986)[29]
	Abdelhai and Upadhyaya (1990)[30]
	Sutton and Parkins (1991)[31]
	Holbert et al. (1994)[32]
Modeling	Matsuoka (1991)[33]
	Terunuma et al. (1990)[34]
	Kitamura et al. (1989)[35]
Reliability	Onisawa and Sugeno (1985)[36]
	Onisawa and Nishiwaki (1988)[37]
	Kuraszkiewicz and Derbis (1990)[38]
	Chun and Ahn (1991)[39]
Site selection	Gencay (1991)[40]

With the use of both a simulation model and the Massachusetts Institute of Technology (MIT) reactor, Bernard[22] demonstrated the application of fuzzy logic in reactor operation. He derived the FLC rules using a three-step process of observing operator actions, observing the instruments that operators monitor, and using a follow-up questionnaire for uncovering the reasons for the operators' control actions. Bernard concurs that fuzzy rule-based controllers are more robust than conventional controllers. He also noted that a more systematic FLC design method needs to be developed. The procedures that are used to tune the controller have been based on iterative improvements or trial and error. This observation by Bernard provided an impetus for the development of a tunable fuzzy logic controller by the authors of this article.[41] This new method overcomes some of the drawbacks of the methods mentioned previously and will be discussed in detail in a future article.

FUZZY LOGIC IN MODELING REACTOR DYNAMICS

The information necessary for a control application can come from the following sources:[32]

1. Mathematical models.
2. Observation based on knowledge and/or experience.
3. Numerical data from instrumentation.
4. Linguistic data.
5. Visual data from actual observations or instrumentation.

When fuzzy logic is used, a combination of inference rules and fuzzy set operations can encode the first four sources of information into representation for computers for control applications. This is possible because the fuzzy set can transform linguistic information into numerical values. The inference scheme of fuzzy logic can capture human knowledge and mathematical models into a set of rules that can be used to interpret the information and respond by proper action. In this sense, a fuzzy approach to control applications can be viewed as a qualitative modeling of the operator's perception of the plant in linguistic terms; for example, fuzzy rules may be as follows:

R^1: If error is negative big and error rate is negative big, then reactivity is positive big.

R^2: If error is negative medium and error rate is negative big, then reactivity is positive medium.

A set of rules $\mathbf{R} = \{R^1, R^2, ..., R^p\}$ is used to define the relationships between the input and output control variables. For a multiple-input and a single-output, a rule R^i is of the form:

$$R^i: \text{ if } x_1 \text{ is } A_1^i \text{ and } x_2 \text{ is } A_2^i \text{ ... and } x_m \text{ is } A_m^i \text{ then y is } B^i \qquad (1)$$

where R^i = ith rule
x_i = input variables
y = output
A_j^i and B^i = fuzzy variables

Fuzzy variables can assume values that are either numeric or linguistic. The linguistic variables and their values (i.e., the fuzzy sets) are context-dependent quantities. Given a control application, for example, the fuzzy variables can assume linguistic values such as "positive medium reactivity" and "positive big reactivity," whose values depend on the situation. This form of knowledge representation is congruous with that used by human operators.

FUZZY LOGIC REPRESENTATION

Let z_k be the raw input data that are collected from various sensors. For n plant variables, the vector $\mathbf{z} = \{z_1, z_2, ..., z_k, ..., z_n\}$ represents the raw input data available for signal processing and control. These data are then transformed through a preprocessor into usable information, which is represented by the vector $\mathbf{x} = \{x_1, x_2, ..., x_j, ..., x_m\}$, where each of the m terms represents one of the preprocessed datum. The vector $\mathbf{x}$ is fed to an array of p fuzzy rules as shown in Fig. 1. Each rule associates the input data with the appropriate fuzzy variables, A_j^i. The degree of association of each input datum with its respective fuzzy variable is numerically represented by the membership value μ_j^i. A membership function is a mathematical description of the distribution of membership values, which characterize the uncertainty of x belonging in A. Common membership functions are triangular and modified versions of the Gaussian distribution, as shown in Fig. 2. The general form for the triangular function, for example, is as follows:

$$\mu_j^i = \mu_{A_j^i}^{x_j}(x_j) = \frac{1 - 2|x_j - \hat{x}_j|}{w_j} \qquad (2)$$

where $\hat{x}_j$ is the location of the peak of the triangle and w_j is the width of its base. The term $\mu_{A_j^i}^{x_j}(x_j)$ is read as the membership of variable x_j (e.g., error) in the fuzzy group A_j^i (e.g., positive small, negative medium, positive large) given a variable value of x_j (i.e., a real number). Once these data sets are fed to the FLC, the inference process of fuzzy logic takes place. In this process the input data become associated with the appropriate control action.

Inference in fuzzy logic is based on the rules of the form "if ... then ...," as demonstrated in Eq. 1. The objective of this formalism is to store knowledge in the form of a set of rules that are well-formed logical formulas. Each rule consists of two parts: an antecedent (x_1 is A_1 and x_2 is A_2 ... and x_m is A_m) and an implicant (y is B). The antecedent part of the rule conjoins the conditions that are required to trigger the implication part of the rule. In the case of multi-input, multi-output, for example, the ith rule is as follows:

$$R^i: \text{ if } \left(x_1 \text{ is } A_1^i\right) \text{ op } \left(x_2 \text{ is } A_2^i\right) \text{ ... op } \left(x_j \text{ is } A_j^i\right) \text{ ... op } \left(x_m \text{ is } A_m^i\right)$$
$$\text{then} \qquad (3)$$
$$\left(y_1^i \text{ is } B_1^i\right) \text{ and } \left(y_2^i \text{ is } B_2^i\right) \text{ ... and } \left(y_k^i \text{ is } B_k^i\right) \text{ ... and } \left(y_n^i \text{ is } B_n^i\right)$$

where "op" stands for one of the fuzzy set theoretic operations, as shown in Table 2. The superscripts i (i = 1, 2, ... , p) are the indices for the fuzzy rules. Subscripts j (j = 1, 2, ... , m) count the input variables, and subscripts k (k = 1, 2, ... , n) correspond to the output control signals.

Once presented with the input variables, each member of the antecedent of a given rule fires its response by

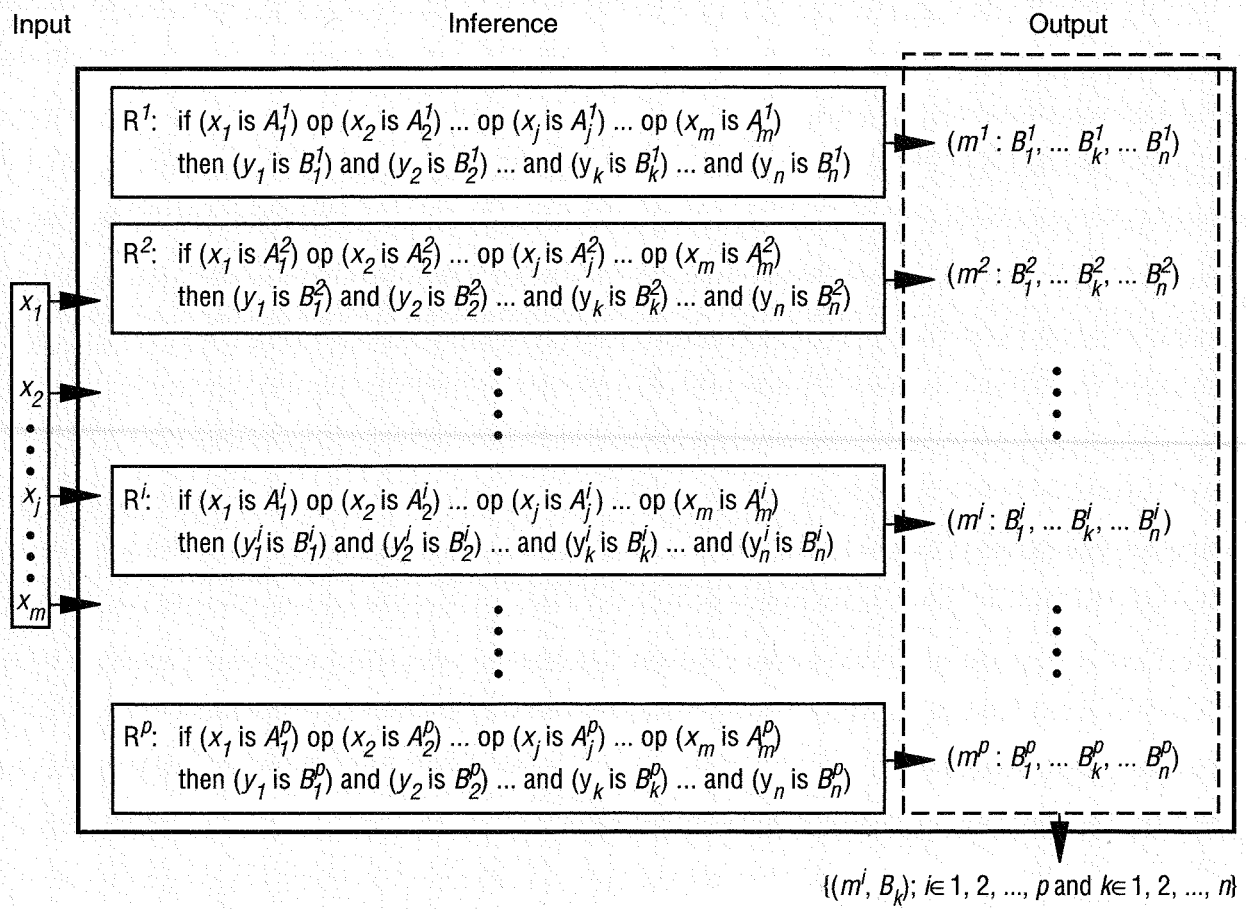

Fig. 1 Internal representation of the fuzzy rules and processing of input data.[28] Superscripts i (i = 1, 2, ..., p) are the indices for the fuzzy rules, subscripts j (j = 1, 2, ..., m) count the input variables, subscripts k (k = 1, 2, ..., n) correspond to the output control signals, R^i is the ith rule, x_i is the input variable, y_i is the output of each rule, A_j^i and B^i are fuzzy variable, m_j^i is the degree of association between x_i and A_j^i or B^i, and m^p represents the degree of membership of the consequence of each rule.

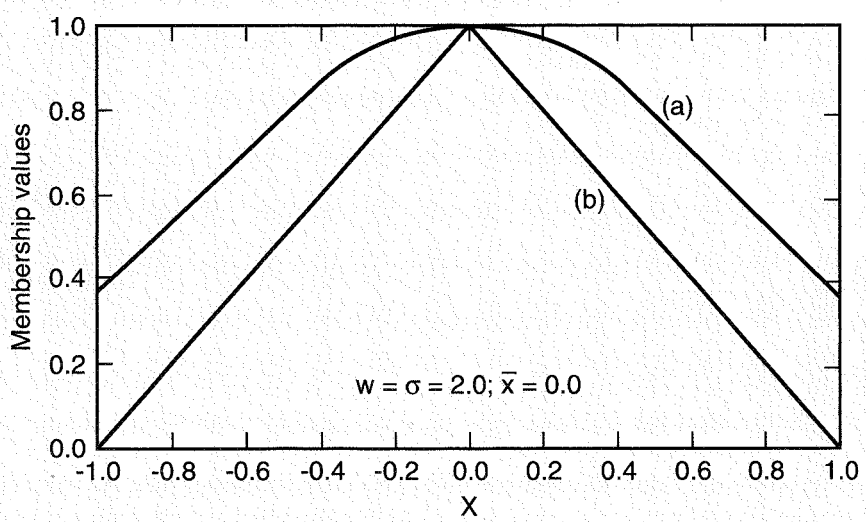

Fig. 2 Membership function curves: Gaussian-like (a) and triangular (b) function.

Table 2 Fuzzy Set Theoretic Operations

Operation (op)	Definition
Equality	$\tilde{x}=\tilde{y}$ iff $\forall_i \mu_{\tilde{x}}(x_i)=\mu_{\tilde{y}}(y_i)$
Intersection	$\mu_{\tilde{x}\cap\tilde{y}}(x)=\mu_{\tilde{x}}(x)\wedge\mu_{\tilde{y}}(x)=\min[\mu_{\tilde{x}}(x),\mu_{\tilde{y}}(x)]$
Union	$\mu_{\tilde{x}\cup\tilde{y}}(x)=\mu_{\tilde{x}}(x)\vee\mu_{\tilde{y}}(x)=\max[\mu_{\tilde{x}}(x),\mu_{\tilde{y}}(x)]$
Complement	$\mu_{\bar{\tilde{x}}}(x)=1-\mu_{\tilde{x}}(x)$

submitting a membership value, μ_j^i. Depending on the fuzzy set operation, as outlined in Table 2, an appropriate membership value is transferred to the consequence part of the rule; for example, if the operator "op" is an "and," then the minimum of μ_j^i is selected. Each rule then submits a set of consequences, B_k^i, and its associated degree of membership, m^i, which is equal to the properly combined μ_j^i from the antecedent of the rule. Finally, the FLC must defuzzify its output.

One possible defuzzification method is centroid defuzzification.[42] The centroid defuzzification scheme gives the crisp controller output, U^*, as the sum of the products of the rule activation strength and the centroid of the output fuzzy sets weighted by the sum of the rule activation strength. This can be written as follows:

$$U^* = \frac{\sum_{i=1}^{N} \mu_{R_i} C_i}{\sum_{i=1}^{N} \mu_{R_i}} \tag{4}$$

where N is the number of primary fuzzy sets in the output fuzzy variable. To illustrate, let two control rules in a two-input one-output FLC be fired. The rules are the following:

*R*1: If error is negative big and error rate is negative big, then reactivity is positive big.

*R*2: If error is negative medium and error rate is negative big, then reactivity is positive medium.

The inference operation, shown graphically in Fig. 3, yields two possible outputs: positive medium reactivity and positive big reactivity. The former has the higher membership values by virtue of the higher activation strength of R2.

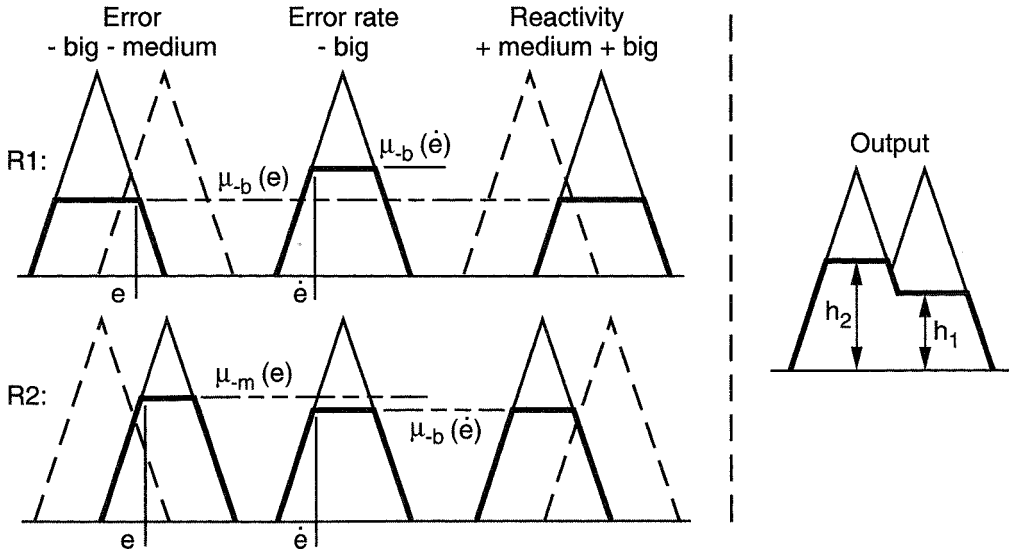

Fig. 3 Max–min composition and centroid defuzzification. R1 and R2 are rules, b = big (–b = negative big), m = medium (–m = negative medium), e = error, ė = error rate, h_1 = output membership function, and μ = the degree of association between the preprocessed datum and the fuzzy variables (membership value).

With the use of the centroid defuzzification scheme, a single, crisp reactivity value is obtained by taking the center of gravity from the resulting output membership functions, shown as output in Fig. 3. This is calculated as

$$\frac{h_2 C_1 + h_1 C_2}{h_2 + h_1}$$

where $h_2 = \mu_b(\dot{e})$, $h_1 = \mu_b(e)$, and C_i = 1,2 are the centroids of the output variable fuzzy sets membership functions (positive big and positive medium).

To build an FLC, the knowledge must be extracted from the expert and transformed into a set of fuzzy rules. Several automated processes for this transformation process exist.[41] In general, this process is the most difficult and crucial step in the design of a fuzzy system because fuzzy rules are derived from a human's experience, which is based mostly on the person's qualitative knowledge of an objective system.[43]

FUZZY LOGIC CONTROLLERS

The thrust of FLC is the automation of control tasks by making use of, as much as possible, the expertise and knowledge of human operators that are relevant to the control of the plant. The process of control can be thought to consist of three tasks executed cyclically and continuously: monitoring, analysis, and implementation of corrective action. The purpose is either to maintain a steady-state operating level or to transfer the plant from one operating level to another following acceptable transition states. The former is called regulating control, and the latter is called tracking or maneuvering control.

At the monitoring stage, variables that are relevant to the determination of the plant's current state are gathered. By comparing the current and the desired plant states, the operator uses personal expertise and knowledge about the plant to decide on the appropriate control actions.

Structure

The structure of an FLC is shown in Fig. 4 (adopted from Ref. 44). It consists of four main parts: a fuzzifier, a fuzzy knowledge base, a fuzzy decision maker, and a defuzzifier.

Fuzzifier. The fuzzifier is the front-end interface of the FLC to the plant to be controlled. It monitors the plant variables, X, that are required for making control decisions. These variables are then transformed into fuzzy variables, or fuzzified, so that they are in the same form as the knowledge base and the decision-maker's logic. The fuzzification process applies the membership function of each input variable to its respective numerical values. The results are vectors of membership values, one for each input variable.

Knowledge Base. The FLC knowledge base comprises a data base and a rule base. The data base consists of definitions of fuzzy variables, their ranges, fuzzification and defuzzification methods, and the inference scheme used by the controller. The rule base is

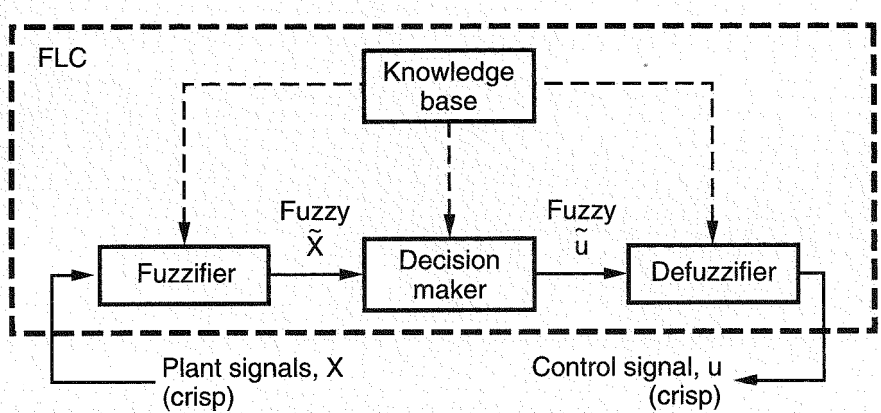

Fig. 4 Structure of a fuzzy logic control unit.

a collection of control rules, similar to the ones used by human operators, that are necessary to control the plant.

Decision Maker. The decision maker generates the degree of activation of each rule that is fired by the input variables. A rule is fired when the condition in its premise is satisfied. The degree to which a control rule is activated is a measure of the appropriateness of the control action. This measure is determined by using the compositional rule of inference, as described in the previous section.

Defuzzifier. The defuzzifier is the FLC back-end interface to the plant for control purposes. It transforms the fuzzy control actions obtained by the decision maker into a single, crisp value of control action.

Fuzzy Logic Controller Modifications

As mentioned previously, the two main ingredients of any FLC are its rule base and membership functions. The rule base contains statements that relate the controller input variable to its output variable(s). The membership functions describe the degree to which a numerical value of a variable belongs in the variable fuzzy sets. For processes with operating experience, such as a nuclear reactor, the rule base can be derived from accumulated operating experience of the reactor operators, process input–output data, or a simulation model of the process. Bernard[22] and Terunuma et al.[24] used the simulation process. Wang and Mendel[45] devised a technique for deriving the FLC rule base from the process input–output data. For novel processes in which no expert knowledge or input–output data are available, the rule base can be derived from the process dynamics or from a simulation model of the process.

The rule base and the membership functions do not always match, thus tuning of the FLC is required. This rule–membership function mismatch arises from lack of information on the specifications of the membership functions. The rules that are incorporated into the FLC rule base are broad generalizations of the operators' control strategy. Although the rules are readily available from the operators, the specifications of the membership functions are harder to define. Overlaps among the primary fuzzy sets of a variable, the slopes, and the functions used in defining the membership values also tend to dilute the generality of the rules and introduce specifics to the FLC. In addition, personal preferences, experience, and the sensitivity of linguistic values to context also contribute to this mismatch. The FLC interpretation of a linguistic value of "small," for example, must coincide with that of the operator's interpretation if the FLC is to achieve consistent control effects with the use of rules that are used by the operators.

Essentially, the tuning of FLCs involves modification of the rules, the membership functions, or both. Procyk and Mamdani[46] and Galluzo et al.[47] present two interesting methods for modifying the FLC rule base. Galluzo et al. construct meta-rules as another level on top of the existing FLC rule base. This arrangement is akin to a two-level controller in which the upper controller monitors and adjusts the performance of the lower one. The upper level controller adjusts the rule base of the lower controller with the use of its own rule base, the meta-rules that are derived empirically. Modifications of the control rules, however, may change the operator-derived FLC rule base, which defeats the advantages of an FLC.

The approaches for forming and modifying the membership functions have been and still are subjects of great interest. The methods that are studied range from the use of neural networks[48] to steepest descent gradient search procedures.[49] Although the work of Yamakawa and Furukawa[48] does not go deep enough into the generation of the control rules, it does deal with membership function generation, where domain expert knowledge is not required. They apply this method to pattern recognition application of fuzzy logic. Nomura et al.[49] use a gradient descent algorithm to adjust both the input and output variable fuzzy subsets membership functions to obtain optimum FLC performance.

EXAMPLE

An experimental FLC was tested in conjunction with the University of New Mexico AGN-201M reactor to validate the simulation and the applicability of the fuzzy logic control methods. The FLC was tested for the following control cases: increasing or decreasing the reactor power from one steady-state level to another or tracking a desired power-level trajectory. The mode of control in this simulation study introduced step reactivity insertion at every sampling interval. The magnitude and sign of the reactivity were determined by the FLC output. Some test results are presented here, and the complete set of experiments appears in Ref. 27.

Error, ER, and error change per sampling interval, DE, were defined for these experiments as the FLC inputs. An externally applied reactivity, RO, was defined as the FLC

output variable. The input and output variables are defined as follows:

$$ER(k) = \bar{p}(k) - \bar{p}_d(k)$$

$$DE(k) = ER(k) - ER(k-1)$$

$$RO(k) = \tilde{f}[ER(k), DE(k)]$$

where k = time steps
$\bar{p}(k)$ = power level at time k
$\bar{p}_d(k)$ = desired power level at time k
$\tilde{f}(\bullet)$ = function representing the fuzzy logic operation on its parameters

The input variable ER has a range of [–100, 100] %FP and is given primary fuzzy sets of {NE, NS, PS, PO}. DE has a range of [–10, 10] %FP with primary fuzzy sets of {NE, NS, ZE, PS, PO}. The output variable RO is in the range of [–1, 1] $ with primary fuzzy sets of {NE, NS, PS, PO}. The primary fuzzy sets have the following meanings: NS denotes "negative small," NE denotes "negative," ZE denotes "zero," PS denotes "positive small," and PO denotes "positive." The membership function parameters of the primary fuzzy sets are given in Table 3, and the membership function curves are shown in Fig. 5.

With this arrangement, as many as 20 rules for the FLC can be developed. The rules describe the relationships between error, ER, error change, DE, and reactivity, RO. Only four rules, however, were used in the experiments because they were found to be reasonable for the type of control problems considered. The rules are as follows:

$$R_1: [(\text{NE} * *) \Rightarrow PO]$$

$$R_2: [(\text{PO} * *) \Rightarrow NE]$$

$$R_3: [(\text{NS} \cap \text{ZE}) \Rightarrow PS]$$

$$R_4: [(\text{PS} \cap \text{ZE}) \Rightarrow NS]$$

where the symbol "*" means ignore the entries. The functions of the rules R_1 to R_4 are as follows: R_1 causes positive reactivity to be inserted so that the reactor power level increases; thus the error, which at the time of the rule activation equals NE, is reduced; R_2 acts conversely to R_1; and R_3 and R_4 are intended to correct for steady-state offset error; for example, the error change, DE, can be zero, which means the reactor power level is off before attaining a desired power level. In this case, R_3 and R_4 cause small reactivity, positive or negative, to be inserted to correct the offset error.

These rules originate from a larger set of rules that describes possible combinations of relationships between ER and DE with RO from a process control standpoint. To illustrate, consider the series of control actions (i.e., reactivity insertions) that are needed for increasing or decreasing a reactor power level. For brevity, let ER, DE, and RO be described only by positive (+ve) and negative (–ve) values. In Fig. 6 the possible values of reactor power, $\bar{p}(t)$, with respect to a steady-state desired value of $\bar{p}_d(t)$ during an increase in power level are shown. Figure 7 shows the possible cases for power decreases. In both figures the values of ER, DE, and the reactivity, RO, that will reduce the error between the actual and the desired power levels are noted.

Condition (a) in Fig. 6 is a situation in which $\bar{p}(t)$ is increasing while ER is negative. This means that DE is positive. Because $\bar{p}(t)$ is moving in the right direction, an appropriate control action is either to do nothing or accelerate the process by introducing +ve RO. Condition (b) of the same figure may arise at the initiation of the control sequence while the reactor is in a steady-state condition. It may also arise as the result of insufficient reactivity insertion. Condition (c) may be induced by disturbance, and condition (d) depicts an overshoot of the reactor power level.

Table 3 FLC Membership Function Parameters

Variable	$\tilde{x}$	$\bar{x}$	x_e
Error, ER	NE	–100.0	+60.0
	NS	–10.0	0.0
	PS	+10.0	0.0
	PO	+100.0	–60.0
Error change, DE	NE	–10.0	+5.0
	NS	–5.0	0.0
	ZE	0.0	+1.0
	PS	+5.0	0.0
	PO	+10.0	–5.0
Reactivity, RO	NE	–1.0	+0.5
	NS	–0.3	+0.3
	PS	+0.3	–0.3
	PO	+1.0	–0.5

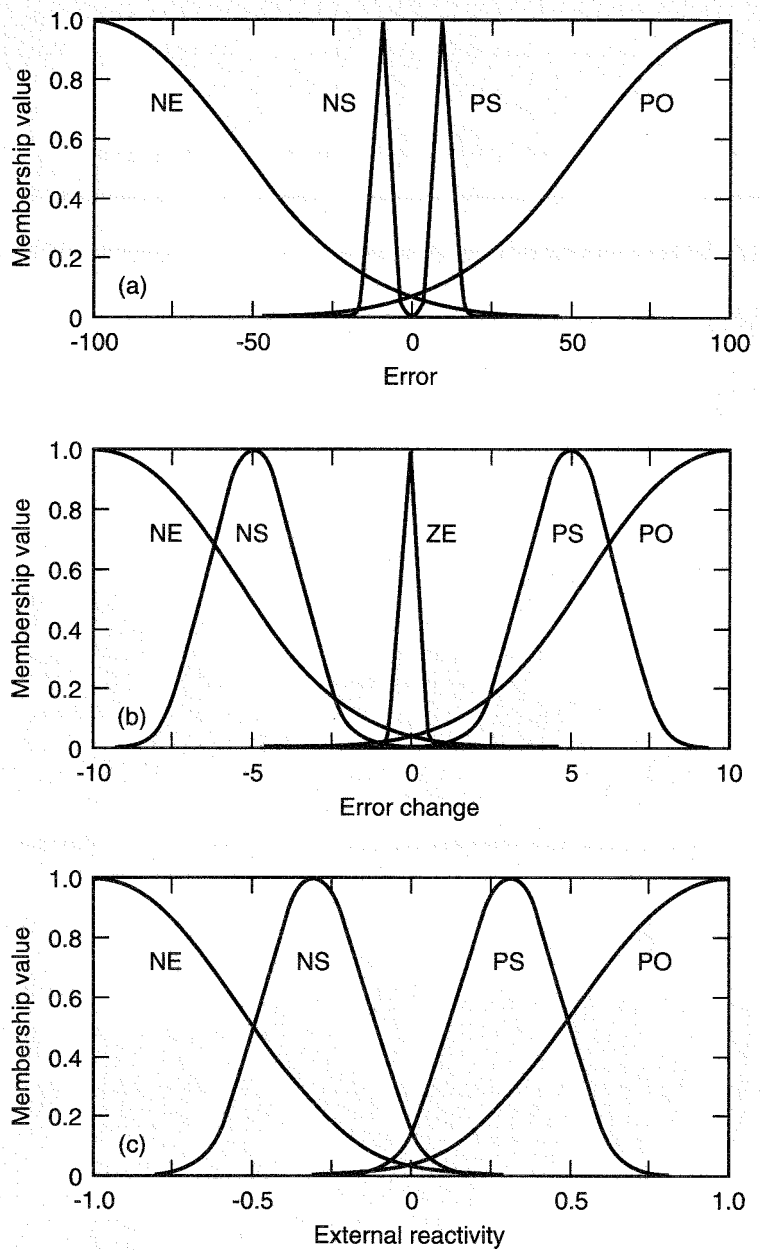

Fig. 5 Membership functions of the fuzzy logic control variables: (a) error, (b) error change, and (c) external reactivity. NS = negative small, NE = negative, ZE = zero, PS = positive small, and PO = positive.

From Figs. 6 and 7, it may be deduced that, in general, whenever ER is negative, RO needs to be positive. Conversely, RO should be negative whenever ER is positive. Rules R_1 and R_2 stem from these conditions. Condition (d) of Fig. 6 also requires action similar to that of condition (c) of Fig. 7. The difference, however, is that just before condition (d) is attained, ER is already small, even though it is still –ve. In this case, unlike conditions (a) to (c), a big reactivity insertion is not needed. The magnitude of reactivity to be applied is calculated by the FLC on the basis of our partitioning of the FLC variables. This leads to the introduction of R_3. The converse of this argument (for decreasing power levels) applies to the deduction of R_4.

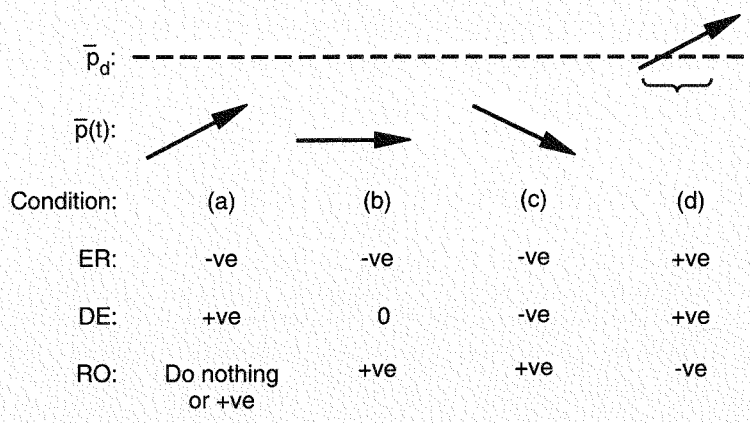

Fig. 6 Rules for reactor power increase. ER = error; DE = error change; RO = reactivity; $\bar{p}_d$ = desired power level of time t, assumed constant; $\bar{p}(t)$ = power level at time t; –ve = negative; +ve = positive.

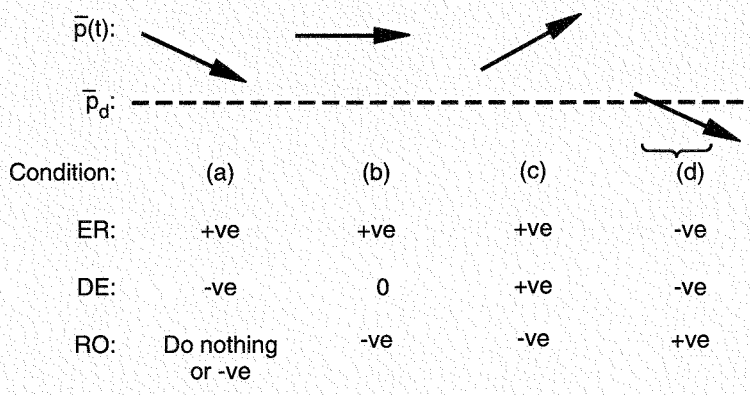

Fig. 7 Rules for reactor power decrease. ER = error; DE = error change; RO = reactivity; $\bar{p}_d$ = desired power level of time t, assumed constant; $\bar{p}(t)$ = power level at time t; –ve = negative; +ve = positive.

Time-Varying Setpoint

A step increase or decrease in reactor power level is naturally desirable if it is safe and attainable. In practice, however, because of, for example, thermal considerations, power change is made following a prescribed trajectory. In this simulation a six-decade power increase, from 20 to 80%FP, was simulated by a step increase in demand by specifying a smoother trajectory. The trajectory is described by $\bar{p}_d(t) = 20 + 60[1 - \exp(-t/20)]$. The reactor response is shown in Fig. 8. The FLC can be seen to closely track the desired power level.

Time-Varying Setpoint with Disturbance

In this simulation the performance of the FLC following a change in the reactor model parameter is tested. The FLC is required to track a desired power trajectory that was described in the previous example. A disturbance is then simulated by increasing the magnitude of the fuel temperature coefficient of reactivity, $\bar{\alpha}_c$. This is equivalent to an increase in fuel temperature or an insertion of neutron poison into the core. The magnitude of $\bar{\alpha}_c$ is changed from $-1.046\$\cdot\bar{T}_f^{-1}(=-4\times10^{-6}\,dk/k\cdot{}^\circ C^{-1})$ to $-3\$\cdot\bar{T}_f^{-1}(=-1.15\times10^{-5}\,dk/k\cdot{}^\circ C^{-1})$ as the steady-state

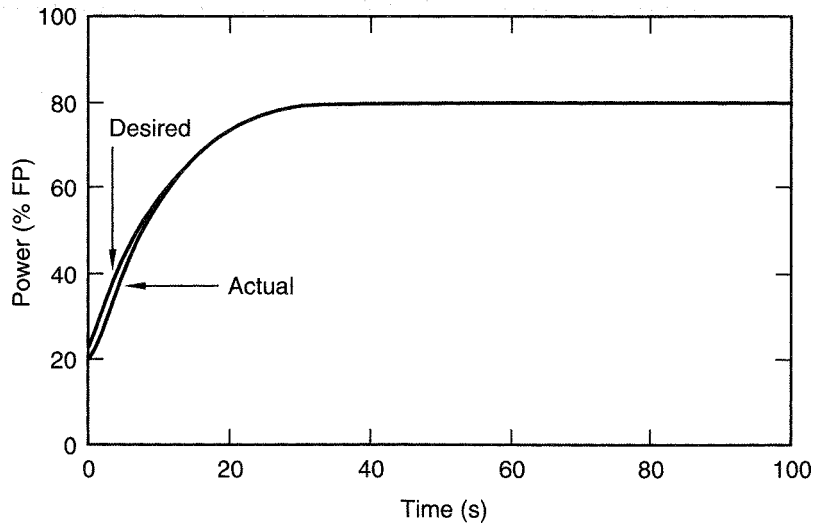

Fig. 8 Tracking control with a fuzzy logic control in response to a six-decade power increase.

power level is attained. As shown in Fig. 9, after a drop in reactor power level the FLC can compensate for the increase in the negative reactivity and bring back the reactor power level to the desired value.

CONCLUSIONS

A control law such as "if the core temperature increases and the reactor power decreases, then withdraw the rod slightly" is a general principle that would be true for many reactors. This introduces the element of universality that carries the advantage that the control rules are better understood by the operators. Regardless of the mathematical formulation used to describe the system, the control principle will still be true. What differs is the quantification of the linguistic measures of "increase," "decrease," and "slightly," or in the terminology of FLC, the specification of the membership functions. Further, such a statement is very familiar to reactor operators so

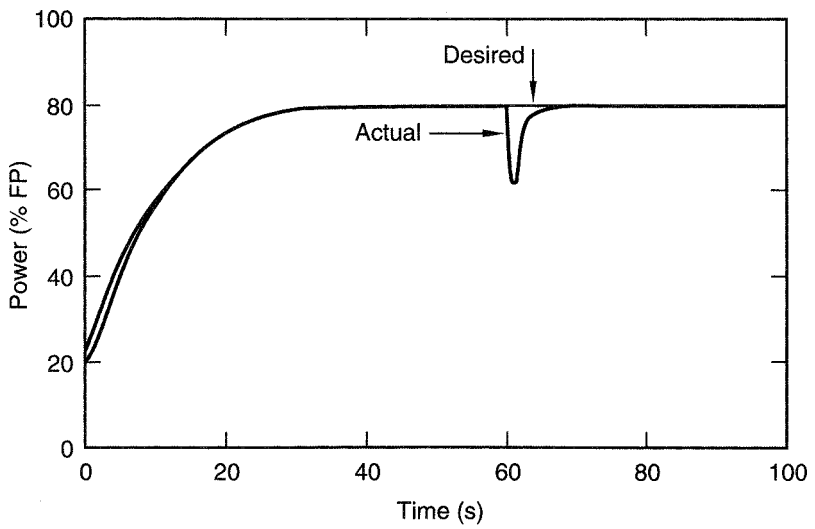

Fig. 9 Reactor response to a disturbance with a fuzzy logic control.

that understanding of the controller behaviors can be almost intuitively anticipated. This helps in controller maintenance, controller troubleshooting, and modifications of controller behavior. The basic tenet of fuzzy logic is to capture these generalities and apply them to specific cases. An FLC transforms information from the linguistic domain to the mathematical domain, operates on it on the basis of a set of prespecified rules, performs the resultant control action, and then transforms the results back to the linguistic domain. These features can provide a powerful tool to capture human knowledge and serve as an effective adviser to human controllers.

REFERENCES

1. C. P. Pappis and E. H. Mamdani, A Fuzzy Logic Controller for a Traffic Junction, *IEEE Trans. Syst., Man, Cybern.*, SMC-7(10): 707-717 (October 1977).
2. L. P. Holmblad and J. J. Ostergaard, Control of a Cement Kiln by Fuzzy Logic, in *Fuzzy Information and Decision Processes*, M. M. Gupta and E. Sanchez (Eds.), North-Holland, Amsterdam, 1982.
3. R. M. Tong, M. B. Beck, and A. Latten, Fuzzy Control of the Activated Sludge Wastewater Treatment Process, *Automatica*, 16(6): 695–701 (November 1980).
4. S. Yasunobu and S. Miyamoto, Automatic Train Operation System by Predictive Fuzzy Control, in *Industrial Applications of Fuzzy Control,* M. Sugeno (Ed.), North-Holland, Amsterdam, 1985.
5. S. Murakami and M. Maeda, Automobile Speed Control System Using a Fuzzy Logic Controller, in *Industrial Applications of Fuzzy Control*, M. Sugeno (Ed.), North-Holland, Amsterdam, 1985.
6. M. Sugeno and K. Murakami, An Experimental Study on Fuzzy Parking Control Using a Model Car, in *Industrial Applications of Fuzzy Control*, M. Sugeno (Ed.), North-Holland, Amsterdam, 1985.
7. Tong, 1977.
8. M. Sugeno, An Introductory Survey of Fuzzy Control, *Info. Sci.*, 36(1–2): 59-83 (August 1985).
9. I. Kliger, Synthesis of an Optimal Nuclear Reactor Control System, in *Neutron Dynamics and Control*, DOE Report CONF-650413, p. 110, U.S. Atomic Energy Commission, 1965.
10. J. J. Roberts and H. P. Smith, Time Optimal Solution to the Reactivity—Xenon Shutdown Problem, in *Neutron Dynamics and Control*, DOE Report CONF-650413, p. 206, U.S. Atomic Energy Commission, 1965.
11. J. L. Melsa, A Closed-Loop, Approximately Time-Optimal Control Method, in *Neutron Dynamics and Control*, DOE Report CONF-650413, p. 207, U.S. Atomic Energy Commission, 1965.
12. R. R. Mohler and C. N. Shen, *Optimal Control of Nuclear Reactors*, Academic Press, New York, 1970.
13. M. Gopal and P. P. Nair, A New Optimal Control Strategy for a Nuclear Boiling Water Reactor, *IEEE Trans. Nucl. Sci.*, NS-32(2): 1180-1189 (April 1985).
14. J. D. Metzger, Development of Model-Reference Adaptive Control with Applications to a Space Nuclear Power System, Doctoral Dissertation, The University of New Mexico, 1989.
15. G. T. Park and G. H. Miley, Application of Adaptive Control to a Nuclear Power Plant, *Nucl. Sci. Eng.*, 94(2): 145-156 (October 1986).
16. A. H. Shoop, S. Silverman, and B. Ramesh, Consolidated Edison System Operation Computer Control System (SOCCS) Alarm Advisor SAA, in *Proceedings of Second Symposium Expert Systems Applications in Power Systems*, pp. 84-88, 1989.
17. R. W. Bijoch, S. H. Harris, and T. L. Volkman, Intelligent Alarm Processor at Northern States Power, in *Proceedings Second Symposium Expert Systems Applications in Power Systems*, pp. 79-83, 1989.
18. M. A. S. Guth, Some Uses and Limitations of Fuzzy Logic in Artificial Intelligence Reasoning for Reactor Control, *Nucl. Eng. Des.*, 113(1): 99-109 (April 1989).
19. R. Uhrig, Artificial Neural Networks in Nuclear Power Plants, *Nucl. News*, 37(9): 38 (1994).
20. R. Uhrig, Use of Neural Networks in Nuclear Power Plants, *ISA Trans.*, 32(2): 139 (July 1993).
21. M. Bubak, J. Moscinski, and J. Jewulski, Fuzzy-Logic Approach to HTR Nuclear Power Plant Model Control, *Ann. Nucl. Energy*, 10(9): 467-471 (1983).
22. J. Bernard, Use of a Rule-Based System for Process Control, *IEEE Control Syst. Mag.*, 3-13 (October 1988).
23. M. Kinoshita, T. Fukuzaki, T. Stoh, and M. Miyake, An Automatic Operation Method for Control Rods in BWR Plants, in *In-Core Instrumentation and Reactor Core Assessment, Proceedings of Specialists' Meeting, Cadarache, France,* pp. 213-220, 1988.
24. S. Terunuma, K. Kishiwada, H. Takahashi, T. Iijima, and H. Hayashi, Application of Fuzzy Algorithms for the Feedwater Control System in Fugen HWR, in *Proceedings of an International Conference on Man–Machine Interface in the Nuclear Industry*, pp. 463-473, 1988.
25. H. L. Akin and V. Altin, Rule-Based Fuzzy Logic Controller for a PWR-Type Nuclear Power Plant, *IEEE Trans. Nucl. Sci.*, 38(2): 883-890 (April 1991).
26. C. C. Kuan, C. Lin, and C. C. Hsu, Fuzzy Logic Control of Steam Generator Water Level in Pressurized Water Reactors, *Nucl. Technol.*, 100(1): 125-134 (October 1992).
27. N. K. Alang-Rashid, Nuclear Reactor Control Using Tunable Fuzzy Logic Controllers, Doctoral Dissertation, The University of New Mexico, 1992.
28. J. Kitowski and M. Bargiel, Diagnostics of Faulty States in Complex Physical Systems Using Fuzzy Relational Equations, in *Approximate Reasoning in Intelligent Systems, Decision and Control*, pp. 175-194, E. Sanchez and L. A. Zadeh (Eds.), Pergamon Press, United Kingdom, 1987.
29. J. A. Hassberger, Simulation-Based Expert System for Nuclear Power Plant Diagnostics, Doctoral Dissertation, University of Michigan, Ann Arbor, Mich., 1986.
30. M. I. Abdelhai and B. R. Upadhyaya, Expert Systems with Fuzzy Logic for Intelligent Diagnosis and Control of Nuclear Power Plants, *Trans. Am. Nucl. Soc.*, 62: 386-388 (1990).
31. R. Sutton and M. J. Parkins, Early Detection of Steam Leaks in Nuclear Plant, in *International Conference on Control '91*, IEEE, London, U.K., 1991.
32. K. E. Holbert, A. S. Heger, and N. K. Alang-Rashid, Redundant Sensor Validation by Using Fuzzy Logic, *Nucl. Sci. Eng.*, 118(1): 54-64 (September 1994).

33. H. Matsuoka, A Simple Fuzzy Simulation Model for Nuclear Reactor System Dynamics, *Nucl. Technol.*, 94(2): 228-241 (May 1991).
34. S. Terunuma et al., 1990.
35. M. Kitamura, T. Baba, M. Takahasi, K. Sugiyama, and T. Washio, Knowledge Acquisition for Diagnosis of Nuclear Power Plant by Qualitative Simulation with Fuzzy Logic, in *Proceedings of the 7th Power Plant Dynamics, Control and Testing Symposium*, Vol. 2, pp. 68.01-68.12, 1989.
36. T. Onisawa and M. Sugeno, An Approach to Failure Analysis Using Fuzzy Unreliability, *Trans. Soc. Instrum. Control Eng.*, 21(8): 835-841 (August 1985).
37. T. Onisawa and Y. Nishiwaki, Fuzzy Human Reliability Analysis of the Chernobyl Accident, *Fuzzy Sets and Systems*, 28(2): 115-127 (November 1988).
38. P. Kuraszkiewicz and P. Derbis, Application of Fuzzy-Sets Methods for Calculating the Reliability of Safety Systems of NPP, in *Proceedings of First International Symposium on Uncertainty Modeling and Analysis*, pp. 382-386, IEEE Computing Society Press, California, 1991.
39. M. H. Chun and K. I. Ahn, Potential Applicability of Fuzzy Set Theory to Analyses Containment Response and Uncertainty for Postulated Severe Accidents, *Trans. Am. Nucl. Soc.*, 64: 398-399 (1991).
40. S. Gencay, Site Selection for Nuclear Plants Using Fuzzy Decision Analysis, *Kerntechnik*, 56(5): 320-327 (October 1991).
41. N. K. Alang-Rashid and A. S. Heger, A Method for Transforming Operators' Skill to Fuzzy Logic Controllers, *Control Theory and Advanced Technology*, 8(3): 513-523 (September 1992).
42. B. Kosko, *Neural Networks and Fuzzy Systems: A Dynamical Approach to Machine Intelligence*, Prentice Hall, New Jersey, 1992.
43. M. Sugeno and T. Yasukawa, A Fuzzy-Logic-Based Approach to Qualitative Modeling, *IEEE Trans. Fuzzy Systems*, 1(1): 7-31 (February 1993).
44. C. C. Lee, Fuzzy Logic in Control Systems: Fuzzy Logic Controller—Part I, *IEEE Trans. Systems, Man, Cybern.*, 20(2): 404-418 (March–April 1990).
45. L. X. Wang and J. M. Mendel, Generating Fuzzy Rules by Learning from Examples, in *1991 IEEE International Symposium on Intelligent Control*, pp. 263-268, 1991.
46. T. Procyk and E. H. Mamdani, A Linguistic Self-Organizing Process Controller, *Automatica*, 15(1): 15-30 (January 1979).
47. M. Galluzo, V. Cappellani, and U. Garofalo, Fuzzy Control of pH Using NAL, *Int. J. Approx. Reasoning*, 5(6): 505-519 (November 1991).
48. T. Yamakawa and M. Furukawa, A Design Algorithm of Membership Functions for A Fuzzy Neuron Using Example-Based Learning, in *IEEE International Conference on Fuzzy Systems*, San Diego, pp. 75-82, IEEE, New York, 1992.
49. H. Nomura, I. Hayashi, and N. Wakami, A Learning Method of Fuzzy Inference Rules by Descent Method, in *IEEE International Conference on Fuzzy Systems*, San Diego, pp. 203-210, IEEE, New York, 1992.

Design Features

Edited by D. B. Trauger

Twenty-Third DOE/NRC Nuclear Air-Cleaning and Treatment Conference

By R. R. Bellamy,[a] J. J. Hayes,[a] and M. W. First[b]

Abstract: *The Twenty-Third Department of Energy/Nuclear Regulatory Commission (DOE/NRC) Nuclear Air-Cleaning and Treatment Conference was held July 25–28, 1994, in Buffalo, New York. The conference was also sponsored by the Harvard Air-Cleaning Laboratory and the International Society of Nuclear Air Treatment Technologies, a nonprofit organization founded to promote technology transfer in the nuclear air-cleaning and treatment area. A total of 192 air-cleaning specialists attended the conference. The United States and 11 foreign countries were represented. The specialists are affiliated with all aspects of the nuclear industry, including government agencies, educational institutions, utilities, architect–engineers, equipment suppliers, and consultants. The high level of international interest is evident from the 40% of papers sponsored by foreign interests. More than 20% of the attendees as well as several members of the Program Committee were from outside the United States. Major topics discussed at this conference included nuclear air-cleaning codes and standards, waste disposal, particulate filter developments (including testing and performance under stress and after aging), sampling and monitoring of process and effluent streams, off-gasses from fuel reprocessing, adsorbents and adsorption, accident control and analysis, and revised source terms for power-plant accidents. A highlight of the conference concerned operations at the DOE facility at West Valley, New York, where construction is under way to solidify radioactive waste. A recurrent theme throughout the sessions was that, in spite of the large number of guidance documents available in the form of regulations, codes, standards, and directives, multiple difficulties arise when all are invoked simultaneously. Gas processing needs, rather than controls for civilian power plants, will provide the principal challenge during the next decade for the air-cleaning specialists of the world.*

The opening plenary session began with a presentation by Dr. M. W. First, Conference Program Committee Chairman, on the history of the Air-Cleaning Conference as an outgrowth as an Atomic Energy Commission (AEC) working group in 1948, to the first meeting in 1951, and the evolution of the conferences over the years.

The keynote address of the opening session was delivered by Admiral R. J. Guimond, Principal Deputy Assistant Secretary, Environmental Management, U.S. Department of Energy (DOE). Admiral Guimond discussed the challenges DOE faces in their environmental cleanup activities at existing and former DOE facilities. Cleanups require the integration of technology with social concerns and call for interactions between DOE and community groups that have a vested interest in the activities. Effective restoration requires that neither worker nor environmental exposure increase and that it avoid creating worse problems than those being solved. Admiral Guimond closed by contrasting the entrepreneur's and bureaucrat's approach to solving problems.

The session concluded with two presentations on the West Valley Demonstration Project established by an Act of Congress for the purpose of developing solidification techniques that can be used for preparing high-level radioactive waste for permanent disposal. The Act directed DOE to (1) develop containers suitable for permanent disposal of the high-level waste, (2) transport the solidified high-level waste to a Federal repository,

[a]Nuclear Regulatory Commission.
[b]Harvard Air-Cleaning Laboratory.

(3) dispose of low-level and transuranic waste produced under the project, and (4) decontaminate and decommission the facilities and materials associated with project activities and the storage tanks originally used to store the liquid high-level radioactive waste. Mr. R. E. Lawrence, West Valley Nuclear Services Company, provided an overview of the current status of the demonstration project: construction is 95% complete; testing began in April 1993. A Safety Analysis Report was submitted to DOE, and Readiness Review activities have begun. Pretreatment activities are scheduled for completion in early 1995. The life of the facility will be 10 years with the period of active operation anticipated to be 30 months. Mr. R. F. Vance, West Valley Nuclear Services Company, described the off-gas treatment systems for the integrated melter. Components include a submerged gas scrubber, mist eliminator, High Efficiency Particulate Air (HEPA) filter, and an NO_x abatement system. He discussed the operating characteristics that were anticipated before testing, the actual characteristics determined from testing, and the design and operational changes initiated to address the problems identified during the testing phase.

STANDARDS: INDIVIDUAL PAPERS AND A PANEL SESSION

The difficulty in adhering to all the provisions of mandatory codes and standards when dealing with ventilation and air-cleaning systems that were neither designed nor constructed according to their provisions was frequently expressed at this session. One paper discussed the challenges of using today's standards to qualify a Class 1E motor now that few companies are qualifying equipment for the nuclear power industry. The author detailed the problems encountered by utilities when using commercial dedication, motor repair, or expedited test methods to qualify equipment.

A second paper presented the results of site acceptance testing of an airborne activity confinement system (AACS) for the K-Reactor at the Savannah River Site. The AACS filter compartments were replaced with seismically qualified compartments designed and constructed to American Society of Mechanical Engineers (ASME) Code AG-1 and ASME Standard N509 specifications and tested according to ASME Standard N510. Manifold qualification testing ambiguities called for an inquiry to the ASME Committee on Nuclear Air and Gas Treatment (CONAGT) to provide a code interpretation on whether artificial leak sites need to be introduced only at the HEPA filter to satisfy Appendix D of ASME N509 or whether artificial leak paths need to be created, one at a time, for both the HEPA filter and the absorber bank. In question was whether adequate mixing would be achieved downstream of the absorber bed. To the Savannah River personnel, the Appendix D methodology seemed inadequate to demonstrate manifold acceptability. Although the reply from the CONAGT committee indicated that artificial leaks needed to be introduced only at the filter bank, Savannah River's tests demonstrated that the filter bank alone may be adequate to demonstrate the adequacy of a sampling manifold for detecting absorber bypass. A test program was initiated to retest the sampling manifold, but project funding was canceled because of DOE's decision to place the K-reactor in a standby condition.

In another paper, a self-contained high-efficiency particulate air filter (SCHEPA), a HEPA filter in a casing with end caps and pipe nipples used at the Hanford Site and elsewhere, was evaluated for compliance with the provisions of ASME N509, ASME N510, ERDA 76-21,[a] MIL-F-51068F,[b] NFPA[c] 90A, and NFPA 91. The SCHEPA failed to meet all the design, fabrication, testing, and documentation requirements of ASME N509, ASME 510, and NFPA. It was concluded that SCHEPA filters do not comply fully with DOE directives and should not be used. Other types of HEPA filters are available for substitution.

The final paper of this session compared the results of laboratory testing of charcoal when using the 1989 ASTM[d] D3803 test protocol relative to other test protocols contained in some nuclear power plant's Technical Specifications (TS). For engineered safety feature (ESF) ventilation systems in fuel-handling areas, first-time use of the 1989 protocol frequently resulted in an absorber efficiency reading of less than 90% and a call for charcoal replacement. However, an absorber efficiency of more than 90% is considered to be a reasonable acceptance criterion when testing carbon at a temperature of 30 °C and a relative humidity (RH) of 95%. When this

[a]ERDA was the Energy Research and Development Administration, which is currently part of DOE.

[b]MIL Specs are Military Specifications published by the Department of Defense (DOD).

[c]NFPA Standards are published by the National Fire Protection Agency (NFPA).

[d]ASTM Standards are published by the American Society for Testing and Materials (ASTM).

same test is conducted at a relative humidity of 70%, rather than 95%, an efficiency of more than 99% can be expected. The author recommended that all spent-fuel pool systems be tested with the use of the 1989 version of ASTM D3803 at an RH based on the presence or absence of heaters. The author concluded that a 2-in.-deep bed of carbon in a control room ESF system would have a difficult time meeting the existing testing requirements of 99% removal efficiency if the 1989 standard is used. A more reasonable efficiency would be 95%, but that would require lowering the assigned efficiencies in the safety analysis for the facility. At 70% RH, an efficiency of more than 99% could be expected for 2-in.-deep beds in control room systems. It was recommended that facilities now using high-temperature testing of control room system carbon should change to a 30 °C test at the RH called for by the 1989 Standard.

A panel discussion on Codes and Standards focused on their application to DOE facilities. Existing codes and standards offer these advantages: (1) they have withstood the test of time; (2) they have a certain reasonableness from both technical and cost standpoints; (3) they have been subjected to public review and frequent use; and (4) they provide cost savings from the use of "standard" components, design, protocols, and testing. Difficulties encountered in the use of the codes and standards include (1) limitation in scope, (2) misapplication, and (3) compliance without understanding. It was emphasized that, although the technology needs to be further developed and standardized before codes and standards can be developed, few nuclear applications are unique, and most technical problems have been solved. Therefore existing codes and standards should always be used as technical guides even when the situation does not fit the exact condition for which the codes and standards were written (i.e., regulatory agencies should not insist on blind adherence). Codes and standards from other industries should be used after modification for nuclear application. New codes and standards are needed to cover long-term operation and operation associated with gas processing [as distinguished from the engineered safety feature (ESF) air-cleaning systems used in nuclear power plant accident control].

A review of DOE facilities showed that filter testing is adequate at all facilities except for the Portsmouth Gaseous Diffusion Plant, but a single standard for in-place testing of HEPA filters at these locations is considered inappropriate. At DOE facilities the application of ASME N509 and N510 may present hazards (e.g., ASME N509 states that heaters shall be electric, but the tank farm complex at Hanford has tanks containing hydrogen). This results in a system that is unsafe, whereas a steam heater would be intrinsically safe. It was recommended that DOE develop a clear statement of expectations for in-place testing that is flexible enough to meet the needs and constraints of all systems.

The panel concluded that a waiver could be requested if, at the start of a project, it was recognized that portions of mandatory codes and standards would not produce the intended results.

NUCLEAR WASTE SESSION

The technical and associated regulatory requirements for the storage and disposal of radioactive wastes were discussed in this session. In a joint project between the Harvard School of Public Health and Massachusetts Institute of Technology, atmospheric releases from a near-grade bunkered low-level waste disposal facility are being modeled. Isotopes of concern are C-14 (the largest component), H-3, I-129, K-85, and Ra-222. Mathematical models are being developed to evaluate natural convection cooling for the heat released during radioactive decay from storage canisters. The models show that natural air convection cooling will suffice to maintain adequate temperatures for stored glass-vitrified wastes and the concrete structures that contain them.

Numerical guidelines for the design of storage facilities at nuclear power plants include: (1) a member of the public should receive less than 1 mrem/yr (10 Sv/yr) from this source; (2) an inadvertent intruder should receive less than 5 mrem/visit (50 Sv/visit); and (3) when the site is released from regulatory control, recycling of the disposed material should result in exposures of less than 1 mrem/yr (10 Sv/yr), calculated as of the time the site is released. Further, the dose from disposal in a sanitary landfill (including any recycling calculated at the time of disposal) should result in doses less than 5 mrem/yr (50 Sv/yr) to any individual.

FILTERS AND FILTRATION SESSION

The U.S. DOE is conducting a complete review of its HEPA filter program to identify areas for improvement. The review encompasses choice of filter materials, manufacturing techniques, applications, acceptance tests, research, and system design. Several areas of concern

have been identified: (1) deterioration from aging and identification of an acceptable service life span for HEPA filters, (2) whether items on a Qualified Products List require further testing, (3) selecting substitutes for di-octyl phthalate (DOP) for in-place testing, (4) a need for consistent guidance to estimate efficiencies of aged filters during accidents, and (5) filter specifications for portable cleaning units and vacuum cleaners. It is anticipated that results of the DOE program will influence other national and international air-cleaning programs.

Work at the University of Southampton in England, previously reported at the Twenty-First Air-Cleaning Conference, has continued on the structure and properties of permanent magnetic filters for radioactive materials. The principle involved is "assisted capture" to retain fine particles more efficiently. Because the targeted material (e.g., $Pu–O_2$) is paramagnetic, no external magnet or power is required. The filter consists of a stack of expanded ferromagnetic metal mash with the aid of a demagnetizing cycle; a small prototype filter is estimated to be able to collect 485 g over 38 years.

Developmental work is being done in England to improve the dust-holding capacity of more conventional HEPA filter media. Two grades under development that use very fine fibers supported on a layer of coarser fibers have shown improved dust holding, but penetration results are not yet acceptable. Graded density papers show promise but need further development. At the Lawrence Livermore National Laboratory, steel fiber filters are being developed and evaluated. Preliminary field results show improved performance in wet environments. Additional field trials are planned. In France, an experimental device has been designed to measure pressure drop across metal filters as a function of dust mass loading. It shows a linear relationship for nonhygroscopic aerosol particles and for hygroscopic aerosol particles when humidities are below the deliquescent point. Above this point, filters become completely clogged for this class of particles.

EFFLUENT AIR STEAMS—MONITORING AND SAMPLING: A PANEL DISCUSSION AND INDIVIDUAL PAPERS

A panel discussion on aerosol sampling focused on a requirement of 40 CFR 61, Subpart H, "National Emission Standards for Hazardous Air Pollutants," that stacks having a potential to emit 1 Sv/yr (0.1 mrem/yr) to the maximally exposed individual must have continuous monitoring. The panel included representatives of the U.S. Environmental Protection Agency (EPA), the ANSI[a] N13.1 Committee, and DOE.

The requirements of the EPA Method 1 were compared with the guidance on sampling points and probe design in ANSI N13.1. An alternative test method, to be used when it is impractical to use ANSI N13.1 because of a potential for underestimating emissions, was discussed along with a need to obtain EPA approval. Three alternatives were discussed: single point sampling; a shrouded, single point sampler; and a computer code to estimate deposition losses. Additional research was recommended on nozzle design and estimation of particle loss in turbulent flow.

The EPA representative stated that the most prevalent problem with an applicant's proposal to use alternative sampling methods is a lack of adequate detail and confirmatory data. He advised applicants to read the requirements carefully, answer all questions, and seek an independent review of the application to ensure that it is complete.

The Chairman of the ANSI N13.1 Committee discussed progress in its revision that will emphasize performance verification rather than the use of look-alike designs. The proposed major changes include (1) omitting workplace and environmental sampling, (2) removing prescriptive and rule-of-thumb guidelines, (3) establishing performance-based criteria (with some set by the user), and (4) focusing sampling requirements on compliance.

Individual papers on 40 CFR 61, Part H, in the session on effluent stack monitoring discussed (1) the development of a real-time stack monitoring system and dose projection program for the Hi-Flux Beam Reactor at Brookhaven National Laboratory and (2) an in-situ measurement method developed for the Hanford Site that uses a portable, low-resolution gamma spectroscope to measure radiation emanating from HEPA filters. The method was developed to estimate the potential unabated dose to the offsite theoretical maximally exposed individual from empirical data rather than from theoretical models. EPA approved use of the method after it was tested and verified. The spectroscope does not measure beta and alpha activity, however, and cannot be applied to unique geometries.

The final paper, from the University of Toronto, on loss of iodine labeled with I-131 in type 316 stainless

[a]ANSI Standards are published by the American National Standards Institute (ANSI).

steel sample lines indicated that deposition depended on such initial surface conditions as the degree and type of oxidation. Pretreatment with nitric acid reduced retention, as did electropolishing. The authors concluded that extensive loss of gaseous elemental iodine would likely occur in the lines leading to the postaccident release monitoring system and that corrections would be unreliable given the complexity of the phenomena involved.

GAS PROCESSING: A PANEL SESSION

This panel included equipment suppliers, representatives from national laboratories, and consultants. Most of the work to date has been on standardization for nuclear applications for power reactors, and more specifically for engineered-safety-feature systems for light-water reactors for gas processing at DOE installations. There are different parameters of importance for gas processing (e.g., temperature, pressure, flow rate, moisture content, corrosive contaminants, radioactive material loads, and efficiency criteria). Guidance is needed on the application of all the components that will be needed for processing gas from equipment such as melters, scrubbers, and absorption columns. Guidance is also needed on how to integrate these components into a well-functioning system as well as for conducting in-place testing of highly contaminated components during decontamination, decommissioning, and disposal. Panel members recommended that new standards be broadly written to permit exercise of engineering judgment and that they be made available as soon as possible.

ADSORPTION

The papers in this session concerned residence time determinations for absorber beds and halide test agent replacements. Residence time differences of about 10% are seen when the calculations, based on ASME AG-1 Code Section FC, use the air volume/carbon volume ratio or the average screen area instead of the smallest screen area. The author concludes that AG-1 should be revised to avoid favoring any particular Type II adsorbent bed design. Chlorofluorocarbons (CFCs), widely used for absorber in-place leak testing, are being phased out, and replacement compounds must be selected that satisfy the following parameters: (1) have similar retention times on activated carbons as CFCs R-11, R-12, R-112, or R-112a; (2) have similar lower detection limit sensitivity; (3) give the same in-place leak-test results; (4) have chemical and radiological stability; (5) cause no degradation of the carbon; and (6) are listed by the EPA as acceptable for commercial use. The most promising compounds evaluated to date are HCFC-123 (a chlorofluorohydrocarbon), 1-bromobutane, bromochloromethane, and chloromethane, but additional work is needed to verify the suitability of these compounds.

PROCESSING AND FUEL REPROCESSING

Because of the lack of U.S. involvement in fuel reprocessing, all papers presented in this session represented foreign interests. Experimental work continues in Japan on iodine expulsion from spent-fuel solutions and its capture by silver-impregnated alumina. The amount of iodine in off-gas streams depends on the nitrous acid concentration that forms from NO_x (generated during spent-fuel dissolution). Iodine is released as the result of (1) oxidation of I to I_2 by nitric acid, (2) oxidation of I_2 by nitrous acid, and (3) formation of colloidal AgI or PdI_2. After the release from solution, two different pore sizes of silver-impregnated alumina are being examined as adsorbents to prevent iodine from reaching the environment. They have excellent removal capability at all humidities [decontamination factor (DF) of 100]. Alumina with 24 wt % silver reduces waste volume.

England is completing construction of its third reprocessing plant, entitled THORP (Thermal Oxide Reprocessing Plant), at its Sellafield site. It is designed to process irradiated fuel from gas-cooled and light-water-cooled reactors. Species of concern for the air treatment system are I-129, C-14, nitrogen oxides, and plutonium and mixed fission-product dust particles from fuel. The system consists of adsorption columns, electrostatic precipitators, dehumidifiers, and HEPA filters designed to process a number of separate off-gas streams. Operational data are limited, but it is expected that emissions from a 125-m stack will ensure that the most highly exposed individual will be below the present limit of 50/μSv committed effective dose equivalent.

Two papers were concerned with treatment of off-gasses from facilities engaged in fusion research in Germany. Construction of a new tritium laboratory at Karlsruhe is complete. The emission control equipment consists of an oxidizing catalyst (for conversion of gaseous tritium or tritiated hydrocarbons to water), heat exchangers, and molecular sieve beds (for water adsorption). Tests show that the reduction in tritium

concentration is independent of catalyst temperature but heavily dependent on gas flow rate; adjustment of these parameters results in a tritium decontamination factor greater than 3000. In Italy, a conceptual study is under way on the tritium inventory and maximum credible accidental dose to the maximally exposed individual from the operation of a tokamak (toroidal magnetic chamber) fusion plant. Exhaust gas is pumped by cryogenic vacuum pumps to an atmospheric decontamination system containing catalytic oxidizers, recombiners, dryers, and molecular sieve absorbers.

AIR TREATMENT SYSTEMS AND ACCIDENT CONTROL

The focus at this session was on the operation of air treatment systems, both component parts and complete systems. Foreign participation was high. In the United Kingdom, a novel glovebox ventilation system was designed to satisfy two deficiencies in existing systems: the only moving part, an exhaust fan, maintains constant exit velocity, and no instrumentation is required. Design exit velocity is achieved in 0.2 second, and containment can be maintained under breach conditions.

Papers from China and Belgium discussed national air-cleaning philosophies. For the 300-MW(e) Qinshan pressurized-water reactor (PWR) in China, 3 years of operation have shown satisfactory operation of the air-cleaning systems. All U.S. design specifications and in-place testing criteria were used except for the use of concrete housings, which were found to be acceptable when sealed. The Chinese experienced no difficulty with airflow distribution upstream of HEPA filters when using different arrangements of inlet and outlet ducts. Belgium generates 60% of its electricity from seven nuclear power plants and believes that they have developed a high level of technical expertise and experience in the air-cleaning area, as evidenced by smooth operation of their reactor ventilation and off-gas treatment systems plus the PAMELA vitrification plant. PAMELA uses a jet scrubber with a cyclone chamber plus three dry stages that contribute to an overall DF of 10^{11}.

The French have improved the ventilation network SIMEVENT computer code to integrate the consequences of fire and mass transfer (gases and aerosols). It now includes gas flow rate, pressure, and temperatures at critical points in the system, which makes it possible to predict undesirable effects. Particularly useful applications are the ability to determine the effect of manipulating ventilation controls (e.g., opening or closing fire dampers) and the ability to maintain confinement. Experimental work continues at Karlsruhe on a low-pressure-drop passive air-cleaning system to dissipate decay heat after a severe accident.

Stainless steel fiber filters and 10-cm-deep adsorbent beds (molecular sieves give the lowest pressure drop) are promising; they have low resistance and give a DF of 10^3 for each component.

A new generation of nuclear generating stations and their air-cleaning systems was presented in a look at the future. The AP600 is a standardized PWR of 600 MW(e) with passive safety features that uses one multifunctional air-cleaning system to achieve greater simplicity, standardization, and a lower cost design. Studies were conducted to ensure that effluent releases and onsite worker exposures would satisfy regulatory requirements. A dual train purge system containing prefilters, HEPA filters, carbon absorbers, and downstream HEPA filters with a capacity of 4000 cfm (1.9 m^3/s) per train was shown to be adequate for the containment and auxiliary buildings and the fuel-handling area exhaust streams.

The final paper in this session discussed damper leak testing. Sulfur hexafluoride, nontoxic, nonreactive, and easily detected in minute quantities by electron-capture gas chromatography, is used as a tracer gas. Four installed bubble-tight dampers at Zion Nuclear Plant in Illinois were tested by this method. Three showed 0.01 to 0.03 cfm (5 to 15 cm^3/s) leakage [two dampers were 1.5 by 1.5 ft (46 by 46 cm) and the third 6 by 6 ft (1.8 by 1.8 m)]. A fourth damper, 4 by 6 ft (1.2 by 1.8 m), which exhibited 21 cfm (0.01 m^3/s) leakage initially, was reduced to 3.8 cfm (0.0018 m^3/s) after adjusting the damper actuator throw and regasketing the blade seats.

SOURCE TERMS AND ACCIDENT ANALYSIS

The NRC is continuing its work on the revised accident source term it published for comment in July 1992. It was discussed at the Twenty-Second Air-Cleaning Conference. It seeks to integrate time of release into the source term by considering the early in-vessel, early ex-vessel, and late in-vessel gap release phases. Publication of a final source term is anticipated in 1994 and will be used for future plants. Existing plants may choose to evaluate the impact of the revised source term on their operations.

In Germany, accident management measures are considered to be a fourth level of safety in their defense-

in-depth concept. Emphasis is placed on offsite emergency planning and plant internal accident management philosophy. There are two accident alert levels: early-warning disaster alert and disaster alert. Work is in progress to develop specific criteria to facilitate decision making.

Two papers discussed subsets of an accident source term. The NAVAHYGROS code is being used to calculate aerosol behavior inside containments, and French researchers are involved in analyzing particle deposition in sampling ducts for various flow regimes to minimize measurement errors.

AGING EFFECTS ON AIR-CLEANING COMPONENTS

The first paper in this session, a part of NRC's Aging Research Program, examined aging effects on HEPA filters and carbon absorbers. It reviewed records of failure-to-identify-stressors aging effects and methods used for surveillance. It was concluded that aging stressors include heat, radiation, volatile solvents, and normal concentrations of atmospheric aerosol particles and gases. Although current inspection, surveillance, and monitoring methods are adequate to detect ruptures and tears, neither pressure drop monitoring nor surveillance leak testing of installed HEPA filters provides indications of aging in terms of reduced filter media strength. Even though aged, intact filters may function adequately under normal conditions, they could fail under accident conditions. The assessment revealed the need for an improved definition of accident stressors as well as additional information on deterioration processes to make possible an evaluation of the performance of aged components under adverse conditions.

A second paper discussed a method of estimating the residual efficiency of aged HEPA filters during and after a design-basis accident. It uses a step-by-step evaluation procedure based on age, temperature, pressure, moisture, and structural damage to assess the filter efficiency on a case-by-case basis.

A third paper described how filter qualification tests were used to evaluate the strength of HEPA filters that had been stored up to 18 years. Tensile strength of the media decreased with age, but the data were insufficient to establish a useful shelf life. Thermogravimetric analyses demonstrated that one manufacturer's paper had low tensile strength because of insufficient binder. When new filter-heated air and overpressure qualification tests were conducted on old filters, they showed that filter age was not the only factor affecting filter performance; materials used and the construction design have a greater influence. An unexpected finding was that substandard HEPA filters have been installed in DOE facilities despite existing regulations and mandatory filter qualification testing. These findings led the authors to recommend that DOE initiate a more vigorous filter qualification program and that additional studies be performed. They should include all the filter components (i.e., gaskets, frames, and sealants in addition to the media) plus the simulation of tornado pulses and smoke plugging.

A final paper presented information to show that some types of welding fumes have little or no effect on carbon absorber efficiency when exposure is short term and loadings are light. The processes studied were shielded metal arc welding, flux cored arc welding, gas tungsten arc welding, and gas metal arc welding. The air-cleaning unit contained prefilters, upstream and downstream HEPA filters, and a carbon absorber section.

WORKING LUNCHEON—CLEAN AIR AND CLEAR RESPONSIBILITY

Dr. Kenneth C. Rogers, in his second 5-year term as an NRC Commissioner, was the featured speaker. He stated that NRC's regulatory approach governing radiation protection is based on the principles of justification, optimization, and limitation but that he was going to focus on a discussion of optimization, expressed as the ALARA principle, "as low as reasonably achievable." NRC believes it is appropriate to set dose design objectives and then require each licensee to make reasonable efforts to maintain doses as far below these objectives as is practical for them. He maintained that where a specific dose limit is mandated licensees will meet that limit but will take no further mitigating steps. The ALARA approach has been effective; a study of 367 randomly chosen NRC licensees showed that all satisfied a 10-mrem/yr (100 Sv/yr) dose design objective based on calculations using industry accepted codes. Seven calculated doses were between 1 and 10 mrem/yr (10 and 100 Sv/yr, respectively), the highest being 8 mrem/yr (80 Sv/yr). The remaining 360 (out of 367) were below 1 mrem/yr (10 Sv/yr). Dr. Rogers concluded that application of the ALARA principle was a major factor in maintaining dose projections an order of magnitude lower than the 10-mrem/yr design objective for all but a handful of licensees.

Dr. Rogers also discussed the dual regulatory regime implemented by NRC and EPA. Radioactive emissions are regulated by both agencies, but where potential conflicts exist, a 1990 Clean Air Act amendment allows EPA to rescind its own authority. Both agencies are working slowly toward its implementation so that the regulated community need only interface with a single federal regulatory agency with a single set of consistent requirements and one set of inspectors.

OPEN END

One of the traditions of air-cleaning conferences is the presentation of short summaries of ongoing work. This session included a discussion of using bar codes on field samples to track custody, analysis, data logging, and calculation of results; a French computer code, ESCADRE, for looking at aerosol particle removal by containment spray systems; degradation of HEPA filters from exposure to dimethyl sulfoxide used as a solvent during dismantling of a nuclear weapons plant; and retrofitting filter plenums to add injection and sampling manifolds for in-place testing. Full reports on these topics are expected at the next Air-Cleaning Conference.

FILTER TESTING

Three papers were presented in this session; two papers concerned replacements for the suspected human carcinogen, di-octyl phthalate (DOP), widely used as a filter test agent. EMORY 3002 had been selected previously by the Edgewood Research Staff (Aberdeen, Md.) (reported at the Twenty-Second Air-Cleaning Conference) for quality assurance testing of personnel filter canisters. Since then they have evaluated EMORY-3004 and EMORY-3006. EMORY compounds are synthetic lubricants of the poly-alpha olefin class that have been approved for this use by the Army's Office of the Surgeon General. Properties of the EMORY compounds and filter testing results duplicate those of DOP. Edgewood recommends EMORY 3002 only for cold dispersion because its flash point is close to the temperature of hot machines. EMORY 3004 may be used in hot monodisperse aerosol generators for bench testing as well as for polydisperse testing. EMORY 3006 can be used in polydisperse aerosol generators used for in-place HEPA filter testing.

The third paper in this session was a review of in-place HEPA filter testing practices at DOE facilities. It was prepared by members of the Lawrence Livermore National Laboratory. Items of concern include (1) selection of representative inspection and sampling locations, (2) adequacy of the challenge aerosol concentration, (3) photometer operation, (4) testing of multiple-phase systems, and (5) lapses of technical support for in-place testing caused by conflicting administrative–organizational–management priorities. A specific recommendation for improvement was to cooperate with the development and refinement of ASME Code AG-1.

VENTILATION FOR DECOMMISSIONING AND DISMANTLING OPERATIONS

In July 1989, production was discontinued at the DOE-owned Fernald site, formerly used for processing uranium metal products for the nation's defense programs. A site-wide Remedial Investigation/Feasibility Study (RI/FS) was completed pursuant to the Comprehensive Environmental Responsibility Compensation and Liability Act (CERCLA) and the Amended Consent Agreement between EPA and DOE. A variety of response actions were identified and brought under one roof as the Fernald Environmental Management Project (FEMP). One of the many response actions in progress is the decontamination and dismantlement (D&D) of Plant One ore silos that were constructed in 1953 for sampling and blending ore concentrates in preparation for refining. From 1955 to 1962, the silos were used for overflow storage of the cold metal oxides, a by-product of ore processing, but have not been used since. The contents were removed except for small amounts of residue. At a panel session, representatives of Fernald Environmental Restoration Management Corporation (FERMCO) and its consultant discussed the design of ventilation and air-cleaning systems and their application for control of radioactive contaminants during D&D operations associated with the silos.

The ventilation system was designed for ease of repair, decontamination, and dismantlement. Sources of radioactivity and methods of control were discussed. They included a description of operations that generate radioactive dust, measured dust concentrations, and job-specific work plans incorporating load restrictions, scaffolding limits, wind speed limits, crane limits, and rigging requirements. Problem areas have been heat, accessibility issues, and wind loading. An "Envoy Program" was established to keep the public informed about the tasks that will be undertaken and the protective measures that have been incorporated in the workplace.

FERMCO believes that such interactions are vital in an environmental project.

COMMENTARY

The Twenty-Third DOE/NRC Air-Cleaning Conference once again provided an excellent opportunity for direct interchange of technical information related to nuclear air cleaning among the world's experts. By means of formal presentations, follow-up questions and answers, informal discussions, and exhibits sponsored by ISNATT, interchanges covering many wide-ranging topics were accomplished in an easy and efficient manner. Interest from countries outside the United States remained high, as evidenced by the large number of attendees and the papers they presented.

This conference was marked by a greater interest in gas-processing activities and a perception that current nuclear air-cleaning regulations, codes, standards, and directives provide inadequate guidance for gas-processing applications, including fuel reprocessing. The need for improvement was presented as the prime challenge facing air-cleaning experts over the next decade. It was emphasized that, when current nuclear guidance documents (written with civilian nuclear power reactors in mind) are invoked, confusion often results. The judgments of experienced engineers must be authorized when site-specific conditions make a word-for-word application of guidance documents dangerous and wasteful. It is anticipated that guidance on an international level can be prepared that will be concise and applicable to both existing and future air-cleaning systems.

Other important themes that were identified include (1) clear recognition that air- and gas-cleaning needs cannot be satisfied by simply installing HEPA filters and carbon absorbers at the end of a pipe; (2) HEPA filters are vulnerable to damage by high temperature, relative humidity, and dust loading, and all these stressors are made worse by aging of the components; and (3) source-term definition is near completion for power reactors, but there is urgent need for similar action for decommissioning and dismantlement operations. The magnitude of the effort that will be required to complete all the outstanding waste storage and encapsulation tasks was made evident by the activities being conducted at West Valley, New York.

The proceedings of the Twenty-Third Conference have been published as CONF-940738/NUREG-CP-0141 and are available from the Superintendent of Documents, U.S. Government Printing Office. Summaries of past conferences reported in *Nuclear Safety* are referenced at the end of this report.[1–15] Plans for the Twenty-Fourth Conference, scheduled for the summer of 1996 on the west coast of the United States, are under way and will continue the outstanding tradition of providing a forum for interchange of technical ideas and discussions among international air-cleaning experts, with ISNATT playing an expanding role.

Table 1, a complete listing of the meeting agenda, contains the titles, authors, and organizational sources for all papers.

REFERENCES

1. R. R. Bellamy, D. W. Moeller, and M. W. First, Twenty-Second DOE/NRC Nuclear Air-Cleaning and Treatment Conference, *Nucl. Saf.*, 33(4): 549-561 (October–December 1992).
2. R. R. Bellamy, D. W. Moeller, and M. W. First, Twenty-First DOE/NRC Nuclear Air-Cleaning Conference, *Nucl. Saf.*, 32(1): 80-88 (January–March 1991).
3. R. R. Bellamy, D. W. Moeller, and M. W. First, Twentieth DOE/NRC Nuclear Air-Cleaning Conference, *Nucl. Saf.*, 30(1): 34-45 (January–March 1989).
4. R. R. Bellamy, D. W. Moeller, and M. W. First, Nineteenth DOE/NRC Nuclear Air-Cleaning Conference, *Nucl. Saf.*, 28(3): 350-361 (July–September 1987).
5. R. R. Bellamy, D. W. Moeller, M. W. First, and J. P. Kotra, Eighteenth DOE/NRC Nuclear Air-Cleaning Conference, *Nucl. Saf.*, 26(3): 318-333 (May–June 1985).
6. R. R. Bellamy, D. W. Moeller, and M. W. First, Seventeenth DOE/NRC Nuclear Air-Cleaning Conference, *Nucl. Saf.*, 24(1): 51-65 (January–February 1983).
7. R. R. Bellamy, D. W. Moeller, D. W. Underhill, and M. W. First, Sixteenth DOE/NRC Nuclear Air-Cleaning Conference, *Nucl. Saf.*, 24(1): 347-361 (January–February 1983).
8. R. R. Bellamy, D. W. Moeller, D. W. Underhill, and M. W. First, Fifteenth DOE/NRC Nuclear Air-Cleaning Conference, *Nucl. Saf.*, 20(1): 63-76 (January–February 1979).
9. D. W. Moeller, D. W. Underhill, and M. W. First, The Fourteenth ERDA Air-Cleaning Conference, *Nucl. Saf.*, 18(2): 174-188 (March–April 1977).
10. D. W. Moeller, D. W. Underhill, and M. W. First, The Thirteenth AEC Air-Cleaning Conference, *Nucl. Saf.*, 16(2): 190-203 (March–April 1975).
11. D. W. Moeller and M. W. First, The Twelfth AEC Air-Cleaning Conference, *Nucl. Saf.*, 14(2): 111-119 (March–April 1973).
12. D. W. Moeller, The Eleventh AEC Air-Cleaning Conference, *Nucl. Saf.*, 12(2): 100-109 (March–April 1971).
13. R. E. Adams and R. D. Ackley, The Tenth U.S. Atomic Energy Commission Air Cleaning Conference, *Nucl. Saf.*, 10(4): 324-327 (July–August 1969).
14. R. E. Adams, Eighth AEC Air-Cleaning Conference, *Nucl. Saf.*, 8(3): 238-244 (Spring 1967).
15. R. E. Adams, Eighth AEC Air-Cleaning Conference, *Nucl. Saf.*, 5(3): 250-254 (Spring 1964).

Table 1 Technical Program of the 23rd DOE/NRC Nuclear Air-Cleaning and Treatment Conference[a]

Plenary Session

Chairmen: J. F. Leonard, DOE, and K. Duvall, DOE

Welcome and Objectives of the Conference	M. W. First, Harvard Air Cleaning Laboratory
Keynote Address	R. J. Guimond, DOE
West Valley Demonstration Project Overview	R. E. Lawrence, WVNS
The Integrated Melter Off-Gas Treatment Systems at the West Valley Demonstration Project	R. F. Vance, WVNS

Nuclear Air-Cleaning Codes and Standards Session

Chairmen: R. R. Weidler, Duke Power Company, and J. J. Hayes, NRC

Challenges of Equipment Qualification Using Today's Standards with Emphasis on a Class 1E Motor Program	K. Deaton, Ellis & Watts
Evaluation of the Self-Contained HEPA Filter	T. E. Arndt, Westinghouse Hanford Company
ASME N510 Test Results for Savannah River Site AACS Filter Compartments	J. D. Paul and T. M. Punch, WSRC
An Evaluation of Efforts by Nuclear Power Plants to Use ASTM D3803-89	W. P. Freeman, NCS

Nuclear Waste

Chairmen: R. Porco, Ellis & Watts, and W. Bergman, LLNL

Generation and Release of Radioactive Gases in LLW Disposal Facilities	M. S. Yim and S. A. Simpson, MIT
Numerical Analysis of a Natural Convection Cooling System for Radioactive Canisters Storage	R. J. Tsal, S. Anwar, and M. G. Mercado, Fluor Daniel, Inc.
Disposal of Slightly Contaminated Radioactive Wastes from Nuclear Power Plants	J. L. Minns, NRC

Filters and Filtration

Chairmen: H. Gilbert, Consultant, and R. G. Dorman, Consultant

HEPA Filter Concerns—An Overview	J. F. Leonard, DOE
A Novel Permanently Magnetized High Gradient Magnetic Filter Using Assisted Capture for Fine Particles	J. H. P. Watson, Institute of Cryogenics, England
Improving the Dust Holding Capacity of HEPA Filters	J. Dyment, Atomic Weapons Establishment, England; C. Hamblin, AEA Technology, England
Effect of Humidity on the Filter Pressure Drop	J. Vendel and P. Letourneau, ISPN
Preliminary Field Evaluation of a High Efficiency Steel Filter	W. Bergman, G. Larsen, R. Lopez, and K. Wilson, LLNL; K. Simon and L. Frye, MMES

Effluent Stack Monitoring

Chairmen: J. J. Hayes, NRC, and J. D. Paul, WSRC

A Real-Time Stack Radioactivity Monitoring System and Dose Projection Program	A. P. Hull and P. A. Michael, BNL; H. J. Bernstein
Potential Radionuclide Emissions from Stacks on the Hanford Site, Part II: Dose Assessment Methodology Using Gamma Spectrometry	J. M. Barnett, Westinghouse Hanford Company
The Retention of Iodine in Stainless Steel Sample Lines	G. J. Evans and C. Deir, University of Toronto; J. M. Ball, Whiteshell Laboratories, Canada

(Table continues on the next page.)

Table 1 (Continued)

Adsorption

Chairmen: P. Sigli, Camfil, and J. L. Kovach, NCS

Residence Time Determinations for Adsorbent Beds of Different Configurations	J. E. Otermat, W. O. Wikoff, and J. L. Kovach, NUCON International, Inc.
Halide Test Agent Replacement Suitability Study	E. M. Banks, W. P. Freeman, B. J. Kovach, R. R. Sommer, and J. L. Kovach, NUCON International, Inc.

Processing and Fuel Reprocessing

Chairmen: J. G. Wilhelm, Bundesministerium fur Umwelt, Germany, and M. Kikuchi, Hitachi Energy Research Laboratory, Ltd., Japan

A Study on the Expulsion of Iodine from Spent-Fuel Solutions	T. Sakurai, A. Takahashi, N. Ishikawa, Y. Komaki, M. Ohnuki, and K. Kato, JAERI
The Development and Design of the Off-Gas Treatment System for the Thermal Oxide Reprocessing Plant (THORP) at Sellafield	P. I. Hudson, C. P. Buckley, and W. W. Miller, BNFL
Development of Silver Impregnated Alumina for Iodine Separation from Off-Gas Streams	M. Kikuchi, T. Fukasawa, K. Funabashi, and F. Kawamura, Energy Research Laboratory, Hitachi; Y. Kondo, Hitachi Works, Japan
Treatment of Tritiated Exhaust Gases at the Tritium Laboratory Karlsruhe	E. Hutter and U. Besserer, KfK; G. Jacqmin, NUKEM GmbH
Review of the Air Cleaning Systems in a Nuclear Fusion Facility and Consideration About Their Safety Significance	A. Boschi, ENEA; T. Palma and G. Sgalambro, ENEA-DISP, Italy

Air Treatment Systems and Accident Control

Chairmen: R. D. Porco, Ellis & Watts, W. R. A. Goossens, PEGO bvba, Belgium, and X. Chen, Shanghai Nuclear Engineering Research & Design Institute, People's Republic of China

Value-Impact Assessment for Resolution of Generic Safety Issue 143—Availability of HVAC and Chilled Water Systems	P. M. Daling, J. E. Marler, T. V. Vo, H. K. Phan, and J. R. Friley, PNL; V. T. Leung, NRC
Leak Testing of Bubble Tight Dampers Using Tracer Gas Techniques	P. L. Lagus, Ph.D., CIH; J. H. Brown, Lagus Applied Technology, Inc.; L. J. Dubois, Commonwealth Edison; K. M. Fleming, NCS
Constant Depression Fan System: A Novel Glovebox Ventilation System	W. V. Milliner, Atomic Weapons Establishment plc, England
Calculation Code Evaluating the Confinement of a Nuclear Facility in Case of Fires	J. C. Laborde, C. Prevost, and J. Vendel, ISPN; G. Perrin, Services Techniques, COGEMA; J. L. Peirano and S. Raboin, Services Calculs Scientifiques SGN, France
Performance of HEPA Filters at LLNL Following the 1980 and 1989 Earthquakes	W. Bergman and J. Elliot, LLNL
The Actual Practice of Air Cleaning in Belgian Nuclear Facilities	W. R. A. Goossens, PEGO bvba, Belgium
An Introduction to the Design, Commissioning and Operation of Nuclear Air Cleaning System for Qinshan Nuclear Power Plant	X. Chen, J. Qu, and M. Shi, Shanghai Nuclear Engineering Research and Design Institute, People's Republic of China
AP600 Containment Purge Radiological Analysis	M. O'Connor, J. Schulz, C. Tan, and M. Kasjaka, Bechtel Power Corporation; N. Alper, Westinghouse Electric Corporation
A Low Pressure Filter System for New Containment Concepts	H. G. Dillmann and H. Pasler, Laboratorium für Isotopentechnik, KfK

Table 1 (Continued)

Source Terms and Accident Analysis

Chairman: R. R. Bellamy, NRC, and R. Zavadoski, DNFSB

Revised Accident Source Terms for Light-Water Reactors	L. Soffer, NRC
Potential Radionuclide Emissions from Stacks on the Hanford Site, Part I: Dose Assessment	W. E. Davis and J. M. Barnett, Westinghouse Hanford Company
The Link Between Off-Site-Emergency Planning and Plant-Internal Accident Management	H. Braun, Bundesministerium für Umwelt, Naturschutz and Reaktorsicherheit; R. Görtz, Bundesamt für Strahlenschutz, Germany
NAUAHYGROS—A Code for Calculating Aerosol Behavior in Nuclear Power Plant Containments Following a Severe Accident	R. Sher, Rudolph Sher Associates; J. Li, TENERA, L. P.
Experimental Study on the Particles Deposition in the Sampling Duct	J. Vendel and J. Charuau, ISPN

Aging Effects on Air Cleaning Components

Chairmen: R. R. Weidler, Duke Power Company, and W. Bergman, LLNL

Filter-Adsorber Aging Assessment	W. K. Winegardner, PNL
A Method for Estimating the Efficiency of HEPA Filters During and After Design Basis Accidents	W. Bergman, LLNL
Performance of HEPA Filters Under Hot Dynamic Conditions	D. P. Frankum and G. Costigan, AEA Technology, England
Studies to Determine the Shelf-Life of HEPA Filters	H. Gilbert, Consultant; F. Rainer, EG&G Rocky Flats Plant; D. Beason and W. Bergman, LLNL
Effects on the Efficiency of Activated Carbon on Exposure to Welding Fumes	D. Ghosh, Southern Company Services

Open End

Chairmen: M. W. First, Harvard Air Cleaning Laboratory, and K. Duvall, DOE

In-Place Test Using Sodium Flame Method for Air Cleaning System of Nuclear District Heating Reactor	Z. H. Lin and S. S. Ye, Institute of Nuclear Energy Technology, Tsing Hua University, People's Republic of China
Air Sample Tracking Utilizing Bar Codes to Assist with New 10 CFR 20 and 10 CFR 835 Regulations	W. H. Bailey, NFS Systems
Experimental Study of Elementary Collection Efficiency of Aerosols by Spray: Design of the Experimental Device	D. Ducret, Association Air-Eau-Environment; S. Le Garrec, Société des Techniques en Milieu Ionisant; J. Vendel, ISPN
Degradation of HEPA Filters Exposed to DMSO	W. Bergman, K. Wilson, R. Lopez, and J. LeMay, LLNL
Proposed Retrofit of HEPA Filter Plenums with Injection and Sampling Manifolds for In Place Filter Testing	J. K. Fretthold, EG&G Rocky Flats

Filter Testing

Chairmen: W. L. Anderson, Consultant, and J. F. Leonard, DOE

New Performance Data for "Emery 3002" and "Emery 3004," Two Army-Approved Safe Materials to Replace DOP in Mask and Filter Testing	H. R. Carlon and M. A. Guelta, U.S. Army Edgewood Research, Development and Engineering Center
Comparison of Emery 3004 and 3006 with DOP for Possible Use in HEPA Filter Leak Tests	B. J. Kovach, E. M. Banks, and G. Kovacs, NUCON International, Inc.
Review of In-Place HEPA Filter Testing at Several DOE Facilities	B. V. Mokler and R. C. Scripsick, LANL

(Table continues on the next page.)

Table 1 (Continued)

[a]Abbreviations of organizations:

BNFL	British Nuclear Fuels, Ltd., United Kingdom	LANL	Los Alamos National Laboratory, U.S.A.
BNL	Brookhaven National Laboratory, U.S.A.	LLNL	Lawrence Livermore National Laboratory, U.S.A.
DNFSB	Defense Nuclear Facilities Safety Board, U.S.A.	MIT	Massachusetts Institute of Technology, U.S.A.
DOE	Department of Energy, U.S.A.	MMES	Martin Marietta Energy Systems, Inc., U.S.A.
ENEA	European Nuclear Energy Association	NCS	Nuclear Consulting Services, U.S.A.
EPA	Environmental Protection Agency, U.S.A.	NRC	Nuclear Regulatory Commission, U.S.A.
ISPN	Institut de Protection et de Surete Nucleaire, France	PNL	Pacific Northwest Laboratories, U.S.A.
JAERI	Japan Atomic Energy Research Institute, Japan	WSRC	Westinghouse Savannah River Company, U.S.A.
KfK	Kernforschungszentrum Karlsruhe, Germany	WVNS	West Valley Nuclear Services Co., Inc., U.S.A.

INTERNATIONAL CONFERENCE ON ADVANCES IN THE OPERATIONAL SAFETY OF NUCLEAR POWER PLANTS

Vienna, Austria, September 4–8, 1995

The International Atomic Energy Agency is preparing for the forthcoming International Conference on Advances in the Operational Safety of Nuclear Power Plants.

For additional information, contact M. Dusic, International Atomic Energy Agency, Safety Assessment Section, Division of Nuclear Safety, Wagramerstrasse 5, P.O. Box 100, A-1400, Vienna, Austria. Phone: (+43 1) 2360. Fax: (+43 1) 234564.

Environmental Effects

Edited by J. Williams

Atmospheric Dispersion and the Radiological Consequences of Normal Airborne Effluents from a Nuclear Power Plant

By D. Fang,[a] C. Z. Sun,[b] and L. Yang[a]

Abstract: *The relationship between the consequences of the normal exhaust of radioactive materials in air from nuclear power plants and atmospheric dispersion is studied. Because the source terms of the exhaust from a nuclear power plant are relatively low and their radiological consequences are far less than the corresponding authoritative limits, the atmospheric dispersion models, their various modifications, and selections of relevant parameters have few effects on those consequences. In the environmental assessment and siting, the emphasis should not be placed on the consequence evaluation of routine exhaust of nuclear power plants, and the calculation of consequences of the exhaust and atmospheric field measurements should be appropriately simplified.*

Calculation of exposure doses resulting from routine exhaust of radioactive materials in air is an important part in siting, applying for construction, and operating nuclear power plants, according to the codes[1-3] stipulated by Chinese regulatory bodies. Atmospheric dispersion, which determines the transport of airborne radioactive material released by nuclear facilities, has been studied carefully. To select an appropriate dispersion model or correct an existing one for assessing consequences and determining dispersion parameters, the combined frequencies of atmospheric stability and the indexes of wind-speed profile, detailed atmospheric experiments, and the hourly collection of weather data for a whole year are needed in the process of constructing a nuclear power plant in China. Many workers and materials will be needed to meet all these requirements also.

The relationship between the factors relative to atmospheric dispersion and the consequences caused by the normal exhaust of radioactive airborne materials is studied with a hypothetical 2 × 1000-MW(e) pressurized-water reactor (PWR) as the reference nuclear power plant. Its main parameters are listed in Table 1.

ATMOSPHERIC DISPERSION MODEL AND PARAMETERS

The range required by regulatory codes in China and other countries for assessing environmental consequences is up to 80 km around the sites. The basic model used in the research of atmospheric dispersion and its consequence assessment is the Gaussian point-source model. Whether the model is applicable to the range of 80 km is not to be considered here. Only the maximum individual exposure doses calculated with various parameters on the site boundaries are compared in the article.

[a]Institute of Nuclear Energy Technology, Tsinghua University, Beijing (100084), People's Republic of China.

[b]Suzhou Nuclear Research Institute, Ministry of Electric Power Industry, Suzhou (215004), People's Republic of China.

Table 1 Main Parameters of Reference PWR

Power, MW(e)	Source term code	Site code	Stack height, m	Building size (h-w)	Site boundary, m	Dispersion parameters
2×1000	RS1[a]	HRB[b]	75	$60\ m \times 120\ m^3$	398	Vogt[c]

[a]RS1: the source term code; see Table 7 for more detailed description.
[b]HRB: an actual site code; its atmospheric stability frequencies are taken from measurements at the site.
[c]See Ref. 4.

The Gaussian continuous point-source model[5] can be written as follows:

$$\left(\frac{\chi}{Q}\right)_i = \left(\frac{2}{\pi}\right)^{1/2} \cdot \frac{8}{x \cdot \pi} \sum_{j=1}^{6} \left[\frac{\exp\left(-\frac{H^2}{2\sigma_{Zj}^2}\right)}{\sigma_{Zj}} \cdot \sum_{m=1}^{M} \frac{P_{ijm}}{u_{jm}} \right] \quad (1)$$

where (χ/Q) = long-term dispersion factor for wind direction i
σ_{Zj} = vertical dispersion parameter with stability class j
u_{jm} = mean wind speed with stability class j and wind-speed grade m at the emission height H
P_{ijm} = weather frequency with stability class j, wind-speed grade m, and wind direction i

The Gaussian model is based on the assumptions of time and space homogeneity. Adjustments of models and parameters are needed to make it more applicable to actual situations. The usual adjustments include changes of wind direction with altitude, the effects of building wake, source depletion, fumigation, mixing heights, dispersion parameters, and the index of wind-speed profile.

The changes of wind direction and terrain modification effects are usually not considered in calculations because of their dependence on actual conditions of terrain and wind fields, which are technically difficult to represent in models.

Source depletion and mixing height have effects only at relatively long distances, more than about 10 km from the exhaust point. Therefore their effects on the maximum individual doses on the site boundary are insignificant.

Fumigation affects only short-term dispersion. Generally its occurrences in a year are very few, and it has little contribution to long-term dispersion factors. At some coastal site fumigation might have more effects.

Building Wake Effects

The exhaust stacks usually are two times lower than the highest structure of pressurized-water-reactor (PWR) power plants and are normally near the reactor building. The plume thermal and momentum rises are small; therefore the building wake effects can be significant. Because the plume rise and the differences among the heights of terrain, building, and vegetation offset one another,[6] modification of the effective source height is not considered.

The σ_y and σ_z in the dispersion model (Eq. 1) can be corrected with Σ_y and Σ_z, respectively, which have the following expressions[6] when the building wake effects are considered:

$$\Sigma_y(x) = \left[\sigma_y^2(x) + \frac{A_G}{\pi}\right]^{0.5}$$
$$\Sigma_z(x) = \left[\sigma_z^2(x) + \frac{A_G}{\pi}\right]^{0.5} \quad (2)$$

$$A_G = h_G \cdot b_G \quad \text{when } b_G \le h_G$$
$$A_G = h_G^2 \quad \text{when } b_G \le h_G$$

where $\Sigma_y(x)$ = lateral dispersion parameter corrected for wake effect
$\sigma_y(x)$ = lateral dispersion parameter
$\Sigma_z(x)$ = vertical dispersion parameter corrected for wake effect
$\sigma_z(x)$ = vertical dispersion parameter
b_G = width of building
h_G = height of building
A_G = cross-sectional area of the building

The long-term dispersion factors from the prevailing-wind direction with the effective source heights of 75 and 100 m and the effective source height of 75 m corrected for wake effects are shown in Fig. 1. The long-term dispersion factors at a distance of 398 m from the source are

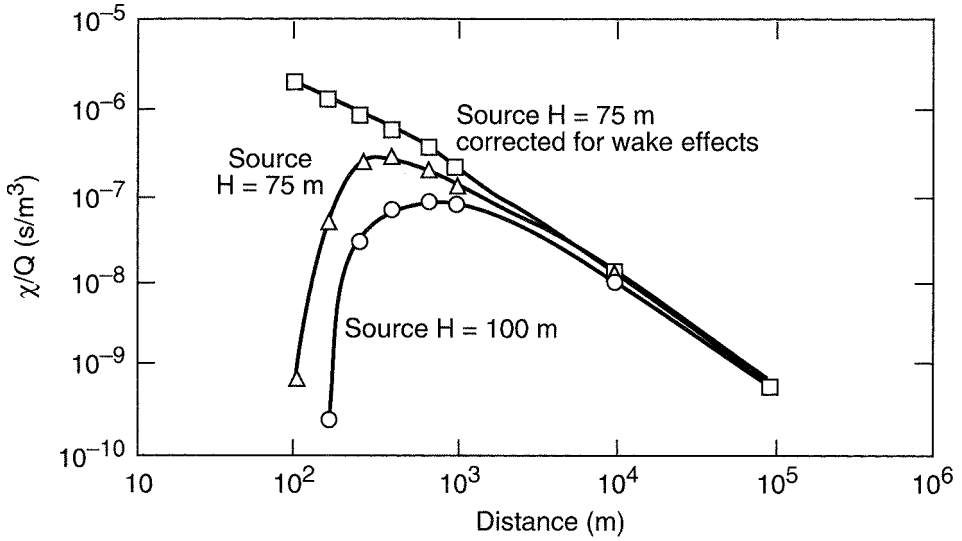

Fig. 1 Long-term atmospheric dispersion factors. χ / Q is the long-term dispersion factor.

5.28×10^{-7} s/m^3 not corrected for wake effects and 2.5×10^{-7} s/m^3 corrected for wake effects, respectively. Their difference is about a factor of 2, and so is the corresponding dose.

Dispersion Parameters

Dispersion parameters are usually determined by such factors as site terrain conditions, surface roughness, and sampling time. They also can be estimated from field measurements on sites. The long-term dispersion factors and the maximum dose equivalent at the distance of 398 m from the site, calculated with different dispersion parameters in downwind direction of prevailing wind, are given in Table 2. The results show a difference of about a factor of 2 caused by different dispersion parameters.

Table 2 Effects of Different Dispersion Parameters on Dispersion Factors and Doses

Dispersion parameters[a]	$(\chi/Q)_{398}$, s/m^3	$Dose_{398}$, mSv/yr
P–G	4.48×10^{-7}	1.64×10^{-3}
Vogt	5.28×10^{-7}	1.93×10^{-3}
Turner	2.42×10^{-7}	8.8×10^{-4}
M. E. Smith	4.32×10^{-7}	1.58×10^{-3}
BNL	4.82×10^{-7}	1.65×10^{-3}

[a]See Ref. 4.

Wind-Speed Profile Index

The vertical wind-speed profile indexes that can be obtained from recommended values or through measurements are often used to calculate the wind speed at the effective exhaust height, H, using the following expression:

$$u_{jm} = u_{0jm}\left(\frac{H}{10}\right)^{k_j} \tag{3}$$

where u_{0jm} is the mean wind speed with stability class j and wind-speed grade m at height 10 m, and k_j is the wind-speed profile index with stability class j.

Table 3 shows two groups of German-recommended indexes, two groups of Chinese-recommended indexes, and the results of dispersion factors and doses calculated with them, respectively. The maximum differences among these results are about a factor of 5, and the difference between these results and those calculated with the observation data at the 10-m height are within a factor of 10.

FREQUENCIES OF ATMOSPHERIC STABILITY

The combined frequencies of atmospheric stability play an important role in the calculation of long-term atmospheric dispersion, as shown in Eq. 1. For a nuclear power-plant site, the hourly atmospheric information for more than 1 year is needed to classify the stability classes and count their frequencies, as required in national codes.

Table 3 German and Chinese Wind-Speed Profile Indexes and Their Effects on Dispersion Factors and Doses

Wind-speed profile index	Atmospheric stability class						$(\chi/Q)_{398}$, s/m^3	$Dose_{398}$, mSv/yr
	A	B	C	D	E	F		
G1[a]	0.09	0.20	0.22	0.08	0.37	0.42	5.28×10^{-7}	1.93×10^{-3}
G2[a]	0.9	1.3	1.7	2.0	1.2	0.4	1.04×10^{-7}	0.37×10^{-3}
GB1[b]	0.15	0.15	0.2	0.25	0.40	0.60	4.85×10^{-7}	1.77×10^{-3}
GB2[b]	0.07	0.07	0.10	0.15	0.35	0.55	5.67×10^{-7}	2.07×10^{-3}

[a]G1 and G2 are from Refs. 5 and 7.
[b]GB1 and GB2 are from Ref. 8.

Characteristics and Variations of Atmospheric Stability in China

A vast territory brings substantial differences among the atmospheric stability frequencies in different terrain conditions and regions in China. The whole territory is classified into six regions; each has a specific stability class, as shown in Fig. 2 (Ref. 4). The frequency ranges of every class are given in Table 4, in which the remarkable differences among these six classes are shown.

Table 4 Ranges of Classification of Atmospheric Stability in Six Stability Regions in China

Atmospheric stability class[a]	Frequency range, %
A	0.40 to 4.63
B	4.40 to 10.24
C	4.70 to 9.62
D	30.17 to 71.20
E	10.60 to 26.52
F	7.30 to 21.72

[a]Pasquill diffusion categories.

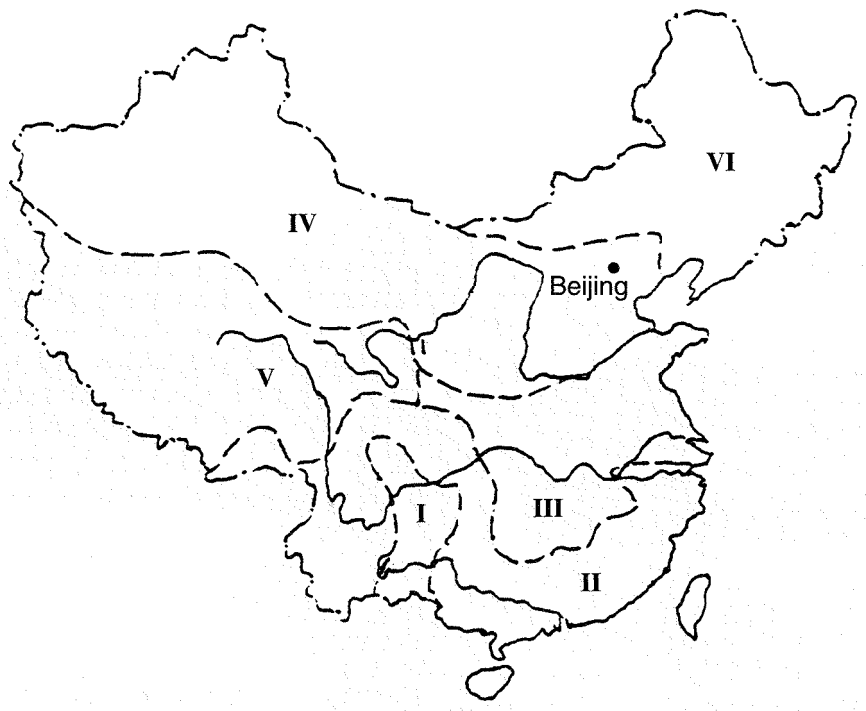

Fig. 2 Six regions of atmospheric stability in China.

The frequency variations of the six classes in ten reference sites (their codes are QS, BEJ, HRB, JLN, LYG, SC, SMZ, YCZ, YY, and BS) distributed in the six regions are given in Fig. 3. The tendencies of frequency variations in Table 4 and in Fig. 3 are the same. Both of them are characterized by the largest frequencies of class D and the smallest frequencies of class A.

Effects of Different Combined Frequencies of Atmospheric Stability Classes on the Consequences of Routine Exhaust

The exposure doses produced by routine exhaust of airborne radioactivity are calculated with the stability frequencies in the ten reference sites as the input data. The calculated individual doses at the ten sites given in Fig. 4 show very low differences, not more than a factor of 3 between the largest and smallest doses on the site boundaries, although the stability frequencies of these sites vary considerably. These doses are two orders of magnitude less than the limit of 0.25 mSv/yr (Ref. 2) required by Chinese authorities for exposure doses received by the public under routine operation of nuclear power plants, and about three orders of magnitude less than the natural background exposure, 2.4 mSv/yr (Ref. 9).

Method of Stability Classification and Acquisition of Atmospheric Information

The methods of stability classification recommended[10] are Pasquill–Gifford (P–G) methods; ΔT method; split σ method; and other widely recommended methods, such as σ_θ, U_R, and ΔT-U.

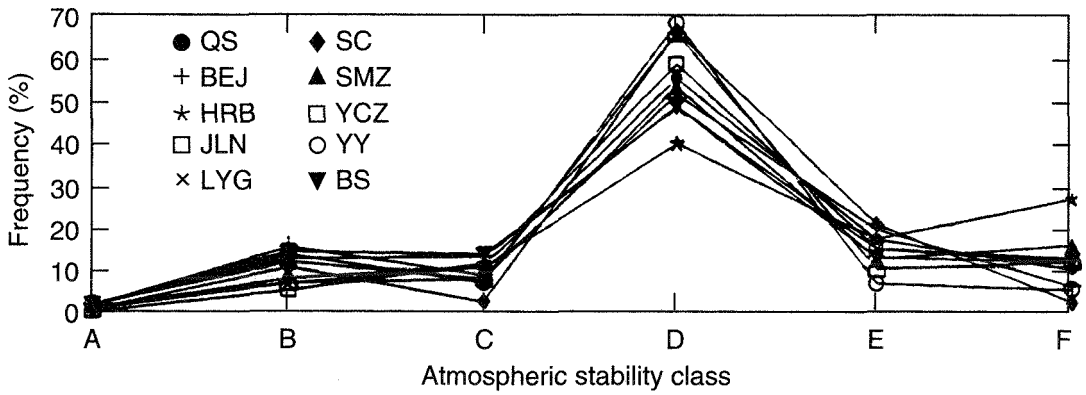

Fig. 3 Atmospheric stability of 10 sites. QS, BEJ, HRB, JLN, LYG, SC, SMZ, YCZ, YY, and BS are site codes.

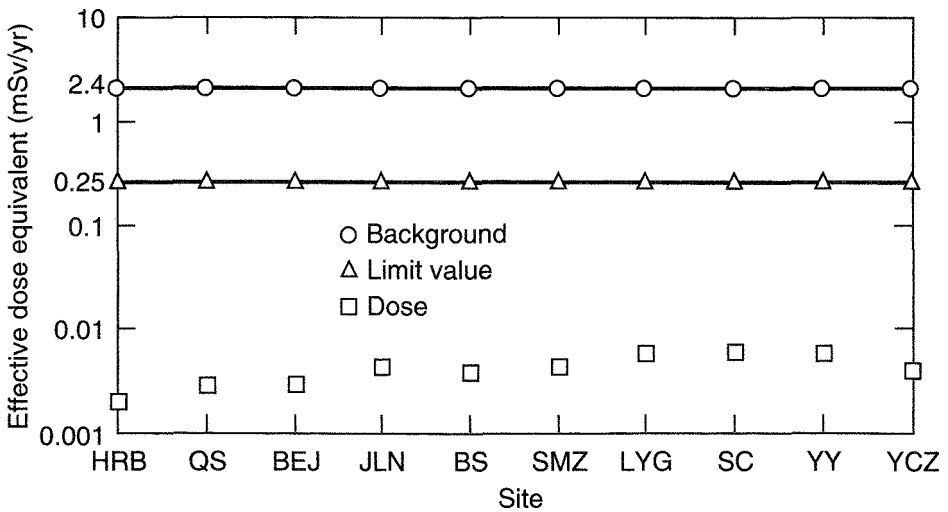

Fig. 4 Maximum individual doses at 398 m for different sites. QS, BEJ, HRB, JLN, LYG, SC, SMZ, YCZ, YY, and BS are site codes.

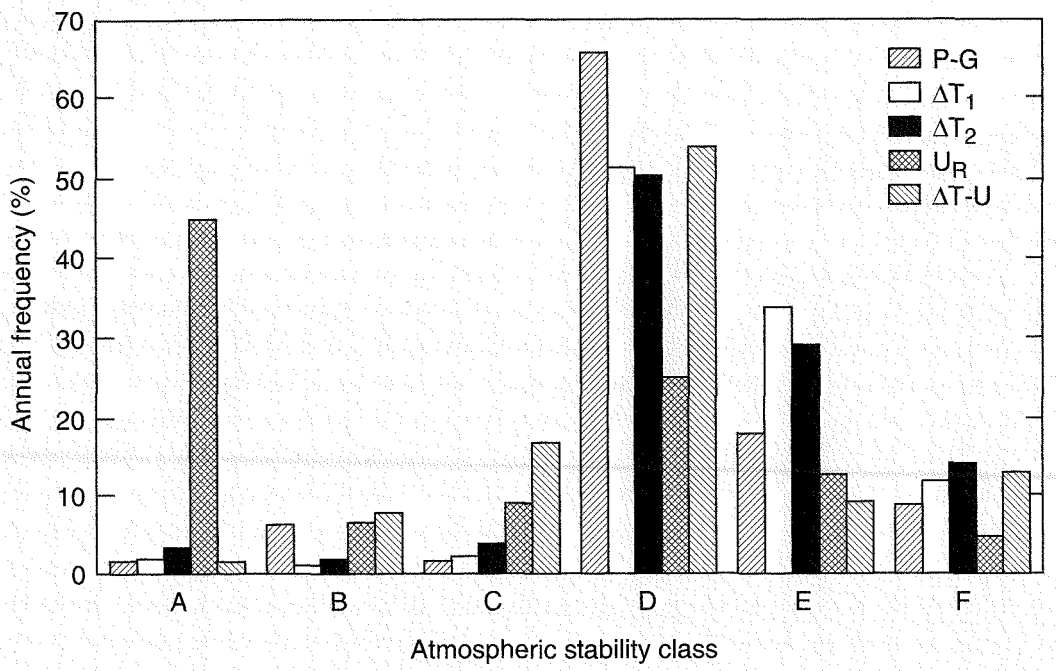

Fig. 5 Annual frequency distributions of different classifying methods. [P–G is the Pasquill–Gifford method. ΔT_1 is based on the temperature difference (ΔT) between 10 m and 100 m in height. ΔT_2 is based on the temperature difference (ΔT) between 10 m and 70 m in height. U_R is based on the wind-speed method. ΔT-U is based on ΔT and the wind-speed method.][11]

The annual distributions of stability frequencies determined, respectively, by the P–G method, ΔT_1 method, ΔT_2 method, U_R method, and ΔT-U method for the same site are shown in Fig. 5. The frequency distribution classified by the ΔT_1 method is based on temperature differences between the 10- and 100-m height, whereas the ΔT_2 method is based on the temperature differences between 10 and 70 m. The maximum long-term dispersion factors calculated with these methods are shown in Table 5.

Table 5 Maximum Long-Term Dispersion Factors Calculated with Different Classification Methods[11]

Method	Distance of downwind, m	Dispersion factor (χ/Q), s/m^3
P–G	500	7.98×10^{-7}
ΔT_1	500	8.57×10^{-7}
ΔT_2	500	7.61×10^{-7}
U_R	500	8.67×10^{-7}
ΔT–U	500	9.49×10^{-7}

From Table 5, the conclusion can be made that, although the different classification methods bring about different distributions of stability frequencies, they do not affect the maximum long-term dispersion factors very much.

Theoretically, the stability classes determined by hourly atmospheric information are more accurate than those determined by the four-times-per-day information (i.e., the information is gathered once every 6 hours) or six-times-per-day information (every 4 hours). In fact, the maximum long-term dispersion factors calculated with them show little difference (more details given in Table 6).

SOURCE TERM

The source term, the amount of radioactive nuclides vented to the environment, is one of the key factors that influences the consequences of normal exhaust of radioactive materials from nuclear power plants. Normally, it is obtained from experience with operating nuclear plants or is calculated by appropriate mathematical models. For a new plant, a mathematical model is the only way. However, the results of the method must be used carefully because mathematical models are based on many

Table 6 Distribution of Stability Frequencies Obtained from Hourly or Four-Times-a-Day Weather Monitoring[12]

Weather station	Frequency of collecting information	Distribution of atmospheric stability frequencies by class, %					
		A	B	C	D	E	F
1	Hourly	1.43	8.4	11.3	40.9	21.8	16.7
	Four times/day	0.62	7.5	11.5	42.8	20.5	17.0
2	Hourly	0.82	4.2	6.8	61.7	18.5	7.9
	Four times/day	1.1	4.9	6.5	61.4	18.0	8.0

Table 7 Different Source Terms of 2 × 1000-MW(e) PWR Under Normal Operating Conditions (Bq/yr)

Nuclide	Source term code			
	RS1	RS2	RS3	RS4
^{3}H	1.23×10^{13}	5.78×10^{13}	1.78×10^{13}	
^{60}Co	6.30×10^{8}	1.68×10^{8}	8.44×10^{8}	
^{88}Kr	1.12×10^{13}	2.64×10^{12}	6.33×10^{13}	4.00×10^{12}
^{133}Xe	1.52×10^{14}	4.92×10^{14}	8.86×10^{14}	9.38×10^{14}
^{138}Xe	1.79×10^{13}	2.46×10^{11}		1.38×10^{13}
^{131}I	1.03×10^{9}	4.44×10^{10}	6.33×10^{9}	3.80×10^{9}
^{134}Cs	9.50×10^{8}	7.00×10^{7}	1.22×10^{8}	
^{137}Cs	6.30×10^{8}	1.20×10^{8}	8.44×10^{8}	
$Dose_{398}$, mSv/yr	1.93×10^{-3}	4.61×10^{-3}	2.75×10^{-3}	3.83×10^{-3}

assumptions and simplifications, and their results are not demonstrated. For PWR plants, much operational experience is available. The exposure doses calculated with source terms collected from various PWR plants show few differences, as shown in Table 7. The results indicate that the doses based on the source terms from operating experiences of nuclear power plants are about two orders of magnitude less than the national dose limits.

CONCLUSIONS

From the previous statements, the following can be concluded:

1. The consequence of routine exhaust of radioactive materials in air is two orders of magnitude lower than the dose limit specified in Chinese codes because the exhaust concentrations are very low.

2. The differences in doses caused by using different adjustments of dispersion models or using different parameters are within a few orders of magnitude.

3. Although the stability frequencies in six regions within Chinese territory vary greatly, the differences of their resulting consequences are small.

In view of these facts, the calculation of the consequences of normal emission should not be taken as critical contents in the siting and environmental assessment for nuclear power plants. A recommended model and parameters are enough to be used to estimate the consequences of exhaust of radioactive airborne materials and to evaluate whether the source terms or the emission limit values of radioactive materials are reasonable, as German SSK Band 17 did.[12]

REFERENCES

1. *Atmospheric Dispersion in Nuclear Power Plant Siting*, Report NNSA-HAF0103, Beijing, 1987 (in Chinese).
2. *Regulations for Environmental Radiation Protection of Nuclear Power Plant*, Report NEPA-GB6249-86, Beijing, 1986 (in Chinese).
3. *Content and Format of Environmental Impact Reports for Nuclear Power Plant*, Report NEPA-RG1, Beijing, 1988 (in Chinese).

4. *Handbook of Urban Air Pollution Total Emission Control*, NEPA Press, Beijing, 1991 (in Chinese).
5. *BMI Stoerfaellberechnungsgrundlagen fuer die Leitlinien des BMI fuer Beurteilung der Auslegung von Kernkraftwerken mit PWR gemaesse*, 28 Abs. 3 Strlsch V, Bundesanzaiger No. 245a, 1983, 12. 31 (in German).
6. D. Gumprecht and M. Mueller-Neumann, *Modelle, Annahmen und Daten mit Erlaueterungen zur Berechnung der strahlenexposition bei der Ableitung radioaktiver Stoffs mit Luft oder Wasser zum Nachweis der Einhaltung der Dosisgrenzwerte nach 45 Strlschv*, Veroeffentlichungen der Strahlenschutzkommission, Stuttgart, 1992 (in German).
7. Allgemaine Berechnungsgroundlage fuer die Strahlenexposition bei radioaktiven Ableitungen mit Abluft oder in Oberflaechengewaesser, *Gemeinsames Ministerialbl.*, 36(19): 380-383 (June 1985) (in German).
8. *Technical Specification and Methods for Making Local Emission Standards of Air Pollutants*, Report NEPA-GB3840-83, Beijing, 1983 (in Chinese).
9. B. G. Bennet, Worldwide Exposures to Ionizing Radiation, in *Proceedings of ASIA Congress on Radiation Protection*, pp. 21-24, Beijing, October 1993.
10. International Atomic Energy Agency, *Atmospheric Dispersion in Nuclear Power Plant Siting, A Safety Guide*, Report 50-SG-S3 (AIX-12-622018), 1980.
11. Hu Erbang, The Effects of Different Atmospheric Stability Classification Methods on the Maximum Long-Term Dispersion Factors, private communication, December 1993 (in Chinese).
12. Zhang Hongyou, The Effects of Hourly and Other Time-Interval Weather Information on the Results of Atmospheric Stability Classification, private communication, 1990 (in Chinese).

Calculation of Distribution Coefficients for Radionuclides in Soils and Sediments

By I. Puigdomènech and U. Bergström[a]

Abstract: *The turnover of radionuclides in parts of the biosphere is usually modeled by use of a sorption distribution coefficient, K_d. Its value has a large influence on calculated concentrations of long-lived radionuclides found in reservoirs, which are important for doses to humans. Sorption is due to several processes and a variety of physical and chemical interactions (e.g., surface complexation and ion exchange). In the commonly used K_d-methodology, however, these processes were usually not considered explicitly. Additionally, many K_d values were obtained from laboratory experiments or from the geosphere, the conditions of which differ from those prevailing in the biosphere. The main objective of this work was to extend the knowledge about the theoretical background for calculation of K_d values. To achieve this objective, theoretical models for ion exchange and surface complexation were adapted to simulation under biospheric conditions. Elements studied were Cs, Ra, Np, U, and Pu. The results show that a triple-layer surface complexation model may be used to estimate K_d values for actinides as functions of some chemical parameters, such as pH and the redox potential (E_H). An area of application is performance assessment of radioactive waste repositories.*

[a]Studsvilk Eco and Safety AB, S-611 82 Nyköping, Sweden.

The possible migration of long-lived radionuclides from repositories of high-level radioactive waste is important when the safety aspects and design of such facilities are being considered. Nuclide behavior has two major aspects: their movement in the geosphere and in the biosphere. The biosphere is the part of Earth's environment inhabited by biological life and comprises parts of the atmosphere, the hydrosphere, and the lithosphere. The geosphere is composed of bedrock, including its water content. In the geosphere the mobility of radionuclides should be so low that most of the released radionuclides from the near-field area will not reach the biosphere in amounts that cause any substantial doses to people. In the biosphere, however, accumulation caused by low mobility may increase the exposure. The exposure pathways may be inhalation caused by dust resuspension or direct consumption of soil, especially by children. Conversely, strong binding yields a high degree of accumulation, which causes low bioavailability of the nuclides and thus decreases their importance for the dose through the exposure pathways of the food chain.

The turnover of elements in the biosphere may be modeled by using compartment theory. The biosphere, for example, is divided into reservoirs; the transport between those reservoirs and the source and sink processes within them are modeled with the use of first-order kinetics. Accumulation in some reservoirs of the biosphere may be described with the use of an equilibrium distribution coefficient, K_d. It can be used as a measure of the sorption of an element at an interface between a solid and a liquid. Sorption is due to several processes and diverse physical and chemical interactions: surface complexation, ion exchange, precipitation, solid solution, entrapment in zeolite structures, complexation by humic and fulvic substances (coating soil particles), etc. At subtrace concentration levels, which concern performance assessments, surface complexation and ion exchange are the most important processes, and complexation by organic materials might be important in some soils. As a first approximation, only surface complexation and ion exchange are considered in this work. With the K_d methodology, which is mostly based on distribution experiments, it is not possible to consider explicitly the underlying physical phenomena. Furthermore, many K_d values used in biospheric models were obtained from the geosphere, the conditions of which are not usually comparable with those prevailing in the biosphere. Other disadvantages of the commonly used methodology for obtaining K_d factors are:

- There is a lack of theoretical background.
- K_d values relevant to a specific problem are often missing. Therefore extrapolated values must be used, which presents some difficulties because of the lack of theory.
- There is no quantitative relation between chemical species in solution and K_d values.
- Precipitation and adsorption processes are difficult to separate.

Many assessment studies for repositories of long-lived radioactive nuclides have also shown that most of the uncertainty related to the calculations is due to uncertainties of the transport parameters.[1,2] These transport parameters are usually based on the use of K_d factors when the accumulation of the nuclides in soil and sediments is described. In addition, the accumulation process (i.e., the K_d parameter) has been identified as a dominating contributor to the uncertainty in calculated results for several scenarios handled within the international BIOMOVS study.[3,4] One reason for this is the large uncertainty assumed for the K_d values, which is due to the lack of theoretical knowledge needed to select more realistic ranges of K_d values for specific conditions.

The main purpose of this study is to extend the knowledge regarding factors that influence the accumulation of long-lived radionuclides in soils and sediments. This will lead to increased accuracy and lower uncertainty in the choice of K_d values. This is particularly important for uncertainty analyses in radiological safety studies. The results will also be applicable for modeling the transport of radionuclides in the geosphere. For this study, theoretical surface complexation models were used to simulate the conditions in the biosphere.

ELEMENTS

The following elements were considered in this study: Cs, Ra, U, Np, and Pu. They were chosen because some of their isotopes were found important in previous safety analyses for spent fuel.[5] This is valid especially for Ra-226 and Np-237. Pu-239 is included because it is potentially important in dose assessments for high-level wastes. In addition, the choice of elements was based on the availability of information about their chemical properties.

The K_d values for soil, previously used in an assessment[6] of conversion factors between unit releases of radionuclides to the biosphere and resulting doses to humans, are shown in Table 1 for comparison and evaluation. The ranges were estimated from the variations of the literature values.[7]

Table 1 Distribution Coefficients (K_d)[a] for Soil/Water[6]

Element	K_d, m^3/kg (best estimate)	Range
Cs	1.0	0.1 to 10
Ra	0.5	0.05 to 5
U	0.1	0.01 to 1
Np	0.1	0.01 to 1
Pu	50	1 to 100

[a] $K_d\,(m^3/kg^{-1}) = 10^3\ g/kg \times 10^{-6}\ m^3/mL \times K_d\,(mL/g) = 10^{-3} \times K_d\,(mL/g)$.

METHODOLOGY

The K_d value for each radionuclide was obtained from chemical equilibrium calculations. The dissolved and adsorbed concentrations for a given solid-to-water ratio were calculated with a combination of chemical models: complexation both within the aqueous solution and on the surface of an iron oxide as well as equilibrium ion exchange on clay (for cesium and radium). For a given chemical element, Me, the distribution coefficient K_d (m^3/kg, equivalent to dm^3/g) was calculated as the quotient between the concentration in the solid (mol/g) and the soluble fraction (mol/dm^3):

$$K_d = \frac{1}{S} \frac{\left[SOMe^{(z-1)+}\right] + \left[SO-MeOH^{(z-2)+}\right] + \left[X_2Me\right] + \ldots}{\left[Me^{z+}\right] + \left[MeOH^{(z-1)+}\right] + \left[MeL^{z-y}\right] + \ldots}$$

where concentrations are in units of mol/L, S is the solid concentration in g/L, L^{y-} represents a ligand (like carbonate or phosphate), X is an ion exchanger (for example, clay), and SO^- *is* a surface complexation site of the iron oxide.

Sorption was described by a set of equilibrium reactions between surface sites and aqueous ions and by mass and charge balance equations.[8–23] One of the main differences between aqueous and surface complexations is that activity coefficients for surface species include an electrostatic term describing the energy required to bring a charged species from the bulk solution to the plane of adsorption. A Boltzmann distribution function is used to relate the variable electrostatic potential at the surface, Ψ; the bulk activity of an ion; and its surface activity: $\{Me^{z+}\}_s = \{Me^{z+}\} \exp(-\Psi/RT)$. The models for surface complexation differ in the number of layers in the electrostatic model. When the surface planes are treated as plate capacitors, it is possible to obtain an expression relating surface charge and potential.

Particle surfaces in contact with aqueous solutions are usually electrically charged. This is due to acid-base reactions of the following type:

$$SOH + H^+ \leftrightarrow SOH_2^+ - \log_{10} K_{a1}^{int} = \log_{10}([SOH_2^+]/[H^+][SOH]) + (\Psi/RT \ln[10]) \quad (1)$$

$$SOH \leftrightarrow SO^- + H^+ \log_{10} K_{a2}^{int} = \log_{10}([SO^-][H^+]/[SOH]) - (\Psi/RT \ln[10]) \quad (2)$$

where $[SO^-]$ and $[SOH]$ represent the molar concentration of surface sites. Metal ion sorption was described with equilibria like the following:

$$SOH + Me^{z+} \leftrightarrow SOMe^{(z-1)+} + H^+$$

for inner-sphere surface complexes and

$$SOH + Me^{z+} \leftrightarrow SO^- - Me^{z+} + H^+$$

for outer-sphere surface complexes in models with more than one surface complexation layer.

As the acid-base reactions (Eqs. 1 and 2) show, particle surfaces in contact with aqueous solutions will be electrically charged, and this charge will depend on the pH value. The charge density in the solid surface, $\sigma_s(C/m^2)$, depends on the specific surface area, $A(m^2/g)$, the solid concentration, $S(g/L)$, and the extent of ionization and sorption, according to the following:

$$\sigma_s = \frac{F}{SA}\left\{\left[SOH_2^+\right] - \left[SO^-\right] + (z-1)\left[SOMe^{(z-1)}\right] + \ldots\right\}$$

The total concentration of surface sites (mol/L) for the chemical system of interest can be calculated from the solid concentration, the specific surface area, and the site density:

$$[SOH]_{TOT} = SAN_s\, 10^{18}/N_A \quad (3)$$

where N_s is the site density ($sites/nm^2$) and N_A is Avogadro's number ($6.02214 \cdot 10^{23}\ mol^{-1}$). The mass-balance constraint for all surface sites is as follows:

$$[SOH]_{TOT} = [SOH] + [SOH_2^+] - [SO^-] + [SOMe^{(z-1)+}] + \ldots$$

The electric potential for the adsorption surface, Ψ, can be estimated with several assumptions, yielding different surface complexation models: constant capacitance, two-layer (or diffuse-layer), Stern, triple-layer, four-layer, etc. The triple-layer model (TLM) was used in this work. This model assumes that protons and strongly binding

cations are placed in the particle's surface plane (the 0-plane), weakly binding ions are placed in a second β-plane, and the third plane is the diffuse-layer *D*-plane. For the 0- and β-planes, there are associated capacitances C_1 and C_2 (F/m^2); the relation between charge (σ) and potential (Ψ) at each plane is given by the following:

$$\Psi_0 - \Psi_\beta = \sigma_0/C_1 \quad \text{and} \quad \Psi_\beta - \Psi_D = (\sigma_0 + \sigma_\beta)/C_2$$

The formula of Gouy–Chapman was used to estimate the diffuse-layer charge, σ_D, from the diffuse-layer potential, Ψ_D (Ref. 24). The total electrical charge of the system must be zero, and electrical charge densities for the different planes are also constrained by the following equation: $\sigma_D = -\sigma_s = -(\sigma_0 + \sigma_\beta)$. Surface charge for the different planes can be calculated from the sum of concentrations of all charged species in the corresponding plane.

The computer program HYDRAQL was used to calculate the chemical equilibrium (including surface complexation and ion exchange).[24] For aqueous complexation, the original data base supplied with the HYDRAQL program was modified as follows. For uranium, the original HYDRAQL values were replaced with those selected in the Organization for Economic Cooperation and Development/Nuclear Energy Agency (OECD–NEA) review.[25] The data bases of Langmuir and Riese[26] for radium, Lemire and Garisto[27] for neptunium, and Puigdomènech and Bruno[28] for plutonium were also used. Preliminary calculations showed anomalous results for uranium sorption. A comparison with plutonium calculations showed that the predicted stability of $U(OH)_4(aq)$ was unusually high. The NEA review[25] indicates a large uncertainty for the formation of $U(OH)_4(aq)$. Grenthe et al.[25] note that the stability of $U(OH)_4(aq)$ "has been overestimated by orders of magnitude." Therefore, in our calculations the value $\log_{10} K_{eq} = -10.0$ was selected for

$$U^{4+} + 4\,H_2O \leftrightarrow U(OH)_4(aq) + 4\,H^+$$

instead of the value -4.5 ± 1.4 selected by the NEA review.[25] This value is more in accordance with the equilibrium constants for Np^{4+} (–10.8) and Pu^{4+} (–9.2) and in better agreement with other reviews concerning uranium hydrolysis.

The ionic strength was kept constant at 0.1 mol/L (NaCl electrolyte) to simplify calculations involving actinide sorption. Precipitation of solid phases was suppressed during the calculations, and equilibrium between the several redox couples was enforced by a prevailing redox potential, E_H. Owing to the structure of the HYDRAQL program, the calculations had to be repeated, which set the main component equal to each of the possible redox states. Calculations for plutonium, for example, had to be repeated, which set the main component successively to PuO_2^{2+}, PuO_2^+, Pu^{4+}, and Pu^{3+}. The results were then collected and integrated into a single K_d-value through the use of a spreadsheet program. The total concentration of radionuclides in the simulations was (in mol/L): 10^{-9} for Cs, 10^{-10} for Ra, 10^{-5} for U, and 10^{-8} for Np and Pu.

The chemical composition of the waters is given in Table 2. Values correspond to average values for Swedish surface waters. Activity coefficients, γ_i, for aqueous ions were estimated with the use of Davies' equation (an extension of the Debye–Hückel limiting law). For neutral aqueous molecules, the approximation $\gamma_i = 1$ was applied.

Important parameters in sorption models are the specific surface area, *A*, the site density, N_S, and the acid-base properties (Eqs. 1 and 2). There is a large scatter in the literature[29] regarding the protolysis constants of iron oxides and hydroxides. The properties of goethite selected for this study were those reported by Lövgren et al.[30] (i.e., $A = 39.9$ m^2/g, $N_S = 1.7$ sites/nm^2, $\log_{10} K_{a1}^{int} = -7.5$, and $\log_{10} K_{a2}^{int} = -9.5$). The swamping electrolyte constants were those reported in Refs. 20 and 31 ($\log_{10} K_{cat}^{int} = -9.3$ and $\log_{10} K_{an}^{int} = 6.2$), and the TLM capacitances are $C_1 = 1.4$ F/m^2 and $C_2 = 0.2$ F/m^2. Surface complexation of CO_3^{2-} and HCO_3^- was not considered in the calculations. Following the work of Bond et al.,[32–34] we assumed that sorption of U, Np, and Pu in soils and sediments is mainly determined by their contents in iron oxyhydroxides, which in this work was

Table 2 Chemical Composition of the Aqueous Solutions Used in the Numerical Calculations

	Average		Range	
Element	**mg/L**	**mol/L**	**mg/L**	**mol/L**
Na	5	2×10^{-4}	1 to 16	$(0.4 \text{ to } 7) \times 10^{-4}$
K	2	5×10^{-5}	0.5 to 5.0	$(1 \text{ to } 10) \times 10^{-5}$
Ca	60	1.5×10^{-3}	2 to 120	$(0.05 \text{ to } 3) \times 10^{-3}$
Mg	2.4	1×10^{-4}	2 to 7	$(0.8 \text{ to } 3) \times 10^{-4}$
HCO_3	30	5×10^{-4}	0 to 122	$(0 \text{ to } 2) \times 10^{-3}$
pH (soil)				4 to 5
pH (sediment)				6 to 7

assumed to be 5% in goethite. This, in essence, agrees with other modeling work on UO_2^{2+} sorption,[35,36] on Zn^{2+} sorption,[37] and on Ni^{2+} sorption.[38] In our K_d calculations, a solid concentration of 1 g/L was used, which corresponds to 0.05 g/L of goethite in the HYDRAQL runs.

The other surface complexation constants are given in Table 3. The same surface complexation constants were used for actinides with the same redox state (for example, UO_2^+, NpO_2^+, and PuO_2^+) because the aim of this work was to test the possibilities of surface complexation models in estimating K_d values in a wide range of conditions, including systems for which there are no surface complexation constants available in the literature. References to the selected values are indicated in Table 3 except a few surface complexation reactions that require some description of the procedure that was followed to select the corresponding equilibrium constant. The surface complexation constant for the carbonate complex of Pu^{4+} (see Ref. 41) was set to a value of $\log_{10} K^{int} = 8.0$ to fit the experimental data for Pu(IV) sorption on goethite as a function of alkalinity (see Fig. 5 in Ref. 41). The equilibrium constant for the surface complexation of NpO_2^+ was adjusted from the values reported in Ref. 16 ($\log_{10} K^{int} = -3.5$) and Ref. 43 ($\log_{10} K^{int} = -3.2$) to $\log_{10} K^{int} = -3.0$ to fit the curves in Fig. 5-2 of Ref. 43 and Fig. 2 of Ref. 44 with our data base of equilibrium constants for complexation in the aqueous phase. When the U(VI) sorption data of Hsi and Langmuir[44] were simulated with the surface complexation constants reported by them, a clear disagreement was obtained. The reasons were the selection of a different data base for the aqueous complexation and our use of different parameter values for goethite. Therefore a slightly different model for UO_2^{2+} sorption was used (see Table 3). Our model approximates the effect of carbonate concentration on the percentage of adsorbed U(VI) (Fig. 8 in Ref. 44) and on the total dissolved uranium (Fig. 4 in Ref. 44).

Table 3 Surface Complexation Equilibrium Constants Used in the Calculations[a]

Reaction	$\log_{10} K^{int}$	Reference
For Np^{3+} and Pu^{3+}		
$SOH + Me^{3+} + H_2O(l) \leftrightarrow SOMe(OH)^+ + 2H^+$	-1.5	30, 39, 40
$SOH + Me^{3+} + 2H_2O(l) \leftrightarrow SOMe(OH)_2^0 + 3H^+$	-9.1	30, 39, 40
For U^{4+}, Np^{4+}, and Pu^{4+}		
$SOH + Me^{4+} + H_2O \leftrightarrow SO^- - Me(OH)^{3+} + 2H^+$	2.5	41
$SOH + Me^{4+} + 2H_2O \leftrightarrow SO^- - Me(OH)_2^{2+} + 3H^+$	-2.0	41
$SOH + Me^{4+} + 3H_2O \leftrightarrow SO^- - Me(OH)_3^+ + 4H^+$	-5.9	41
$SOH + Me^{4+} + 4H_2O \leftrightarrow SO^- - O_2^0 + 5H^+$	-12.0	41
$SOH + Me^{4+} + 4H_2O + CO_3^{2-} \leftrightarrow SOH_2^+ - Me(OH)_4CO_3^{2-} + 3H^+$	8.0	See text
For NpO_2^+ and PuO_2^+		
$SOH + MeO_2^+ \leftrightarrow SOMeO_2^0 + H^+$	-3.0	See text
For UO_2^{2+}, NpO_2^{2+}, and PuO_2^{2+}		
$SOH + MeO_2^{2+} + H_2O \leftrightarrow SOMeO_2(OH)^0 + 2H^+$	-4.5	See text
$SOH + MeO_2^{2+} + 2H_2O \leftrightarrow SOMeO_2(OH)_2^- + 3H^+$	-12.2	See text
$SOH + MeO_2^{2+} + 3CO_3^{2-} + H^+ \leftrightarrow SOH_2^+ - MeO_2(CO_3)_3^{4-}$	33.5	See text
For Ra^{2+}		
$SOH + Ra^{2+} \leftrightarrow SO^- - Ra^{2+} + H^+$	-5.0	20, 31, 42
$SOH + Ra^{2+} + H_2O \leftrightarrow SO^- - Ra(OH)^+ + 2H^+$	-14.5	20, 31, 42

[a] *SOH* stands for a surface site. Outer-layer complexes in the triple layer model are indicated with a "–" between the surface site and the complexed metal species.

For Cs^+ and Ra^{2+}, model calculations included ion exchange in competition with Na^+, K^+, Ca^{2+}, and Mg^{2+}. Ion-exchange reactions are described in the literature.[45] For the simulation of ion exchange between two ions "Me" and "N" (usually two metal cations) at the ion exchanger "X" (for example, clay), the following reaction was used:

$$zX_yN + yMe^{z+} \leftrightarrow yX_zMe + zN^{y+}$$

If the activity for ion-exchanged species may be assumed to be proportional to their molar concentrations, the equilibrium constant for the preceding reaction can be written as follows:

$$\log_{10} K_X(N/Me) = z \log_{10}\{N^{y+}\} - y \log_{10}\{Me^{z+}\} + y \log_{10}[X_zMe] - z \log_{10}[X_yN]$$

The activity coefficients for the ion-exchanged species are thus assumed to be constant and included in K_X. This assumption will be appropriate if only trace amounts of "Me" are ion exchanged. The total concentration of ion exchanger is given as the cation exchange capacity (CEC). The amount of ion exchange (clay) was set in the calculations to 1 g/L, and a value of CEC = 0.2 meq/g was used. The ion-exchange equilibrium constants are $\log_{10} K_X(Na/K) = 0.5$ and $\log_{10} K_X(Na/Cs) = 1.4$, as given in the tables of Ref. 46. For interchange between cations of charge +1 and +2 (for example, Na^+ and Ca^{2+}), the K_N values tabulated in Ref. 46 ($K_N \approx 4$ for Na/Ca and Na/Mg exchange) refer to ionic equivalent fractions in the ion exchanger. If K_N is constant, then the value of K_X (as defined previously) depends on the total cation exchange capacity of the system (CEC, in equivalents per liter of solution):

$$2XNa + Ca^{2+} \leftrightarrow X_2Ca + 2Na^+$$

$$K_N = 2 \cdot CEC \cdot K_X(Na/Ca)$$

The ion-exchange constants selected in this work are similar to those reported in Ref. 47. For Ra^{2+}, a combination of ion exchange and surface complexation was used. Precipitation of calcite and aragonite was suppressed in the calculations. The sorbent was assumed to be 1 g/L of clay and 0.05 g/L of goethite. Surface complexation constants for Ra^{2+} were assumed to be equal to those for Ca^{2+} reported in Refs. 31 and 42.

RESULTS

The calculations carried out gave K_d values as functions of environmental conditions, such as pH, E_H, alkalinity, and concentrations of cations. Results are presented graphically in three-dimensional plots against the major parameter influencing the K_d values for the respective element. The ranges of these model parameters may be wider than those normally occurring in the environment. Normal background values for soil pore waters are given in Table 2. Major differences between the sediment properties compared with those of soil are that reducing conditions may occur, and the pH values may be higher than in the soil, presumably about 7. The redox potential is positive in surface soil and upper sediment, whereas reducing conditions occur in deeper sediments.

Cesium

For cesium, ion exchange is the main process for retaining the element on solid materials. The calculations show this through decreasing K_d values, when the concentrations of cations increase (see Fig. 1). However, all obtained values are lower than those found in experimental studies.[45,48,49] This may be due to the experimental design but also because many measurements include the total irreversibly bound cesium pool, whereas our calculations are based on reversibly sorbed cesium. These two pools of bounded Cs^+ in soil are described in the literature.[45,48]

Radium

For radium as well, ion exchange is the main sorption process. The calculations show that the calcium concentration is the main parameter influencing the K_d values (see Figs. 2 and 3), where the K_d values are plotted against calcium concentration and the concentration of the alkali metals Na and K or pH, respectively. The influence of alkali metals is due to their competing with radium for ion-exchange sites.

Uranium

The calculations show that pH, inorganic carbon, and E_H are the major parameters influencing the K_d values. The relationship between calculated K_d values by a surface complexation model vs. E_H and pH with a constant carbonate concentration of 1 mM is plotted in Fig. 4. Calculated K_d values for a constant redox potential

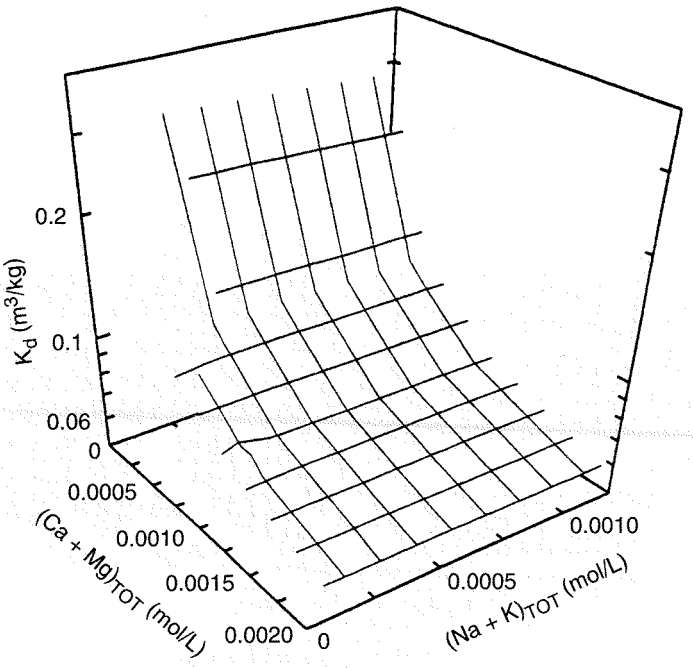

Fig. 1 The relationship between calculated K_d values for Cs by ion exchange vs. concentration of the alkali metals Na and K and concentration of Ca+Mg, when pH is 5.

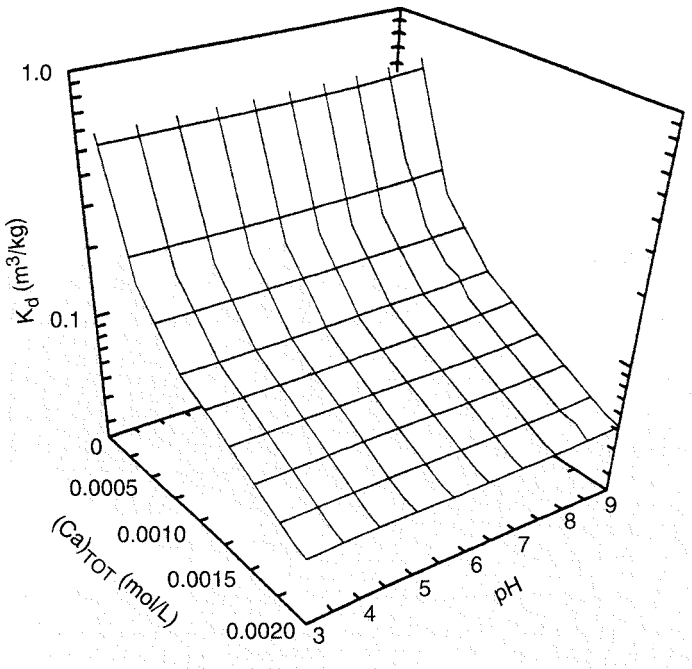

Fig. 2 The relationship between calculated K_d values for Ra by ion exchange and surface complexation models vs. pH and the concentration of Ca^{2+} for $[NA^+]_{TOT} + [K^+]_{TOT} = 0.00025$ mol/L.

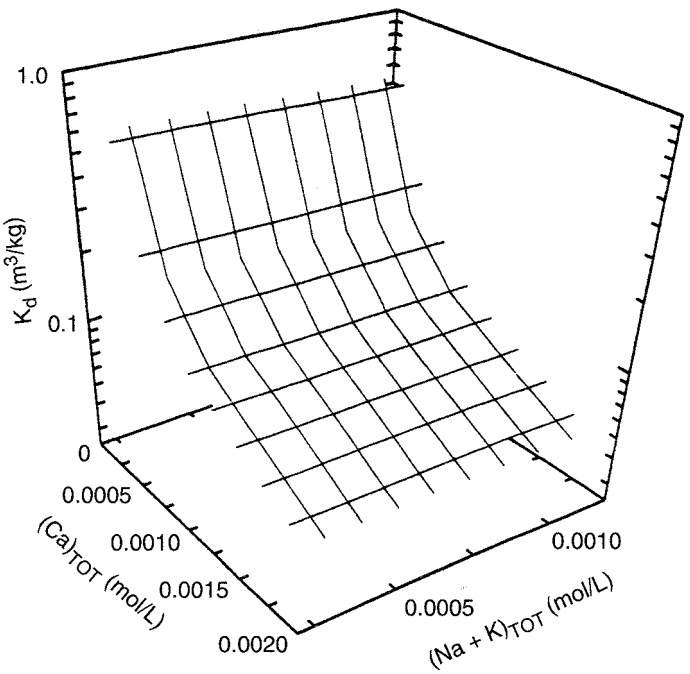

Fig. 3 The relationship between calculated K_d values for Ra both by ion exchange and surface complexation models vs. the calcium concentration and the alkali metal concentration for pH = 5.

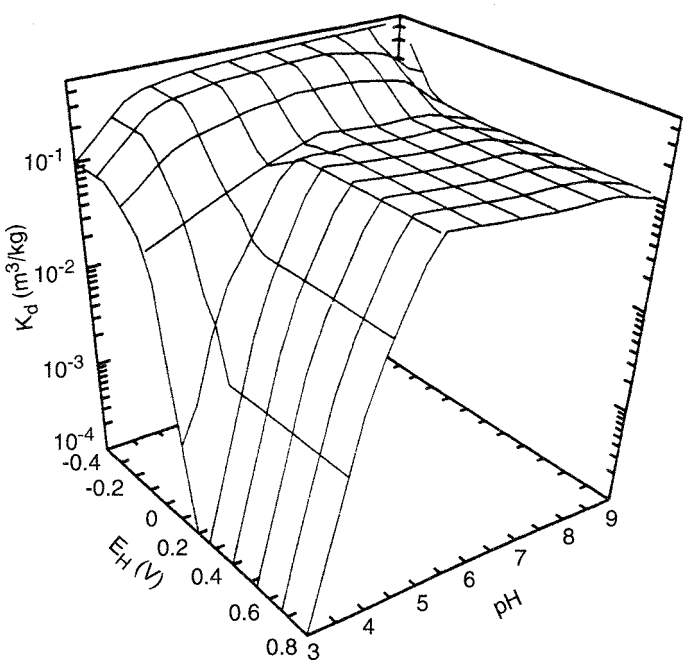

Fig. 4 The relationship between calculated K_d values by a surface complexation model vs. pH and redox potential, E_H, when $\left[CO_3^{2-}\right]_{TOT}$ = 0.001 mol/L.

(0.6 V) are shown in Fig. 5 as a function of the content of inorganic carbon and pH. As shown in Fig. 4, reducing conditions gave the highest K_d values. The effect of pH increases considerably under oxidizing conditions. Under such conditions, in combination with pH values above 6, the K_d values obtained are about 0.1 m^3/kg. When the concentration of inorganic carbon was high and pH values were higher than 6, the K_d values decreased considerably. Calculated K_d values are about 0.1 m^3/kg, considering normal values of alkalinity and pH for soil and sediments. These values agree with those used earlier in dose assessments, as discussed in the "Elements" section and elsewhere.[6]

Neptunium

The K_d values were high under reducing conditions (see Fig. 6). This agrees with the few investigations made under reducing conditions,[50,51] as well as the low solubility of the tetravalent neptunium, which is the dominating state under reducing conditions.[52] The pH dependence of K_d shown in Fig. 6 agrees with experimental studies of the adsorption behavior of neptunium in soil.[53–57]

Plutonium

In contrast to neptunium, the K_d values were not as sensitive to E_H at neutral and acid conditions (see Fig. 7), where the K_d values are plotted against pH and E_H for a constant total inorganic carbon content of 61 mg/L. The dependence on pH, however, is clearly seen in Fig. 7. Experimental studies of pH adsorption have also shown this, but the dependence is not so fully pronounced as our calculations demonstrate.[41,58] The extreme values are due to extreme combinations of chemical conditions not occurring naturally. There is a large scatter of values in the literature concerning K_d values for Pu (see, for example, Ref. 59 and the recent compilation by Albinsson[58]).

CONCLUSIONS

This study was made to determine whether surface complexation models for sorption would be applicable for performing assessment studies for radioactive waste repositories. Many of the surface complexation equilibrium constants had to be estimated to perform the

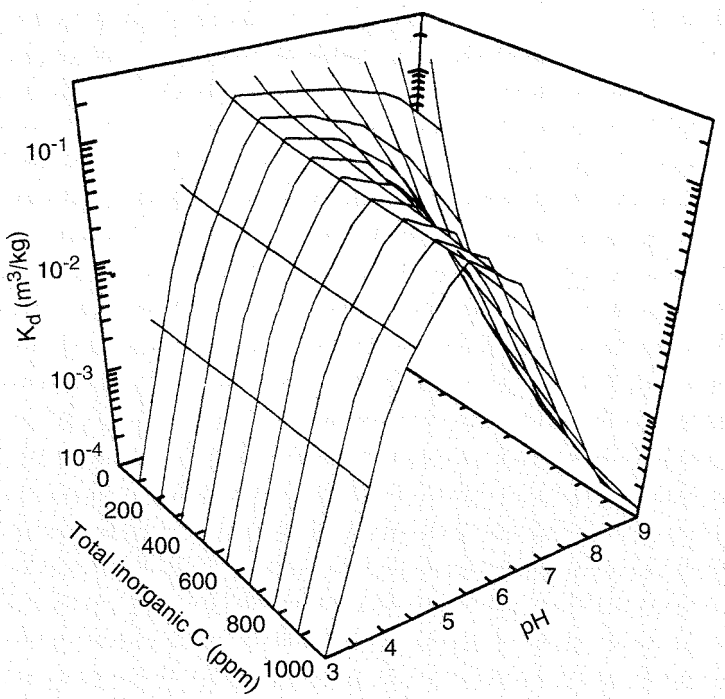

Fig. 5 The relationship between calculated K_d values for U by a surface complexation model vs. pH and inorganic carbon concentration for redox potential E_H = 0.6 V.

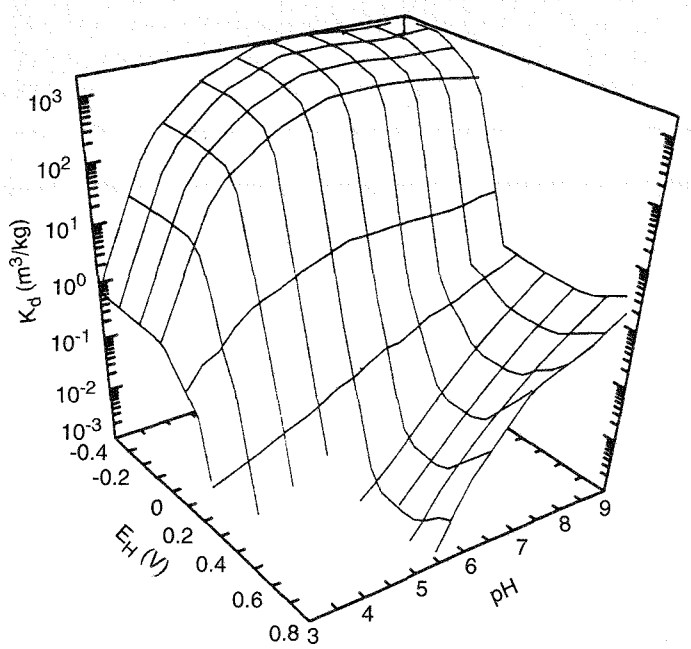

Fig. 6 The relationship between calculated K_d values for Np by a surface complexation model vs. pH and redox potential, E_H, for $\left[CO_3^{2-}\right]_{TOT}$ = 0.001 mol/L.

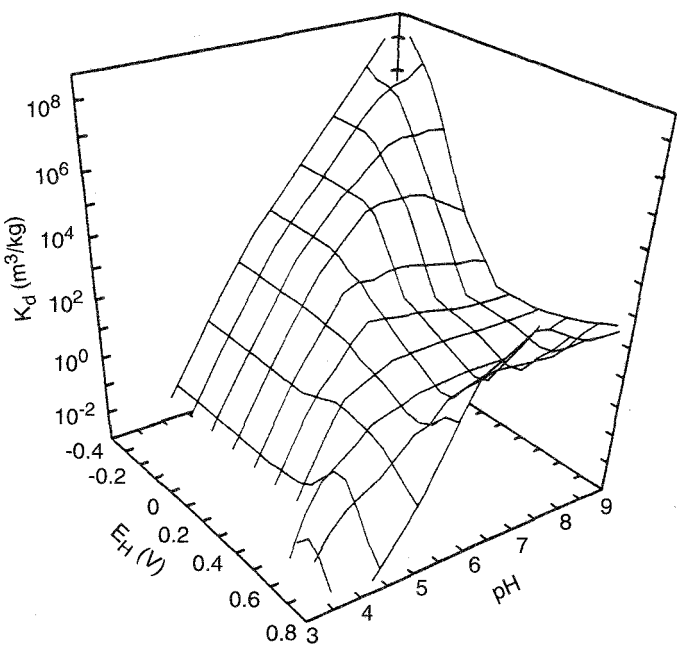

Fig. 7 The relationship between calculated K_d values for Pu by a surface complexation model vs. pH and redox potential, E_H, and pH for $\left[CO_3^{2-}\right]_{TOT}$ = 0.001 mol/L.

calculations. Nevertheless, the results show that the triple-layer surface complexation model is suitable for the estimation of the dependence of K_d on chemical parameters. A combination of experimental and estimated surface complexation constants was used for all studied actinides. This method appeared to give a correct variation of calculated K_d values. Nevertheless, this should not be interpreted as a suggestion that experimental values are unnecessary. Instead, we believe that this work might contribute to an increase in the usefulness of surface complexation models for the understanding of the results obtained in natural systems and in laboratory measurements. Results from ongoing experimental efforts will be added in the future to the model presented here to allow more accurate K_d predictions.

Reasonable parameter values were used for the properties of the sorbing phase. The calculated K_d values depend on, for example, the concentration of sorption sites per liter of aqueous solution, or the total cation-exchange capacity per liter. This is affected by several parameters, such as the specific cation-exchange capacity of the clays, or the iron–oxyhydroxide percentage of the soil or sediment, or the assumed specific surface area. In other words, the system modeled is overdefined; Eq. 3 shows the interdependence of some of the parameters to consider. If some of them are quantified by, for example, chemical analysis of a given soil, the specific surface area might still be an unknown parameter, which can be adjusted to fit some in situ migration experiments. Our calculations show, however, that refitting surface complexation equilibrium constants to specific sorption data on soil or sediment samples will, in general, create a set of surface complexation reactions that do not adequately represent sorption under different experimental conditions. No advantage would thus be gained as compared with the use of the K_d concept. The power of the surface complexation model is instead that equilibrium constants obtained under well-controlled laboratory conditions on well-determined minerals can easily be used to estimate sorption under a much wider variety of conditions in the field. If equilibrium constants are not available for the surface complexation of a given metal ion, a chemical analogue may be used to obtain plausible K_d values that reflect the correct dependence on such chemical parameters as pH.

Care must be taken when surface complexation equilibrium constants are extracted from experimental studies. This study showed that it is necessary to do some preliminary calculations to check that it is possible to reproduce the experimental fractions of metal sorbed and the measured dissolved metal concentrations reported in the literature. Differences in the aqueous data base and in the properties of the solid phase might require a readjustment of the $\log_{10} K^{int}$ values to allow reproduction of reported experiments. Furthermore, these preliminary calculations indicate whether the reported sorption reactions refer to inner- or outer-sphere complexes.

If some environmental conditions are known, such as the concentration of calcium, the K_d value for radium could be estimated more precisely with the method described here. However, the sorption of cesium consists of such complicated processes that further analysis needs to be done to judge the applicability of ion-exchange models for performance assessment.

One phenomenon that is not considered in our calculations is the formation of solid solutions, which might be important, especially for the system $Ra^{2+}/Ca^{2+}/CO_3^{2-}$. Some approximate calculations may be done, as proposed by Langmuir and Riese,[26] if the radium content of the calcium carbonate in a soil or sediment is known. Most soils and sediments in the Swedish biosphere scenarios are very poor in carbonate, however, and therefore the formation of solid solution was not considered in this work.

ACKNOWLEDGMENTS

The support from the Swedish Nuclear Fuel and Waste Management Company for this study is gratefully acknowledged. We thank Dr. B. Hallberg for help with this manuscript and Dr. I. Aggeryd and Mr. S. Nordlinder for valuable comments.

REFERENCES

1. U. Bergström and S. Nordlinder, Uncertainties Related to Dose Assessments for High Level Waste Disposal, *Nucl. Saf.*, 32(3): 391-402 (July–September 1991).
2. NEA PSAG User Group, *Psacoin Level 1B Intercomparison*, R. Klos, J. E. Sinclair, C. Torres, J. S. Martin, D. A. Galson, and U. Bergström (Eds.), Nuclear Energy Agency, OECD Publications, Paris, 1993.
3. H. Grogan (Ed.), *Irrigation with Contaminated Groundwater*, BIOMOVS TR 6, Swedish Radiation Protection Institute, Stockholm, 1989.
4. C. Jones (Ed.), *Transport of Radionuclides to Root-Zone Soil from Contaminated Groundwater*, BIOMOVS TR 9, Swedish Radiation Protection Institute, Stockholm, 1989.
5. U. Bergström, *Dose and Dose Commitment Calculations from Groundwater Borne Radioactive Elements Released from a Repository for Spent Nuclear Fuel*, Report SKBF-KBS-TR-83-49, Stockholm, 1983.

6. U. Bergström and S. Nordlinder, *Individual Radiation Doses from Unit Releases of Long-Lived Radionuclides*, Report SKB-TR 90-09 (STUDSVIK-NS-90-42), Stockholm, 1990.
7. I. Puigdomènech and U. Bergström, *Calculated Distribution of Radionuclides in Soils and Sediments* (to be issued as an SKB Technical Report, TR 95-??, Swedish Nuclear Fuel and Waste Management Co., Stockholm, 1995).
8. W. Stumm and J. J. Morgan, *Aquatic Chemistry*, 2nd edition, p. 780, John Wiley & Sons, New York, 1981.
9. G. A. Cederberg, R. L. Street, and J. O. Leckie, Groundwater Mass Transport and Equilibrium Chemistry Model for Multicomponent Systems, *Water Resour. Res.*, 21: 1095-1104 (1985).
10. L. Balistrieri and J. W. Murray, Surface of Goethite (FeOOH) in Sea Water, in Chemical Modeling in Aqueous Systems, Speciation, Sorption, Solubility and Kinetics, E. A. Jenne (Ed.), *ACS Symp. Ser.*, 93: 275-298 (1979).
11. A. C. M. Bourg, Adsorption of Trace Elements by Suspended Particulate Matter in Aquatic Systems, Section 8 in *The Determination of Trace Metals in Natural Waters*, T. S. West and H. W. Nurnberg (Eds.), pp. 256-286, IUPAC, Blackwell Scientific Publications, Oxford, 1988.
12. D. A. Dzombak and F. M. M. Morel, *Surface Complexation Modeling*, John Wiley & Sons, New York, 1990.
13. L. J. Evans, Chemistry of Metal Retention by Soils, *Environ. Sci. Technol.*, 23(9): 1046-1056 (1989).
14. K. F. Hayes and J. O. Leckie, Mechanism of Lead Ion Adsorption at the Goethite–Water Interface, in Geochemical Processes at Mineral Surfaces, J. A. Davis and K. F. Hayes (Eds.), *ACS Symp. Ser.*, 323: 114-141 (1986).
15. B. D. Honeyman and P. H. Santschi, Metals in Aquatic Systems, *Environ. Sci. Technol.*, 22(8): 862-871 (1988).
16. D. B. Kent, V. S. Tripathi, N. B. Ball, J. O. Leckie, and M. D. Siegel, *Surface-Complexation Modeling of Radionuclide Adsorption in Subsurface Environments*, Report NUREG/CR-4807 (SAND-86-7175), and Stanford University Technical Report 294, 1988.
17. J. P. McKinley and E. A. Jenne, Experimental Investigation and Review of the "Solids Concentration" Effect in Adsorption Studies, *Environ. Sci. Technol.*, 25(12): 2082-2087 (1991).
18. F. M. M. Morel, J. G. Yeasted, and J. C. Westall, Adsorption Models: A Mathematical Analysis in the Framework of General Equilibrium Calculations, Chapter 7 in *Adsorption of Inorganics at Solid–Liquid Interfaces*, M. A. Anderson and A. J. Rubin (Eds.), pp. 263-294, Ann Arbor Science Publishing, Inc., 1981.
19. P. W. Schindler and W. Stumm, The Surface Chemistry of Oxides, Hydroxides, and Oxide Minerals, in *Aquatic Surface Chemistry*, W. Stumm (Ed.), pp. 83–110, John Wiley & Sons, New York, 1987.
20. R. W. Smith and E. A. Jenne, Recalculation, Evaluation, and Prediction of Surface Complexation Constants for Metal Adsorption on Iron and Manganese Oxides, *Environ. Sci. Technol.*, 25(3): 525-531 (1991).
21. J. C. Westall, Adsorption Mechanisms in Aquatic Surface Chemistry, in *Aquatic Surface Chemistry*, W. Stumm (Ed.), pp. 3-32, John Wiley & Sons, New York, 1987.
22. J. Westall and H. Hohl, A Comparison of Electrostatic Models for the Oxide/Solution Interface, *Adv. Colloid Interface Sci.*, 12(4): 265-294 (1980).
23. G.-T. Yeh and V. S. Tripathi, A Model for Simulating Transport of Reactive Multispecies Components: Model Development and Demonstration, *Water Resour. Res.*, 27(12): 3075-3094 (1991).
24. C. Papelis, K. F. Hayes, and J. O. Leckie, *HYDRAQL: A Program for the Computation of Chemical Equilibrium Composition of Aqueous Batch Systems Including Surface-Complexation Modeling of Ion Adsorption at the Oxide/Solution Interface*, Technical Report 306, Deptartment of Civil Engineering, Stanford University, 1988.
25. I. Grenthe, J. Fuger, R. J. Lemire, A. B. Muller, C. Nguyen-Trung, and H. Wanner, *Chemical Thermodynamics of Uranium*, H. Wanner and I. Forest (Eds.), Elsevier Science Publishing Co., Amsterdam, 1992.
26. D. Langmuir and A. C. Riese, The Thermodynamic Properties of Radium, *Geochim. Cosmochim. Acta*, 49(7): 1593-1601 (1985).
27. R. J. Lemire and F. Garisto, *The Solubility of U, Np, Pu, Th, and Tc in a Geological Disposal Vault for Used Nuclear Fuel*, Report AECL-10009, 1989.
28. I. Puigdomènech and J. Bruno, *Plutonium Solubilities*, Report SKB-TR 91-04, 1991.
29. K. F. Hayes, G. Redden, E. Wendell, and J. O. Leckie, Surface Complexation Models: An Evaluation of Model Parameter Estimation Using FITEQL and Oxide Mineral Titration Data, *J. Colloid Interface Sci.*, 142(2): 448-469 (1991).
30. L. Lövgren, S. Sjöberg, and P. W. Schindler, Acid/Base Reactions and Al(III) Complexation at the Surface of Goethite, *Geochim. Cosmochim. Acta*, 54(5): 1301-1306 (1990).
31. *Environ. Sci. Technol.*, 26: 1251-1954 (1992), comment on Ref. 20.
32. K. A. Bond, J. E. Cross, and F. T. Ewart, Thermodynamic Modelling of the Effect of Organic Complexants on Sorption Behaviour, *Radiochim. Acta*, 52/53(2): 433-437 (1991).
33. K. A. Bond, A. Haworth, S. M. Sharland, A. C. Smith, and C. J. Tweed, Modelling Studies of the Sorption of Uranium and Plutonium in the Far Field of a Nuclear Waste Repository, in *Scientific Basis for Nuclear Waste Management XIV*, T. A. Abrajano and L. H. Johnson (Eds.), pp. 585-592, Mater. Res. Soc., Pittsburgh, Pa., 1991.
34. K. A. Bond and C. J. Tweed, *Geochemical Modelling of the Sorption of Tetravalent Actinides*, Report NSS-R-227 (AEA-D and R-0072), 1991.
35. T. E. Payne and T. D. Waite, Surface Complexation Modelling of Uranium Sorption Data Obtained by Isotope Exchange Techniques, *Radiochim. Acta*, 52/53(2): 487-493 (1991).
36. D. Read, P. J. Hooker, M. Ivanovich, and A. Milodowski, A Natural Analogue Study of an Abandoned Uranium Mine in Cornwall, England, *Radiochim. Acta*, 52/53(2): 349-356 (1991).
37. A. Davis and D. D. Runnells, Geochemical Interactions Between Acidic Tailings Fluid and Bedrock: Use of the Computer Model MINTEQ, *Appl. Geochem.*, 2(3): 231-241 (1987).
38. J. Gruber, Natural Geochemical Isolation of Neutron-Activated Waste: Scenarios and Equilibrium Models, *Nucl. Chem. Waste Manage.*, 8(1): 13-32 (1988).
39. D. Stammose and J-M. Dolo, Sorption of Americium at Trace Level on a Clay Mineral, *Radiochim. Acta*, 51(4): 189-193 (1990).
40. V. Moulin, D. Stammose, and G. Ouzounian, Actinide Sorption at Oxide–Water Interfaces: Applications to an Alumina and Amorphous Silica, *Appl. Geochem.*, Suppl. 1: 163-166 (1992).
41. A. L. Sanchez, J. W. Murray, and T. H. Sibley, The Adsorption of Plutonium IV and V on Goethite, *Geochim. Cosmochim. Acta*, 49(11): 2297-2307 (1985).

42. C. E. Cowan, J. M. Zachara, and C. T. Resch, Cadmium Adsorption on Iron Oxides in the Presence of Alkaline-Earth Elements, *Environ. Sci. Technol.*, 25(3): 437-446 (1991).
43. D. C. Girvin, L. L. Ames, A. P. Schwab, and J. E. McGarrah, Neptunium Adsorption on Synthetic Amorphous Iron Oxyhydroxide, *J. Colloid Interface Sci.*, 141(1): 67–78 (1991).
44. C-K. D. Hsi and D. Langmuir, Adsorption of Uranyl onto Ferric Oxyhydroxides: Application of the Surface Complexation Site-Binding Model, *Geochim. Cosmochim. Acta*, 49(9): 1931-1941 (1985).
45. K. H. Lieser and T. Steinkopff, Chemistry of Radioactive Cesium in the Hydrosphere and in the Geosphere, *Radiochim. Acta*, 46(1): 39-47 (1989).
46. M. G. M. Bruggenwert and A. Kamphorst, Survey of Experimental Information on Cation Exchange in Soil Systems, Chapter 5 in *Soil Chemistry B. Physico-Chemical Models*, G. H. Bolt (Ed.), p. 141, Elsevier Science Publishing Co., Amsterdam, 1982.
47. H. Wanner, Modeling Interaction of Deep Groundwaters with Bentonite and Radionuclide Speciation, *Nucl. Technol.*, 79: 338 (1987).
48. R. N. J. Comans, M. Haller, and P. De Preter, Sorption of Cesium on Illite: Non-Equilibrium Behaviour and Reversibility, *Geochim. Cosmochim. Acta*, 55(2): 433-440 (1991).
49. J. K. Miettinen, A. Nikula, and S. Leskinen, Distribution Coefficients of Radionuclides Between Finnish Soils and Groundwater, *Environmental Migration of Long-Lived Radionuclides*, Report STI/PUB/597, pp. 153-158, IAEA, Vienna, 1982.
50. Y. Albinsson, B. Christiansen-Satmark, J. Engkvist, and T. C. Johansson, Transport of Actinides and Tc Through a Bentonite Backfill Containing Small Quantities of Iron or Copper, *Radiochim. Acta*, 52/53: 283 (1991).
51. K. H. Lieser and U. Muhlenweg, Neptunium in the Hydrosphere and in the Geosphere: I. Chemistry of Neptunium in the Hydrosphere and Sorption of Neptunium from Groundwaters on Sediments Under Aerobic and Anaerobic Conditions, *Radiochim. Acta*, 46: 27-35 (1988).
52. B. Allard and B. Torstenfelt, *Actinide Solubilities and Speciation in Repository Environment*, Report NAGRA-NTB-85-18, 1985.
53. Y. Sakamoto, M. Konishi, K Shirahashi, M. Senoo, and N. Moriyama, Adsorption Behaviour of Neptunium for Soil, *Radioac. Waste Manage. Nucl. Fuel Cycle*, 15: 13-25 (1990).
54. R. E. Meyer, W. D. Arnold, and F. I. Case, *Valence Effects on the Sorption of Nuclides on Rocks and Minerals II*, Report NUREG/CR-4114 (ORNL-6137), 1985.
55. G. W. Beall, B. Allard, T. Krajewski, and G. D. O'Kelley, Chemical Reactions in the Bedrock–Groundwater System of Importance for the Sorption of Actinides, *Sci. Basis Nucl. Waste Manage.*, 2: 625-631 (1980).
56. K. Andersson, B. Torstenfelt, and B. Allard, Sorption Behavior of Long-Lived Radionuclides in Igneous Rock, in *Environmental Migration of Long-Lived Radionuclides*, Report STI/PUB/597, pp. 111–131, IAEA, Vienna, 1982.
57. G. Bidoglio and A. De Plano, Neptunium Migration in Salt Brine Aquifers, *Nucl. Technol.*, 74(3): 307-316 (1986).
58. Y. Albinsson, *Sorption of Radionuclides in Granitic Rock*, Report SKB Technical Note 91-07, Stockholm, 1991.
59. J. J. W. Higgo, *Radionuclide Interactions with Marine Sediments*, Report NSS/R-142, 1987.

Operating Experiences

Edited by G. A. Murphy

Reactor Shutdown Experience

Compiled by J. W. Cletcher[a]

This section presents a regular report of summary statistics relating to recent reactor shutdown experience. The information includes both numbers of events and rates of occurrence. It was compiled from data about operating events entered into the SCSS data system by the Nuclear Operations Analysis Center at the Oak Ridge National Laboratory and covers the six-month period of July 1 to December 31, 1994. Cumulative information, starting from May 1, 1984, is also shown. Updates on shutdown events included in earlier reports are excluded.

Table 1 lists information on shutdowns as a function of reactor power at the time of the shutdown for both boiling-water reactors (BWRs) and pressurized-water reactors (PWRs). Only reactors in commercial operation at the start of the reporting period (July 1, 1994) are included. The second column for each reactor type shows the annualized shutdown rate for the reporting period. The third and fourth columns list cumulative data (numbers and rates) starting as of May 1, 1984.

Table 1 Reactor Shutdowns by Reactor Type and Percent Power at Shutdown[a] (Period Covered is the Second Half of 1994)

	BWRs (37)				PWRs (76)			
Reactor power (P), %	Number	Shutdown rate (annualized for period)	Cumulative number	Cumulative shutdown rate per reactor year[b]	Number	Shutdown rate (annualized for period)	Cumulative number	Cumulative shutdown rate per reactor year[c]
0	5	0.27	670	1.78	10	0.26	469	0.63
$0 < P \leq 10$	2	0.11	131	0.35	4	0.10	170	0.23
$10 < P \leq 40$	5	0.27	164	0.44	3	0.08	319	0.43
$40 < P \leq 70$	5	0.27	155	0.41	2	0.05	177	0.24
$70 < P \leq 99$	11	0.59	376	1.00	2	0.05	511	0.68
$99 < P \leq 100$	12	0.64	478	1.27	34	0.89	1172	1.57
Total	40	2.15	1974	5.24	55	1.44	2818	3.76

[a]Data include shutdowns for all reactors of the designated type while in commercial service during all or part of the period covered. The cumulative data are based on the experience while in commercial service since the starting date of Jan. 1, 1984, through the end of the reporting period; it includes the commercial service of reactors now permanently or indefinitely shut down.

[b]Based on cumulative BWR operating experience of 376.43 reactor years.

[c]Based on cumulative PWR operating experience of 748.82 reactor years.

[a]Oak Ridge National Laboratory.

Table 2 shows data on shutdowns by shutdown type: *Shutdowns required by Technical Specifications* are automatic scrams under circumstances where such a shutdown was required; *Intentional or required manual reactor protection system actuations* are manual shutdowns in which the operators, for reasons that appeared valid to them, took manual actions to actuate features of the reactor protection system; *Required automatic reactor protection system actuations* are actuations that the human operators did not initiate but that were needed; *Unintentional or unrequired manual reactor protection system actuations* are essentially operator errors in which the human operators took action not really called for; and *Unintentional or unrequired automatic reactor protection system actuations* are instrumentation and control failures in which uncalled-for protective actuations occurred. Only reactors in commercial operation are included. The second column for each type of reactor shows the annualized rate of shutdowns for the reporting period. Cumulative information is shown in the third and fourth columns for each reactor type.

Table 3 lists information about shutdowns by reactor age category, both total numbers and rates in that category; it also shows cumulative results. Note that the age groups are not cohorts; rather reactors move into and out of the specified age groups as they age. The reactor age as used in this table is the number of full years between the start of commercial operation and the beginning of the reporting period (July 1, 1994, for this issue). The first line of this table gives the information for reactors licensed for full power but not yet in commercial operation on that date.

Table 2 Reactor Shutdowns by Reactor Type and Shutdown Type[a] (Period Covered is the Second Half of 1994)

	BWRs (37)				PWRs (76)			
Shutdown (SD) type	Number	Shutdown rate (annualized for period)	Cumulative number	Cumulative shutdown rate per reactor year[b]	Number	Shutdown rate (annualized for period)	Cumulative number	Cumulative shutdown rate per reactor year[c]
SDs required by Technical Specifications	7	0.38	258	0.69	9	0.24	409	0.55
Intentional or required manual reactor protection system actuations	6	0.32	194	0.52	12	0.31	370	0.49
Required automatic reactor protection system actuations	17	0.91	923	2.45	30	0.78	1589	2.12
Unintentional or unrequired manual reactor protection system actuations	0	0.00	9	0.02	0	0.00	19	0.03
Unintentional or unrequired automatic reactor protection system actuations	10	0.54	590	1.57	4	0.10	431	0.58
Total	40	2.15	1974	5.24	55	1.44	2818	3.76

[a]Data include shutdowns for all reactors of the designated type while in commercial service during all or part of the period covered. The cumulative data are based on the experience while in commercial service since the starting date of Jan. 1, 1984, through the end of the reporting period; it includes the commercial service of reactors now permanently or indefinitely shut down.

[b]Based on cumulative BWR operating experience of 376.43 reactor years.

[c]Based on cumulative PWR operating experience of 748.82 reactor years.

Table 3 Reactor Shutdowns by Reactor Type and Reactor Age[a] (Period Covered is the Second Half of 1994)

Years in commercial operation (C.O.)	BWRs (37)						PWRs (76)					
	Exposure during the period (in reactor years)	Number		Shutdown rate (annualized for the period)	Cumulative number	Cumulative shutdown rate per reactor year	Exposure during the period (in reactor years)	Number		Shutdown rate (annualized for the period)	Cumulative number	Cumulative shutdown rate per reactor year
		Reactors	Shutdowns					Reactors	Shutdowns			
Not in C.O.[b]	0.504	1	0	0.00	330	22.02	0.000	0	0	0.00	336	34.24
First year of C.O.	0.000	0	0	0.00	121	9.00	0.090	1	0	0.00	281	9.96
Second through fourth year of C.O.	0.000	0	0	0.00	264	6.29	0.665	3	2	3.01	528	5.57
Fifth through seventh year of C.O.	2.294	5	3	1.31	181	4.23	4.298	10	6	1.40	324	3.20
Eighth through tenth year of C.O.	3.496	9	10	2.86	213	5.15	7.001	15	13	1.86	383	3.63
Eleventh through thirteenth year of C.O.	1.262	4	2	1.58	273	5.63	3.841	10	3	0.78	502	4.17
Fourteenth through sixteenth year of C.O.	0.504	1	1	1.99	397	6.16	2.322	7	5	2.15	369	3.22
Seventeenth through nineteenth year of C.O.	1.925	5	1	0.52	281	4.52	6.103	13	9	1.47	263	2.61
Twentieth through twenty-second year of C.O.	5.459	13	11	2.01	166	4.29	10.100	22	13	1.29	109	1.99
Twenty-third through twenty-fifth year of C.O.	3.025	8	9	2.97	58	3.58	2.355	8	3	1.27	33	2.04
Twenty-sixth through twenty-eighth year of C.O.	0.170	2	0	0.00	8	2.53	1.008	2	1	0.99	17	2.43
Twenty-ninth through thirty-first year of C.O.	0.000	0	0	0.00	9	3.00	0.000	0	0	0.00	5	1.67
Thirty-second through ninety-ninth year of C.O.	0.504	1	3	5.96	3	3.94	0.504	1	0	0.00	0	0.00
Total	19.143		40	2.09	2304	5.89	38.286		55	1.44	3150	4.15

[a]Age is defined to be the time (in years) from the start of commercial operation to the time of the shutdown event, except for the first line, which lists reactors not yet in commercial service (see b below).
[b]This category includes reactors licensed for full-power operation but not yet in commercial operation. During this reporting period reactors in this category included 1 BWR (Shoreham) and no PWRs.

U.S. Nuclear Regulatory Commission Information and Analyses

Operating Experience Feedback Report—Reliability of Safety-Related Steam Turbine-Driven Standby Pumps Used in U.S. Commercial Nuclear Power Plants

John R. Boardman[a]

Abstract: *Pump failure experience is collected by two primary means: 1) Licensee Event Reports, and 2) Nuclear Plant Reliability Data System failure reports. Certain safety-related turbine-driven standby pumps were identified by these data systems as experiencing significant ongoing repetitive failures of their turbine drivers, resulting in low reliability of the pump units. The root causes of identified failures were determined, and actions to preclude these repetitive failures were identified.*

INTRODUCTION AND SCOPE

This study of safety-related standby turbines was initiated because of the continuing and repetitive operational failures of these turbine assemblies (turbines with their associated governors, valves, valve operators, overspeed trip mechanisms, circuit breakers, and fuses) used as drivers for safety-related standby pumps installed in U.S. commercial nuclear power generating plants.[1] In pressurized water reactor (PWR) plants, the turbine-driven pumps are used as an independent and redundant means of removing reactor core heat by providing Auxiliary Feed Water (AFW) to the steam generators in the event of the operational failure of the Main Feed Water (MFW) system. In Boiling Water Reactor (BWR) plants, these turbine-driven pumps are used in the High Pressure Cooling Injection (HPCI) and Reactor Core Isolation Cooling (RCIC) systems to provide automatically initiated redundant and independent sources of reactor grade water to assure reactor core heat removal under specified off-normal and accident conditions of plant operation when the MFW system is not available.

Pump failure experience is collected by two primary means: 1) Licensee Event Reports (LERs), and 2) the Nuclear Plant Reliability Data System (NPRDS) failure reports. NPRDS failure reports relating to these turbine assemblies for the years 1985 through 1992 were analyzed, as were LER abstracts from 1974 through 1992. When additional details were needed, NRC Office of Nuclear Reactor Regulation project managers and resident inspectors were contacted.

Over 60 NRC and industry generic communications and studies addressing these standby pump turbine-drivers were reviewed. Plant Updated Safety Analysis Reports (USARs), recent individual licensee plant annual reports to the NRC, and NRC inspection reports were also reviewed for information pertinent to standby pump turbine-driver reliability.

[a]U.S. Nuclear Regulatory Commission, Office for Analysis and Evaluation of Operational Data, Safety Programs Division, Washington, DC 20555 USA. Phone: (301) 415-6354; Fax: (301) 415-6359.

Appropriate personnel were contacted at selected plants to gain a better insight into the details of specific failures that had been reported. DRESSER-RAND Terry-Turbodyne (Terry), and Woodward, the manufacturers of the standby turbines and their governors, respectively, were also contacted to gain a better understanding of the components provided by each company, and to discuss failure initiators involving the design, installation, modification, maintenance, and operation of these components.[a]

Recurring failures identified during this study were analyzed for root causes and failure initiators that had not been previously addressed in generic communications.

STANDBY PUMP–TURBINE DESIGN FACTORS AFFECTING RELIABILITY

All Terry turbines use governors manufactured by the Woodward Governor Company (Woodward). The General Electric Company (GE), the Nuclear Steam System Supplier (NSSS), was the designer for the HPCI and RCIC turbines and their governor systems. The design of AFW turbine installations, including the governor systems, was performed by the Architect–Engineer (AE) for each plant, and appears to be essentially plant specific. The scope of design included standby service in a cold shut-down condition and turbine cold quick-starts.

Turbine cold quick-starts are required to meet pump starting time limits in plant USARs for AFW, RCIC, and HPCI Engineered Safety Features (ESF) actuations, and other specified actuations to meet the reactor safety analysis requirements of the NSSS vendors. A cold start typically has been considered to be a start that occurs when a turbine has not been operated for at least 72 hours. Turbine "quick-starts" occur when the turbines are required to reach rated speed and pump flow [speeds vary from 3550 to 5900 revolutions per minute (rpm)] in 30 to 120 seconds.

Some AFW turbines use the trip and throttle valve supplied by Terry as the steam stop valve. This design requires the trip and throttle valve to be closed at turbine startup, and at startup to rapidly open coordinated with the position of the governor valve to prevent an overspeed trip. Other AFW turbines have separate steam stop valves. This design permits the trip and throttle valve to be open at startup as designed by the turbine manufacturer. This configuration requires the opening speed of the turbine steam stop valve to be coordinated with governor valve position to prevent a turbine overspeed trip during a cold quick-start.

Many turbines do not have pressurized lubricating oil systems to provide lubrication at startup, others have shaft-driven lube oil pumps which do not provide oil pressure until the turbine is operating. Except for one AFW turbine, only the HPCI turbines were identified as having an auxiliary motor-driven lube oil pump to provide prelubrication at turbine startup. Safety-related standby turbines typically utilize turbine lubricating oil as the hydraulic operating fluid for their governors or valve actuators.

Basic governor types include both mechanical/hydraulic governors and electric governors with an electrical/mechanical/hydraulic actuator. HPCI and RCIC turbines use the same basic electric governor, although the HPCI governor fails high and the RCIC governor fails low. AFW turbines use several variations and modifications of Woodward governors. Governor modifications appear to be plant and pump/turbine specific, customized to control all flow conditions that the pump will encounter. Turbine governors having the same model numbers may not be interchangeable *per se* because of optional parts and subassemblies, such as buffer springs, which can significantly affect governor operation.

The physical location of AFW turbines varies widely between plants, resulting in different ambient temperature and humidity ranges with their environmental effects on turbine deterioration, maintenance, and operational performance.

Normal commercial applications for these turbines and their speed control governors involve continuous operation. Normal turbine startup is slow and preceded by proper warmup of the steam lines and turbine to minimize transients and wear. By contrast, standby turbine-driven pumps in nuclear power plant applications are normally in a cold shutdown condition in areas where humidity is typically high, and temperatures can vary from high to almost 0°C (32°F) depending on the specific plant. Leaking steam inlet valves can worsen the situation by contaminating the turbine lubricating oil with water, which is a primary cause of failure for governors and actuators. These standby conditions can lead to accelerated deterioration of the turbine governor that may not be identifiable until pump–turbine startup.

Reliable operation of Terry governor valves to meet design demands and prevent overspeed trips during cold quick-starts is dependent upon governor operation,

[a]The use of such terms as "Terry-Turbodyne stated . . .," or "Woodward stated. . .," are used to indicate information provided by the manufacturer's staff and not an official company position.

including a rapid buildup of hydraulic pressure in the governor system. For most standby turbines, the rate of governor speed change during turbine startup is controlled by a ramp generator circuit for electric governors, and by a ramp bushing for mechanical–hydraulic governors.

Woodward type PGD mechanical–hydraulic governors and some earlier Woodward type EG-M electrical governor systems were not provided with speed increase ramp features to reduce overspeed during quick-starts. This fact could contribute to increased standby turbine overspeed trips during cold quick-starts with these governors.

Terry turbine lube oil is an International Standards Organization (ISO) Viscosity number 32 (Society of Automotive Engineers [SAE] 30) or 10W-30[a] weight oil, with possible additives for turbine service, including vapor inhibitor (VI) additives to prevent the turbine from rusting during standby service. Oils of other types and grades are permitted for governor use within certain bounding viscosity limits that are defined in Woodward technical literature, which shows that the maximum oil viscosity (minimum fluidity) for reliable governor and actuator response during Terry turbine quick-starts is 300 Saybolt Seconds Universal (SSU). A standby turbine could trip on a cold quick-start because of viscous oil, but not trip on subsequent starts after the oil had circulated and become more fluid, resulting in the initial overspeed being declared spurious or unknown.

According to Woodward[2], an ISO-viscosity number 32 (SAE 30) weight oil would have a viscosity of 300 SSU at approximately 112°C (130°F) while an SAE 10W-30 oil would have a viscosity of 300 SSU at about 37°C (98°F). Woodward further states that governor oil should not be cooled below 38°C (100°F).[3]

Certain standby turbine installations are in environments that can be lower than these temperatures, especially AFW pump turbines which are installed out-of-doors. Though certain plants have heaters for their governor or actuator oil, heated oil typically is not circulated until turbine startup. As a result, governor and actuator oils of higher viscosities may not be sufficiently fluid to close the turbine governor valve in time to prevent a turbine overspeed trip during initial cold quick-starts at ambient temperatures between 38°C (100°F) and 54.4°C (130°F) (depending on the viscosity of the oil used).

[a]There is no equivalent ISO-Viscosity number for SAE multi-viscosity oils.

Woodward literature states that governor and EGR actuator operation can be sluggish due to excessive oil cooling. Certain reported unexplained overspeed trips during cold quick-starts could have been caused by viscous (thick) governor oil not being able to flow through small passages in the governor (or EGR actuator), such as the compensation needle valve port, and hence not rapidly close the governor valve to prevent a turbine overspeed trip.

Viscous oil makes it difficult for the integral oil pump of a governor, or actuator, to prime itself and to force oil though certain small passages of the governor and actuator in the initial few seconds of a turbine cold quick-start. Slow oil pressure build-up in hydraulic governors and actuators could result from inadequate pump priming with viscous oil, caused by the governor, or actuator, pump taking suction from the turbine oil sump through a small [~1/8-inch iron pipe size (IPS)] line.

An annual report of completed changes, tests, and experiments submitted to the NRC by the licensee of a BWR in 1989 stated that the plant had completed a RCIC turbine governor control oil system modification designated as Terry Design Improvement DI-6, revision 1, dated April 28, 1978.[b] This design improvement adds an oil sump to EGR actuators used with Woodward type EG-M governors. The oil sump provides an oil supply to the actuator's oil pump, enhancing oil pressure buildup and governor valve response time during a turbine cold quick-start.

SAFETY-RELATED TURBINE-DRIVEN STANDBY PUMP OPERATING EXPERIENCE

Operating experience has shown that failure detection for these standby pumps is sensitive to the way in which surveillance testing is carried out. The closer the testing mimics the cold quick-start profile of an actual demand, the more likely it is to disclose situations where the dynamic response of the turbine-governor-valve combination is out of calibration, resulting in an overshoot and trip on overspeed. Surveillance testing requirements have historically allowed a range of approaches, some of which do not fully test that dynamic response.

[b]General Electric Company, San Jose, California, stated that they issued field instructions to all affected BWRs in February 1976 defining the installation of the RCIC turbine EG-R actuator oil sump as identified in Terry Design improvement No. 6 (DI-6).

Certain plants have tested their safety-related standby turbines using cold quick-starts. Other plants have used hot quick-starts, which do not challenge the governor hydraulic system and turbine lube oil systems. Certain plants have used hot slow start surveillance tests, which preclude the turbine experiencing failures during cold quick-start transients, and do not reflect the safety-related operational requirements of standby turbines. AFW turbines typically experience more cold quick-starts than either HPCI or RCIC turbines. Depending upon specific plant requirements, the number of cold quick-starts could vary by a factor as great as eighteen times, from one test start per month to one per eighteen month fuel cycle. This variance in test methodologies can result in a proportional variance in failure rates between plants.

Over time, more plants have begun using cold quick-starts for routine surveillance testing as a result of industry and regulatory feedback. Such factors as the changing mixture of hot-start and cold-start testing, and plant-specific changes in maintenance practices in response to operational feedback, make it difficult to accurately quantify turbine reliability, or to trend failure frequency from NPRDS failure reports and LERs. Thus data on failure frequencies could be misleading. However, the continuing receipt of reports of the same repetitive failures observed for a number of years, as well as the emphasis given in industry improvement efforts, are strong indications that additional effort appears warranted.

For this study, 660 failures of safety-related turbines and their associated components, such as governors, valves, valve operators, overspeed trip mechanisms, circuit breakers, and fuses were identified covering the period of January 1985 through December 1989. Approximately 2000 LER abstracts were reviewed for the period of 1969 through 1989, in conjunction with individual plant USARs. Selected full text LERs were retrieved and reviewed. The analysis of these failures confirmed the continuing validity of earlier studies by the US NRC and by US industry that the most significant factors in failures of turbine-driven standby pumps have been the failures of the turbine drivers and their controls, especially during cold quick-start transients. For example, a historical overview of failures through 1986 for the auxiliary feedwater system, found that the standby turbine was a principal contributor to AFW system failures and the turbine governor.[4] An analysis of these failures confirmed the validity of earlier studies by the US NRC and by US industry that the most significant factors in failures of turbine-driven standby pumps have been the failures of the turbine drivers and their controls, especially during cold quick-start transients. The present study has extended the data review to include more recent failures, and has assembled an integrated and comprehensive compilation of the failure mechanisms or root causes of the reported failures, as well as remedies developed by the industry which should prove effective if implemented.[1] Details of the causes of turbine failures and the increase in reliability that has been generated through the operational feedback improvement process are given below.

STANDBY TURBINE FAILURES RELATED TO COLD QUICK-STARTS

Turbine failures during cold quick-start transients appear to primarily result from failures of governor control. Root cause determinations during this study, as well as other NRC studies, industry studies, and generic correspondence, are discussed in the following subsections.

Maintenance Related Failures Affecting Standby Turbine Cold Quick-Starts

A significant number of standby turbine governor failures identified during the study which appeared to be maintenance related are capable of being eliminated with the effective implementation of plant-specific preventive maintenance (PM) programs. Failure mechanisms identified from failure reports during this study include:

• *Operational failures of turbine and governor sub-components and piece-parts presently identified by the turbine manufacturer as being covered by periodic preventive maintenance, for which maintenance was not, or may not have been, performed completely, or with specified periodicities.* These failures range from the loss of turbine lube oil caused by a clogged filter, to an apparent failure to calibrate an electric governor ramp generator circuit causing an overspeed trip. A primary factor in plant-specific failures to accomplish the turbine manufacturer's identified periodic preventive maintenance appeared to be the use by certain plants of early versions of the turbine manual which did not contain all preventive maintenance dictated by turbine operational experience. Some plants still use their original manufacturer's manuals. Certain manuals were published as early as 1969 and do not contain the presently identified preventive maintenance actions and periodicities.

• *Failures caused by the mispositioning of valves in turbine lubricating oil systems.* Since these valves are part of the pump–turbine assembly ("skid mounted"), typically they may not have check lists to verify their position.

• *Governor failures caused by the failure of instrument air used for remote turbine speed setting with mechanical/hydraulic governors, and by the simultaneous mispositioning of the governor high speed stop.* The turbine manufacturer stated that the original design concept for these turbines did not include the use of the connection of instrument air to these turbine governors, though it is an optional feature of certain governors to permit remote setting of the turbine speed.

• *Apparent failures of sub-components and piece-parts as a result of aging phenomena.* A recent example was the identified repetitive failures of voltage dropping resistors in electric governors. Certain electrical component piece-parts such as voltage dropping resistors, and aluminum electrolytic capacitors, as well as mechanical/hydraulic component piece-parts such as elastomeric seals, will exceed their design life span during plant life. Determination of required replacement intervals is the responsibility of the individual plant because of plant specific conditions affecting component aging. Only one plant was identified during this study that accomplishes extensive periodic replacement of component parts to prevent age-related governor system failures. This plant replaces their electric governors and actuators every eight years because of age related failures.

Turbine Cold Quick-Start Failures Related to Configuration Control

Several turbine governor failures were caused by the removal of required, but uncontrolled and unidentified, modifications to the governors. The past frequency of this failure mechanism *per se* does not raise a concern, as it appears to be low. However, this failure mechanism by its nature potentially can affect all plants using Woodward governors, and could lead to common cause failure for plants which have redundant turbine-driven standby pumps.

These failures were caused by plant-specific governor modifications which were not documented, or indicated on the governors' identification plates. The modifications were removed during governor refurbishment at the manufacturer's plant when the governor was restored to its "as-built" configuration based on the governors' identification plates and factory records. Plant design control and quality assurance organizations did not identify the removal of the modification when the governors were returned to the plant after refurbishment. Failures caused by the removal of the modification apparently occurred when the plant changed its standby turbine-pump operability verification surveillance test methodology from hot start to cold quick-start.

Operational failures have resulted from the apparent lack of coordination of the opening of the turbine steam inlet stop valve, or the turbine trip and throttle valve, with the required response time and movement of the governor valve to prevent turbine overspeed trip during turbine startup. For RCIC and AFW turbines, the turbine manufacturer supplies the turbine trip and throttle and governor valves. Another design agent provides the turbine inlet steam stop valve, or uses the trip and throttle valve as the steam stop valve. One study identified that as many as 20 percent of turbine failures may be attributed to the improper opening speed of the trip and throttle valve, causing turbine overspeed before the governor valve can control steam flow. Originally, the trip and throttle valve was designed by the turbine manufacturer to remain open at all times unless it is tripped closed. Marginal valve timing coordination between the stop valve, the trip and throttle valve, and the governor valve could cause turbine overspeed trips during quick-cold starts.

STANDBY TURBINE/PUMP PERFORMANCE FEEDBACK BASED ON THE ANALYSIS OF OPERATIONAL FAILURE DATA

Since 1978, the US NRC, using operational experience, has issued 17 notices, circulars, and studies dealing with various problems affecting the reliability of safety-related standby turbines. Pertinent US NRC documents are listed in Table 1. This study identified an even larger number of documents issued by US industry organizations since 1980, which covered the history of operational failures of the subject pump/turbines. Certain industry documents identified specific methodologies to enhance the reliability of safety-related standby turbines.

The most extensive and focused source of operational data to enhance the reliability of standby turbines identified during this study were five GE Nuclear Service Information Letters (SILs) listed below. These SILs contain design and operational changes that appear to significantly enhance the reliability of HPCI and RCIC standby turbine-driven pumps. These SILs were not

Table 1 NRC Studies, Information Notices and Circulars Reviewed

Report Number	Title of Report	Comments
AEOD Case Study Reports		
AEOD/C602	Operational Experience Involving Turbine Overspeed Trips	
NRC Studies		
NUREG/CR-5404 Vol. 1	Auxiliary Feedwater System Aging Study	
NRC Circulars (IECs)		
IEC 78-02	Proper Lubricating Oil for Terry Turbines	This circular deals with the use of lubricating oils containing vapor phase inhibitors in Terry turbines used for pump-drivers for AFW/EFW, RCIC and HPCI standby pumps to prevent excessive rusting of the turbine interiors.
NRC Information Notices (INs)		
IN 81-24	Auxiliary Feed Pump Turbine Bearing Failures	This IN identifies damage to Terry Turbine type GS-2 auxiliary feed pump turbine bearings as a result of the failure to maintain turbine lube oil levels within the required operating band. The involved turbines used CA pickup rings only. Types GS-2 and GS-1 turbines have been built using a combination of force feed lubrication and oil pickup rings. Maintenance of proper oil level is required for both oil system designs.
IN 81-36	Replacement Diaphragms for Robertshaw Valve (Model No. VC-210)	This notice identified a failure of a neoprene diaphragm in the ROBERTSHAW diaphragm control valve installed in the mechanical-hydraulic overspeed complex of a Terry Turbine used with a HPCI pump. Because of the lube oil used in such standby pumps, a non-standard, fabric reinforced diaphragm is required for this application. Replacement valves will have the incorrect diaphragm. The correct diaphragm must be ordered separately and installed by the end-user.
IN 84-66	Undetected Unavailability of the Turbine-Driven Auxiliary Feedwater Pump	This IN identified five events at operating reactors during 1982-1983 where standby turbine driven AFW pumps were inoperable because the steam supplies were isolated. The isolations were caused by a failure to return AFW pump turbines to operability after the performance of surveillance or maintenance, or to verity operability after work had been performed in the area of the turbine control systems.
IN 86-14	PWR Auxiliary Feedwater Pump Turbine Control Problems	This IN dealt with four overspeed trip events during AFW pump turbine startup, or restart. Two of the trips resulted from residual oil pressure in the governor control oil system prior to turbine restart. Two trips resulted from condensate in the turbine steam supply lines at startup causing loss of speed control.
IN 86-14 (Supplement 1)	Overspeed Trips of AFW, HPCI, and RCIC Turbines	This IN dealt with four generic standby turbine speed control problems which result in overspeed trip. This IN was based on AEOD study AEOD/C602, "Operational Experience Involving Turbine Overspeed Trips." The four speed control problems were: • Slow response of the governor during quick startup (including binding of the governor valve stem-disc assembly). • Entrapped oil in the governor speed setting cylinder. • Incorrect governor setting. • Water induction into the turbine (condensate in the steam supply line at startup).
IN 86-14 (Supplement 2)	Overspeed Trips of AFW, HPCI, and RCIC Turbines	This IN dealt with turbine speed control problems which result in overspeed trip caused by an accumulation of dirt and grit in the turbine governor's control oil system.

(Table continues on the next page.)

Table 1 (Continued)

Report Number	Title of Report	Comments
IN 87-53	Auxiliary Feedwater Pump Trips Resulting From Low Suction Pressure	This IN deals with AFW pump trips resulting from low AFW pump suction pressure caused by the simultaneous starting of two AFW pumps.
IN 88-09	Reduced Reliability of Steam-Driven Auxiliary Feedwater Pumps Caused by Instability of Woodward PG-PL Type Governors	This IN covers a series of interrelated problems at Calvert Cliffs involving speed control of their AFW pumps. The causal factors in these problems were identified as: • Use of replacement governors with incorrect buffer springs. The correct buffer springs are required to dampen out turbine speed oscillations. The installed springs were of less than the degree of stiffness that was originally specified by Woodward for this installation and resulted in unacceptable oscillations. • Degraded and improperly adjusted governor linkage, resulting in excessive tolerances. • Binding of the governor valve stem-disc assembly, resulting in improper control of turbine speed control. • Damaged and misaligned turbine overspeed trip linkage and mechanisms, which resulted in an over sensitivity to tripping when disturbed by vibration, jarring, or water hammer in adjacent piping. • A failed governor. • Excessive condensate in the turbine steam supply line when the turbine was started. The condensate resulted in damage to the governor valve and the governor linkage, and in loss of turbine speed control as condensate impinged upon the governor valve and the turbine wheel.
IN 88-67	PWR Auxiliary Feedwater Pump Turbine Overspeed Trip Failure	This IN deals with a failure of a standby turbine for an AFW pump to trip on overspeed. The overspeed trip failure was caused by an excessively worn polyurethane tappet ball in the turbine overspeed trip system linkage.
IN 89-14	Inadequate Dedication Process for Commercial Grade Components Which Could Lead to Common Mode Failure of a Safety System	This IN deals with the inadequate 10 CFR 21 dedication by a licensee of packing for an AFW pump.
IN 90-45	Overspeed of the Turbine-Driven Auxiliary Feedwater Pumps and Overpressurization of the Associated Piping Systems	This IN deals with the combined failures of the turbine governor and overspeed trip mechanism, with resulting turbine overspeed and overpressurization of the AFW system.
IN 90-51	Failures of Voltage Dropping Resistors in the Power Supply Circuitry of Electric Governor Systems	This IN deals with the effect on governor operability of the failure or degradation of voltage dropping resistors (dual voltage dropping resistor assemblies) installed in the power supplies of electric governors used for the speed control of standby turbines and emergency diesel generators.
IN 90-51 (Supplement 1)	Failures of Voltage Dropping Resistors in the Power Supply Circuitry of Electric Governor Systems	This IN deals with additional failures of dual voltage dropping resistor assemblies used in standby turbine and emergency diesel generator electric governor power supplies, and the Woodward Governor Company (Woodward) letter to the NRC which stated that Woodward did not concur in the continued use of the dual voltage dropping resistor assembly, since battery charge voltage could result in increased current and heat that could cause these assemblies to fail or degrade.
IN 93-51	Repetitive Overspeed Tripping of Turbine-Driven Auxiliary Feedwater Pumps	This IN deals with repetitive tripping on turbine-driven auxiliary feedwater pump (TDAFWP) turbines at both units of a two unit site, where the proximate cause was determined to be water intrusion into the turbine resulting from deficiencies in the steam drain systems, in conjunction with other degraded and off normal conditions.

mandatory, and their implementation in the field varies. These SILs addressed operational problems affecting HPCI and RCIC turbine reliability. The RCIC SILs are also technically applicable to certain AFW turbines.

- GE SIL 336, dated July 11, 1980, emphasized the need to perform cold quick-start tests of these standby turbines to duplicate actual operational demands for the turbines to start, since most failures occur during the cold quick-start transient. The SIL provided guidance on the sequencing of the HPCI turbine stop valve and methodology for the performance of periodic surveillance tests for pump operability, including test instrumentation to enhance the assurance of pump and turbine operability.
- GE SIL 352, dated February 18, 1981, identified operational problems resulting from the improper adjustment of the HPCI turbine steam stop valve's steam balance chamber which resulted in overspeed trips during the cold quick-start transient. The SIL included a detailed procedure for the proper adjustment of this balance chamber.
- GE SIL 377, dated June 1982, identified operational problems with RCIC turbine speed control during the cold quick-start transient. It provided a design modification for a turbine steam by-pass line to significantly reduce this transient and overspeed trips.
- GE SIL 480, dated February 3, 1989, identified a design change to provide oil pressure from the HPCI turbine's electric auxiliary lubricating oil pump to the governor valve's model EGR hydraulic actuator prior to the turbine rolling to assure instant governor response during a cold quick-start. This SIL also changed the Woodward type EG electric governor's turbine idle speed voltage setting.
- GE SIL 336, Revision 1, dated December 8, 1989, updated the original version, incorporating additional operational data. Enhanced procedures were included for the assurance of proper turbine operation and testing.

Other design features that GE addressed included such potential turbine failure mechanisms as 1) the maximum allowable particle size when using turbine lube oil as a hydraulic fluid for mechanical/hydraulic governors and actuators, and 2) fluctuations in the reference voltage of electric governors.

MAINTENANCE GUIDANCE DOCUMENT, NP-6909, titled TERRY TURBINE CONTROLS, was issued in late October 1990 by the Electric Power Research Institute (EPRI).[5] This document provides manufacturers' data on the preventive maintenance of standby turbines and their governors that generally have not been available at specific plants to support the maintenance of these turbines and governors.

SUMMARY AND CONCLUSIONS

While failures of safety-related standby turbine-driven pumps continue to occur, analysis of existing operational experience indicates that the majority of failures have been repetitive in nature. Elimination of the causes of these failures, with the resultant improvement in the reliability of standby turbines, appears to be achievable by enhanced industry-wide implementation for these turbines of presently available guidance, such as more rigorous design control and dedication of commercial grade items used in safety-related applications, and by the accomplishment of actions specifically relating to these standby turbines based on failure report root cause determinations such as:

- Implementation of the design and test changes contained in the GE SILs for all applicable HPCI and RCIC standby turbines. Some enhancements contained in SILs address design and test weaknesses of certain AFW turbines.
- Implementation of the latest applicable Terry-Turbodyne identified maintenance for the standby turbines, and the maintenance guidance contained in EPRI NP-6909 for the turbine governors. Applicable plant specific design features relating to these turbines and their governors need to be identified, maintained, and incorporated in the appropriate plant procedures.
- Replacement of component piece-parts which affect plant safety before the end of their design life to prevent failures.
- Verification that the opening of turbine steam inlet stop valves is coordinated with the opening of their associated turbine trip and throttle valve and governor valve based on the criteria of the turbine manufacturer, who supplied the trip and throttle, and governor valves.
- For plants which use the AFW turbine trip and throttle valve as the turbine steam inlet stop valve, assurance of the proper coordination of its opening with governor valve response during cold quick-starts.
- Verification that the extremes of all variables, such as internal governor and model EGR actuator hydraulic fluid temperature and viscosity at the initiation of startup, and of variations in electric governor reference voltages resulting from maximum and minimum station battery voltage, are included in the design time responses for standby turbine cold quick-start transients, as well as continuous turbine operation.

REFERENCES

1. J. R. Boardman, *Operating Experience Feedback Report—Reliability of Safety-Related Steam Turbine-Driven Standby Pumps,* NUREG-1275, Vol. 10, U.S. Nuclear Regulatory Commission, October 1994.
2. Woodward manual 25071, "Oils for Hydraulic Controls," Table 4-1, "Viscosity and Operating Temperature of Oils," 1986.
3. Woodward manual 36641F, "Governor Oil Heat Exchanger Remote and Integral Types," 1971.
4. D. A. Casada, "Auxiliary Feedwater System Aging Study," NUREG/CR-5404, Vol. 1, U. S. Nuclear Regulatory Commission, March 1990.
5. "Terry Turbine Controls," Maintenance Guidance Document NP-6909, Electric Power Research Institute (EPRI), October 1990.

Turbine Building Hazards

By H. L. Ornstein[a]

Abstract: *This paper describes a study of turbine building hazards at U.S. plants which is being performed by the U.S. Nuclear Regulatory Commission's (NRC's) Office for Analysis and Evaluation of Operational Data (AEOD). In addition, it presents observations and lessons learned from recent operating experience.*

INTRODUCTION

In U.S. nuclear power plants, the turbine buildings are characterized as primarily containing "balance of plant" equipment, and as such, hazards in turbine buildings are not perceived as being a large contributor to plant risk. However, the turbine overspeed event at Salem Unit 2 on November 9, 1991, and the turbine blade failures at Fermi Unit 2 on December 25, 1993, have stimulated interest and helped focus utilities' and NRC's attention on the potential hazards and risks from equipment in nuclear plant turbine buildings.

DISCUSSION

Subsequent to the turbine overspeed event which resulted in fires and explosions at the Salem Unit 2 nuclear power plant on November 9, 1991, the NRC's Office for Analysis and Evaluation of Operational Data (AEOD) initiated studies on turbine-generator overspeed events (AEOD S94-02[1] and NUREG-1275, Vol. 11[2]) and on turbine building hazards.[3] The turbine overspeed studies noted that (1) the likelihood for a catastrophic overspeed event is much greater than previously estimated, and (2) the hazards from a catastrophic turbine-generator overspeed event could be much more extensive than previously envisioned. AEOD S94-02 raised questions about the completeness of plant safety analysis regarding damage from vibration and discharge of flammable or explosive fluids and collateral flooding which can result from turbine overspeed.[b]

The Salem overspeed event showed that protection from turbine overspeed events should not be limited to only damage from missiles. Previous U.S. NRC licensing activities did not focus on the potential for fires, explosions, and flooding that could result from a destructive turbine overspeed. The Salem event demonstrated that the likelihood for having low trajectory missiles penetrate the turbine casing was orders of magnitude higher than had been predicted by the turbine manufacturer. The turbine manufacturer's estimated probability of a missile ejection was about 2.7×10^{-7} per year, whereas a point estimate based on operating experience is 1.25×10^{-3} per year (90 percent confidence interval). Both Salem and Fermi turbine failures demonstrated that fires, explosions, or flooding could result from the vibrations which accompany large turbine blade losses.

Fortunately, many of the design features of the Salem and Fermi plants limited the damage which resulted from their respective events. In addition, many actions taken by the respective plant personnel limited the damage from the events. Based on examinations of other plant

[a]U.S. Nuclear Regulatory Commission, Office for Analysis and Evaluation of Operational Data, Washington, DC, 20555. Phone: (301) 415-7574, Fax: (301) 415-6359.

[b]*Title 10, U.S. Code of Federal Regulations, Part 50,* "Domestic Licensing of Production and Utilization Facilities," Appendix A, "General Design Criteria for Nuclear Power Plants," Criterion 4, "Environmental and Dynamic Effects Design Bases."

designs, it is not clear that all other U.S. plants would have fared as well as Salem and Fermi if they had experienced similar events.

AEOD's present study of turbine building hazards entails reviewing plant operating experience such as Immediate Notification Reports (10 CFR 50.72), Licensee Event Reports, NRC inspection reports, plant safety analyses, Appendix R submittals, individual plant evaluations, insurance industry loss data, and NRC sponsored studies (NUREGs). The study will also include visits to nuclear plants to interview plant staff and to conduct turbine building walk through examinations.

Examples of recent turbine building events and recently discovered turbine building deficiencies are shown in Table 1.

OBSERVATIONS AND LESSONS LEARNED FROM RECENT OPERATING EXPERIENCE

Theoretically, full implementation of U.S. NRC requirements for fire protection[4–6] would assure that a challenge to nuclear plant safety would not occur as a result of an internally generated fire or explosion in the turbine building or any other part of the plant. Our industry is still on a learning curve, even though the industry is not a new one. As a result, new operating experience teaches us about subtleties which may not have been recognized but which can introduce risk.

The December 25, 1993, turbine failure at Fermi Unit 2 has taught us several important lessons. For example, the flooding (a total of about 1 million gallons) that resulted from piping failures, deluge system actuation, and leaking from the condenser was contained in the radwaste storage building, which is annexed onto the turbine building. However, there were paths from the radwaste storage building to each of the reactor building emergency core cooling system (ECCS) "corner" rooms, which are on lower elevations. Fortuitously, the single check valve in the drain pipe leading to each ECCS room held and the ECCS rooms were unaffected by the turbine building flood water. It is also important to note that those check valves were not subject to any in-service testing or in-service inspection. To rectify this potential problem, the Fermi plant is introducing two isolation valves in the flow path from the radwaste storage building to each corner room. In addition, each of those valves will be subject to periodic in-service testing.

Another lesson learned was that, although the turbine building flooding was contained, high conductivity, high chloride content water from Lake Erie, which entered through the condenser, intruded into the reactor, the reactor coolant system, and the control rod drive system. The licensee cleaned up the impurities, and inspections have not revealed any metallurgical damage thus far. However, the licensee will be implementing an extensive program to inspect for longer term stress corrosion cracking of the aforementioned equipment.

CONCLUSIONS

At many U.S. plants, turbine building concerns have been limited to turbine missiles and damage that the missiles can do to safety-related equipment in the containment building. Operating experience has shown that the turbine building can be a major source of fires, explosions, and flooding. The hazards from turbine failures such as overspeed, blade failure, etc., can be much more significant than originally envisioned when the industry was in its infancy, and the likelihood for a turbine failure is much higher than originally estimated. Operating experience has also shown that repetitive inspections may not necessarily find turbine building vulnerabilities. The recent operating experience has sparked many U.S. utilities' and the NRC's interest in the subject of turbine failures and consequences. The knowledge gained from this turbine experience can be used to reduce the likelihood of turbine failures and minimize the safety impact of any subsequent failures.

REFERENCES

1. U.S. Nuclear Regulatory Commission, Special Study AEOD/S94-02, *Turbine-Generator Overspeed Protection Systems at U.S. Light-Water Reactors*, September 1994.
2. H. L. Ornstein, *Operating Experience Feedback Report—Turbine-Generator Overspeed Protection Systems*, Report NUREG-1275, Vol. 11, U.S. Nuclear Regulatory Commission, April 1995.
3. H. L. Ornstein, Turbine Building Hazards, U.S. Nuclear Regulatory Commission, to be published.
4. *Title 10, U.S. Code of Federal Regulations, Part 50*, "Domestic Licensing of Production and Utilization Facilities," Appendix R, "Fire Protection Program for Nuclear Power Facilities Operating Prior to January 1, 1979."
5. *Title 10, U.S. Code of Federal Regulations, Part 50*, "Domestic Licensing of Production and Utilization Facilities," Appendix A, "General Design Criteria for Nuclear Power Plants," General Design Criterion 3, "Fire Protection."
6. U.S. Nuclear Regulatory Commission, *Standard Review Plan for the Review of Safety Analysis Reports for Nuclear Power Plants*, Branch Technical Position 9-5.1, "Guidelines for Fire Protection for Nuclear Power Plants," Report NUREG-0800, June 1987.

Table 1 Recent Turbine Building Events

Date	Plant	Country	Type of plant	Event
09/94	Fitzpatrick	USA	BWR	(1) Contrary to safety analyses, two electric switchgear rooms containing safety related equipment were not isolated to protect against a high energy line break in the turbine building. (2) A safety-related ventilation control panel needed for accident mitigation (emergency service water) was not installed in the "protected" switchgear rooms.
12/93	Fermi 2	USA	BWR	Turbine blade fatigue failure. Missiles penetrated the turbine casing. Turbine vibrations caused seal and piping failures resulting in hydrogen explosion and fires, oil fires, and flooding. Extensive damage to the turbine, the generator, and the main condenser. Flooding in turbine building had potential to flood emergency core cooling system equipment in reactor building. Lake water intrusion into control rod drive system and reactor vessel pose long-term stress corrosion cracking concerns. Resulted in about a 1-year outage.
12/93	Millstone 1	USA	BWR	Safety-related switchgear in an unanalyzed condition. Turbine building railway access roll-up door was closed. Door is required to be open to ensure safety-related switchgear remains within equipment qualification limits if a steam line pipe rupture occurred in the turbine building.
03/93	Narora 1	India	PHWR	Fire led to an extended station blackout which compromised decay heat removal. Accident management using diesel driven fire pumps was credited with preventing serious consequences. Believed to be caused by turbine blade fatigue failure. Turbine vibrations caused seal and piping failures resulting in hydrogen explosion and fires, oil fires, and flooding. Extensive damage resulted in about $1^{1}/_{2}$-year outage.
12/92	Not specified	Non-U.S with potential for similar problem in U.S.	BWR/3	General Electric notified U.S. plants that a non-U.S. plant postulated that a hydrogen gas line break in the turbine building mezzanine could result in a hydrogen detonation. Blast waves from the hydrogen detonation could damage vital 1E buses.
11/91	Salem 2	USA	PWR	Turbine overspeed resulted in missiles (blades) penetrating the turbine casing. A hydrogen explosion, hydrogen fires, and turbine lube oil fires resulted. Extensive damage to the turbine, the generator, and the main condenser resulted in a 6-month outage.
10/91	Chernobyl 2	Ukraine	RBMK	Turbine building fire caused by an electrical short. Fire caused a roof to collapse on all five auxiliary feedwater pumps and three emergency feedwater pumps. Operator actions utilizing an auxiliary water system to cool the core was credited for preventing serious consequences.
09/91	Pickering 2	Canada	PHWR	Turbine fire originated from a generator hydrogen gas leak. Quick response to smoke/fire detectors and rapid deployment of fire fighters successfully minimized consequences of the fire.
10/89	Vandellos	Spain	GCR	Turbine vibration resulted in severing lubrication oil lines resulting in oil fires. Flooding of the turbine and reactor building led the licensee to decommission the plant instead of undertaking extensive repair and restoration.

Recent Developments

Edited by M. D. Muhlheim

Reports, Standards, and Safety Guides

By D. S. Queener

This article contains four lists of various documents relevant to nuclear safety as compiled by the editor. These lists are: (1) reactor operations-related reports of U.S. origin, (2) other books and reports, (3) regulatory guides, and (4) nuclear standards. Each list contains the documents in its category which were published (or became available) during the October 1994 through March 1995 reporting period. The availability and cost of the documents are noted in most instances.

OPERATIONS REPORTS

This category is listed separately because of the increasing interest in the safety implications of information obtainable from both normal and off-normal operating experience with licensed power reactors. The reports fall into several categories shown, with information about the availability of the reports given where possible. The NRC reports are available from the Nuclear Regulatory Commission (NRC) Public Document Room, 2120 L Street, NW, Washington, DC 20555.

NRC Office of Nuclear Reactor Regulation

The NRC Office of Nuclear Reactor Regulation (NRR) issues reports regarding operating experience at licensed reactors. These reports, previously published by the NRC Office of Inspection and Enforcement (IE), fall into two categories of urgency: (1) NRC Bulletins and Generic Letters, which require remedial actions and/or responses from affected licensees; and (2) NRC Information Notices and Administrative Letters, which are for general information and do not require any response from the licensee. The Administrative Letters are relatively new generic communications issued by the NRC. They contain information of an administrative or informational nature and were previously distributed under the generic letter category. No specific action is required in response to these Administrative Letters.

NRC Bulletins

NRC B 94-02 Corrosion Problems in *Certain Stainless Steel Packagings Used to Transport Uranium Hexafluoride,* November 14, 1994, 3 pages plus 2 pages of attachments.

NRC Information Notices

NRC IN 94-7 *Degradation of Scram Solenoid Pilot Valve Pressure and Exhaust Diaphragms,* October 4, 1994, 4 pages plus 3 pages of attachments.

NRC IN 94-72 *Increased Control Rod Drop Time from Crud Buildup,* October 4, 1994, 3 pages plus 2 pages of attachments.

NRC IN 94-73 *Clarification of Criticality Reporting Criteria,* October 12, 1994, 4 pages plus 2 pages of attachments.

NRC IN 94-74 *Facility Management Responsibilities for Purchased or Contracted Services for Radiation Therapy Programs,* October 13, 1994, 3 pages plus one-page attachment.

NRC IN 94-75 *Minimum Temperature for Criticality,* October 14, 1994.

NRC IN 94-76 *Recent Failures of Charging/Safety Injection Pump Shafts,* October 26, 1994, 5 pages plus 3 pages of attachments.

NRC IN 94-77 *Malfunction in Main Generator Voltage Regulator Causing Overvoltage at Safety-Related Electrical Equipment,* November 17, 1994, 2 pages plus one-page attachment.

NRC IN 94-78 *Electrical Component Failure Due to Degradation of Polyvinyl Chloride Wire Insulation,* November 21, 1994.

NRC IN 94-79 *Microbiologically Influenced Corrosion of Emergency Diesel Generator Service Water Piping,* November 23, 1994, 4 pages plus 4 pages of attachments.

NRC IN 94-80 *Inadequate DC Ground Detection in Direct Current Distribution Systems,* November 25, 1994.

NRC IN 94-81 *Accuracy of Bioassay and Environmental Sampling Results,* November 25, 1994.

NRC IN 94-82 *Concerns Regarding Essential Chiller Reliability During Periods of Low Cooling Water Temperature,* December 5, 1994.

NRC IN 94-83 *Reactor Trip Followed by Unexpected Events,* December 6, 1994.

NRC IN 94-84 *Air Entrainment in Terry Turbine Lubricating Oil System,* December 2, 1994.

NRC IN 94-85 *Problems with the Latching Mechanism in Potter and Brumfield R10-E3286-2 Relays,* December 21, 1994, 3 pages plus one-page attachment.

NRC IN 94-86 *Legal Actions Against Thermal Science, Inc., Manufacturer of Thermo-Lag,* December 22, 1994.

NRC IN 94-87 *Unanticipated Crack in a Particular Heat of Alloy 600 Used for Westinghouse Mechanical Plugs for Steam Generator Tubes,* December 22, 1994, 2 pages plus 3 pages of attachments.

NRC IN 94-88 *Inservice Inspection Deficiencies Result in Severely Degraded Steam Generator Tubes,* December 23, 1994, 4 pages plus one-page attachment.

NRC IN 94-89 *Equipment Failures at Irradiator Facilities,* December 28, 1994, 5 pages plus 6 pages of attachments.

NRC IN 94-90 *Transient Resulting in a Reactor Trip and Multiple Safety Injection System Actuations at Salem,* December 30, 1994, 5 pages plus one-page attachment.

NRC IN 95-01 *DOT Safety Advisory: High Pressure Aluminum Seamless and Aluminum Composite Hoop-Wrapped Cylinders,* January 4, 1995, 3 pages plus 4 pages of attachments.

NRC IN 95-02 *Problems with General Electric CR2940 Contact Blocks in Medium-Voltage Circuit Breakers,* January 17, 1995, 4 pages plus 4 pages of attachments.

NRC IN 95-03 *Loss of Reactor Coolant Inventory and Potential Loss of Emergency Mitigation Functions While in a Shutdown Condition,* January 18, 1995, 4 pages plus one-page attachment.

NRC IN 95-04 *Excessive Cooldown and Depressurization of the Reactor Coolant System Following a Loss of Offsite Power,* January 19, 1995, 3 pages plus one-page attachment.

NRC IN 95-05 *Undervoltage Protection Relay Settings Out of Tolerance Due to Test Equipment Harmonics,* January 20, 1995, 4 pages plus one-page attachment.

NRC IN 95-06 *Potential Blockage of Safety-Related Strainers by Material Brought Inside Containment,* January 25, 1995, 4 pages plus one-page attachment.

NRC IN 95-07 *Radiopharmaceutical Vial Breakage During Preparation,* January 27, 1995, 3 pages plus one-page attachment.

NRC IN 95-08 *Inaccurate Data Obtained with Clamp-On Ultrasonic Flow Measurement Instruments,* January 30, 1995, 4 pages plus one-page attachment.

NRC IN 95-09 *Use of Inappropriate Guidelines and Criteria for Nuclear Piping and Pipe Support Evaluation and Design,* January 31, 1995, 3 pages plus one-page attachment.

NRC IN 95-10 *Potential for Loss of Automatic Engineered Safety Features Actuation,* February 3, 1995, 3 pages plus 2 pages of attachments.

NRC IN 95-10, Suppl. 1 *Potential for Loss of Automatic Engineered Safety Features Actuation,* February 10, 1995, 3 pages plus one-page attachment.

NRC IN 95-11 *Failure of Condensate Piping Because of Erosion/Corrosion at a Flow-Straightening Device,* February 24, 1995, 3 pages plus one-page attachment.

NRC IN 95-12 *Potentially Nonconforming Fasteners Supplied by A&G Engineering II, Inc.,* February 21, 1995, 3 pages plus one-page attachment.

NRC IN 95-13 *Potential for Data Collection Equipment to Affect Protection System Performance,* February 24, 1995, 3 pages plus one-page attachment.

NRC IN 95-14 *Susceptibility of Containment Sump Recirculation Gate Valves to Pressure Locking,* February 28, 1995.

NRC IN 95-15 *Inadequate Logic Testing of Safety-Related Circuits,* March 7, 1995.

NRC IN 95-16 *Vibration Caused by Increased Recirculation Flow in a Boiling Water Reactor,* March 9, 1995.

NRC IN 95-17 *Reactor Vessel Top Guide and Core Plate Cracking,* March 10, 1995.

NRC IN 95-18 *Potential Pressure-Locking of Safety-Related Power-Operated Gate Valves,* March 15, 1995.

NRC IN 95-18, Suppl. 1 *Potential Pressure-Locking of Safety-Related Power-Operated Gate Valves,* March 31, 1995, 4 pages plus 2 pages of attachments.

NRC IN 95-19 *Failure of Reactor Trip Breaker to Open Because of Cutoff Switch Material Lodged in the Trip Latch Mechanism,* March 22, 1995.

NRC IN 95-20 *Failures in Rosemount Pressure Transmitters Due to Hydrogen Permeation into the Sensor Cell,* March 22, 1995.

NRC Administrative Letters

NRC AL 94-15 *Reorganization of the Office of Nuclear Reactor Regulation,* October 6, 1994, 1 page plus 3 pages of attachments.

NRC AL 94-16 *Revision of NRC Core Inspection Program for Annual Emergency Preparedness Exercise,* November 30, 1994, 2 pages plus 2 pages of attachments.

Other Operations Reports

These are other reports issued by various organizations in the United States dealing with power-reactor operations activities. Most of the NRC publications (NUREG series documents) can be ordered from the Superintendent of Documents, U.S. Government Printing Office (GPO), P.O. Box 37082, Washington, DC 20013.

NRC draft copies of reports are available free of charge by writing the NRC Office of Administration (ADM), Distribution and Mail Services Section, Washington, DC 20555. A number of these reports can also be obtained from the NRC Public Document Room (PDR). Specify the report number when ordering. Telephone orders can be made by contacting the PDR at (202) 634-3273.

Many other reports prepared by U.S. government laboratories and contractor organizations are available from the Technology Administration, National Technical Information Service (NTIS), U.S. Department of Commerce, Springfield, VA 22161, and/or DOE Office of Scientific and Technical Information (OSTI), P.O. Box 62, Oak Ridge, TN 37831. Reports available through one or more of these organizations are designated with the appropriate information (i.e., GPO, PDR, NTIS, and OSTI) in parentheses at the end of the listing, followed by the price, when available.

NUREG-0090, Vol. 17, No. 2 *Report to Congress on Abnormal Occurrences for April–June 1994,* October 1994, 41 pages (GPO).

NUREG-0090, Vol. 17, No. 3 *Report to Congress on Abnormal Occurrences for July–September 1994,* January 1995, 35 pages (GPO).

NUREG-1272, Vol. 8, No. 1 *Office for Analysis and Evaluation of Operational Data. 1993 Annual Report—Power Reactors,* December 1994, 261 pages (GPO).

NUREG-1275, Vol. 10 *Operating Experience Feedback Report—Reliability of Safety-Related Steam Turbine-Driven Standby Pumps. Commercial Power Reactors,* J. R. Boardman, October 1994, 91 pages (GPO).

NUREG-1517 *Report of the South Texas Project Allegations Review Team,* L. Kokajko et al., March 1995, 200 pages (GPO).

NUREG/CR-2850, Vol. 12 *Dose Commitments Due to Radioactive Releases from Nuclear Power Plant Sites in 1990,* D. A. Baker, Pacific Northwest Labs., WA, November 1994, 194 pages (GPO).

NUREG/CR-6192 *Aging and Service Wear of Spring-Loaded Pressure Relief Valves Used in Safety-Related Systems at Nuclear Power Plants,* March 1995, 86 pages (GPO).

NRC Office for Analysis and Evaluation of Operational Data

The NRC Office for Analysis and Evaluation of Operational Data (AEOD) is responsible for the review and assessment of commercial nuclear power plant operating experience. AEOD publishes a number of reports, including case studies, special studies, engineering evaluations, and technical reviews. Individual copies of these reports may be obtained from the NRC Public Document Room (PDR).

AEOD/S95-01 *Reactor Coolant System Blowdown at Wolf Creek on September 17, 1994,* J. Kauffman and S. Israel, March 1995, 40 pages.

AEOD/T95-01 *Major Disturbances on the Western Grid and Related Events,* Mary S. Wegner, March 10, 1995, 10 pages.

DOE- and NRC-Related Items

NUREG-0383, Rev. 17 *Directory of Certificates of Compliance for Radioactive Materials Packages. Report of NRC-Approved Packages,* 513 pages, October 1994 (GPO).

NUREG-1435, Suppl. 4 *Status of Safety Issues at Licensed Power Plants. TMI Action Plan Requirements, Unresolved Safety Issues, Generic Safety Issues, Other Multiplant Action Issues,* 157 pages, December 1994 (GPO).

NUREG-1465 *Accident Source Terms for Light-Water Nuclear Power Plants,* 40 pages, February 1995 (GPO).

NUREG-1470 *Financial Statement for Fiscal Year 1994,* 84 pages, March 1995 (GPO).

NUREG-1497 *Interim Licensing Criteria for Physical Protection of Certain Storage of Spent Fuel,* P. A. Dwyer, 20 pages, November 1994 (GPO).

NUREG-1511 *Reactor Pressure Vessel Status Report,* J. Strosnider et al., 174 pages, December 1994 (GPO).

NUREG/CP-0138 *Proceedings of Workshop I in Advanced Topics in Risk and Reliability Analysis. Model Uncertainty: Its Characterization and Quantification,* A. Mosleh et al., Univ. of Maryland, College Park, 259 pages, October 1994 (GPO).

NUREG/CP-0139 Transactions of the Twenty-Second Water Reactor Safety Information Meeting, S. Monteleone, Brookhaven National Lab., NY, 141 pages, October 1994.

NUREG/CP-0141 *Proceedings of the 23rd DOE/NRC Nuclear Air Cleaning Conference,* 800 pages, February 1995 (GPO).

NUREG/CP-0143 *Proceedings of the Third International Workshop on the Implementation of ALARA at Nuclear Power Plants,* 822 pages, March 1995 (GPO).

NUREG/CR-4838 *Microcomputer Applications of and Modifications to the Modular Fault Trees,* A. C. Payne et al., Sandia National Labs., NM, 300 pages, October 1994 (GPO).

NUREG/CR-6284 *Criticality Safety Criteria for License Review of Low-Level Waste Facilities,* 45 pages, March 1995 (GPO).

NUREG/CR-6285 *Severe Accident Natural Circulation Studies at the INEL,* 200 pages, February 1995 (GPO).

Other Items

NCRP Commentary No. 10 *Advising the Public About Radiation Emergencies. A Document for Public Comment,* National Council on Radiation Protection and Measurements (NCRP), MD, November 30, 1994, 28 pages (available from NCRP Publications, 7910 Woodmont Avenue, Suite 800, Bethesda, MD 20814-3095).

NCRP Report 120 *Dose Control at Nuclear Power Plants,* NCRP, MD, December 30, 1994, 136 pages (available from NCRP).

STI/PUB/946 *The Nuclear Power Option. Proceedings Series,* International Atomic Energy Agency (IAEA), Vienna, March 1995, 763 pages (available from UNIPUB, 4611-F Assembly Drive, Lanham, MD 20706-4391).

STI/PUB/958 *Quality Assurance for the Safe Transport of Radioactive Material. Safety Series No. 113,* IAEA, Vienna, November 1994, 92 pages (available from UNIPUB).

STI/PUB/963 *Periodic Safety Review of Operational Nuclear Power Plants—A Safety Guide. Safety Series No. 50-SG-O12,* IAEA, Vienna, November 1994, 50 pages (available from UNIPUB).

STI/PUB/964 *Operating Experience with Nuclear Power Stations,* IAEA, Vienna, October 1994, 930 pages (available from UNIPUB).

STI/PUB/967 *Inspection of Fire Protection Measures and Fire Fighting Capability at Nuclear Power Plants—A Safety Practice. Safety Series No. 50-P-6,* IAEA, Vienna, January 1995, 70 pages (available from UNIPUB).

STI/PUB/968 *Treatment of External Hazards in Probabilistic Safety Assessment for Nuclear Power Plants—A Safety Practice. Safety Series No. 50-P-7,* IAEA, Vienna, February 1995, 58 pages (available from UNIPUB).

STI/PUB/976 *Design of Spent Fuel Storage Facilities. Safety Series No. 116,* IAEA, Vienna, February 1995, 50 pages (available from UNIPUB).

STI/PUB/977 *Operation of Spent Fuel Storage Facilities. Safety Series No. 117,* IAEA, Vienna, February 1995, 54 pages (available from UNIPUB).

STI/PUB/981 *Safety Assessment for Spent Fuel Storage Facilities. Safety Series No. 118,* IAEA, Vienna, February 1995, 68 pages (available from UNIPUB).

REGULATORY GUIDES

To expedite the role and function of the NRC, its Office of Nuclear Regulatory Research prepares and maintains a file of Regulatory Guides that define much of the basis for the licensing of nuclear facilities. These Regulatory Guides are divided into 10 divisions as shown in Table 1.

Table 1 Regulatory Guides

Division 1	Power Reactor Guides
Division 2	Research and Test Reactor Guides
Division 3	Fuels and Materials Facilities Guides
Division 4	Environmental and Siting Guides
Division 5	Materials and Plant Protection Guides
Division 6	Product Guides
Division 7	Transportation Guides
Division 8	Occupational Health Guides
Division 9	Antitrust and Financial Review Guides
Division 10	General Guides

Single copies of the draft guides may be obtained from NRC Distribution Section, Division of Information Support Services, Washington, DC 20555. Draft guides are issued free (for comment) and licensees receive both draft and final copies free; others can purchase single copies of active guides by contacting the U.S. Government Printing Office (GPO), Superintendent of Documents, P.O. Box 37082, Washington, DC 20013. Costs vary according to length of the guide. Of course, draft and active copies will be available from the NRC Public Document Room, 1717 H Street, NW, Washington, DC, for inspection and copying for a fee.

Revisions in these rates will be announced as appropriate. Subscription requests should be sent to the National Technical Information Service, Subscription Department, Springfield, VA 22161. Any questions or comments about the sale of regulatory guides should be directed to the Chief, Document Management Branch, Division of Technical Information and Document Control, Nuclear Regulatory Commission, Washington, DC 20555.

Actions pertaining to specific guides (such as issuance of new guides, issuance for comment, or withdrawal), which occurred during the reporting period, are listed below.

Division 1 Power Reactor Guides

1.16 *Work and Job Functions of Personnel Who Received Greater Than 100 MREM of Exposure in 1994,* December 1994.

1.82 (Draft Proposed Rev. 2) *Water Sources for Long-Term Recirculation Cooling Following a Loss-of-Coolant Accident,* November 1994.

Draft Reg Guide DG-1028 *Periodic Testing of Electric Power and Protection Systems,* October 1994.

Division 8 Occupational Health Guides

8.013 (Draft Revision 3) *Instructions Related to Prenatal Radiation Exposure,* October 1994.

8.029 (Draft Revision 1) *Instruction Concerning Risks from Occupational Radiation Exposure,* December 1994.

Division 10 General Guides

10.005 (Second Proposed Revision 2) *Application for Licenses of Broad Scope,* October 1994.

10.027 (Draft) *Format and Content of Application for Approval for Thermal Annealing of Reactor Pressure Vessels,* October 1994.

NUCLEAR STANDARDS

Standards pertaining to nuclear materials and facilities are prepared by many technical societies and organizations in the United States, including the Department of Energy (DOE) (NE Standards). When standards prepared by a technical society are submitted to the American National Standards Institute (ANSI) for consideration as an American National Standard, they are assigned ANSI standard numbers, although they may also contain the identification of the originating organization and be sold by that organization as well as by ANSI. We have undertaken to list here the most significant nuclear standards actions taken by organizations from October 1994 through March 1995. Actions listed include issuance for comments, approval by the ANSI Board of Standards Review (ANSI-BSR), and publication of the approved standard. Persons interested in obtaining copies of the standards should write to the issuing organizations.

American National Standards Institute

ANSI does not prepare standards; it is devoted to approving and disseminating standards prepared by technical organizations. However, it does publish standards, and such standards can be ordered from ANSI, Attention: Sales Department, 1430 Broadway, New York, NY 10018. Frequently, ANSI is an alternate source for standards also available from the preparing organization.

ANSI A1264.1-1995 (Revision of ANSI A1264.1-1989, approved by ANSI/BSR) *Safety Requirements for Workplace and Wall Openings, Stairs and Railing Systems.*

ANSI HPS N13.11-1993 (Published) *Personnel Dosimetry Performance—Criteria for Testing,* $24.00.

ANSI/N15.41-1984 (R1994, approved by ANSI/BSR) *Derivation of Measurement Control Programs—General Principles.*

ANSI/NFPA 801-1995 (Revision of ANSI/NFPA 801-1994, approved by ANSI/BSR) *Facilities Handling Radioactive Materials.*

American Nuclear Society

Standards prepared by ANS can be obtained from ANS, Attention: Marilyn D. Weber, 555 North Kensington Avenue, LaGrange Park, IL 60525.

ANSI/ANS 3.2-1994 (Revision of ANSI/ANS 3.2-1988, approved by ANSI/BSR) *Administrative Controls and Quality Assurance for the Operational Phase of Nuclear Power Plants.*

ANSI/ANS 5.1-1993 (Revision of ANSI/ANS 5.1-1979, R1985, approved by ANSI/BSR) *Decay Heat Power in Light Water Reactors.*

ANSI/ANS 58.8-1994 (Revision of ANSI/ANS 58.8-1984, approved by ANSI/BSR) *Time Response Design Criteria for Safety-Related Operator Actions.*

BSR/ANS 3.7.1 [Revision of ANSI/ANS 3.7.1-1979(R1986), for comment] *Facilities and Medical Care for On-Site Nuclear Power Plant Radiological Incidents,* $7.50.

BSR/ANS 8.7 [Revision of ANSI/ANS 8.7-1975(R1987), for comment] *Nuclear Criticality Safety in the Storage of Fissile Materials,* $10.00.

BSR/ANS 8.19 [Revision of ANSI/ANS 8.19-1984(R1989), for comment] *Administrative Practices for Nuclear Criticality Safety,* $7.50.

BSR/ANS 18.1 (Revision of ANSI/ANS 18.1-1984, for comment) *Radioactive Source Term for Normal Operation of Light Water Reactors,* $10.00

BSR/ANS 57.5 (New Standard, for comment) *Light Water Reactors Fuel Assembly Mechanical Design and Evaluation,* $7.50.

BSR/ANS 58.9 [Revision of ANSI/ANS 58.9-1981(R1987), for comment] *Application of the Single Failure Criterion for Light Water Reactor Safety-Related Fluid Systems,* $7.50.

BSR/ANS 59.51 (Revision of ANSI/ANS 59.51-1989, for comment) *Fuel Oil Systems for Safety Related Emergency Diesel Generators,* $7.50.

American Society of Mechanical Engineers

Standards prepared by ASME can be obtained from ASME, Attention: R. D. Palumbo, 345 East 47th Street, New York, NY 10017.

ANSI/ASME NQA-1-1994 (Published) *Quality Assurance Requirements for Nuclear Facility Applications,* $140.00.

ANSI/ASME NQA-1a-1995 (Addenda to ANSI/ASME NQA-1-1994, for comment) *Quality Assurance Requirements for Nuclear Facility Applications,* $20.00.

Institute of Electrical and Electronics Engineers

Standards prepared by IEEE can be obtained from IEEE, Attention: M. Lynch, 345 East 47th Street, New York, NY 10017.

ANSI/IEEE 334-1994 (Published) *Qualifying Continuous Duty Class 1E Motors for Nuclear Power Generating Stations,* $65.00.

BSR/IEEE 379 (Revision of ANSI/ISA 379-1988, for comment) *Standard Application of the Single-Failure Criterion to Nuclear Power Generating Stations Safety Systems,* $26.00.

BSR N42.20 (New standard, for comment) *Performance Criteria for Active Personnel Radiation Monitors,* $35.50.

Instrument Society of America

Copies of ISA standards may be purchased by contacting ISA Member and Customer Services,

67 Alexander Drive, P.O. Box 12277, Research Triangle Park, NC 27709.

BSR/ISA S67.10 (Revision of ANSI/ISA S67.10-1986, for comment) *Sample-Line Piping and Tubing Standard for Use in Nuclear Power Plants,* $20.00.

International Standards

This section includes publications for any of the three types of international standards:

—IEC standards (International Electrotechnical Commission)
—ISO standards (International Standards Organization)
—KTA standards [Kerntechnischer Ausschuss (Nuclear Technology Commission)].

Standards originating from the IEC and ISO can be obtained from the American National Standards Institute (ANSI), International Sales Department, 1430 Broadway, New York, NY 10018.

The KTA standards are developed and approved by the Nuclear Safety Standards Commission (KTA). The KTA, formerly a component of the Gesellschaft für Reaktorsicherheit (GRS), is now integrated in the Federal Office for Radiation Protection (Bundesamt für Strahlenschutz BfS) in Salzgitter, Germany. Copies of these standards can be ordered from Dr. T. Kalinowski, KTA-Geschäftsstelle, Postfach 10 01 49, 3320 Salzgitter 1, Germany. These standards are in German and, unless otherwise noted, an English translation is available from the KTA.

Prices for the international standards are shown in German currency (DM). The IEC and ISO standards are included in this issue.

IEC

IEC 45A(Central Office)142 (Draft) *Nuclear Power Plants—Main Control Room-Application of Visual Display Units (VDU),* $50.00.

ISO

ISO 9889:1994 (Published) *Determination of Carbon Content in Uranium Dioxide Powder and Sintered Pellets—Resistance Furnace Combustion—Titrimetric/Coulometric/Infrared Absorption Method,* $40.00.

ISO 10648-2:1994 (Published) *Containment Enclosures—Part 2: Classification According to Leak Tightness and Associated Checking Methods,* $48.00.

ISO 12184:1994 (Published) *Determination of Solubility in Nitric Acid of Plutonium in Unirradiated Mixed Oxide Fuel Pellets* $(U,Pu)O_2$, $29.00.

ISO/DIS 4037-2 (Draft) *X and Gamma Reference Radiations for Calibrating Dosimeters and Doserate Meters and for Determining Their Response as a Function of Photon Energy—Part 2: Dosimetry of X and Gamma Reference Radiations for Radiation Protection Over the Energy Range from 8 keV to 1.3 MeV and from 4 MeV to 9 MeV,* $101.00.

ISO/DIS 11929-1 (Draft) *Determination of the Lower Limits of Detection and Decision for Ionizing Radiation Measurements—Part 1: Fundamentals and Applications to Counting Measurements with the Influence of Sample Treatment,* $52.00.

ISO/DIS 8769-2 (Draft) *Reference Sources for the Calibration of Surface Contamination Monitors—Part 2: Electrons of Energy Less than 0.15 MeV and Photons,* $40.00.

ISO/DIS 11934 (Revision of ISO 1758:1976, ISO 1759:1976 and ISO 4071:1978, Draft) *Indirect or Direct Reading Capacitor-Type Pocket Dosimeters,* $65.00.

Proposed Rule Changes as of Dec. 31, 1994[a,b]

(Changes Since the Previous Issue of *Nuclear Safety* Are Indicated by Shaded Areas)

Number of part to be changed	Date published for comment	Date comment period expired	Date published; date effective	Topic or proposed effect	Current action and/or comment, *Federal Register* volumes and page numbers
10 CFR 1	6-19-92	8-18-92; 9-30-92		Review of reactor licensee reporting requirements	Published for comment in 57:119 (27394); comment period extended in 57:153 (34886)
10 CFR 1			12-12-94; 12-12-94	Statement of organization and general information; agency consolidation and minor adjustments	Final rule in 59:237 (63881)
10 CFR 2	12-23-92	3-8-93		Availability of official records	Published for comment in 57:247 (61013)
10 CFR 2 10 CFR 72	6-3-93	8-17-93; 10-1-93		Interim storage of spent fuel in an independent spent fuel storage installation; site-specific license to a qualified applicant	Published for comment in 58:105 (31478); comment period extended in 58:176 (48004)
10 CFR 2	9-29-93	11-15-93		Informal hearing procedures for materials licensing adjudications	Published for comment in 58:187 (50858)
10 CFR 2	5-11-94	6-10-94		Summary reports on the status of petitions for rulemaking; frequency	Published for comment in 59:90 (24371)
10 CFR 2, 30, 40, 70, 72			7-15-94; 8-15-94	Licensee submittal of data in computer-readable form	Final rule in 59:135 (36026)
10 CFR 2	8-23-94; 9-27-94; 11-28-94	10-24-94; 12-28-94		Reexamination of the NRC enforcement policy	Published for comment in 59:162 (43298); correction in 59:171 (46004); expanded scope in 59:186 (49215); revised in 59:227 (60697)
10 CFR 2, 51, 54	9-9-94	12-8-94		Nuclear power plant license renewal; proposed revisions	Published for comment in 59:174 (46574)
10 CFR 2			11-25-94; 11-25-94	Change in organizational title and telephone numbers	Final rule in 59:226 (60551)
10 CFR 2	11-30-94	12-30-94		NRC size standards, proposed revision	Published for comment in 59:229 (61293)
10 CFR 11 10 CFR 25	12-28-94	1-27-95		NRC licensee renewal/ reinvestigation program	Published for comment in 59:248 (66812)
10 CFR 19 10 CFR 20	2-3-94	4-4-94		Radiation protection requirements; amended definitions and criteria	Published for comment in 59:23 (5132)

(Table continues on the next page.)

Proposed Rule Changes as of Dec. 31, 1994 (Continued)

Number of part to be changed	Date published for comment	Date comment period expired	Date published; date effective	Topic or proposed effect	Current action and/or comment, *Federal Register* volumes and page numbers
10 CFR 19, 20, 21, 26, 51, 70, 71, 73, 74, 76, 95	2-11-94	4-12-94	9-23-94; 10-24-94	Certification of gaseous diffusion plants	Published for comment in 59:29 (6792); final rule in 59:184, Part II (48944)
10 CFR 19, 20, 35, 40			8-15-94; 8-15-94	Standards for protection against radiation; clarification	Final rule in 59:156 (41641)
10 CFR 20	2-25-94	5-26-94		Disposal of radioactive material by release into sanitary sewer systems	Advanced notice of proposed rulemaking published in 59:38 (9146)
10 CFR 20 10 CFR 61	4-21-92	7-20-92		Low-level waste shipment manifest information and reporting	Published for comment in 57:77 (14500)
10 CFR 20	6-18-93	8-15-93; 9-20-93		Radiological criteria for decommissioning of NRC-licensed facilities; generic environmental impact statement (GEIS) for rulemaking, notice of intent to prepare a GEIS and to conduct a scoping process	Published for comment in 58:116 (33570); comment period extended in 58:154 (42882)
10 CFR 20	2-2-94	3-11-94		Radiological criteria for decommissioning of NRC-licensed facilities; enhanced participatory rulemaking, availability of the staff's draft of the rule	Published for comment in 59:22 (4868)
10 CFR 20 10 CFR 35	6-15-94	8-29-94		Criteria for the release of patients administered radioactive material	Published for comment in 59:114 (30724)
10 CFR 20, 30, 40, 50, 51, 70, 72	8-22-94	12-20-94; 1-20-95		Radiological criteria for decommissioning	Published for comment in 59:161, Part III (43200); comment period extended in 59:236 (63733)
10 CFR 20, 30, 40, 61, 70, 72	12-28-94	3-28-95		Termination or transfer of licensed activities: recordkeeping requirements	Published for comment in 59:248 (66814)
10 CFR 21	10-24-94	1-9-95		Procurement of commercial grade items by nuclear power plant licensees	Published for comment in 59:204 (53372)
10 CFR 26	5-11-94	9-9-94		Consideration of changes to fitness-for-duty (FFD) requirements	Published for comment in 59:90 (24373)
10 CFR 30, 40, 70, 72	1-13-93	3-29-93		Timeliness in decommissioning of materials facilities	Published for comment in 58:8 (4099)

Proposed Rule Changes as of Dec. 31, 1994 (Continued)

Number of part to be changed	Date published for comment	Date comment period expired	Date published; date effective	Topic or proposed effect	Current action and/or comment, *Federal Register* volumes and page numbers
10 CFR 30 10 CFR 32 10 CFR 35	6-17-93	10-15-93	12-2-94; 12-19-94; 1-1-95	Preparation, transfer for commercial distribution, and use of byproduct material for medical use	Published for comment in 58:115 (33396); final rule in 59:231 (61767); correction to final rule in 59:242 (65243)
10 CFR 30 10 CFR 40 10 CFR 70 10 CFR 72	6-22-94	9-20-94		Clarification of decommissioning funding requirements	Published for comment in 59:119 (32138)
10 CFR 31 10 CFR 32	11-27-92	3-29-93		Requirements concerning the accessible air gap for generally licensed devices	Published for comment in 57:229 (56287)
10 CFR 34 10 CFR 150	2-28-94	5-31-94		Licenses for radiography and radiation safety requirements for radiographic operations	Published for comment in 59:39 (9429)
10 CFR 34, 35, 50, 73, 110			10-5-94; 10-5-94	NRC library; address change	Final rule in 59:192 (50688)
10 CFR 35	11-3-94	3-3-95		Request for comments regarding potential modifications of NRC's therapy regulations	Published for comment in 59:212 (55068)
10 CFR 40	10-28-92	1-26-93		Licensing of source material	Published for comment in 57:209 (48749)
10 CFR 40 10 CFR 72 10 CFR 74 10 CFR 75 10 CFR 150	1-26-93	4-26-93	7-13-94; 10-11-94	Licensee submittal of data in computer-readable form	Published for comment in 58:15 (6098); final rule in 59:133 (35618)
10 CFR 50	9-28-92	12-28-92		Acceptability of plant performance for severe accidents; scope of consideration in safety regulations	Published for comment in 57:188 (44513)
10 CFR 50 10 CFR 52 10 CFR 100	10-20-92	2-17-93; 3-24-93; 6-1-93; 2-14-95		Reactor site criteria, including seismic and earthquake engineering criteria for nuclear power plants and proposed denial of petition for rulemaking from Free Environment, Inc., et al.	Published for comment in 57:203 (47802); comment period extended in 58:2 (271); extended again in 58:57 (16377); extended again in 59:199 (52255)
10 CFR 50	6-28-93	9-13-93		Production and utilization facilities; emergency planning and preparedness-exercise requirements	Published for comment in 58:122 (34539)

(Table continues on the next page.)

Proposed Rule Changes as of Dec. 31, 1994 (Continued)

Number of part to be changed	Date published for comment	Date comment period expired	Date published; date effective	Topic or proposed effect	Current action and/or comment, *Federal Register* volumes and page numbers
10 CFR 50	1-7-94	3-23-94; 4-25-94		Codes and standards for nuclear power plants; subsection IWE and subsection IWL	Published for comment in 59:5 (979); comment period extended in 59:59 (4373)
10 CFR 50			7-12-94; 7-12-94	Regulation of Advanced Nuclear Power Plants; Statement of Policy	Final rule in 59:132 (35461)
10 CFR 50	9-19-94	12-5-94		Steam generator tube integrity for operating nuclear power plants	Published for comment in 59:180 (47817)
10 CFR 50	9-20-94	12-5-94		Technical specifications	Published for comment in 59:181 (48180)
10 CFR 50	10-4-94	1-3-95		Fracture toughness requirements for light water reactor pressure vessels	Published for comment in 59:191 (50513)
10 CFR 50	10-19-94; 10-25-94	1-3-95		Shutdown and low-power operations for nuclear power reactors	Published for comment in 59:201 (52707); correction in 59:205 (53613)
10 CFR 50 10 CFR 55 10 CFR 73	11-2-94	12-19-94		Reduction of reporting requirements imposed on NRC licensees	Published for comment in 59:211 (54843)
10 CFR 51	9-17-91	12-16-91; 3-16-92; 9-8-94		Environmental review for renewal of operating licenses	Published for comment in 56:180 (47016); comment period extended in 56:228 (59898); supplemental proposed rulemaking in 59:141 (37724)
10 CFR 52	11-3-93	1-3-94		Rulemakings to grant standard design certification for evolutionary light water reactor designs	Advance notice of proposed rulemaking published in 58:211 (58664)
10 CFR 55	5-20-93	7-19-93		Operator's licenses	Published for comment in 58:96 (29366)
10 CFR 60	7-9-93	10-7-93		Disposal of high-level radioactive wastes in geologic repositories; investigation and evaluation of potentially adverse conditions	Published for comment in 58:130 (36902)
10 CFR 61	8-3-94	10-3-94; 12-2-94		Land ownership requirements for low-level waste sites	Published for comment in 59:148 (39485); comment period extended in 59:202 (52941)
10 CFR 72	5-24-93	8-9-93; 11-9-93		Emergency planning licensing requirements for independent spent fuel facilities (ISFSI) and monitored retrievable storage facilities (MRS)	Published for comment in 58:98 (29795); comment period extended in 55:166 (45463)

Proposed Rule Changes as of Dec. 31, 1994 (Continued)

Number of part to be changed	Date published for comment	Date comment period expired	Date published; date effective	Topic or proposed effect	Current action and/or comment, *Federal Register* volumes and page numbers
10 CFR 72	9-14-93	11-29-93	12-14-94; 1-13-95	Notification of events at independent spent fuel storage installations and the Monitored Retrievable Storage installation	Published for comment in 58:176 (48004); final rule in 59:239 (64283)
10 CFR 72	6-2-94	8-16-94; 9-30-94	12-22-94; 1-23-95	List of approved spent fuel storage casks: addition	Published for comment in 58:176 (48004); comment period extended in 59:166 (44381); final rule in 59:245 (65898)
10 CFR 73	10-6-93	12-20-93	7-28-94; 8-29-94	Annual physical fitness performance training for tactical response team members, armed response personnel, and guards at Category 1 licensees	Published for comment in 58:192 (52035); final rule in 59:144 (38347)
10 CFR 73	11-4-93	1-3-94	8-1-94; 8-31-94	Protection against malevolent use of vehicles at nuclear power plants	Published for comment in 58:212 (58804); correction in 58:217 (59965); final rule in 59:146 (38889)
10 CFR 73			7-29-94; 8-29-94	Temporary access to safeguards information	Final rule in 59:145 (38533)
10 CFR 110	2-7-90	3-9-90		Import and export of radioactive wastes	Advance notice of proposed rulemaking for comment in 55:26 (4181); corrections in 55:57 (10786);
	4-28-92	7-13-92			published for comment in 57:82 (17859)
10 CFR 110	3-17-93	4-16-93	9-26-94; 11-10-94	Specific licensing of exports of certain alpha-emitting radionuclides and byproduct material	Published for comment in 58:50 (14344); final rule in 59:185 (48944)
10 CFR 170 10 CFR 171	4-19-93	7-19-93		NRC fee policy; request for public comment	Published for comment in 58:73 (21116)
10 CFR 170 10 CFR 171	5-10-94	6-9-94	7-20-94; 8-19-94	Revision of fee schedules; 100% fee recovery, FY 1994	Published for comment in 59:89 (24065); final rule in 59:138 (36895)
48 CFR 20	10-2-89	12-1-89		Acquisition regulation (NRCAR)	Published for comment in 54:189 (40420); corrections in 58:43 (12988)

[a]NRC petitions for rule making are not included here, but quarterly listings of such petitions can be obtained by writing to Division of Rules and Records, Office of Administration, U.S. Nuclear Regulatory Commission, Washington, DC 20555. Quarterly listings of the status of proposed rules are also available from the same address.

[b]Proposed rules for which the comment period expired more than 2 years prior to the start of the period currently covered without any subsequent action are dropped from this table. Effective rules are removed from this listing in the issue after their effective date is announced.

The Authors

The Chornobyl Accident Revisited, Part II: The State of the Nuclear Fuel Located Within the Chornobyl Sarcophagus

Aleksandr Aleksandrovich Borovoi, doctor of mathematical physics, is head of the Department of the Methods and Technologies of Radiation Research at the Kurchatov Russian Research Institute in Moscow. Borovoi has coauthored five monographs and authored or coauthored more than 120 articles/preprints and reports—20 of which are published. He has supervised several doctoral dissertations, including that of his coauthor for this article. Since April 1986 he has taken an active part in the mitigation of the consequences of the Chornobyl accident. During 1986 he worked as scientific consultant to the U.S.S.R. Governmental Chornobyl Commission; during 1987 he was scientific head of one of the operational groups at the Kurchatov Institute charged with investigating the accident. From 1988 to 1992 he was head of the Kurchatov Institute's Chornobyl Complex Expedition—charged with monitoring the state of the melted nuclear fuel located within the destroyed Unit 4 and monitoring the environmental impact of the sarcophagus. Since 1992, at the request of the Ukrainian Academy of Sciences, he has remained to continue his work in the newly formed Inter-Branch Scientific and Technical Center "Shelter" in Chornobyl as acting director of the Division of Nuclear and Radiation Safety. Current address: Ukrainian Academy of Sciences, Kyjiv, Ukraine, and Kurchatov Russian Research Institute, Moscow, Russia.

Alexander Roman Sich received his Ph.D. degree in February 1994 from the Department of Nuclear Engineering at the Massachusetts Institute of Technology (Cambridge, Massachusetts), where he completed his dissertation on reconstructing the sequence of events of the active phase of the Chornobyl accident. He spent a unique one and one-half years living in the town of Chornobyl as the first Westerner permitted to work closely with members of the Chornobyl Complex Expedition—the small group of Russian and Ukrainian scientists studying the remains of the ill-fated Unit 4 reactor. Prior to his doctoral work, he earned the B.S. degree from Rensselaer Polytechnic Institute (Troy, New York) in 1984, where he majored in nuclear engineering and minored in physics, and earned the M.A. degree from Harvard University (Cambridge, Massachusetts) in 1992, majoring in Soviet studies. He has traveled extensively in Russia, Ukraine, Uzbekistan, and Lithuania, and lived in Ukraine from July 1990 to April 1993. Current address: Massachusetts Institute of Technology, Cambridge, Massachusetts.

Nuclear Power Safety in Central and Eastern Europe

Richard Wilson [redacted] received his M.A. and D. Phil. degrees in physics at Oxford University, England, in 1949, and has been at Harvard University since 1955. He traveled to Chernobyl soon after the accident and helped to make a film for public television about the accident. He was given the FORUM AWARD of the American Physical Society in 1990 for "his outstanding research and promotion of public understanding on a broad spectrum of issues dealing with physics, the environment, and public health, including his work on reactor safety, estimation of hazards posed by environmental pollution and pioneering use of comparative risk analysis." Current address: Department of Physics, Harvard University, Cambridge, MA 02138.

Safety of Nuclear Power Reactors in the Former Eastern European Countries

Sabyasachi Chakraborty received the B.S. degree in physics from Calcutta University, India, in 1961 and the diploma in nuclear physics from the University of Kiel in Germany. He joined the Swiss Federal Nuclear Safety Inspectorate in 1975 after a variety of research work in the field of nuclear physics. He has continually applied and extended his knowledge to nuclear power safety issues. He has authored three books dealing with different aspects of risk management in industrial societies and is head of Research and International Programs of the Swiss Regulatory Body. He is a member of the Committee on the Safety of Nuclear Installations of the Nuclear Energy Agency and of the Board of Management of the Halden Reactor Project of the Organization for Economic

Cooperation and Development. He is presently chairman of the International Atomic Energy Agency Steering Committee on the Safety of RBMK Reactors. Current address: Swiss Federal Nuclear Safety Inspectorate, Ch-5232 Villigen-HSK, Switzerland.

Technical Note: On the Definition of Common-Cause Failures

Henrique Paula. Current address: JBF Associates, Inc., Knoxville, TN 37932-3353.

Modeling and Analysis of Core-Debris Recriticality During Hypothetical Severe Accidents in the Advanced Neutron Source Reactor

S.-H. Kim, V. Georgevich, D. B. Simpson, C. O. Slater, and ***R. P. Taleyarkhan.*** Current addresses: Oak Ridge National Laboratory, Oak Ridge, TN 37831.

Ignitability of Hydrogen/Oxygen/Diluent Mixtures in the Presence of Hot Surfaces

R. K. Kumar is currently a research engineer at the Atomic Energy of Canada Limited (AECL). His current work deals with hydrogen combustion studies relevant to nuclear reactors. Previously he worked in the area of gas turbine combustion research at the Gas Turbine Research Establishment in India. He received the B.Eng. degree from the University of Mysore; the M.Eng. degree from the Indian Institute of Science, India; and M.A.Sc. and Ph.D. degrees in mechanical engineering from the University of Waterloo, Canada. He has over 20 years of experience in various aspects of combustion and has published extensively. Current address: AECL Research, Whiteshell Laboratories, Pinawa, Manitoba R0E 1L0, Canada.

Grant W. Koroll is currently acting branch manager of the Containment Analysis Branch of Reactor Safety Research at Atomic Energy of Canada Limited (AECL). He received the B.Sc. degree in chemistry from the University of Saskatchewan and the M.Sc. degree in physical chemistry from the University of Manitoba. He joined AECL in 1975 and has been working in safety-related hydrogen combustion since 1981. His current activities include research of combustion phenomena (ignition and combustion in complex geometrics) and development of catalytic combustion systems. Current address: AECL Research, Whiteshell Laboratories, Pinawa, Manitoba R0E, 1L0, Canada.

Coupled RELAP5 and CONTAIN Accident Analysis Using PVM

Kevin A. Smith received the Ph.D. degree in nuclear engineering from The Pennsylvania State University in 1992. He held a limited-term position at the KEMA Institute in the Netherlands during his graduate work. His interests include computational thermal hydraulics, severe-accident analysis, and high-performance computing. Current address: Oak Ridge National Laboratory, Oak Ridge, TN 37831-6392.

Anthony J. Baratta received the Ph.D. degree in physics from Brown University in 1978. He worked with the U.S. Navy nuclear propulsion program for 10 years before becoming a faculty member at The Pennsylvania State University College of Engineering in 1978. His research interests include reactor safety, probabilistic risk assessment, transport theory, and radiation effects on semiconductor devices and materials. Current address: The Pennsylvania State University, University Park, PA 16802.

Gordon E. Robinson received the Ph.D. degree in mechanical engineering from The Pennsylvania State University (PSU) in 1970. He is an associate professor of nuclear engineering at PSU. His research interests include basic boiling phenomena and light-water-reactor transient analysis. Current address: The Pennsylvania State University, University Park, PA 16802.

Application of Fuzzy Logic in Nuclear Reactor Control. Part I: An Assessment of State-of-the-Art

A. Sharif Heger is an assistant professor at the University of New Mexico. He has developed, modified, and taught several graduate and undergraduate courses in medical radioisotopes, nuclear reactor theory, thermodynamics, and risk assessment. He has also been

the Technical Advisor for the Environmental Risk Management Series that was broadcast to national and international sites. He has developed new methods for performance assessment of waste management and environmental restoration sites as well as calculation of exact values of complex systems fault tree models (SigmaPi Method). His search in intelligent systems concentrates on the application of pattern recognition techniques in risk assessment and use of fuzzy logic in instrument fault detection, isolation, and correction. Current address: Chemical and Nuclear Engineering Department, University of New Mexico, Albuquerque, N.M.

Nahrul Khair Alang-Rashid [redacted] received the B.Sc. degree with Honors in electrical and electronics engineering from the University of Glasgow, U.K., in 1977 and the M.S. degree in nuclear instrumentation from the University of Edinburgh, U.K., the following year. In 1992 he obtained the Ph.D. degree in nuclear engineering from the University of New Mexico, Albuquerque, U.S.A. He joined the Malaysian Institute for Nuclear Technology Research (MINT), formerly known as Nuclear Energy Unit (UTN), in 1976 as a research engineer, headed the Reactor Department of MINT starting in 1982, and became the Institute's Deputy Director General in May 1993. He spent about a year each at Oregon State University, U.S.A., to obtain the U.S. Nuclear Regulatory Commission Senior Reactor Operator's License; at General Atomic Company, California, U.S.A., as trainee engineer; and at Oak Ridge National Laboratory, U.S.A., as guest engineer between 1979 and mid-1981. He has written several papers in his area of interest: fuzzy logic control and intelligent systems. Current address: Malaysian Institute for Nuclear Technology Research, Kompleks PUSPATI, Bangi, Selangor, Darul Ehsan, Malaysia.

Mohammad "Mo" Jamshidi received the B.S.E.E. degree (cum laude) from Oregon State University in June 1967; he received the M.S.E.E. and Ph.D. degrees from the University of Illinois in June 1969 and February 1971, respectively. Currently, he holds the AT&T Professorship of manufacturing engineering. He is also Professor of Electrical and Computer Engineering and Director of Computer-Aided Design Laboratory for Intelligent and Robotic Systems at the University of New Mexico, Albuquerque, N.M. He is a consultant with the Los Alamos National Laboratory. He has over 400 technical publications, including 35 books and edited volumes primarily in English. Four books have been translated into Chinese and Russian. He is the Founding Editor or co-founding editor or editor of five journals and a magazine (*IEEE Control Systems Magazine*). He has been on the executive editorial boards of a number of journals and two encyclopedias. He has been the series editor for ASME Press Series on *Robotics and Manufacturing* since 1988 and for the Prentice Hall Series on *Environmental and Intelligent Manufacturing Systems* since 1991. He is a Fellow of IEEE, a recipient of the IEEE Centennial Medal and IEEE Control Systems Society Distinguished Member Award, a member of five honor societies, and honorary chaired professor at three Chinese universities. He is the General Chairman of World Automation Congress, a multidisciplinary multisymposia technological and scientific meeting taking place every two years. Current address: Electrical and Computer Engineering Department, University of New Mexico, Albuquerque, N.M.

Twenty-Third DOE/NRC Nuclear Air-Cleaning and Treatment Conference

Ronald R. Bellamy, Ph.D., is Chief of the Nuclear Materials Safety Branch for Region I of the Nuclear Regulatory Commission (NRC) in King of Prussia, Pa. He directs a staff of specialists responsible for inspection at medical institutions and research and development facilities, industrial radiographers, and sealed source users in the northeastern United States. Previously stationed at Three Mile Island, he presently serves on several industry standards committees pertaining to air cleaning. Current address: NRC, 475 Allendale Road, King of Prussia, PA 19406.

John J. Hayes is a senior health physicist in the Emergency Preparedness and Radiation Protection Branch for the Office of Nuclear Reactor Regulation of the Nuclear Regulatory Commission (NRC) in Rockville, Md. He worked for electrical utilities and as an engineering consultant prior to joining the NRC. He is a member of the ASME Committee on Nuclear Air and Gas Treatment and ANS Standards Committee 59.2. Current address: NRC, Mail Stop OWFN 10D4, Washington, DC 20555-0001.

Melvin W. First, Sc.D., is professor of environmental health and engineering and Director of the Harvard Air-Cleaning Laboratory. He has been a leading figure in air-cleaning research for over 30 years. Current address:

School of Public Health, Harvard University, 665 Huntington Avenue, Boston, MA 02115.

Atmospheric Dispersion and the Radiological Consequences of Normal Airborne Effluents from a Nuclear Power Plant

D. Fang is an associate professor in the Institute of Nuclear Energy Technology at Tsinghua University in China. He graduated from the Department of Engineering Physics of Tsinghua University in 1964. His research areas are radiological consequences, environmental impact assessment, environment and health risk analysis, and air pollution control. Current address: Institute of Nuclear Energy Technology, Tsinghua University, Beijing (100084), People's Republic of China.

C. Z. Sun is a senior engineer at Suzhou Nuclear Research Institute, Ministry of Electric Power. He graduated from Jilin University in 1963. Prior to his current assignment, he worked on nuclear chemical research at China's Northwest Nuclear Technology Research Institute. He has been responsible for the environmental impact evaluation of several sites and siting of some nuclear power plants. Current address: Suzhou Nuclear Research Institute, Ministry of Electric Power Industry, Suzhou (215004), People's Republic of China.

L. Yang is a research assistant in the Institute of Nuclear Technology at Tsinghua University. She received the B.Eng. degree in reactor engineering from Tsinghua University in 1989. Her research areas are accident consequences, environmental assessment, radiation shielding, and decommissioning. Current address: Institute of Nuclear Energy Technology, Tsinghua University, Beijing (100084), People's Republic of China.

Calculation of Distribution Coefficients for Radionuclides in Soils and Sediments

Ignasi Puigdomènech [redacted] After his graduation in the Universidad Autonoma de Barcelona, he undertook his Ph.D. studies at the Department of Inorganic Chemistry of the Royal Institute of Technology in Stockholm, Sweden. He was employed at Studsvik in 1987, and since then he has been working in the fields of thermodynamics of aqueous solutions and geochemical modeling of natural water systems. He has also been involved in the compilation of thermodynamic data for americium during a three-year stay at the Nuclear Energy Agency in Paris, France. Current address: Studsvik Eco & Safety AB, S-61182 Nyköping, Sweden.

Ulla Bergström [redacted] received the M.Sc. degree from the Department of Mathematics and Science at the University of Uppsala, Sweden, in 1972 and continued her studies in hydrologics and advanced mathematics before she joined AB Atomenergi in 1974 as a member of the Environmental Protection Section. Since then she has been working with modeling of radionuclide turnover in the biosphere and resulting doses to man from releases of radionuclides from nuclear power plants and radioactive waste repositories. She has participated in several international model intercomparisons and validation projects. Current address: Studsvik Eco & Safety AB, S-61182 Nyköping, Sweden.

Operating Experience Feedback Report—Reliability of Safety-Related Steam Turbine-Driven Standby Pumps Used in U.S. Commercial Nuclear Power Plants

J. R. Boardman attended Emory University for three years and is a 1955 graduate of the U.S. Naval Academy. He was on active duty for four years serving in amphibious ships and the guided missile cruiser Canberra and was in the Naval Research Reserve for fourteen years. From 1959 he was employed by Litton Industries Ingalls Shipbuilding Division in Pascagoula, Miss., until 1980 when Litton ended its work on nuclear powered attack submarines. At Ingalls he held increasingly responsible positions in its Nuclear Power Division in the functional areas of startup testing, design and systems engineering, and nuclear quality assurance. He subsequently was Ingalls Director of Nuclear Material and Nuclear Overhaul Planning, initiating the nuclear overhaul planning organization, and as a collateral duty, he established and directed the reactor plant engineering group that defined the requirements for commercial-grade dedication of electrical, instrumentation and control, and fluid/mechanical items. From 1980 to 1990,

he was a reactor inspector with the Nuclear Regulatory Commission (NRC) in Region IV, where he performed both construction- and operation-phase inspections, and completed NRC training for all U.S. commercial reactor types except high-temperature gaseous reactors. In 1990 he joined the NRC's Office for Analysis and Evaluation of Operational Data (AEOD). He is presently a Senior Reactor Systems Engineer with the Reactor Analysis Branch of AEOD's Safety Programs Division.

Turbine Building Hazards

Harold L. Ornstein is a Senior Reactor Systems Engineer with the U.S. Nuclear Regulatory Commission's Office for Analysis and Evaluation of Operational Data (AEOD). He received his B.S., M.S., and Ph.D. degrees in Mechanical Engineering from City College of New York, Rensselaer Polytechnic Institute, and the University of Connecticut, respectively. From 1961 to 1966 he was a Senior Analytical Engineer with Pratt & Whitney Aircraft. From 1966 to 1971 he worked as an instructor of Mechanical Engineering at the University of Connecticut and performed research on water desalination analyzing the thermohydraulics of flash evaporators. During this time he also worked at the New England Research Application Center applying aerospace technology to other fields. He joined the U.S. Atomic Energy Commission (now the U.S. Nuclear Regulatory Commission) in 1971 where he worked on the development of sodium to air heat exchangers for the Breeder Reactor Program (specifically, the Fast Flux Test Facility). With the NRC, he provided testimony for Congress regarding safety margins at Browns Ferry during the March 22, 1975, fire, was a member of the Three Mile Island Special Inquiry Group, and has authored numerous AEOD case studies as well as special study reports (notably, studies on air systems, solenoid-operated valves, loss of decay heat removal, and turbine-generator overspeed).

Indexes to *Nuclear Safety,* Volumes 34 and 35

Cumulative Keyword in Context (KWIC) indexes of issues of *Nuclear Safety* through Volume 22 were published as separate documents and are available from the National Technical Information Service. Starting with Volume 23 (1982), author and KWIC indexes are published in the first issue of the following volume. This issue contains these indexes for *Nuclear Safety*, Volumes 34 and 35, because only 2 issues per year were published for these years. Both indexes use a six-digit number to indicate the location of the indexed material. The six-digit number is divided into four parts (00-0-000), which stand, respectively, for volume-number-page. The authors are indexed alphabetically. In the KWIC index, the article titles are permuted around the various significant words contained therein; for example, the title "A Scheme for Passive Isolation of the Containment of a Reactor" is indexed under the words *Passive*, *Isolation*, *Containment,* and *Reactor*. The index words are arranged alphabetically in a column in the center of the page with the titles permuted around them. A slash (/) indicates the end of a title. The two indexes follow.

KWIC Indexes to Volumes 34 and 35

Author List

30th TENNESSEE INDUSTRIES WEEK

Knoxville, Tenn., August 14–18, 1995

The University of Tennessee is offering eight short courses during the week of August 14, 1995. These courses, which are designed to help practitioners apply new technology, are as follows: Predictive Maintenance Technology (Aug. 14–16), Bayesian Reliability Analysis (Aug. 14–18), Radiological Assessment (Aug. 14–18), Nuclear Criticality Safety (Aug. 14–18), Computational Methods in Reactor Analysis & Shielding (Aug. 14–18), Applied Artificial Intelligence for Engineering Applications (Aug. 14–18), Contemporary Issues in Nuclear Reactor Safety (Aug. 14–16), and An Introduction to Fusion Technology for the Practicing Engineer (Aug. 14–18).

For additional information, contact Professor T. W. Kerlin, 315 Pasqua Engineering Building, The University of Tennessee, Knoxville, TN 37996-2300. Phone: (615) 974-2525. Fax: (615) 974-0668.

DOE TECHNICAL STANDARDS PROGRAM 1995 WORKSHOP

St. Louis, Mo., October 3–6, 1995

The U.S. Department of Energy (DOE) Technical Standards Program workshop for 1995 will present "The Strategic Standardization Initiative—A Technology Exchange and Global Competitiveness Challenge for DOE." The workshop is to inform the DOE technical standards community of strategic standardization activities taking place in the Department, other Government agencies, standards developing organizations, and industry. Individuals working on technical standards will be challenged to improve cooperation and communications with the involved organizations in response to the initiative.

Workshop sessions include presentations by representatives from various Government agencies that focus on the coordination among and participation of Government personnel in the voluntary standards process; reports by standards organizations, industry, and DOE representatives on current technology exchange programs; and how the road ahead appears for "information superhighway" standardization. Another session highlights successful standardization case studies selected from several sites across the DOE complex. The workshop concludes with a panel discussion on the goals and objectives of the DOE Technical Standards Program as envisioned by senior DOE management.

For additional information, contact Becky Harrell, Technical Standards Program Office, Oak Ridge National Laboratory, P.O. Box 2009, Oak Ridge, TN 37831-8065. Phone: (615) 574-0396. Fax: (615) 574-0382.

MULTIPHASE FLOW EXPERIMENTS AND INSTRUMENTATION

San Francisco, Calif., October 29–November 2, 1995

The Thermal–Hydraulics Division of the American Nuclear Society is sponsoring a technical session on Multiphase Flow Experiments and Instrumentation. Technical papers will discuss advancements in two-phase flow instrumentation and related experimental studies in two-phase flow.

For additional information, contact

Prof. J. N. Reyes, Jr., Dept. of Nuclear Engineering, Oregon State University, Radiation Center, C116, Corvallis, OR 97331-5902, Phone: (503) 737-4677. Fax: (503) 737-4678.

or

Prof. F. B. Cheung, Dept. of Mechanical Engineering, Penn State University, University Park, PA 16802, Phone: (814) 863-4261. Fax: (814) 863-8682.

(Continues from page ii)

it with nuanced completeness. In this connection, I have a personal "stylistic" debt to Ernest that I have never publicly acknowledged. In 1970, at a meeting of the American Nuclear Society, I first characterized nuclear energy as a Faustian Bargain (much to the annoyance of many nuclear colleagues). I entitled the paper *The Moral "Dilemma" of Nuclear Energy*. It was Ernest who pointed out that "Dilemma" was not quite the right word: there was inherent in nuclear energy a Moral *Imperative,* and that was the title I published without ever giving Ernest full credit for this felicitous improvement. As editor of *Nuclear Safety,* Ernest has been responsible for innumerable improvements both in style and substance, but, because he was editor, these improvements have had to go unacknowledged. On behalf of the hundreds of authors who published in *Nuclear Safety*, I hereby explicitly thank Ernest for using his editorial pencil so precisely, yet anonymously.

Ernest spent three years with me at the Institute for Energy Analysis. While there he became an expert in the whole field of energy—not just nuclear energy—and perhaps grew to appreciate that nuclear energy did place unusual demands on its practitioners, standards of excellence and dedication that Ernest himself exhibited to so admirable a degree. When Ernest returned to Oak Ridge National Laboratory, he first joined the Fast Breeder Reactor program and then, at Bill Cottrell's invitation, the staff of *Nuclear Safety.*

So we pioneers of the First Nuclear Era once again thank Ernest for editing *Nuclear Safety.* We know that his retirement will be filled with exciting and meaningful activities—always marked by Ernest's perceptive, good-natured, and witty interventions.

Alvin M. Weinberg

SUBSCRIPTIONS

For current price of subscription or single copies, please contact the Superintendent of Documents, P.O. Box 371954, Pittsburgh, PA 15250-7954. Telephone requests can be made from 8:00 a.m. to 4:00 p.m. eastern time, at (202) 512-1800.

FUTURE ARTICLES

THE CHORNOBYL ACCIDENT

Chornobyl Source Term Release Dynamics and Reconstruction of Events During the Active Phase, *A. R. Sich*

GENERAL SAFETY

Western Nuclear Safety and Licensing Practices, *S. Chakraborty*

A Decision Support System for Maintenance Management of a Boiling Water Reactor, *J. H. Shen, A. Ray, and S. Levine*

Role of Experimental Measurements in Criticality Technology, *R. E. Malenfant*

Elements of a Nuclear Criticality Safety Program, *C. M. Hopper*

Technology and Competence in Criticality Safety, *R. E. Wilson*

ACCIDENT ANALYSIS

Transient Analyses of the PIUS Advanced Reactor Design with the TRAC-PF1/MOD2 Code, *B. E. Boyack, J. L. Steiner, S. C. Harmony, H. J. Stumpf, and J. F. Lime*

The Hierarchy-by-Interval Approach to Identifying Important Models that need Improvement in Severe Accident Simulation Codes, *T. J. Heames, R. P. Jenks-Johnson, M. Khatib-Rahbar, and Yi-Shung Chen*

RELAP5/MOD3 Code Coupling Model, *R. P. Martin*

Missiles Caused by Severe PWR Accidents, *R. Krieg*

DESIGN FEATURES

Validation of COMMIX with Westinghouse AP-600 PCCS Test Data, *J. G. Sun, T. H. Chien, J. Ding, and W. T. Sha*

Modern Tornado Design of Nuclear and Other Potentially Hazardous Facilities, *J. D. Stevenson and V. Zhao*

ENVIRONMENTAL EFFECTS

Potential Accident Radiological Consequences and Siting of Commercial Nuclear District-Heating Reactor, *Zhongqui Shi*

A Method of Calculating Risk from a Spent Fuel Facility, *L. Canas*